Contents

1 Introduction

The discovery of the Deoxyribonucleic acid (DNA) double helix is arguably one of the greatest scientific breakthroughs of the 20th Century. Since then, DNA has captured the imagination of many great scientists and with every new development so the excitement grows. There have been many milestones including the development of the polymerase chain reaction,[1] DNA fingerprinting, [2] and the remarkable completion of the human genome project.[3] Through years of scientific endeavour, we have acquired a comprehensive understanding of the structure, function and reactivity of DNA, yet there remains great potential for the use of DNA in numerous applications. Emerging technologies including anti-sense therapy, nanotechnology, catalysis and aptamer ligands are all utilising the inherent characteristics of DNA. In the first 50 years since its discovery, DNA has been propelled to the forefront of research and all indicators seem to suggest that interest in this molecule will continue in the next 50 years.

1.1 Aptamers

1.1.1 Background

Aptamers are short strands of artificial nucleic acids. They can either be single stranded deoxyribonucleic acid (ss DNA) or ribonucleic acid (RNA) and can act as ligands that can be specifically targeted against particular molecules.[4] This is in contrast to traditional guest – host interactions whereby the target molecules are often referred to as ligands.

The word aptamer comes from the Latin “aptus” meaning fitted.[5] They can adopt tertiary structures, which can discriminate between small differences in target molecules. Consequently, they have specificity, selectivity and affinity comparable to and sometimes in excess of antibodies.[6] Aptamers were first reported in 1990 when 3 different laboratories

independently developed methods for selecting aptamers to targets ranging from small dye molecules, [5] single stranded DNA [7] and an enzyme.[8]

Firstly, it is important to illustrate the structure of an aptamer template molecule and distinguish from the aptamer sequence (see Figure 1.1). It can be thought of as consisting of two parts; the first contains two primer regions of known sequence each typically around 15-25 bases, with the other is a region of unknown sequence, typically around 30-80 bases. The latter region provides the complexity and diversity that make aptamer selection such a powerful tool. It is within this region that the aptamer sequence is to be found.

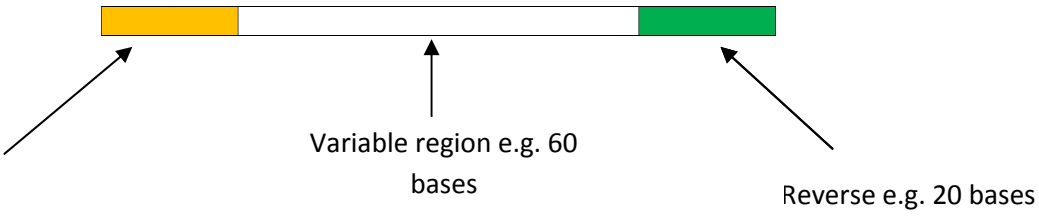

Figure 1.1: Diagram of an aptamer template molecule.

It is possible to calculate the theoretical maximum number of different molecules arising from, for example, a 60 base variable region. Each base can be one of four; adenine (A), cytosine (C), guanine (G) and thymine (T)

$$4^{60} = 1.33 \times 10^{36} \text{ different molecules.}$$

In reality, however, this number is limited by the sample size. The pool of aptamer molecules is often generated on the µmole scale.

1 mole contains	➔	6.022×10^{23} (Avagadro's number) molecules
1×10^{-6} moles contains	➔	6.022×10^{17} different molecules

The figures detailed above help illustrate a unique property of aptamers. Although the building blocks of aptamers (nucleic acids) lack chemical diversity, the sheer number of possible sequence variations can produce structural diversity to such an extent that, theoretically,

aptamers may be selected against any target molecule, ion or species, as illustrated by the aptamer database.[9] Examples include small ions such as Zn(II)[10], toxins such as ricin,[11] enzymes such as thrombin[12] and whole cells.[13] This variation is also reflected in the binding constants observed between aptamer and target. Dissociation constants (K_D) values range from high micromolar (arginine 125 μM)[14] to low picomolar (keratinocyte growth factor 0.3 pM).[15] Often there is a compromise to be made between affinity and selectivity. However, the theophylline aptamer is a good example of one with both properties.[6] This aptamer has an affinity for theophylline that is 10,000 times that of caffeine despite the fact that these two molecules differ in only one methyl group (see Figure 1.2).

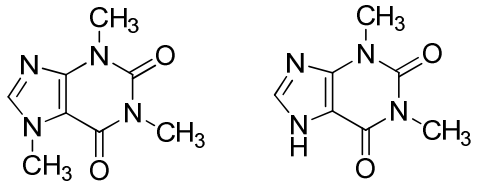

Figure 1.2: Structures of caffeine (left) and theophylline (right).

RNA aptamers dominate the literature over DNA (a search in the aptamer database gives 206 hits for RNA compared to 84 hits with DNA, search performed Sept '10). Although the discussion thus far has only focussed on nucleic acids, peptide aptamers now represent an emerging class in this field. Each class of aptamer has its own properties which will be considered in detail in subsequent sections.

1.1.2 Introduction to nucleic acids

Nucleic acids are arguably the most important biological molecule. They hold and convert genetic material responsible for the construction of all living organisms and form the basis of genetic inheritance. There are two types of nucleic acids; deoxyribonucleic acid (DNA) and ribonucleic acid (RNA). In general, genetic material is stored in genes and chromosomes and consists of DNA whereas RNA translates the information into proteins that sustain the

organism. However, there are exceptions for instance the genetic material of RNA viruses consists of RNA. The nucleic acid molecule can be broken down into phosphate backbone, sugar and base.[16] The phosphate backbone (depicted in Figure 1.3) is common to both DNA and RNA.

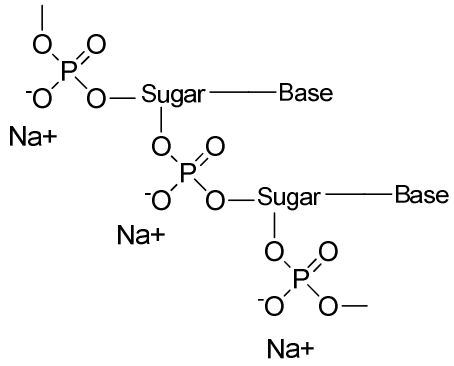

Figure 1.3: Illustration of the phosphate backbone present in nucleic acids.

Figure 1.3 highlights the characteristic negatively charged backbone common to nucleic acids. However, the two acids differ in their sugar molecules. As the name suggests, RNA contains ribose sugar, whereas DNA contains deoxyribose sugar (illustrated in Figure 1.4).

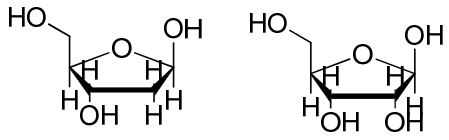

Figure 1.4: Structures of the 2 sugar molecules present in nucleic acids, β-D-ribose (right) and β-2-deoxy-D-ribose (left).

Although the structures in Figure 1.4 would indicate only subtle differences between the two molecules, the two differ significantly in their reactivity (which will be discussed in a section 1.1.5). Another difference between RNA and DNA is the bases. The bases in RNA and DNA can be one of four; adenine, guanine, cytosine and thymine (in DNA) or uracil (in RNA). The structures of all five bases are shown in Figure 1.5.

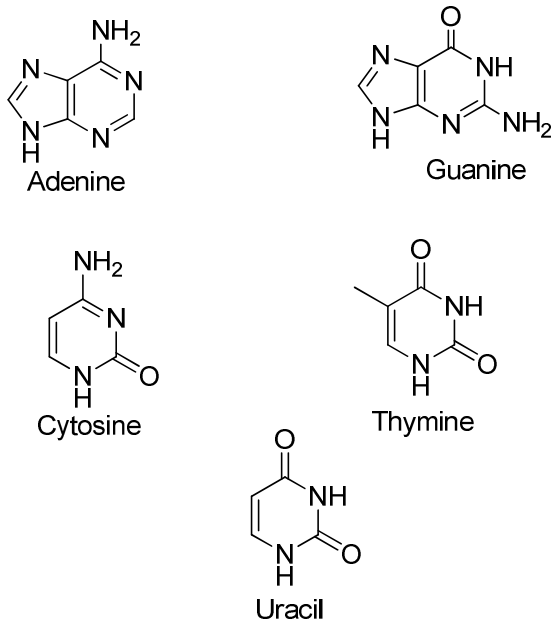

Figure 1.5: Structures of all 5 bases of nucleic acids.

As shown in Figure 1.5, all structures fall into either the bicyclic purine type or the monocyclic pyrimidine type. Their size and ability to hydrogen bond play key roles in determining the complementary base pairing.

1.1.3 Complementary base pairing

In DNA, the bases pair up to form a double stranded molecule famously termed the double helix. It was the combined work of Wilkins, Franklin, Watson and Crick that lead to the discovery of the structure.[17 18 19] Crucial to the discovery was the complementary nature of the base pairing i.e. adenine binds only to thymine and guanine binds only to cytosine. Hydrogen bonding is responsible for the base pairing, shown in Figures 1.6 – 1.8.

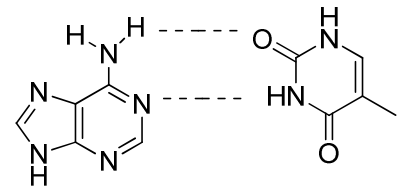

Figure 1.6: A - T hydrogen bonding.

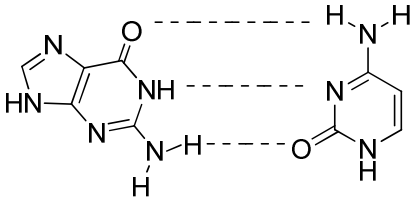

Figure 1.7: G - C hydrogen bonding.

In RNA the base thymine is replaced by the base uracil which also bonds to adenine via two hydrogen bonds.

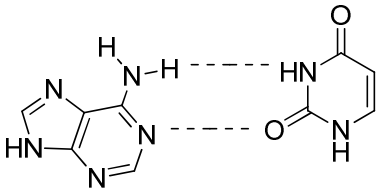

Figure 1.8: A - U hydrogen bonding.

1.1.4 Double helix

The double helix (illustrated in Figure 1.9) is formed by the connection of two, anti-parallel single strands of DNA joined together via hydrogen bonding between the bases.

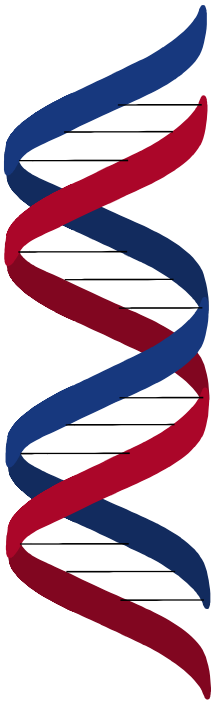

Figure 1.9: Double helix structure of DNA.

The sequence of the DNA bases is of utmost importance. It is at the core of the "central dogma of molecular biology" together with RNA and protein. DNA acts as the template upon which proteins are synthesised thus sustaining and propagating all life forms. It directs the transcription into RNA and subsequent translation into the amino acid building blocks of proteins.

Because DNA is such an important molecule, it is essential to gain insight into and understanding of its properties, function and reactivity. Since the initial findings of Wilkins, Franklin, Watson and Crick, scientists have been fascinated by this molecule and consequently a plethora of knowledge has been acquired.

1.1.5 Comparison of DNA and RNA

Although DNA and RNA are structurally similar molecules they do differ significantly in their reactivity. This difference can be attributed to the presence of the hydroxyl group on the ribose sugar molecule. RNA is far more reactive than DNA and as such has implications on its stability. The phosphodiester bond is very susceptible to hydrophilic attack to form a 2' – 3' cyclic phosphate, as shown in Scheme 1.1

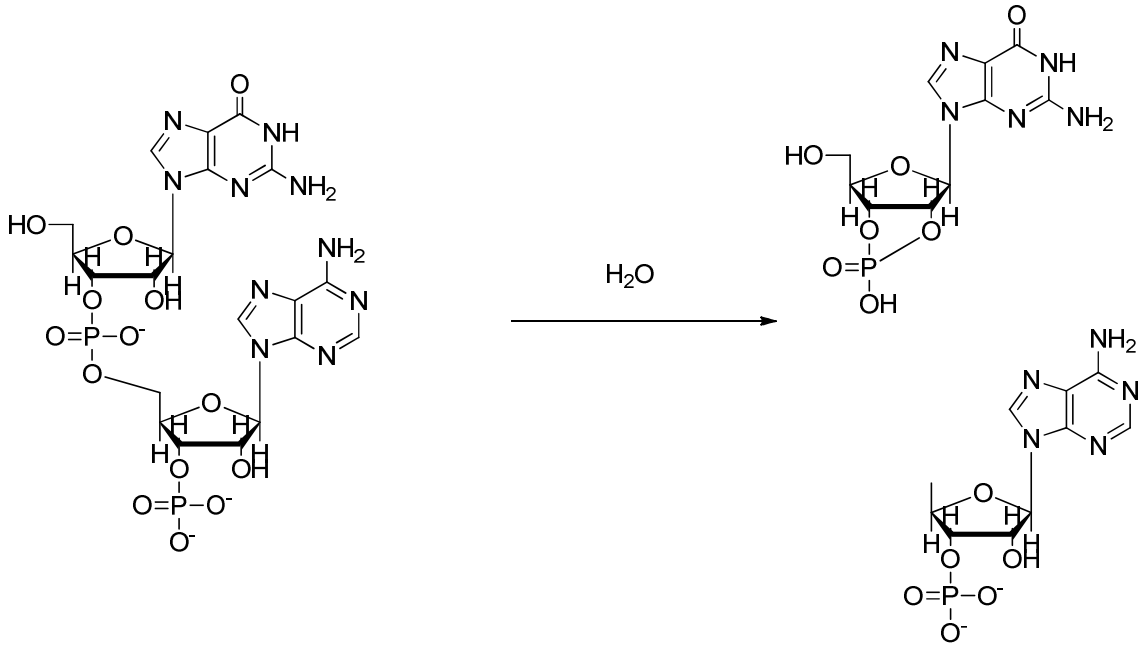

Scheme 1.1: Reaction of RNA degradation resulting in formation of a cyclic phosphate.

The other factor contributing to the degradation is ribonucleases (RNases). These are ubiquitous enzymes which catalyse the degradation of RNA.

Although there are disadvantages associated with RNA, they are often the nucleic acid of choice to be used as aptamers. The same OH responsible for the reactivity of RNA allows for more complex folding of the RNA structure compared with DNA and thus confers greater tertiary structure. This has an advantage as it gives the greatest possible chance of an aptamer to form the best fit to a target.

There are numerous examples of RNA aptamers in the literature. Indeed the very first aptamers

isolated were RNA.[5 7 8] It is possible for RNA and DNA aptamers to bind to the same target (the classic example being thrombin). This protein has both a DNA[12] and RNA aptamer.[20] The two sequences are unrelated and bind at different sites of the target. In the 20 years since the first isolation of aptamers, DNA and RNA have become well established and characterised. Peptide aptamers, however, are starting to feature in the literature. They do differ from their nucleic acid counterparts and are discussed in the subsequent section.

1.1.6 Peptides

Peptide aptamers were first isolated by Colas *et al*.[21] They are defined as combinatorial protein species containing a variable peptide region. They are composed of a protein scaffold which confers structural rigidity to the aptamer and a variable region responsible for binding to the target, typically consisting of around 20 amino acids.[22] The aptamers are generated by inserting a DNA sequence encoding for the amino acids into the protein scaffold. The constrained nature of the aptamer confers high specificity, an essential requirement.[23] The nature of the scaffold is important, ideally it should have little reactivity or enzyme activity i.e. biologically neutral. This can be achieved by inserting the peptide sequence into an area of the protein which will disrupt its function.

The majority of peptide aptamers in the literature act as interferents on protein – protein interactions. One such example is the Hepatitis B virus (HBV) peptide aptamer. This aptamer binds to a protein which prevents replication of the virus. HBV is associated with liver cancer and the antiviral potential of such an aptamer could open up novel routes for liver cancer therapy.[24] Peptide aptamers have proved to be very specific as they are capable of differentiating between mutant and wild type proteins.[25] Although, peptides are the most recent class of aptamer, they have great potential in many areas including proteomics, cell biology and drug binding validation. Indeed all classes of aptamer are emerging as an exciting new branch of science. The most powerful aspect of aptamers comes from the vast range of potential targets.

1.1.7 Targets

The first aptamers isolated in 1990 were all RNA based but selected against three very different targets; single stranded DNA,[7] organic dyes[5] and polymerase enzyme.[8] Immediately, the potential for aptamer technology was demonstrated. In addition to a wide range of species being targeted successfully, Robertson *et al*.[7] generated a ribozyme (i.e. RNA with catalytic activity) capable of cleaving single stranded DNA. From here, research into the field of aptamers has grown exponentially. Proteins are the most common target for aptamers (as shown in Table 1.1).

Table 1.1: Summary of different aptamer targets from the Aptamer Database.

Target	***No. of hits on database****
Protein	141
Organic / small molecule	64
Peptide	29
Nucleic acid	25
Aminoglycoside	9
Carbohydrate	4
Other	36

* Search performed Sept'10

However, small molecules are beginning to feature in the literature. One of the most well known is the cocaine aptamer, developed by Stojanovic *et al*.[26] and has been used in numerous different ways to detect cocaine ranging from fluorescence spectroscopy,[27] electrochemical detection[28] to the use of aptamer functionalised quantum dots.[29] It is possible, therefore, that other drug molecules could be potential targets for aptamers.

1.1.8 Amphetamine / methamphetamine

One drug of particular interest is amphetamine. Amphetamine is the commonly used name for the aromatic amine 1-phenylpropan-2-amine.

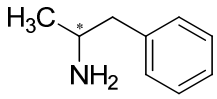

Figure 1.10: Structure of amphetamine.

As can be seen from Figure 1.10, the molecule posses a steroegenic centre at this position (*) and it is the *D* enantiomer which is the active form of the drug.

However, amphetamine is often used as a broad term to describe a family of drug compounds; including methylenedioxymethamphetamine (MDMA also known as ecstasy) and methamphetamine (also known as methylamphetamine) (see Figure 1.11). They are all controlled in UK law under The Misuse of Drugs Act, 1971 but are categorised under different classifications. They act on the central nervous system (CNS) and have stimulatory effects including increasing heart rate and blood pressure. However, amphetamines have medicinal properties and have been known to treat Attention – deficit hyperactivity disorder (ADHD). The American Food and Drug Administration FDA have licensed the drug Adderall which contains a racemic mixture of neutral sulfate salts of *D* and *L* amphetamine.

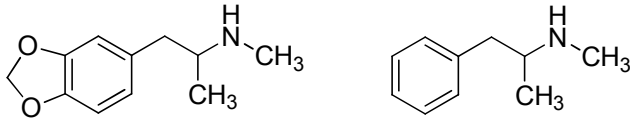

Figure 1.11: Structure of MDMA (left) and methamphetamine (right).

The pharmacological action of amphetamine is thought to involve producing increased levels of the neurotransmitters dopamine and serotonin, however the mode of therapeutic action for treatment of ADHD is not known.

There are existing analytical techniques to detect amphetamine and are often divided into screening and confirmation tests. The majority of screening tests are immunoassays. Enzyme linked immuosorbent assays (ELISA) are common as they offer good detection limits (typically ng/mL)[30], can be easily automated to allow for rapid, high throughput screening[31] and are compatible with numerous sample types, for example blood,[32] urine[33] and hair.[34] Immunoassays are used ubiquitously in drug detection with the application of antibodies being utilised successfully for decades. However, one must consider the method of antibody production. Animals are still predominantly used to generate antibodies and with current efforts being made within the scientific community to reduce the number of animals involved in research, there is a need to develop complementary techniques in parallel with the well established immunoassays. Thin layer chromatography (TLC) is another technique used for screening purposes[35] and, as it is purely a chemical analysis, can overcome the disadvantage of the use of animals in the production of antibodies.

These screening tests are only indicative and so confirmation tests are required to fully identify a sample as an amphetamine. Consequently, instrumental techniques such as gas chromatography (GC) are often the analysis of choice. They have detection limits in the ng/mL (nM) range and when coupled to a characterising technique like mass spectrometry (MS) it can yield to conclusive data as to the identity of a compound.[36] [37] [38] Unlike immunoassays and TLC techniques, GC-MS is cumbersome, relatively expensive and not portable.

Therefore, the generation of a novel aptamer sequence selected against amphetamine has the potential to solve some of the problems identified and, in parallel with existing techniques, could improve drug detection. The process required to generate aptamers is systematic evolution of ligands by exponential enrichment (SELEX).

1.2 Systematic Evolution of Ligands by Exponential Enrichment (SELEX)

1.2.1 Outline of Process

SELEX is the name given to the process whereby a large aptamer library pool (containing a random assortment of different sequences) is created and then selectively enriched in order to produce only a few molecules which display excellent binding to the target. The process was developed independently by three different laboratories.[5 7 8] Since its inception, the SELEX process has undergone numerous developments (which will be discussed later) but most can be characterised by four common steps and is summarised in Figure 1.12:

- *Generation of aptamer library*

  A random assortment of molecules with unique nucleotide sequences is created, using solid phase synthesis.

- *Selection*

  The aptamer library is passed through a matrix containing the target and incubated to allow binding to occur. The target immobilisation can be carried out in numerous ways as summarised by Stoltenburg *et al*.[39] and is discussed in more detail in Section 1.2.5). In the early rounds, only an extremely small proportion of the library have any affinity and the remaining molecules are removed.[40] Molecules which do exhibit some binding are eluted and taken into the next round.

- *Amplification*

  The polymerase chain reaction (PCR) is carried out on the eluted aptamer library molecules in order to increase the concentration of molecules which show affinity for the target. This is termed the enriched aptamer pool.

  The double stranded (ds) DNA product from the PCR must be rendered single stranded before being reintroduced into the column.

  This enriched aptamer pool is then passed again through the column containing the target. This iterative process continues with increases in the stringency of each cycle.

  Usually 10-15 cycles are needed, as this is sufficient to reduce the large library pool to a few molecules which exhibit excellent binding. Counter and negative selections are also

carried out intermittently during this time, the details of which are discussed further at the end of this section.

- *Isolation of Aptamers*

  The aptamer pool is then cloned into bacteria. This separates the mixture of DNA eluted at the end of the process into individual aptamer library molecules. This is often carried out through the use of commercial kits whereby unique DNA sequences are inserted into a vector provided in the kit. (This process is explained in depth in Section 3.3). The molecules have to then be tested for efficacy and efficiency of binding to the target. There are a variety of different ways to assess this including assay formats like Enzyme Linked Oligonucleotide Assay (ELONA) patented by NexStar[41] or Enzyme-Linked Immunosorbent Assay (ELISA),[42] surface plasmon resonance (SPR),[43] electromoblity shift assay (EMSA)[44], fluorescent labelling[45] and equilibrium dialysis.[46]

  These molecules are purified and sequenced. Their sequences are compared using alignment software and conserved regions or consensus sequences (if present) are identified.

This consensus over many aptamer library molecules forms the basis of a single aptamer which is synthesised. This is a very important stage as it represents the transition from an aptamer template molecule to an aptamer. This then becomes the molecular probe or detector. It can be linked to fluorophores,[26] [47] redox labels for electrochemical detection,[48] dye labels for colorimetric determination,[49] [50] attached to nanoparticles,[51] [52] or quantum dots[29] to create assays for diagnostic and biosensing applications.

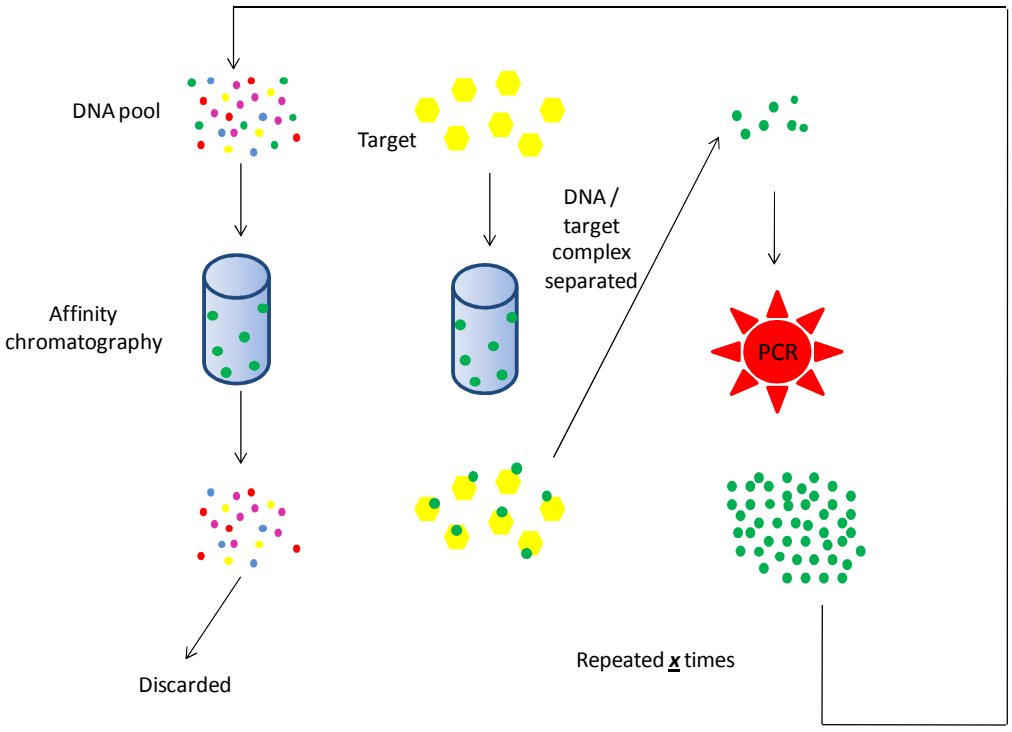

Figure 1.12: Schematic of SELEX, showing binding, elution and amplification of aptamer library molecules.

Although Figure 1.12 illustrates the SELEX cycle, there are a few steps not included. Counter SELEX is an essential step in which the DNA pool is passed through a column containing the matrix only (no target). Some molecules are retained in the column. The purpose of this step is to exclude any molecules which have an affinity for the medium from being included in further steps. Negative selection is another requirement in the SELEX process. This is usually carried out in the middle of the cycle and involves the use of a molecule with a similar chemical structure to elute any aptamer library molecules which are not selectively binding to the target.

Figure 1.12 gives only a limited overview of the generic process . The main observation applicable to all SELEX formats is that it is iterative in nature and that PCR often features. This is a revolutionary amplification technique that has radicalised the field of DNA / RNA research.

1.2.2 Polymerase chain reaction

The polymerase chain reaction allows many identical copies of DNA to be synthesised from a small amount of starting material. Kary Mullis was the prominent figure in PCR research and is cited for its invention and patent approval in 1987.[1] It has been responsible for the proliferation of research in the general molecular biology field. More specifically, PCR has featured in medicinal applications including the monitoring and diagnosis of leukaemia[53 54] in addition to genetic disorder detection of, for example, cystic fibrosis[55] and sickle cell anaemia.[56] Early PCR work coincided with the development of genetic fingerprinting[2] and the explosion of this technology has lead to the current situation where DNA fingerprinting is ubiquitously used in forensic science. The DNA from trace samples recovered from crime scenes e.g. blood and skin cells can be amplified using this reaction. Millions of copies of DNA can be produced in a few hours and so provide sufficient material for genetic fingerprinting and subsequent suspect identification.

Another important area is The Human Genome Project,[3] which involves the mapping of the complete set of human chromosomes. This was an international collaborative effort, spanning 13 years, to discover the estimated 25,000 human genes and to determine the complete sequence of the 3 billion DNA bases pairs present in the genome. This has only been made possible by the advent of this reaction.

In order to carry out PCR, there are several requirements:

- a small sample of DNA to be copied,
- DNA polymerase (a thermally stable enzyme),
- primers (short strands of ss DNA which “prime” the enzyme),
- free deoxyribose nucleotides (dNTP’s),
- PCR buffer (this ensures the correct conditions for the enzyme),
- $MgSO_4/MgCl_2$ (Mg^{2+} ions are essential).

All reagents are placed in a thermocycler (a very accurate automated heating device) and a series of temperatures are stepped through.

An example temperature programme is as follows:

- Step A @ 95 °C (10 minutes) - the hotstart
- Step B @ 95 °C (20 seconds) - the denaturing step
- Step C[#]@ 55 °C (20 seconds) - the annealing step
- Step D @ 72 °C (20 seconds) - the elongation step

These steps are repeated in a number of cycles (usually 30)

The denaturing step is where the hydrogen bonds are broken thus separating the two original DNA strands.

The annealing stage is where primers and template interact. The primers are short pieces of single stranded (ss) DNA specifically designed to flank target regions on the DNA template. Their bases are complementary to those at the beginning and end of the DNA sequence. The polymerase enzyme extends the primers in the 5'→3' direction.

The elongation step occurs with the formation of two identical molecules of DNA (each containing one strand from the original molecule). The Mg^{2+} ions produce the substrate for the polymerase to recognise by forming soluble complexes with the dNTPs. It is the DNA polymerase which catalyses the addition of free nucleotides to the template strands.

Evidently, with the repetition of the above steps, numerous copies of DNA can be produced; i.e. 2^x copies, where x = no. of cycles.

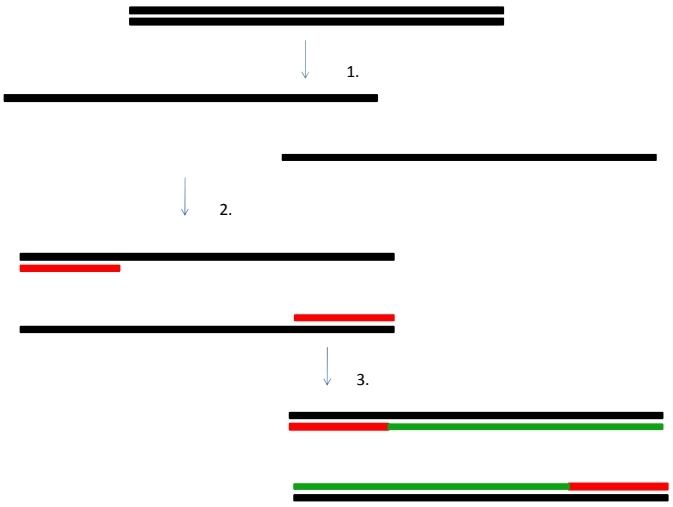

Figure 1.13: Schematic of PCR showing all the steps; 1. – denaturation, 2. – annealing, 3 – elongation.

[#] The temperature of this step can vary according to which primers are used.

Although PCR is common in most SELEX processes, it is possible to introduce variation into the selection process of aptamers. This can be done in numerous ways including chemical modification of the aptamer, selection of catalytic aptamers, the use of different target immobilisation techniques, the ability to tune binding parameters and complete automation of the process. Each of these will be considered in turn in sections 1.2.3 – 1.2.7.

1.2.3 Aptamer modifications

The interactions upon which traditional SELEX is based are non covalent, namely hydrogen bonding, hydrophobic interactions, van der Waals and electrostatic forces between aptamer and target. However, some aptamer / target interactions are very strong (binding constants in the picomolar range[15]) and so it is the accumulation of all the interactions which react synergistically to produce a strong bond between aptamer and target. Aptamers can be chemically modified to alter the binding; a property exploited in the development of photoSELEX.[57] In this work the cytosine base was modified (as illustrated in Figure 1.14) to produce 5-bromo-deoxycytidine (the photo active form).

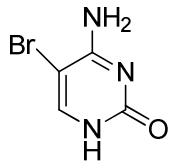

Figure 1.14: Bromine modified cytosine base.

When irradiated with UV light, the base cross-links to the protein target thus forming a strong covalent bond. This helps transform a relatively delicate, complex process into a far more robust one.

Care needs to be taken when modifying aptamers sequences. It can be done both pre and post SELEX, depending on end use. Pre modifying nucleic acids means specific attention is required to ensure they are compatible with PCR. However, post modification also poses problems. It is generally accepted that converting a full length DNA or RNA aptamer sequence into its

modified counterpart can weaken or even totally disrupt its binding. To overcome this, it is often necessary to modify specific bases which are known not to be critical in the binding of aptamer to target.[58]

The use of locked nucleic acids (LNA) has also being employed in aptamer research, and was the subject of a review by Wengel and Veedu.[59] As shown in Figure 1.15, LNA is a conformationally restricted molecule owing to the presence of a methylene bridge on the sugar, which prevents degradation occurring (as detailed in Scheme 1.1).

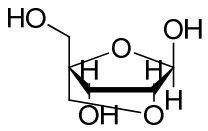

Figure 1.15: Structure of LNA sugar molecule

They are regarded as RNA analogues but their increased stability[60 61] offers another dimension to the field of aptamer research. Nucleic acid enantiomers (also known as a Spiegelmers®, patented by NOXXON Pharma AG) also feature in the literature. The ultimate aim is to create an *L*-nucleic acid oligonuloetide aptamer as it will be nuclease resistant. In order to achieve this, *D*-DNA is used in the SELEX process and the mirror image of the target used. Consequently, only peptides, proteins and other chiral molecules are appropriate. Once isolated, the *L*-DNA sequence is synthesised and binding studies carried out on the correct enantiomer of the target. Several groups have used this approach.[62 63 64]

There are a number of other possible modifications applicable to aptamers and will be discussed in Section 1.3.2.

However, more radical modifications can be achieved through the catalytic formation of covalent bonds.

1.2.4 Catalytic aptamers

There are numerous examples of catalytic aptamers. [65] [66] [67] The majority are composed of RNA and are sometimes called aptazymes. This term is derived from ribozymes which are naturally occurring RNA molecules which catalyse reactions involving phosphodiester bonds. However, the term aptazyme denotes all catalytic RNA aptamers which are involved in a variety of reactions. Examples of catalytic bond formation include C-C,[68] C-N,[69] and C-S.[70] They have proved a useful addition to the field of organic chemistry. One such reaction is the Diels – Alder reaction as an RNA aptamer has been isolated.[71] Many more organic reactions may benefit from the inclusion of aptamers in order to reduce temperature requirements, reduce reactions times or raise reaction yields.

1.2.5 Selection procedures

The SELEX process described in 1.2.1 falls into the category of affinity chromatography. The most common media used are agarose[72] sepharose[46] or magnetic beads.[73] Filter binding is an alternative technique in which nitrocellulose membrane filtration is used. This was the basis of one of the first aptamers isolated[8] and is also considered the most efficient.[74] Consequently, this is often the preferred method and is used in current aptamer research.[75] [76] [77] However, this is only applicable to peptide and protein targets. Only protein / peptides bind to the nitrocellulose so free nucleic acids pass through the filter. Any DNA / RNA remaining on the filter must be bound to the target.

Over the past 20 years a variety of analytical techniques have been developed including flow cytometry[78] and surface plasmon resonance (SPR).[79] Capillary electrophoresis has also been used and has seen improved binding kinetics as a result and offers advantages over traditional affinity column methods.[44] This separation technique has been modified through the years and has lead to the development of non – equilibrium capillary electrophoresis of the equilibrium mixture (NECEEM).

1.2.6 Non – Equilibrium Capillary Electrophoresis of the Equilibrium Mixture (NECEEM)

This technology has generated interest because of the rapid nature of the technique and the possibility of generating "smart" aptamers.[80] The term "smart" aptamers was coined by Krylov *et al*. [81] which describes aptamers that have a variety of different kinetic parameters. In this technique, the DNA aptamer library and target protein are mixed together and allowed to come to equilibrium. This equilibrium mixture is then injected into a capillary tube. A high voltage is applied and thus the different species (i.e. free DNA and protein / aptamer complexes) can be separated due to their different electrophoretic mobilities. The kinetic parameters can be tuned by selecting and amplifying aptamers from fractions eluted at time-controlled windows. It is this control of kinetic characteristics which offers a real advantage in the field of aptamer selection.

1.2.7 Automated SELEX

The last variation to the SELEX process to be discussed here is arguably the most exciting and holds the greatest potential. Automated SELEX may provide the solution to the four main limitations associated with the process. The *in vitro* selection systems detailed previously are unsuitable for high throughput applications, are time consuming, labour intensive and repetitive. Cox and Ellington conducted initial work into the development of an automated SELEX process[82] and continued their research with the development of a robotic workstation for the selection of anti-protein aptamers.[82] The work station was created and run without any direct intervention steps. There have been numerous studies into automated SELEX and in particular Chambers and co-workers developed an inexpensive alternative to the workstation based on a microfluidic chip.[83] With advances being made every year, this could lead to an explosion in aptamer research.

1.3 Applications of Aptamers

1.3.1 Introduction

Aptamer function can be classified into three general areas; therapeutics, binding study validation and drug screening and diagnostics and biosensors. All will be discussed in some detail, although it must be mentioned that the area studied in the greatest detail is use of aptamers in diagnostic applications and their use as biosensors.

1.3.2 Therapeutic aptamers

Aptamers have a number of attractive properties with respect to therapeutic applications, that is, good specificity, affinity and, most importantly for medicinal purposes, they have high selectivity. They are produced *in vitro* and thus give rise to the possibility of creating aptamers against both toxic and non-immunogenic targets. An aptamer based drug has been developed by the company EyeTech Pharmaceuticals called Pegaptanib sodium, also known as Macugen. This was the first (and currently the only) aptamer approved by the Food and Drug Administration (FDA). The drug can treat age related macular degeneration (AMD) by acting as an antagonist to the growth factor responsible for the condition (vascular endothelial growth factor isoform 165 (VEGF 165). VEGF is a cytokine which causes proliferation of new blood vessels (angiogenesis).[84] The initial SELEX work was carried out by Jellink *et al*. who isolated a number of RNA ligands which bound to VEGF selectively and with affinities as low as 0.14 nM.[85] Their ultimate goal, however, was to develop a VEGF antagonist capable of therapeutic action *in vivo*. Consequently, different modifications of the RNA nucleotide were attempted. The first such modification was the amination of the sugar molecule. When compared to unmodified RNA oligonucleotides, the amino modified molecules confer a vast improvement in stability (around 1000-fold increase in the presence of human serum).[86]

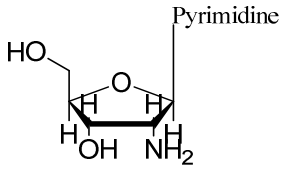

Figure 1.16: 2'-aminopyrimidine nucleoside.

Figure 1.16 illustrates the replacement of the 2' hydroxyl group with the amine moiety. This simple modification is known to confer excellent resistance to nucleases and therefore represented progress towards *in vivo* applications.[87] The next modification investigated was the presence of a 2' fluorine.

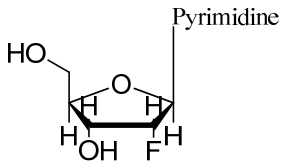

Figure 1.17: 2'-fluoropyrimidine nucleoside.

The fluorine modification yielded promising results,[88] however, the actual drug is a 28-nucleotide 2-O-methoxy modified RNA aptamer (replacement of 2' hydroxyl group with a methoxy group) with a 40 kDa polyethylene glycol (PEG) group incorporated at the 5' end. PEG is commonly used in biological studies as its neutral properties confer stability (when compared to highly charged DNA). The aptamer selectively binds to $VEGF_{165}$ and inhibits angiogenesis. The final aptamer composition was determined following an in depth study by Healy *et al*.[89] In this work, they investigated eight different RNA modifications and observed the following in vivo properties; circulatory half life, clearance rates and biodistribution to different organs (notably the kidneys). Their results suggested that the PEG moiety confers the most desirable properties and consequently it was this form that would go on to become the active pharmaceutical ingredient (API) which gained a license from the FDA in 2004.[90] Trujillo et al. published a good review summarising the development of the aptamer.[91]

As mentioned previously, Macugen is the only aptamer based drug currently on the market. This highlights the challenges with respect to developing therapeutic aptamers. Although great

strides have been made in tuning aptamer properties through manipulation of their chemical composition, it will take more time and effort before the real potential of aptamers in this field is realised. The above example illustrates the use of an aptamer selected against an extracellular target. There is, however, a drive to develop intramers that is, aptamers targeted against intracellular targets. Indeed, there are examples of such aptamers in the literature.[92] [93] [94]

Protein Kinase C is an intracellular protein for which both a DNA[44] and RNA[95] aptamer have been isolated. PKC as the name suggests, is part of the kinase family. They are enzymes that transfer phosphate groups i.e. they faciliate phosphorylation and are involved in cell signalling processes causing "cell growth, differentiation and apoptosis".[96] The ability to use an aptamer that could bind to, and have an inhibitory effect on, PKC could have great potential in, for example, the control of tumour growth. Indeed one of the isoforms of PKC (delta) has been identified as playing a key role in tumour growth.[96] This is therefore another area of research which could help realise the full potential of aptamers.

The thrombin aptamer is also another promising example. This aptamer is by far the most well studied aptamer and currently is linked to hundreds of publications. Indeed, a search of web of knowledge with the term "thrombin aptamer" produced 622 hits (12/09/10). The majority of the research is based on *in vitro* detection, however, early work did focus on clinical uses. The main area of interest is investigating heparin alternative therapies. The aptamer was first isolated by Bock *et al*.[12] and consisted of a 15 mer DNA oligonucleotide composed of thymine and guanine bases. Further work was carried out as a result of thrombin's biological significance. Consequently, an RNA aptamer[20] has been isolated in addition to another DNA aptamer.[97]

An initial study using the unmodified DNA aptamer showed good anticoagulant properties in monkeys.[98] However, the disadvantage with this aptamer was the short *in vivo* half life of approximately 2 minutes. A few studies indicated the aptamer had some therapeutic properties however, as is common to this technology, nuclease degradation was an issue.[99] [100]

A combination of chemical modification and aptamer – antidote pairs, produced a suitable reagent for *in vivo* therapy.[101] The aptamer – antidote technique employs the use of

complementary oligonucleotide to the aptamer in order to better regulate the aptamer activity *in vivo*. Because the aptamer prevents blood clotting, it is essential to regulate this function as uncontrollable bleeding could be fatal. In this type of set-up, a 5' cholesterol modification was incorporated into the aptamer sequence as this was found to increase the half life of the aptamer *in vivo*.[101] As a result of its biological significance, thrombin has proved a popular target for aptamer research and has led to the compilation of a large body of research.

Another promising therapeutic aptamer is the nucleolin targeting aptamer and it is currently being investigated for cancer treatment. Nucleolin is a binding protein and is present at elevated levels in the cytoplasm and on the surface of cancer cells.[102] [103] The aptamer is a 26 mer with the following sequence:

5'-GGTGGTGGTGGTTGTGGTGGTGGTGG – 3'

It is G- rich (65%) and is known by the code AS1411. It was developed by Aptamera (Louisville, USA) and was formerly known as ARGO100.[104] This is the most advanced anti cancer aptamers currently in the literature, indeed, the compound is in phase II clinical trials (Antisoma, UK) and has shown promising results in the treatment of two cancers; renal cell carcinoma and acute myeloid leukaemia. It should be noted that the aptamer was not generated through the SELEX process, but through the isolation of G-rich oligonucleotide (GROs) sequences.[105] Such sequences have been identified as cell growth inhibitors.[106] [107]

These are only a few, selected examples which hopefully highlight the potential of aptamers as therapeutic agents. As mentioned previously, this is only one area which has been explored by aptamers. Binding validation studies is one other field currently being investigated.

1.3.3 Binding validation studies

As mentioned previously, aptamer-target interactions differ form guest- host interactions due to the fact that the aptamer is considered to be the ligand. This approach can be exploited in the drug discovery process as aptamers can mimic the activity of a small drug molecule because numerous aptamers are antagonists to the normal function of their binding targets. Potential

drug molecules could be investigated at relatively low cost by comparing drug / target interactions with known aptamer / target interactions.

In order for a protein to be inhibited directly in its native environment, the molecules used in such investigation must be "routinely obtained and applied independently of the target, act at low concentrations and with high specificity and in an intracellular context".[108] Aptamers can fulfil these requirements and as such they have the capability of identifying potential drug molecules capable of acting as protein antagonists.

One common method in such work is a competitive binding assay. The aim is to discover molecules that bind to targets upon which aptamers have already been selected for and thus assess the effectiveness of a possible drug molecule. In this type of study, small molecule libraries are searched for compounds which can compete with the aptamer for binding to the target. This set-up has been used in numerous studies and was the subject of a recent review by Mayer.[109] Three targets show the most promise; HIV-1 reverse transcriptase, cytohesin and PDGF.

Famulok and co-workers identified an inhibitor of HIV-1 reverse transciptase by screening small molecules for competitive binding against a known aptamer.[110] They used a library of 2500 small molecules and using (amongst other techniques) aptamer displacement assays they isolated an antagonist for the enzyme. Their investigation identified regions of the enzyme which have not previously been targeted in HIV therapy and so could provide an alternative route for treatment. In a similar type study, Hafner *et al*.[111] screened a library of 1000 small molecules to investigate antagonists to cytohesins. This has relevance in understanding type 2 diabetes and may help better understand insulin activity and the "molecular pathogenesis of this disease".[111] They used fluorescence polarization to assess aptamer displacement and identified the compound SecinH3 as a potential drug candidate.

The platelet – derived growth factor (PDGF) aptamer was first isolated by Green *et al*. in 1996.[112] This protein has a number of biological functions including embryonic development,[113] lung abnormalities[114] and malignant transformation in cancer cells.[115] Subsequent work by the same group used the displacement assays to assess the potential of anions as drugs. They tested 12 organic anion anti-tumor drugs and all were able to disrupt the aptamer / PDGF target.[116]

Although there are numerous examples of binding validation studies using aptamers, the area where aptamers have made a real impact is in the diagnostic and biosensor type applications.

1.3.4 Diagnostics and Biosensors

This is by far the most common field for aptamer applications. This is due to the range of molecules already targeted by aptamers, the ease of modification (e.g. radio, fluorescence and electrochemical labelling) and consequently the number of detection methods available. Although radio-labelled aptamers have been used,[117] this is not ideal and there is a general trend towards the decreasing use of radioactive materials especially in a medicinal environment. Drolet *et al*.[41] conjugated the enzyme alkaline phosphatase to VEGF aptamers and performed an ELISA type assay. Fluorophores have also been used. In one such study, fluorescein was conjugated to human neutrophil elastase (HNE) aptamers and flow cytometry was used to quantify the fluorescence.[118]

The thrombin aptamer has been used in a variety of diagnostic settings, including molecular beacon type platforms. In this technique, the binding of aptamer to target is accompanied by a conformational change which results in emission of fluorescence. Traditional molecular beacons are illustrated in Figure 1.18.

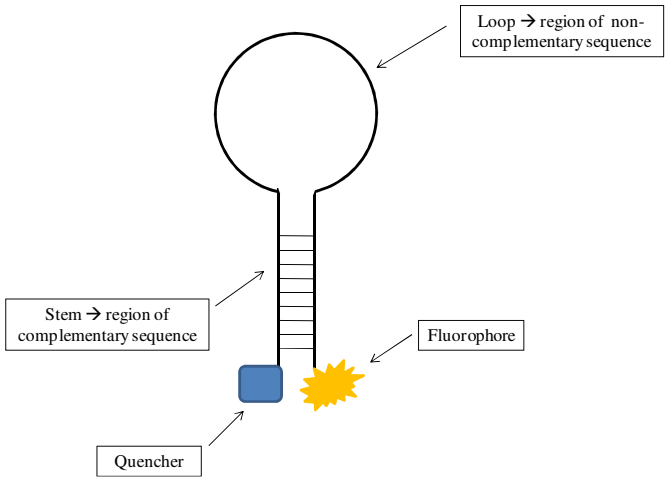

Figure 1.18: Schematic of molecular beacon. The stem region brings the fluorophore and quencher into close proximity and results in fluorescence inhibition.

In the presence of a complementary DNA sequence, the beacon "opens up" to separate the fluorophore and quencher which results in the emission of fluorescence. This is a traditional molecular beacon; however, aptamer beacons are somewhat different. They are based on the opposite logic i.e. upon binding to the target, the aptamer forms a tight, rigid structure in which the fluorophore and quencher are brought into close proximity and fluorescence emission decreases. With the thrombin aptamer, it is the formation of the G-quartet which brings the fluorophore and quencher into close proximity, as shown in Figure 1.19.

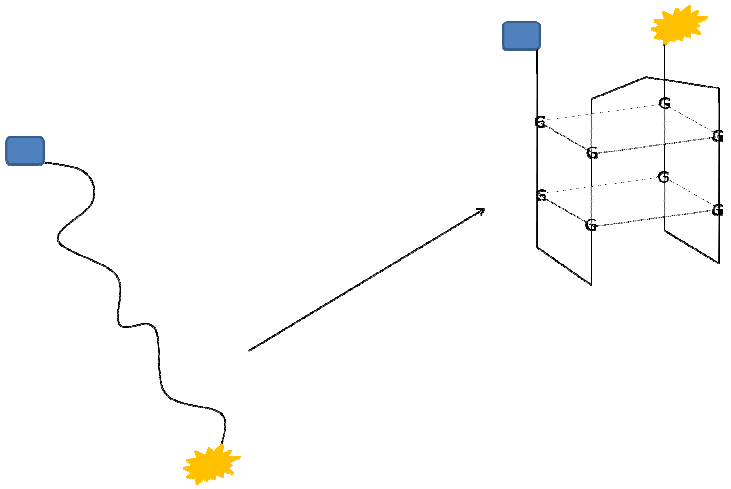

Figure 1.19: Thrombin aptamer forming the G-quartet (Blue – quencher, yellow – fluorophore).The G bases are present at the apexes of the quartets.

This format has been used in a variety of studies into the thrombin aptamer including fluorophore and quencher[47] and charge transfer incorporating electrochemical detection.[119] This concept was expanded and modified to incorporate nanoparticles,[120] an area of growing research in aptamer technology.

1.4 Nanoparticles

1.4.1 General

Although aptamer technology has been around 20 years, the combination of aptamers and nanoparticles has been a recent development.[121] Work has continued and has focused on mainly the use of gold nanoparticles.[122] [123] Often, these types of study utilise molecular recognition events between aptamer and target, thus changing the nanoparticle environment which can be monitored both visually and by UV – visible (UV – vis) spectroscopy.

In order to understand the advantages associated with using nanoparticles, it is necessary to have a basic appreciation of their fundamental properties. One of the most common forms of nanoparticles are colloidal suspensions. Although nanotechnology is often regarded as a very recent addition to the science field, examples of colloidal gold have been traced back to the "4th or 5th century BC".[124] However, major scientific investigation really began with Michael Faraday's experiments in 1857 where he reduced aqueous solution of chloroaurate to form a red solution of gold colloid.[125]

Nanoparticles can be composed of numerous materials, come in a range of different sizes and can have a variety of properties; metallic, soft, hollow shells.[126] However, they can all be generally defined as a structure whose dimensions are 100 nm or less. The surface chemistry of nanoparticles is of particular importance. Unlike bulk materials where the proportion of molecules at the surface is insignificant compared to the total number of molecules, at the nanoscale, the number of molecules is indeed significant. The nanoscale can be thought of as an intermediate phase, neither bulk level nor molecular level. It is this unique property of nanomaterials which has been (in part) responsible for the proliferation of interdisciplinary research across the fields of proteomics, nanotechnology and molecular diagnostics, as reviewed by Johnson *et al*.[127]

Metallic nanoparticles, especially gold and silver are often the preferred choice in biosensing, diagnostic and the medicinal fields due to their superior properties which are discussed in

section 1.4.2. The work detailed in this thesis will deal with gold and silver nanoparticles only and consequently the discussion will be limited to the two metals.

1.4.2 Gold and silver nanoparticles

Although both gold and silver nanoparticles have similar properties which make them ideal for numerous applications, including a colour transition between the unaggregated and aggregated state, the ability to attach bio-molecules to the surface and ease of synthesis, it is gold which dominates the literature with respect to aptamer / nanoparticle conjugates. The catalyst for this can be attributed to the pioneering work by Mirkin and co-workers.[128] They exploited the ability of bond formation between sulfur and gold in order to attach thiol-modified oligonucleotides to the surface of the nanoparticles. The ability to attach DNA to nanoparticles has generated interest with respect to aptamers. From there, work has continued and expanded with particular interest in three main targets namely, thrombin,[129 130] cocaine[131 132 133] and adenosine.[134 51 135] Silver / aptamer conjugates[136 137] do feature in the literature with the latter using a silver film as opposed to nanoparticles.

One of the main advantages of using nanoparticles is the simplicity of detection. An on / off switch can be created which exploits the colour change between aggregated (blue for gold and grey for silver) and unaggregated (red for gold and yellow for silver) nanoparticles. This aggregation is caused by attractive forces between the nanoparticles. The colour associated with metallic nanoparticles is due to the oscillations of the surface electrons (also known as surface plasmons). When light interacts with the surface plasmons, oscillation of the plasmons is induced which results in the propagation of electromagnetic radiation parallel to the metal / dieletric interface. The properties of colloidal nanoparticles are greatly affected by the changes in the dielectric medium. The production of gold colloid e.g. citrate reduction of chloroaurate $AuCl_4^-$ yields nanoparticles with a negatively charged surface. Each nanoparticle is electrostatically repelled from each other and so exists in a monodispersed suspension. If the environment is modified, i.e. the addition of salt, those forces are disturbed and aggregation can occur. This clustering of nanoparticles causes the individual surface plasmons of each to

couple together, causing a broadening and / or shift in energy of the surface plasmon resulting in a colour change. Modification of the surface of nanoparticles can allow the control and manipulation of the aggregation properties. Another important property of nanoparticles is their extinction coefficient. Silver nanoparticles have a much higher value than gold ($2.87x10^{10}$ and $2.7x10^{8}$ M^{-1} cm^{-1} respectively).[138] However, gold is often the preferred metal due to its increased stability compared with silver.[139] [140]

As already mentioned, DNA molecules can be attached to nanoparticles via modifications to the sequences e.g. thiol modifiers. Figure 1.20 illustrates a DNA conjugated gold nanoparticles.

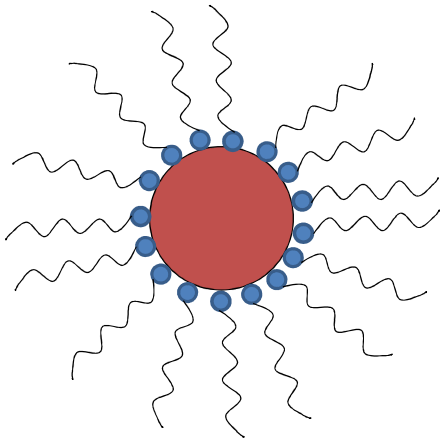

Figure 1.20: Gold nanoparticle (red centre circle) conjugated with thiol modified DNA molecules. DNA represented by the lines and the thiol modification by the blue circles.

Increasingly, more biological applications are being found as a result of the discovery that nanoparticles can pass through cell membranes into the cytosol.[141] In this study, unmodified nanoparticles were used and non-specific cellular uptake was achieved. Often, however, this general uptake by all cells is not appropriate. Instead, specific uptake (through receptor – ligand interactions) is necessary. Transferrin and folate receptors exist on the surface of the cell and this has been exploited in studies where transferrin and folic acid have been conjugated to the surface of gold nanoparticles and cell penetration accomplished through the specific receptor channels.[142] [143] Cancer cell research is another growing area of aptamer / nanoparticle technology. In 2007 Tang *et al.*[144] used cellSELEX to isolate aptamers which recognise a cancer

cell known as Burkitt's lymphoma and a subsequent study used this aptamer to develop a colorimetric assay for the detection of cancer cells.[123] The same group expanded the technology to allow for simultaneous detection of three different cancer cell types.[145]

Aptamer / nanoparticle conjugates, therefore, have the potential to make a real impact into the development of anticancer therapies.

As mentioned previously, three targets have ignited the field of aptamer / nanoparticle research; adenosine, cocaine and thrombin. The main reason these aptamers feature prominently in the literature is due to the fact that they have been well studied and their aptamer / target complex well defined and measured. The cocaine aptamer, for example, exists in a 3-way junction when bound to the target[26] as depicted in Figure 1.21.

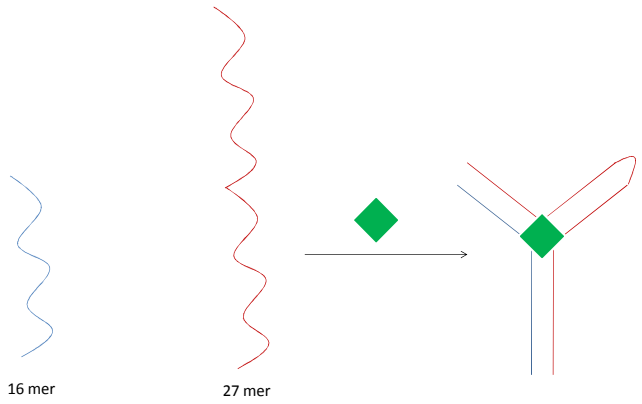

Figure 1.21: Illustration showing the formation of the cocaine aptamer; the two strands of DNA assemble into the 3-way junction only in the presence of cocaine (green diamond).

Once the DNA aptamer had been isolated, the sequence was separated into two sub units based on the predicated loop structure. Upon cocaine binding, self assembly of the DNA occurs to form the 3-way junction. When combined with nanoparticles, visual detection was used and micromolar detection limits have been achieved.[131 132] The aptamer / nanoparticles conjugates were incorporated into a microfluids set –up (dipstick). The advantage of moving away from solution based assays in the ability to detect cocaine in complex biological mixture i.e. undiluted human blood serum.[48]

The adenosine aptamer is very similar to the cocaine one, indeed a study included both

aptamers in their experiments.[131] In other work, the aptamer / nanoparticles conjugates have been attached to gold electrodes and cyclic voltametry used to detect the binding event between aptamer and target.[134] One area not mentioned thus far is vibrational spectroscopy, with examples including Raman, Surface Enhanced Raman (SERS) and Surface Enhanced Resonance Raman (SERRS) scattering. These techniques will be discussed in the next section, however, when incorporated in the adenosine work, low detection limits (10 nM) were achieved and a stable, reproducible system was created which was capable of being regenerated.[135] The structure of the aptamer / target complex is critical to such assays. Thrombin has two aptamer binding sites[146] and this has been exploited in many aptamer studies. An aptamer from two different nanoparticles can bind to the one thrombin molecule, bringing the nanoparticles into close proximity and causing aggreagation (as illustrated in Figure 1.22).

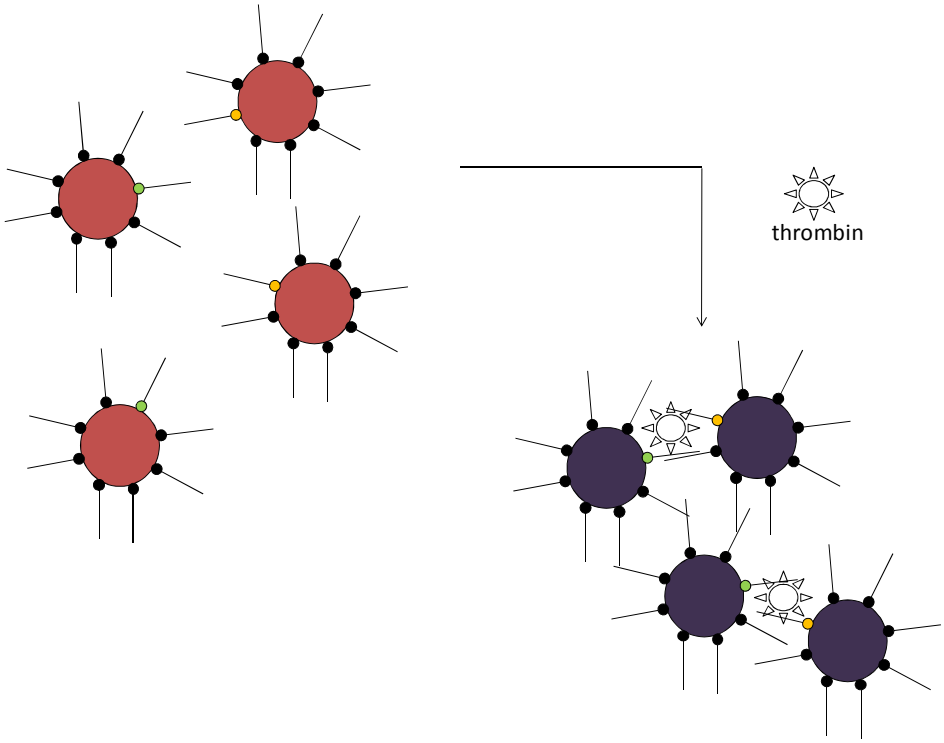

Figure 1.22: Aggregation of aptamer conjugated nanoparticles in the presence of thrombin and the resultant colour change (from un-aggregated red particles to aggregated purple particles).The yellow and green colours represent the binding between thrombin and aptamers form two different nanoparticles.

As mentioned previously, the use of nanoparticles allow the incorporation of SERS and SERRS

into the analysis. The subsequent section details the theory, background and reasons why such detection is desirable.

1.5 SE(R)RS

1.5.1 Raman scattering

Surface Enhanced Resonance Raman Scattering is a variation of Raman spectroscopy which incorporates two different enhancement phenomena namely, surface and resonance enhancements. This is necessary because Raman scattering is a very weak process and consequently not ideal for sensitive analyses. Before detailing these enhancement processes it is first necessary to gain an understanding of Raman spectroscopy, first observed by Raman and Krishnan in 1928.[147]

In this technique, the molecule of interest is interrogated with light (usually laser). The photons interact with the electrons of the molecules in one of three ways; absorption, scattering or no interaction. The scattering process causes the photons to polarise the electron cloud. The scattered photon is of approximately the same energy as the incident photon and this is termed elastic scattering (or Rayleigh scattering) and is the more common process. However, in addition to the distortion of the electron cloud, the scattering process can also induce nuclear motion. This is termed inelastic scattering (or Raman scattering) as the energy of the scattered photon differs from that of the incident photon by one vibrational unit. The polarisation of the electron cloud creates a short lived state called the virtual state and it is the transitions between the vibrational and virtual states which give rise to the characteristic Raman spectrum observed. Rayleigh scattering is the dominant process, with only 1 in 10^6 - 10^8 photons being scattered inelastically. The main disadvantage, therefore, with Raman spectroscopy is the inefficiency of scattering.

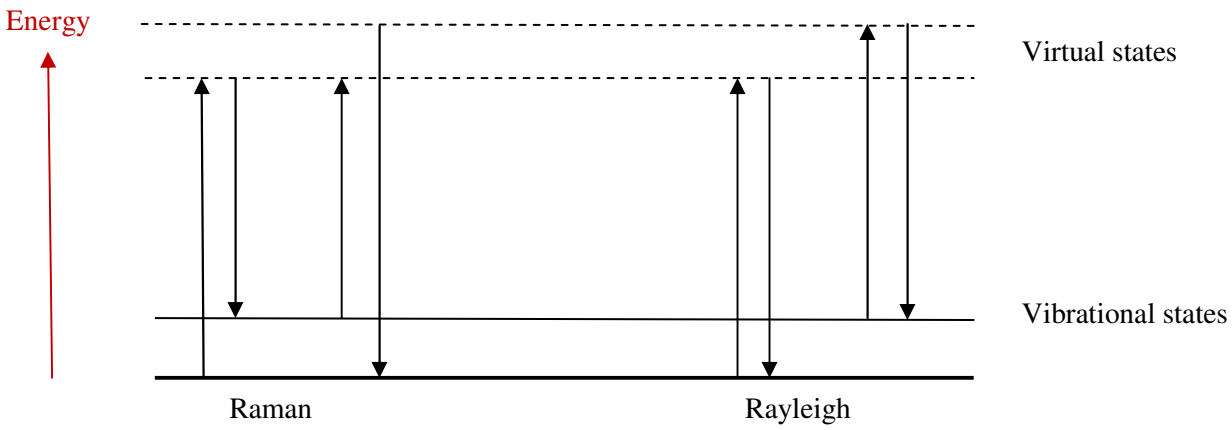

Figure 1.23: Line diagram illustrating the transitions which produce different scattering types.

The first enhancement of Raman scattering was observed by Fleischmann *et al*. in 1974.[148] In this work, pyridine was adsorbed onto a roughened silver electrode and the Raman signal was increased by a factor of 10^5 – 10^6. When attempting to explain this effect, it is necessary to discuss surface plasmons. These are waves of electrons which oscillate across the metal surface. On a flat surface, the plasmons move only in a parallel direction with respect to the surface. Scattering efficiency, however, is greatly increased if the plasmons can oscillate in a perpendicular direction and hence a rough surface can facilitate this.[149]

1.5.2 SERS

Roughened surfaces can generally be classed into two groups; engineered surfaces and colloidal suspensions. The first example of SERS was achieved using a silver electrode engineered electrochemically.[150] Other examples include lithography type techniques, [151] [152] island films and cold deposited films and are reviewed by Moskovits.[153] Although these surfaces can be engineered very reproducibly, they can be problematic to manufacture and can require sophisticated instrumentation. One way to overcome this problem is to use colloidal suspensions. This type of surface usually comes in the form of suspensions of metallic nanoparticles. These colloids can be made very easily only requiring simple reagents. However,

certain types of nanoparticles can suffer from poor reproduclibilty with batch to batch variation including different sizes, shapes and degree of dispersity (i.e. monodispersed or partially aggregated). In addition, the stability of colloidal suspensions is of critical importance and can be affected by a number of parameters, ionic strength, pH, electrolyte and composition.[154] Despite this, nanoparticles are often used and have been discussed in detail in the previous section.

1.5.3 Resonance

The second enhancement is termed Resonance Raman. This phenomenon is observed when the molecule of interest contains a chromophore. The wavelength of the incident laser light is chosen such that it coincides with an electronic transition within the molecule. In previous work, enhancements of up to 10^6 have been observed.[155]

1.5.4 SERRS

The combination of the two enhancements produces the SERRS effect[155] and has been utilised in numerous studies across a broad range of fields. Figure 1.24 summarises the SERRS effect.

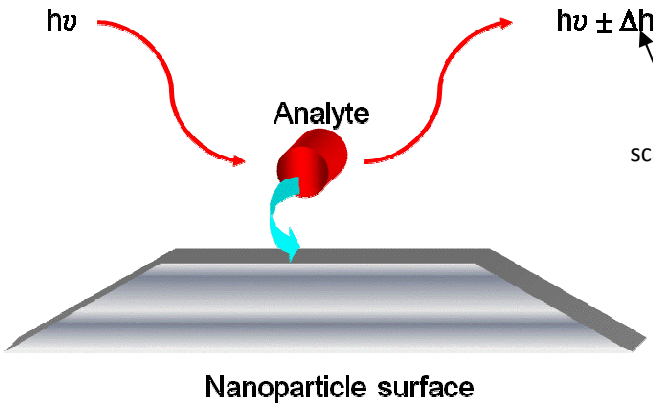

Figure 1.24: Diagram illustrating the SERRS process whereby an analyte is adsorbed onto the nanoparticle surface and the subsequent irradiation and scattering produced.

Molecular recognition is one such field where SE(R)RS has proved useful. Numerous biological interactions have been studied using the technique including DNA-DNA hybridisations, protein-protein interactions and protein-DNA interactions.[156 - 166] The work can be generally divided into homogenous and heterogeneous SERRS. The former is solution based where analytes are adsorbed onto the surface of colloidal nanoparticles whereas the latter involves interaction of a solution with a SERRS active surface. Each method has its own associated advantages and disadvantages.

1.5.5 DNA – DNA interactions

DNA – DNA interactions are often based on the attachment of a Raman reporter molecule to a complementary strand of DNA. The other strand of DNA is attached to the surface of a nanoparticle. When hybridisation occurs, the dye is brought into close proximity of the nanoparticle and enhancement takes place. This set-up has been used to detect a breast cancer gene (BRCA1).[156] In this study, Rhodamine dyes were used together with a silver surface. Similar work carried out by the same group where atomic force microscopy (AFM) was used to analyse the surface topography to indicate the binding of DNA onto the SERS substrate.[157] One of the main advantages of SER(R)S is the ability to multiplex i.e. to detect numerous analytes / dyes.[158] Raman scattering produces narrow spectral bands (as opposed to the broad spectrum produced by fluorescence). Consequently, different spectral lines can be selected and so different species identified using SER(R)S. This is demonstrated by Irudayaraj and co-workers.[159] Using four non-fluorescent Raman tags, four different DNA sequences (all common to the previously mentioned gene BRCA1) were detected simultaneously. In this work, gold-coated glass slides were used to immobilise capture strands and then hybridisation occurred using complementary DNA strand modified with the tag. The four tags used were; 4-mercaptopyridine, 2-thiazoline-2-thiol, 4,6-dimethyl-2-pyrimidinethiol and 2-thiouracil. The concept of DNA-DNA hybridisations for the development of array – type technology was exploited by Green *et al*.[160] whereby island lithography was used to attach DNA sequences to specific areas of a platform of silicon wafer. SERS was used as the detection method as no chromophore was present; indeed the focus of their work was to develop a label free array

system.

1.5.6 Protein – protein interactions

Often protein – protein interactions are based on antibody chemistry. Han *et al*. used an isothiocyanate dye to detect IgG antibody – anti human IgG interaction.[161] The reaction occurred on a glass surface and detection limits of 0.1 pg/mL were achieved. Other antibody work has been carried out by Li *et al*.[162] They use IgG antibodies and Protein A (which binds immunoglobins). They used the dye, fluorescein, and employed SERRS to detect IgG at 1 ng/mL. The work by Douglas *et al*. used SERRS to detect a protein kinase (p38) in a sandwich assay using a rhodamine dye labelled antibody.[163]

1.5.7 Protein – DNA interactions

There are some examples of DNA aptamers binding to protein in SERRS analysis and often involves the thrombin aptamer,[164] [165] however, some DNA binding proteins have been used. One example is DNA cytosine–C5 methyltransferase M.HhaI. This protein has a recognition site of GCGC and a gold nanoparticle scaffold was created using DNA hybridisation.[166]

This introduction offers an insight into potential and numerous applications of aptamer technology. There exists real scope for exciting and novel research and this thesis undertakes to detail such attempts.

2 Aims

The aim of this research centred on the use of aptamers as biosensors, with both the selection of novel aptamers, and the application of existing aptamers investigated. This PhD thesis details four key areas of research:

- To develop a SELEX program with the aim to select novel aptamer sequences capable of detecting amphetamine and methamphetamine, involving the isolation of numerous potential aptamer sequences and the subsequent testing to assess binding capability.
- To develop a SELEX program based around the reaction of a diene and dieneophile with the aim to select a sequence capable of catalysing the Diels-Alder reaction in biological conditions. The potential for catalysis will be assessed by carrying out different Diels-Alder reactions in the presence of aptamer sequence(s) identified and product formation identified using conventional analytical techniques including UV-vis spectoroscopy, High performance liquid chromatography (HPLC) and mass spectrometry (MS).
- The application of an aptamer specific for protein kinase C to create functionalised gold nanoparticles. Initial work will focus on the synthesis of such conjugates with a variety of variables investigated. Optimisation of UV-visible spectroscopy assay conditions will then be investigated with the aim of developing a system for the detection of protein kinase C.
- The application of two different thrombin aptamers to create functionalised gold and silver nanoparticle conjugates. The development of, firstly, a UV-visible spectroscopy assay to detect thrombin was investigated. Dye labelled silver conjugates were then synthesised with the ultimate aim of creating a solution phase SERRS assay based upon the interaction between the aptamer and protein.

3 Generation of a novel aptamer for the detection of amphetamine and methamphetamine

3.1 Introduction

Drug abuse is a constant issue facing society with deep and wide ranging consequences resulting in crime, serious health problems and family breakdown. Consequently, there is a need to develop, and improve upon existing detection methods in order to assist with identification of suspected controlled substances and identify individuals under the influence of such substances.

One of the aims of this research was to create an aptamer raised against the amphetamine class of drugs. It was hoped that such a development be used in parallel with antibody type amphetamine detection in current use and could complement instrumental techniques to improve drug detection. A split SELEX was carried out in an attempt to create two different aptamers capable of detecting amphetamine and methamphetamine independently, sensitively and with high specificity. As shown in Figure 3.1, their structures differ only by the presence of an additional methyl group on methamphetamine. The ability to detect these two molecules, therefore, presents quite a challenge.

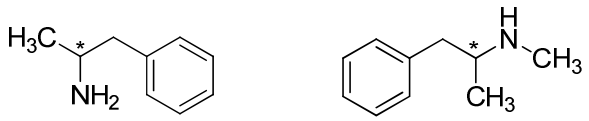

Figure 3.1: Structure of amphetamine (left) and methamphetamine (right).

The molecules possess a steroegenic centre at the positions indicated (*). The *D*-enantiomer of each molecule was studied in this project as this is the active form of the drug.

The SELEX process centred on column chromatography with epoxy activated Sepharose™ 6B resin used as the medium to immobilise the target molecule. Scheme 3.1 depicts the coupling reaction between the resin and amphetamine.

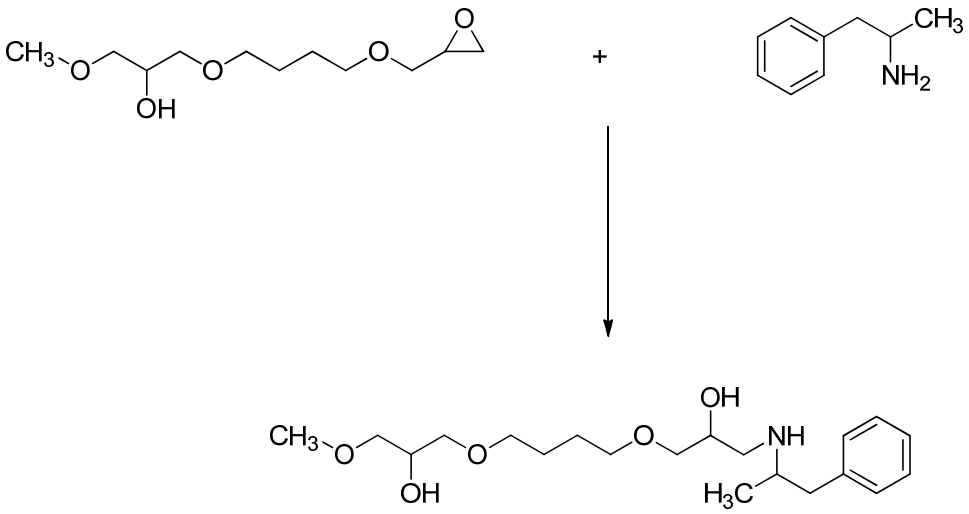

Scheme 3.1: Reaction between amphetamine and resin.

.

The SELEX process involved iterative rounds of column chromatography, with decreasing concentrations of target, the results of which are detailed in the subsequent section.

3.2 SELEX

The first part of the work detailed in this chapter focuses on the development and execution of a programme of SELEX with the aim of isolating aptamer sequences capable of detecting amphetamine and methamphetamine. The SELEX was initially carried out with amphetamine only and then diverged after completion of 11 SELEX cycles to incorporate methamphetamine (refer to Table 3.1).

3.2.1 Counter SELEX

In all rounds of SELEX, after amphetamine functionalisation, the column was blocked with ethanolamine. This ensured that there were no free epoxy sites which could result in non-specific interactions between the DNA in the aptamer pool and the resin. However, this could give rise to the selection of aptamers with an affinity for ethanolamine as opposed to amphetamine. A counter selection was carried out in order to prevent this. To counter select, the epoxy resin was first passivated by the addition of ethanolamine. The aptamer pool was then introduced into this column and any molecules that had an affinity for ethanolamine would be retained. The remaining molecules passed through the column, were collected and could then be introduced into the first amphetamine column. Counter selection was carried out at the start of the process, before cycle 1 and then again before cycle 5.

3.2.2 Negative SELEX

Negative selection was another essential process which ensured the aptamers selected were specific for the target as opposed to a structurally similar molecule. The negative selection was carried out using the molecule aniline (also known as amino benzene or phenylamine). As shown in Figure 3.2, aniline shares some structural similarity to amphetamine and so was appropriate for the negative selection.

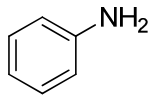

Figure 3.2: Structure of aniline.

In theory, this should remove any aptamers which had a general affinity for an amine group or benzene moiety.

All the epoxide sites on the resin (of the target column) were reacted with amphetamine or with ethanolamine. Therefore, when carrying out the negative selection, the aniline was free in

solution. This was carried out immediately prior to SELEX 8.

3.2.3 SELEX Results

The work carried out in this project is summarised in the Table 3.1. Throughout the SELEX process PCR[1] and gel electrophoresis were used ubiquitously.

Previous work within the Graham group had been carried out to optimise the PCR conditions for amplification of the aptamer library.[167] All PCR was carried out according to the following temperature program:

10 minutes	@ 94 °C	
20 seconds	@ 94 °C	
20 seconds	@ 53 °C	x 15
20 seconds	@ 72 °C	
30 seconds	@ 94 °C	
1 minute	@ 53 °C	
5 minutes	@ 72 °C	
2 hours	@ 4 °C	

Gel electrophoresis was then used to assess the PCR and purify the DNA. This is a separation technique whereby a potential difference is set up. The DNA migrates towards the positive electrode, due to the electrostatic attraction between it and the negatively charged phosphate groups on the DNA. As the agarose sets and polymerises, pores are created allowing smaller fragments of DNA to migrate further than larger fragments. When carrying out gel electrophoresis, it is essential to have a size marker reference in order to identify the size of the resulting DNA bands. In this work, a commercially available ladder, Hyperladder V, was chosen. In order to visualise the DNA, ethidium bromide was used as an intercalating agent which, under UV light, exhibits fluorescence. A typical gel is displayed in Figure 3.3:

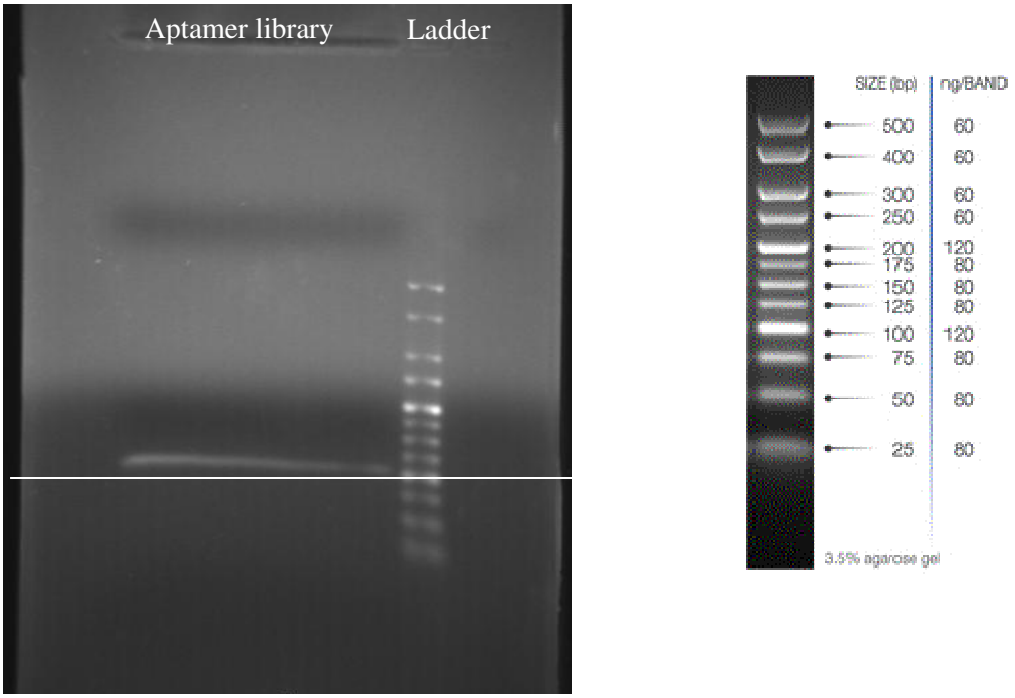

Figure 3.3: Gel image of aptamer library (left) with the 100bp size indicated (white line) and illustration of Hyperladder V showing the different size markers (right).

The gel band at 100 bp was excised and purified using a commercial kit to remove agarose and ethidium bromide. It was then rendered single stranded ready to be re-introduced into the next round of SELEX. One of the primers used in PCR was modified with a phosphate group incorporated into the 5' end. This allowed for enzymatic digestion to produce ss DNA. As shown in Figure 3.4, lambda exonuclease digests double stranded DNA in the 5' – 3' direction upon recognition of the phosphate moiety.

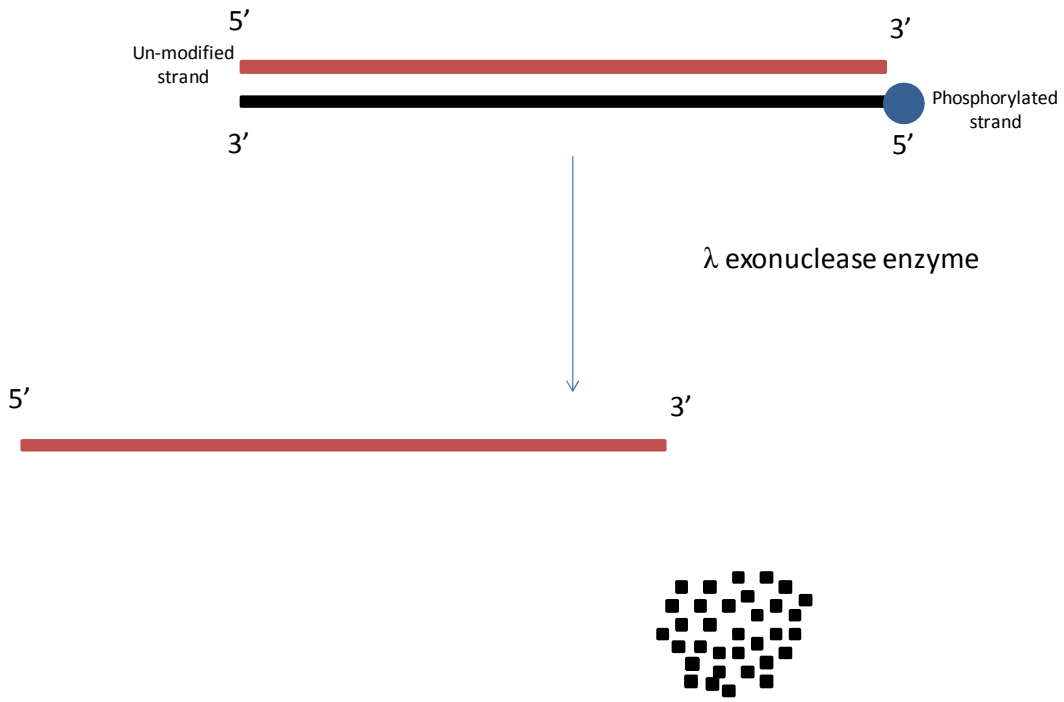

Figure 3.4: Schematic of the enzyme digestion of double stranded DNA producing mononucleotides.

Once rendered single stranded, the sample was purified using ethanol precipitation to remove the mononucleotides and the concentration of the pool determined by UV-vis absorbance measurement at 260 nm.

A repetitive process of PCR, gel electrophoresis and purification was carried out after each SELEX cycle until the aptamer library was concentrated enough to proceed to the next round of SELEX. The final steps of enzyme digestion and purification were carried out immediately prior to commencing the next round of SELEX.

Table 3.1 summarises the work carried out, including the number of PCR rounds required to achieve sufficient amplification of the aptamer library.

Table3.1: Summary of SELEX results

SELEX no.	Aptamer library concentration (μM)	Column loading (μM)	Elution concentration of target (μM)	No. of PCR
1	5.0	10	12	1
2	12.8	10	12	1
3	11.3	5	7	3
4	11.9	5	7	3
5	10.2	5	7	1
6	10.7	5	7	2
7	5.1	2.5	4	1
Negative*	7.4	2.5	10	2
8	7.3	5	7	5
9	8.2	2.5	4	1
10	8.6	1	3	3
11	10.0	1	3	3
12*	10.4	1	2.5 (meth)	2
13	15.2	2	4	2
14	9.3	5	50 (amp) 50 (meth)	2
15	6.3	5	80 (amp) 80 (meth)	3
16*	5.8	2.5	100 (amp)	2

*The negative SELEX was carried out using aniline. * indicates the three stages where cloning was carried out. The final column indicates the number of PCR required to produce the aptamer library prior to the next SELEX cycle.*

Table 3.1 summaries all the SELEX work carried out with respect to amphetamine and

methamphetamine. The results are significant in themselves in that aptamer library molecules with an affinity for amphetamine and methamphetamine were produced, recovered and selectively enriched. As can be observed, the general trend is towards a decreasing concentration of target, 10 μM gradually being stepped down to a minimum of 1 μM used in SELEX 10 – 12. This was to increase the stringency of selection conditions with a view to increasing the affinity of the aptamers towards the target.

The process was then split during SELEX 12, at which point, a methamphetamine wash was introduced. Before the bound aptamers were eluted from the column (with amphetamine) a solution of methamphetamine (2.5 μM) was used to select aptamers that preferentially bound to methamphetamine. This fraction was collected and continued through SELEX 14, 15 and 16 while the amphetamine eluted aptamers from SELEX 12 were carried through to the final amphetamine cycle, SELEX 13.

After carrying out the SELEX process, aptamer molecules had to be separated into individual sequences *via* cloning, sequenced and then analysed for consensus identification.

3.3 Cloning

3.3.1 Theory

It is necessary to clone the aptamers before they could be assessed. This allows the DNA pool to be separated into individual DNA sequences. The Perfectly Blunt® Cloning kit (Novagen) is a good example of this and was used in this project. This process can be divided into several steps which are illustrated in Figure 3.5:

- End conversion
- Ligation
- Transformation
- Colony selection
- Outgrowth
- DNA preparation

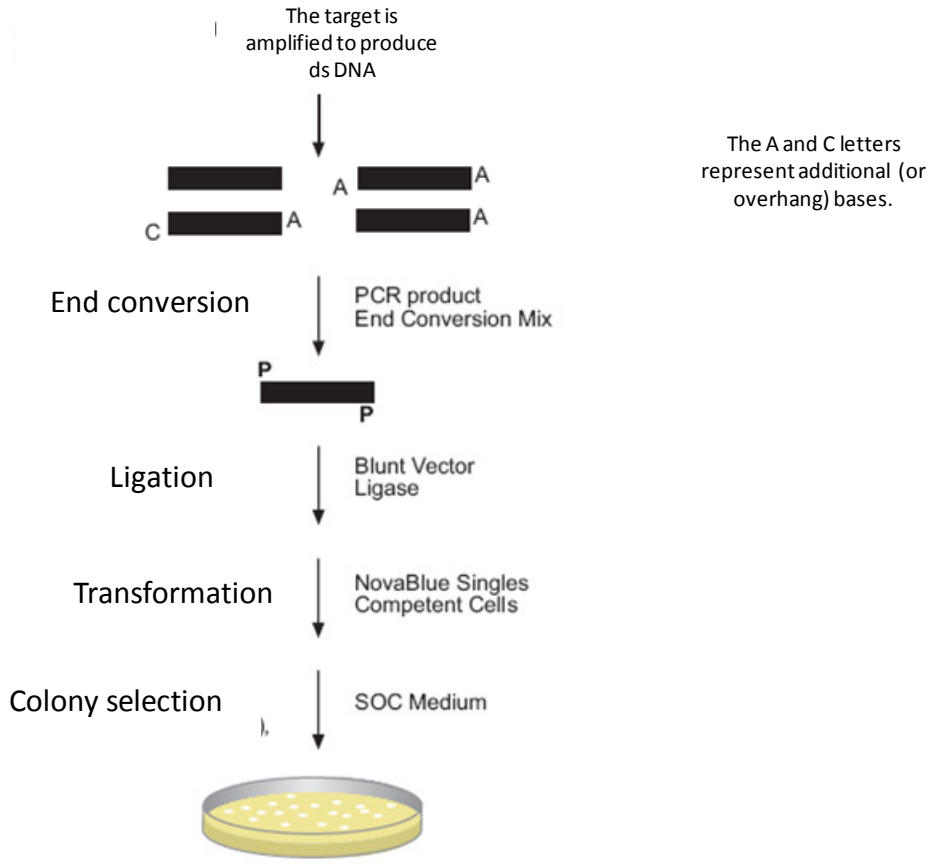

Figure 3.5: Schematic of cloning process.

The end conversion step had two main functions; the first was to add bases onto the ends of each strand to ensure they were flush and the second was to add phosphate groups to both the 3' and 5' ends (which is an essential requirement for the ligation step).

The ligation step inserts the target DNA into the vector provided. Phosphate groups on each of the strands of DNA donate into the two dephosphorylated ends of the linear vector, allowing the synthesis of a phosphodiester bond and the creation of a plasmid capable of replication. A plasmid is a term describing a circular piece of DNA and often has the following properties: a gene which confers antibiotic resistance, a galactosidase gene, an origin of replication (to allow the plasmid to make numerous copies of itself) and multiple cloning sites. The vector carried a gene that confers resistance to the antibiotic cabenicillin. The medium on which the clones were to be grown contained cabenicillin and so only those cells carrying this resistance gene, and therefore the construct, would survive.

The transformation step involved competent cells. These are cells engineered to easily uptake foreign DNA. As DNA is a very polar molecule, it is unable to pass through the bacterial cell wall. This problem is overcome by making the cells competent. The process of making cells competent involves the creation of pores in the bacterial cell wall by introducing a high concentration of Ca^{2+} ions. When heated, briefly, to 42 °C the DNA is able to pass through the pores. The plasmid DNA (containing the insert of interest) is therefore transferred into the competent cells. Transferred cells are then added to an antibiotic containing plate consisting of growth medium solidified with agar and incubated overnight at 37 °C.

Blue / white screening was used to select aptamer containing colonies. As already stated, the vector contains a galactosidase gene. The agar plates upon which the colonies are grown are first coated with two compounds, namely, isopropyl-β-D-thiogalactopyranoside (IPTG) and 5-bromo-4-chloro-3-indoyl-β-D-galactopyranoside (X-Gal), depicted in Figures 3.7. IPTG induces the transcription of the galactosidase gene present on the vector (see Figure 3.6).

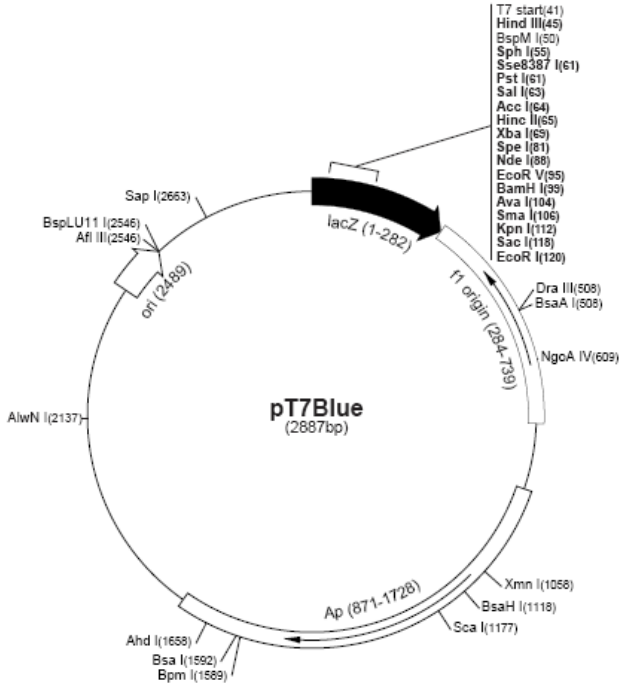

Figure 3.6: Vector map of plasmid used in the cloning process. The lacZ site indicated by the black arrow shows the location of DNA insertion and the galactosidase gene.

The resulting enzyme cleaves X-Gal to produce a blue coloured product. However, the DNA inserts are cloned into the same area of the vector where the gene is located and inhibit expression of the enzyme thus preventing the formation of the blue coloured compound. Therefore, the blue / white screening can be employed to distinguish between colonies which lack or possess the insert, respectively.

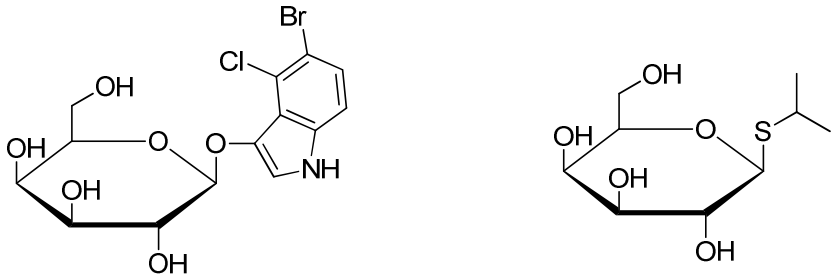

Figure 3.7: Structure of X-Gal (left) and IPTG (right). X-Gal is cleaved by β- galactosidase to produce a blue colour and IPTG induces activity of β- galactosidase.

Once the white colonies had been picked, the outgrowth step was carried out, whereby a culture was created containing millions of identical copies of the colonies from which the plasmid DNA could be extracted. In order to extract the DNA, alkaline lysis of the bacterial cell was carried out, isolating the plasmid DNA whilst leaving the bacterial genomic DNA behind. At this point the inserted DNA is ready to be extracted from the plasmid DNA via a restriction enzyme digest. This is where the plasmid DNA is cut thus releasing the 104 bp DNA insert of interest which can then be used in further work. The DNA preparation step yielded 50 µl of eluted DNA, which was then used in the final step (the restriction enzyme digest).

Two agarose gels had to be run to ensure that, firstly, the plasmid DNA had been extracted and secondly, the restriction enzyme digest had been successful i.e. a 104bp fragment had been cut from the plasmid DNA. For the plasmid DNA gel electrophoresis experiment, a 1 % (w/v) gel was run. This was because the DNA fragment of interest was 4 kbases in length and so a relatively thin gel was required to allow DNA of such length to migrate during the electrophoresis. The ladder used was λ *Hin*D III (see Figure 3.8) as this was suitable for a DNA fragment of this length.

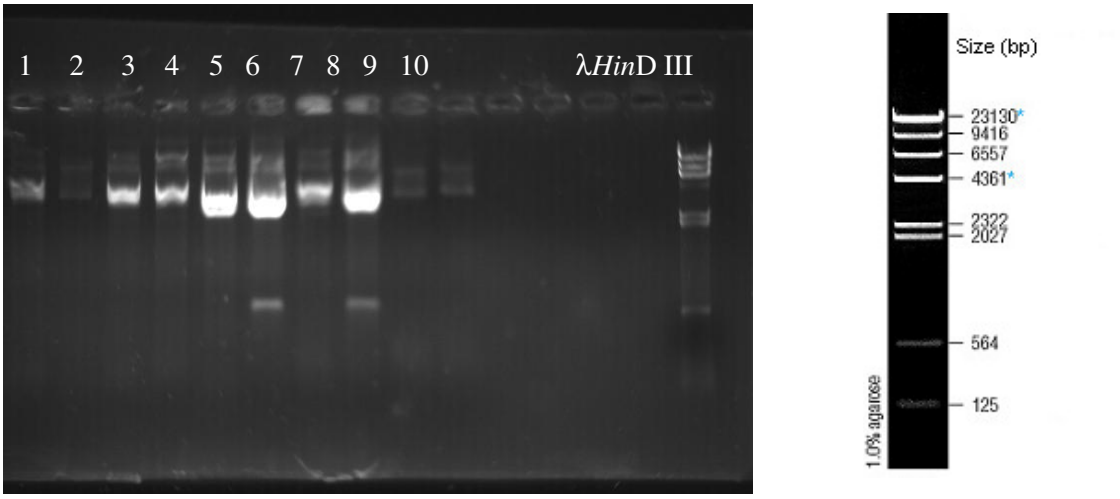

Figure 3.8: UV gel image of plasmid samples from the first set of cloning (after Negative SELEX) on the left and illustration of λ HinD III ladder showing the different size markers on the right.

To investigate whether the digest was successful, a 2.5% gel was run together with HyperLadderV, similar to the gel shown in Figure 3.9.

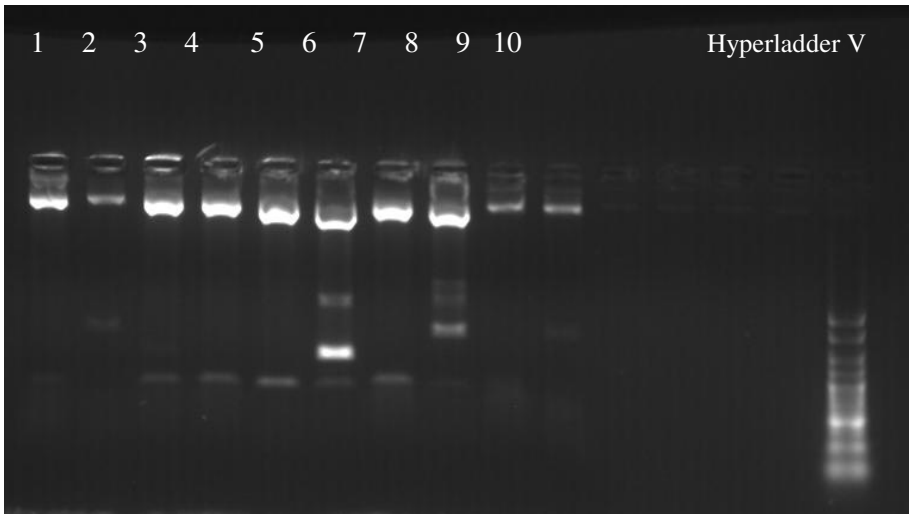

Figure 3.9 Typical UV image of gel electrophoresis of plasmid samples subjected to a restriction enzyme digest (100 bp indicated by white line).

The bands present at 100 bp indicate the insert has successfully been isolated from the samples. As indicated in Table 3.1, this process was carried out three times, after negative SELEX, after SELEX 13 and after SELEX 16, with the results detailed in section 3.3.2.

3.3.2 Cloning results

All steps listed in 3.3.1 were carried out, with white colonies being picked from agar plates and subsequently prepared to yield plasmid samples and finally the 100 bp insert. Table 3.2 summarises the results obtained from the three sets of cloning carried out.

Table 3.2: Summary of cloning results for all three sets.

Cloning cycle	No. of colonies picked	No. of plasmids present	No. of inserts present
Negative	30	30	30
13	20	18	17
16	21	-	21

On each plate, there were in excess of 100 colonies, however, for convenience and ease of sample preparation not all were picked.

Once the presence of the insert had been identified, the plasmid samples were sent off for sequencing. This was carried out by Rothwell Tate at Strathclyde Institute of Pharmacy and Biomedical Sciences, Molecular Biology Facility.

3.4 Summary of all sequencing results

All three set of sequencing results were interpreted in the same way in order to identify the two primer regions and the random 60 base region. The sequence of each 60 base region is summarised in Table 3.3.

Table 3.3: Summary of sequencing results

		Sequence of 60 base random regoin
	CD.N.1	ACGACNTNNAGCAGCACAACGACAACCGGCGCGTAGGAGGACGGGGAAGGTGGGCATAA
	CD.N.3	ACGCCCNTNNAGNAGCACAACGACGACCGGCGCGTAGGAGGACGGGAANGTGGGCATAG
	CD.N.4	TTGGGACCCTTNGNAGTAACTAGACGAGTCCGGGTCGATGTTAAATACGTGCAGGTCTAA
	CD.N.5	GCCGNNNNGTTNTGAGCCACACCAACCGAAGTGACTGCAGGGAACAATCACGCTGAGGTAAAT
	CD.N.8	ACGCCCTTNCAGACAGCACAACGACGACCGGCGCGTAGGAGGACGGGGCAAGGTGGGCATA
N	CD.N.9	CTATGCCCCNNTTTNNCGGTCCTCCTACGCGCCGGTCGTCGTTGTGCTGCTGTTTGGCGT
E	CD.N.19	GAGGGATGTGCGCTTGGGAAAGTTGTCGCTCGTGTTGGGAAATAGGGAAAGGNGTGGGAAAA
G	CD.N.20	ACCCNTTGNNNGCGGTGCGGGTCGCTGTAGAGGGTGAGGGGGGACGAAGGAAGGATAGT
A	CD.N.21	ACCCCTTACAGCAGCACCACGACGACCGGCGCGTAGGAGGACGGGGAAGGTGGGCATAG
T	CD.N.22	GAACCNNTGGGAAACGGGGCTGGTCAGGCACGGTCCACGCGTCTCTGTGAGTGACATGTCA
I	CD.N.23	GGNCCTGTACTGGGCAATGAGTGCCGGAGTGCCCGGACGAAGCTGGAGGGACTGGGGGGAA
V	CD.N.24	ACGCCACCCTTCANCACAACGACGACCGGCGCGTAGGAGGACGGGGAAGGTGGGCATAG
E	CD.N.25	CCGCGCTGGTGATGCACCTGACGCGTGTATCACGTGTAGGGTGGCGTGACGCGAGACGGGG
	CD.N.26	ACGCCTNACAGCAGCACAACGACGACTGGCGCGTAGGAGGATGGGGAAGGTGGACATAG
	CD.N.27	ACCCCTTNNANCAGCACAACGACGACCGGCGCGTAGGAGGACGGGGCAAGGTGGGCATAG
	CD.N.28	GCAGCTGCACACGACTATAGGCGGGATTTGTGCAGGTGCATGGGNGTNAAGGGGGTC
	CD.N.29	GTACGGATCTGAAATGTCACGTACAGTATACGGCGGTAAACAAGGGAAATGNANGGTACG
	CD.N.30	CCCNNAAAGGTTAAGGAAAGTGTTACGTTGTGGCTGAGGGAAGGTGCGCTCTGGGGTAAA
	CD.13.4	ACCCNTAACAGCAGCACAACGACGACCGGCGCGTAGGAGGACGGGGTAAGGTGGGCATAG
	CD.13.6	CGAAGCCGTGCATGCCGACAGTGAGTGCCTAAGTGCGGTGGGCGGTGTGCAAGAAGAGGA
	CD.13.7	CAAGGGTGCAGTACTACACCCGCGGGCGTATAAGCGAACCTGACACACGCGTTAGGAGTC
S	CD.13.9	GGCTCNTTGCTCGGGGAAGTTAGGGGACACTTCGTGAAATGGCATGCTTGGGTCAATTAAA
E	CD.13.10	TCGTACACCCCTGTCCCGTGTACCAGTATCCTCGGTCGTTCCGACCCGCGCCATGAAGTG
L	CD.13.11	AAGCGAGCAAANTNGGACCCTACCGAACAACTTGTGCCCATGGGTGCTTGTGAANGGGGTTA
E	CD.13.13	AACGCANCAACTAGGACCCTACCGAACAATTTGTGCCCATGGATGCTTGCGGCTGGGTTA
X	CD.13.14	AATGCNGNATGTGAGTACAGCACTGGAATCGACATGCCATACACGTCTGTGGAATGGGAAACA
1	CD.13.15	ACGACAAACAGCAGCACAACGACAACCGGCGCGTAGGAGGACGGGGAAGGTGGGCATAA
3	CD.13.16	AATTGCGATCAGAGCAAGTGCATGAACCAATAAAGTCGTGAAGTGTTGCAATGAACGTGCGTTA
	CD.13.17	ACGTAGTAGTGCAGAGTGTGAGCACTGTACTGTAGGTCGTGCAAGGAAGCCGGGGAGGTAN
	CD.13.18	CAAGGGTGCAGTACTACANCCCGCGGGCGTATAAGCGAACCTGACACACGCGTTAGGAGTC
	CD.13.19	TTGGGACAGCGGGCAGTAACTAGACGAGTCCGGGTCGATGTTAAATANCGTGACGACAGGNGG
	CD.16.48	ATTNNNGGGNNCACGACCCAGTACACCTGCGCAACGTACCGTGACACGGTCTCATGTTGCC
	CD.16.52	TGATTGCGGGACCTGGGTCTGCTGTTGGTGACAAGTGCGTTATCAACGGCGAGTTTGGAGA
	CD.16.58	GAGGGATGTGCGCTTGGGAAAGTTGTCGCTCGTGTTGGGAAATAGGGAGATTGTGGGAAA
	CD.16.59	AAGAATAAGCCGCAATCAAAGTGCAGTACGAGATCAACCTTGGCCGTAATGCCACTCAGT
	CD.16.60	AATGCGGATCAACGCGGGCATACTCATGTGCGAATCGCAACACGTGTCGGCTGGTAAACG
S	CD.16.61	GAAACCATGGGAACGGGGCTGGTCAGGCACGGTCCACGCGTCTCTGTGAGTTGACAGTTTCA
E	CD.16.63	TTTCTCCCACCCCGAGCTAGCACCATCAGTAGCGTTGTCCTGGTGCAACTGTGTCGCATA
L	CD.16.64	TGTGGCAGTACCGGCCGCATATTGCCACATGGGCGTACCGGGAGACAGCGTGGTCTCACA
E	CD.16.67	TTGGGACAGCGGGCAGTAACTAGACGAGTCCGGGTCGATGTTAAATACGTGCAGGTCTAA
X	CD.16.71	AACGTAGCCGACCGTGCACGTACCGGGTTGGCTATACGACGAATGGGGAGGTGTTAAAAA
1	CD.16.74	ACGCTACGGACGTCACGACGCGGTAGTAACACGGTAACGCGTCGTGTGGCTGGGTAGTGA
6	CD.16.75	NNCNNACGCGNGACGATCGAGCNNNAGTCNTGCGTACCGGGAGNNNAGCGTGGTCGCACA
	CD.16.80	ANGNCAAACNNCAGCNCANCAANGNCCGGNNNGTANGAGGACGGGGGAAAGTNGGCATAGC
	CD.16.82	TGTGCAATCGGGATACGGAGTCAGTGCACAGCGTAAGGGACACGTATAAGTGGTTGGGG
	CD.16.83	AAGAATAAGCCGCAATCAAAGTGCAGTACGAGATCAACCTTGGCCGTAATGCCACTCAGT
	CD.16.84	GTAAGAATAAGCCGCAATCAAAGTGCAGTACGAGATAACCTTGGTCGTAATGCCACTCAG
	CD.16.85	TGTNNNCAGTGCAGGCCGCATATTGCCACATGGGCGTACCGGGGACAGCGTGGTCGCAC

The sequencing refers to the 60 base random region on the aptamer library molecule. (The letter N denotes that the software was unable to assign an identity to a particular base).

A total of 18 samples from negative SELEX, 13 samples from SELEX 13 and 17 samples from SELEX 16 were successfully sequenced. It was then necessary to examine the sequences in an attempt to identify patterns or areas of consensus. The first analysis was in the form of a linear comparison. This was carried out using Multialn software.[168] This is a freely available online algorithm which can compare numerous sequences simultaneously and has the capability to divide sequences into clusters / subsets. The three sets of cloning data were investigated individually and then a comparison between the different sets carried out, using the Multialin software.

3.4.1 Negative SELEX sequencing results

The 18 sequences isolated from the negative cloning stage (see Table 3.3) were input into the algorithm and the output displayed in Figure 3.10.

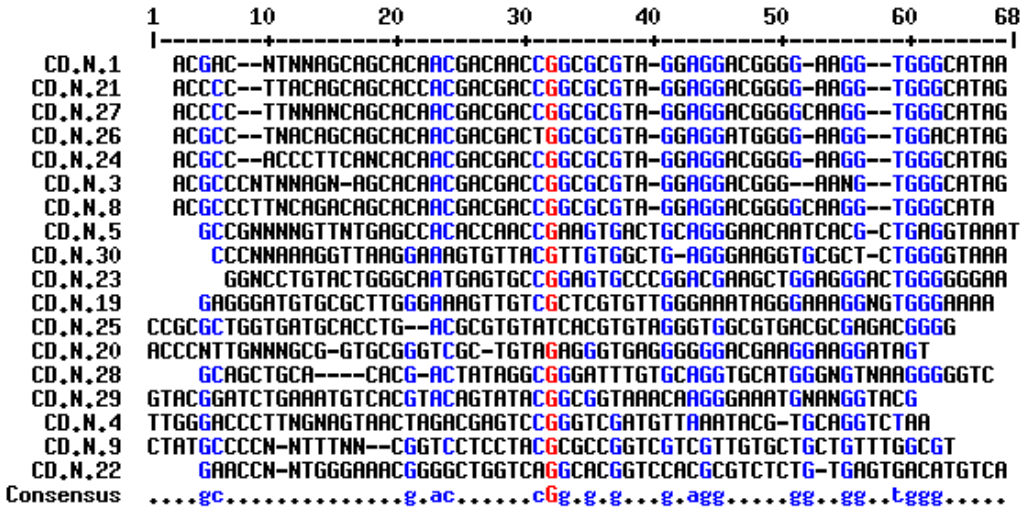

Figure 3.10: Sequence alignment for 18 aptamer library molecule.

The blue areas represent partial matches with > 50% agreement and the red areas represent full alignment i.e. >90%. The horizontal lines are gaps that have been inserted into the sequence by the algorithm. From an initial inspection it was observed that the 7 sequences at

the top of the alignment diagram were very similar and so separate alignment was carried out on those 7 only, CD 1, 3, 8, 21, 24, 26 and 27, as shown in Figure 3.11.

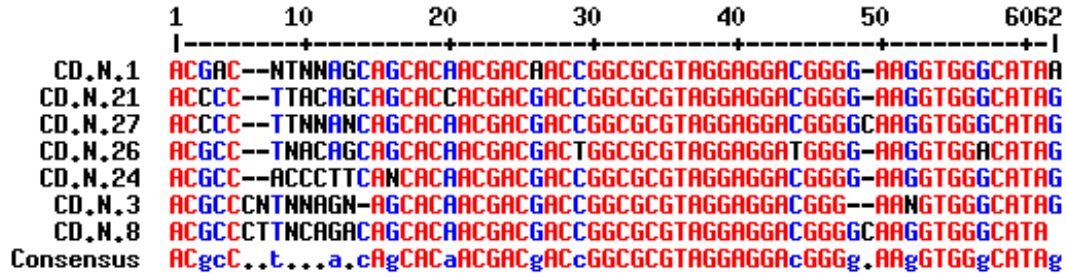

Figure 3.11: Sequence alignment for the top 7 aptamer library molecules.

As shown in Figure 3.11, there is a high degree of consensus between the 7 sequences (indicated by the presence of the red areas). This high level of consensus may lead one to conclude that the sequences are in fact identical. Upon greater scrutiny, it was noted that there were at least three differences present when each sequence was compared to the other. This provided good evidence that all 7 sequences were unique. Another technique used to assess the sequences is to determine the total of GC content. This was expressed as a percentage and varied from 60% (samples CD 1 and 26) to 67% (samples CD 8 and 27). Statistically, it would be expected that GC and AT content would each be ~ 50%. This therefore reinforces the consensus between the sequences. As already mentioned this is only a linear analysis. One should bear in mind that these molecules adopt 3-D structures and so this simplistic approach may not be the most appropriate means of analysis. It is, therefore, important not to exclude the other 11 sequences from further testing.

3.4.2 SELEX 13 sequencing results

As can be observed from Table 3.2, 20 samples were sent for sequencing. 7 sequences failed thus producing raw data for 13 samples. After data processing, sequence alignment was carried out and the result shown in Figure 3.12.

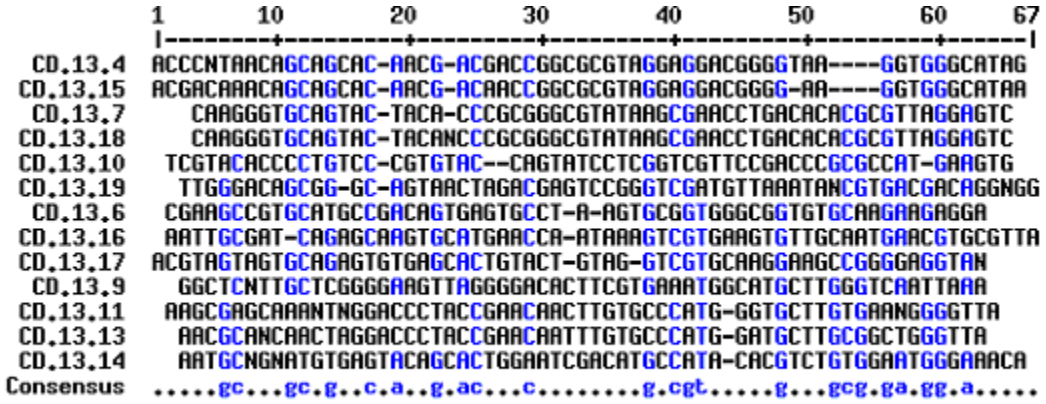

Figure 3.12: Alignment of sequence from SELEX 13.

There are sporadic areas of blue and so it was therefore necessary to try and identify groups / families of similar sequences. Upon closer inspection, there were a number of very similar pairs of sequences within the set e.g. CD.13.11 and 13, CD.13.4 and 15, CD.13.19 and 6. The alignments of these pairs are displayed in Figure 3.13.

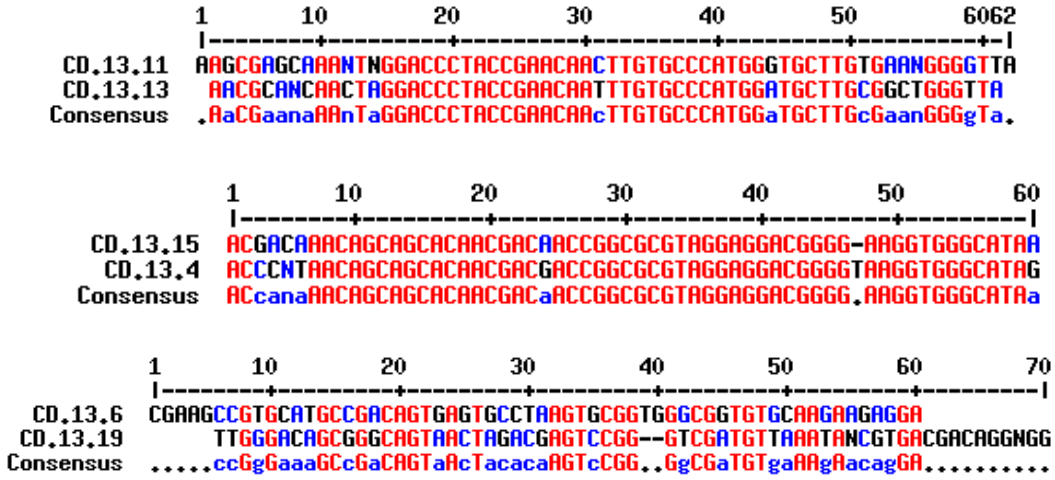

Figure 3.13: Alignment of pairs of sequences.

There is great consensus between the above set of pairs (as shown in Figure 3.13) and an aptamer sequence with a high affinity and specificity for amphetamine may well be contained within the sequences above. As can be seen from Figure 3.12, there are a number of sequences

which display no such consensus. However, it must be remembered all 13 aptamer library molecules may have the potential to display selective affinity for amphetamine. Accordingly, an aptamer for amphetamine may well be contained within any one of the sequences.

3.4.3 SELEX 16 sequencing results

As highlighted in Table 3.2, 21 samples were sent for sequencing. 4 sequences failed thus producing raw data for 17 samples. After data processing, sequence alignment was carried out and the result shown in Figure 3.14.

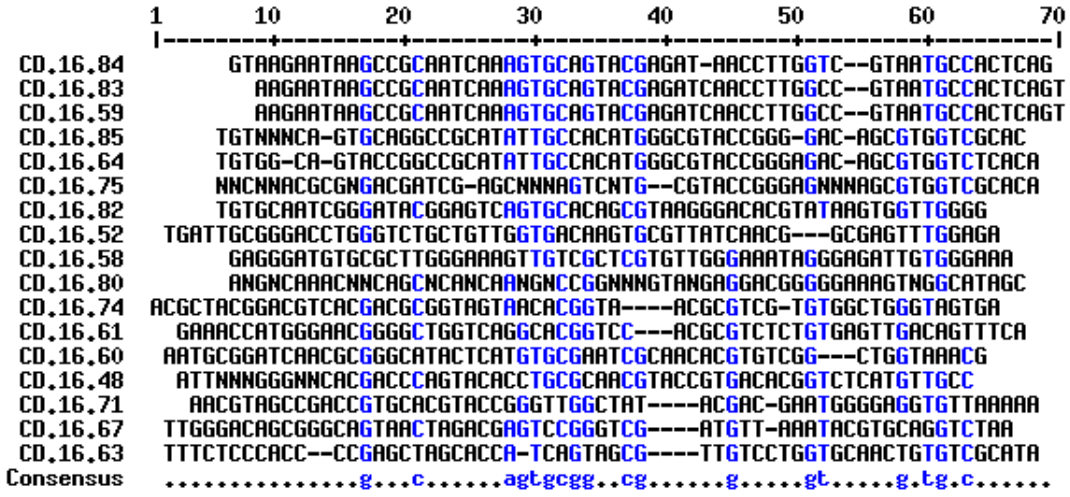

Figure 3.14: Alignment of all sequences from SELEX 16.

Although there are some blue areas, it would appear that no significant consensus exists between the sequences. Some similarities exist between individual sequences, in particular, CD.M.59,83 and 84 are almost identical (as shown in Figure 3.15).

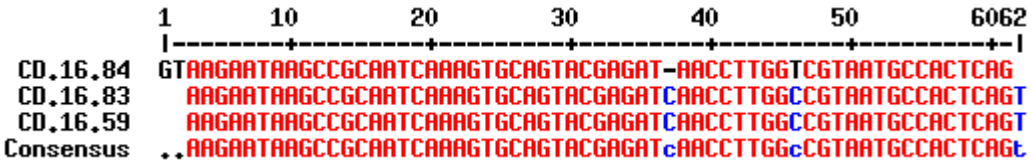

Figure 3.15: Alignment of sequences 59, 83 and 84.

All three sets of sequencing data have been compared; however, it was necessary to see if any consensus existed between the different sets.

3.4.4 Evaluation of consensus between different sets

Using the sequencing results from sections 3.4.1 – 3.4.3, different combinations of sequences from all three sets were compared, the results of which are displayed in Figure 3.16.

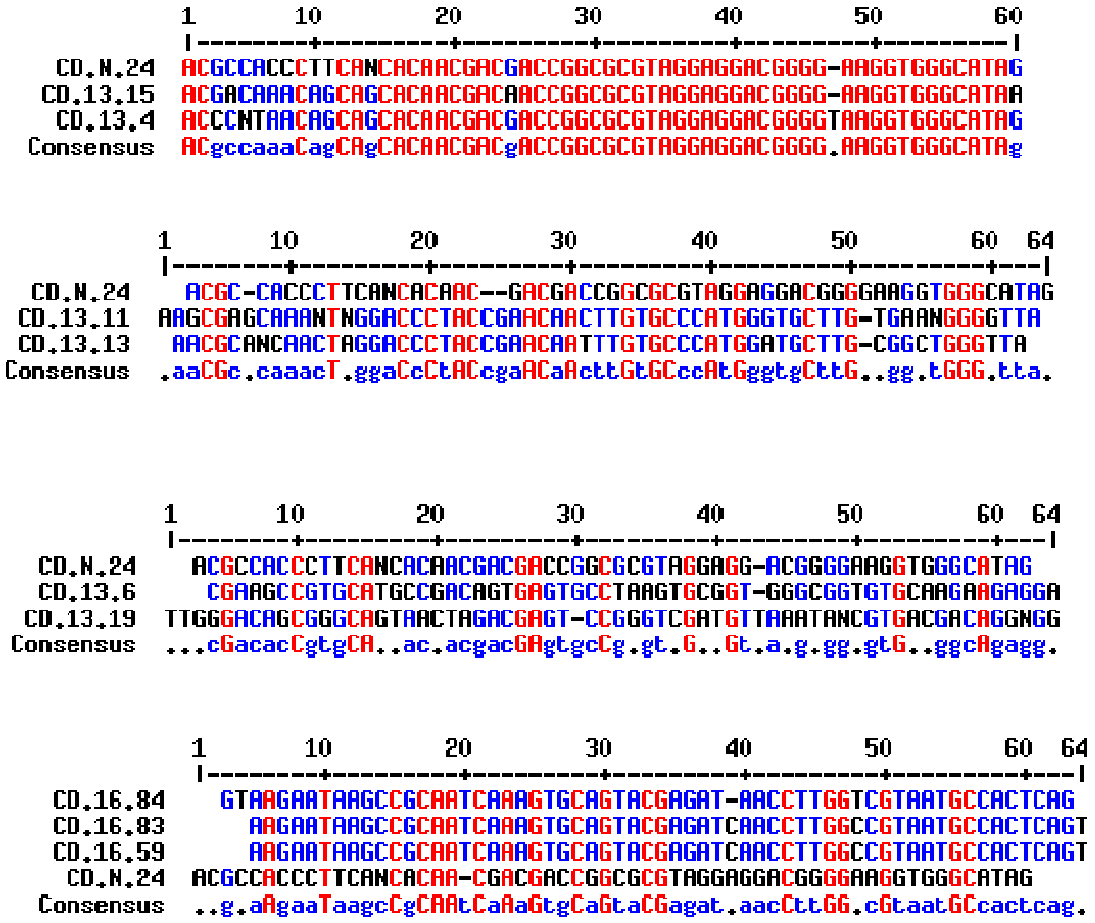

Figure 3.16: Comparison of selected sequences from all three sets of data; SELEX N, 13 and 16.

CD.N.24 originates from the Negative SELEX sequencing and is one of the top 7 sequences which displayed good consensus. This consensus is continued into the second round of cloning as sequence 11 and 13 (which are almost identical) from SELEX 13 share similarities with CD.N.24 as do sequences 6 and 19 from the same set. The final set of sequencing originated from the pool of aptamers selected against methamphetamine and in theory should have a preferential affinity for methamphetamine as opposed to amphetamine. However, the consensus from both the previous sequencing results has been carried through to the final set with samples 59, 83 and 84 (which are almost identical) showing similarities with CD.N.24. It can only be theorized at this stage as to whether each set of sequences were preferential towards amphetamine, methamphetamine or both. It was therefore necessary to assess the binding of the different sequences to the targets.

3.4.5 Mfold analysis

Before carrying out the binding investigation, further sequence analysis was attempted. Analysis of sequences using the Multialin algorithm is limited as only a linear comparison is employed. It is therefore necessary to employ a more sophisticated system to provide information on the secondary structure of the DNA sequences. The mfold webserver is a freely available online software application which can predict the folding of DNA.[169] A number of different parameters are used to predict the most stable secondary structure for a given sequence. This analysis was carried out for all 48 sequences. A selection is shown in Figures 3.17 – 3.20 and the remaining are located in the appendix.

The main conclusion drawn for the secondary structure analysis is that similar sequences do not necessarily adopt the same secondary structure. For example, sequences CD.N.1, CD.N.3 and CD.N.8 are all very similar (refer to Figure 3.11) however, they do differ in predicted secondary structure (see Figure 3.17).

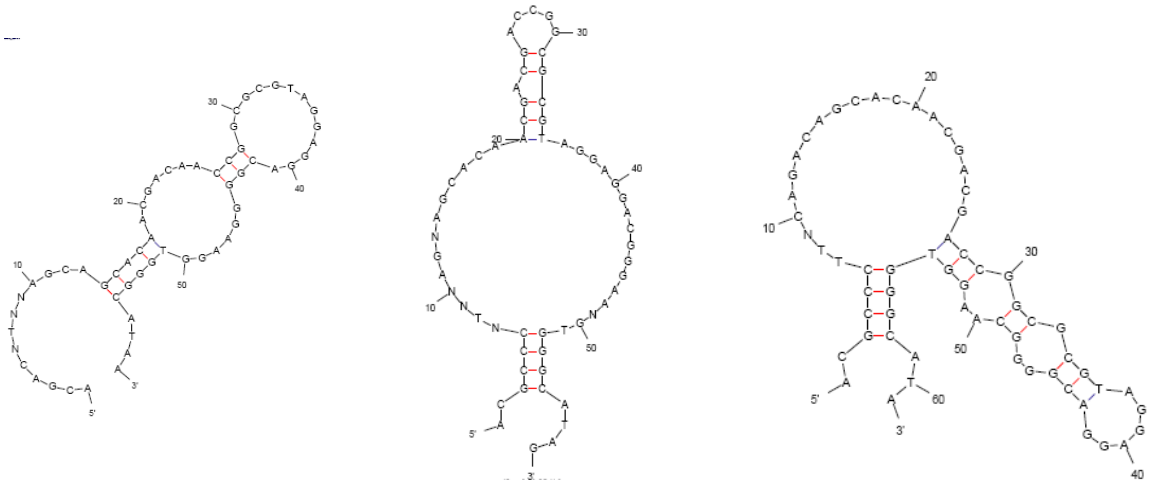

Figure 3.17: Predicted secondary structure of CD.N.1, CD.N.3 and CD.N.8 (going from left to right).

When a similar comparison was carried out using the samples CD.16.59, CD.16.83 and CD.16.84, identical secondary structures were predicted (as shown in Figure 3.18). This is hardly surprising given the fact that all three sequences were almost identical (see Figure 3.15.

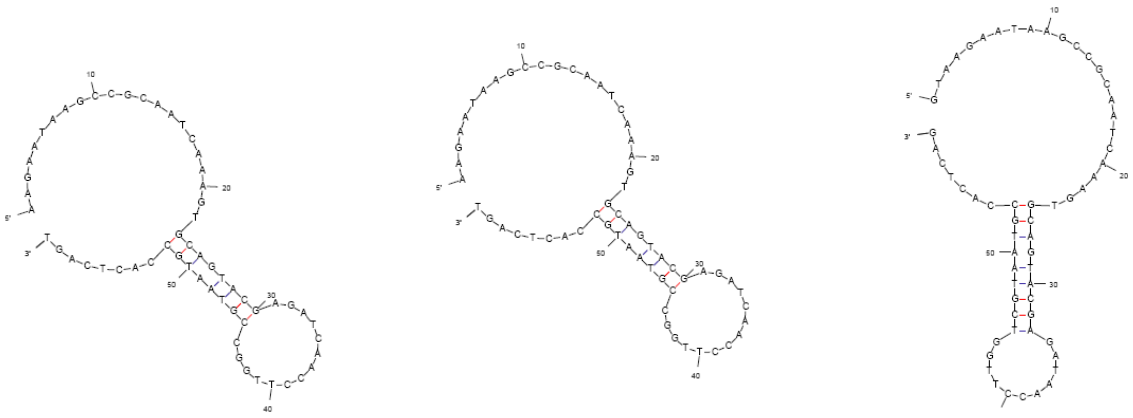

Figure 3.18: Predicted secondary structure of CD.16.59, CD.16.83 and CD.16.84 (going from left to right).

The inverse can also occur, that is, two unrelated sequences can have similar secondary structures as present in the comparison between CD.N.30 and CD.13.17, see Figures 3.19 and 3.20).

```
                1        10        20        30        40        50        60 63
                |--------+---------+---------+---------+---------+---------+--|
CD.N.30         CCCNNAAAGGTTAAG---GAAAGTGTTACGTTGTGGCTGAGGGAAGGTGCGCTCTGGGGTAAA
CD.13.17         ACGTAGTAGTGCAGAGTGTGAGCACTGTACTGTAGGTCGTGCAAGGAAGCCGGGGAGGTAN
Consensus       .aCnnAaaaGTgaAG...GaaAGcacTacacTGTaGcTcagGcAAGGaaccCgcgGaGGTAa.
```

Figure 3.19: Sequence alignment of CD.N.30 and CD.13.17

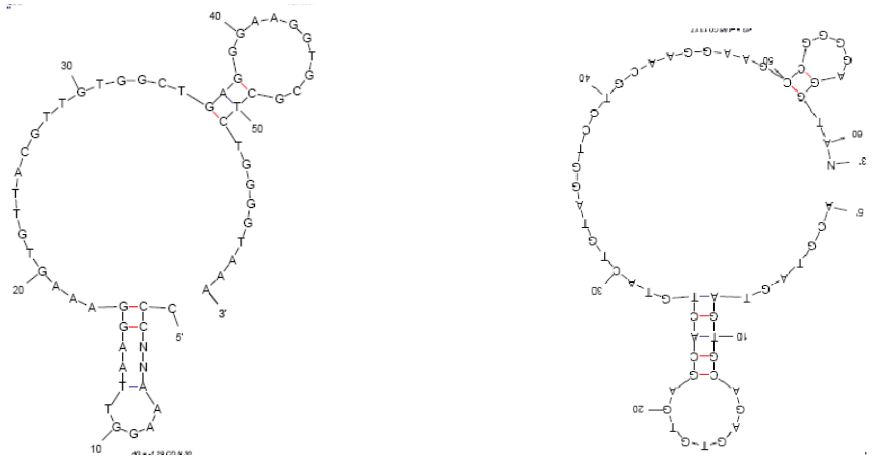

Figure 3.20: Predicted secondary structure of CD.16.59, CD.16.83 and CD.16.84 (going from left to right).

Although both the linear analysis and the secondary structure predictions did provide useful information, it was not possible to correlate a relationship between primary and secondary DNA structure to potential aptamer binding to amphetamine and methamphetamine. It was, therefore, necessary to try and prove the binding between potential aptamer sequences and the target. The rest of this chapter is dedicated to the results of efforts striving towards that goal.

3.5 Evaluation of binding

3.5.1 Enzyme Linked Immunosorbant Assay

An enzyme linked immunosorbent assay (ELISA) is an immunoassay technique, first pioneered in 1971.[170 171 172]

An immunoassay is a process involving reagents taken from the immune system and is a means of testing a sample for the presence of a known substance. These reagents (called antibodies) are often produced *in vivo* with rabbits, mice and sheep often being the animals of choice.

Before detailing this process, it is necessary to define some key terms:

- Antigen – a substance which, when introduced into an animal will stimulate the immune response to produce antibodies.
- Epitope – the specific part of the antigen that is recognized by the antibody.
- Antibody – a protein that binds to a specific antigen. This is the active component that is derived from the animal.

Although conventional ELISA techniques use antibodies, aptamers can be utilized in a similar way. There are four main variations of this technique; it can be performed indirectly or as a sandwich and can involve either the aptamer/antibody being immobilised or the antigen being immobilised (see Figure 3.21).

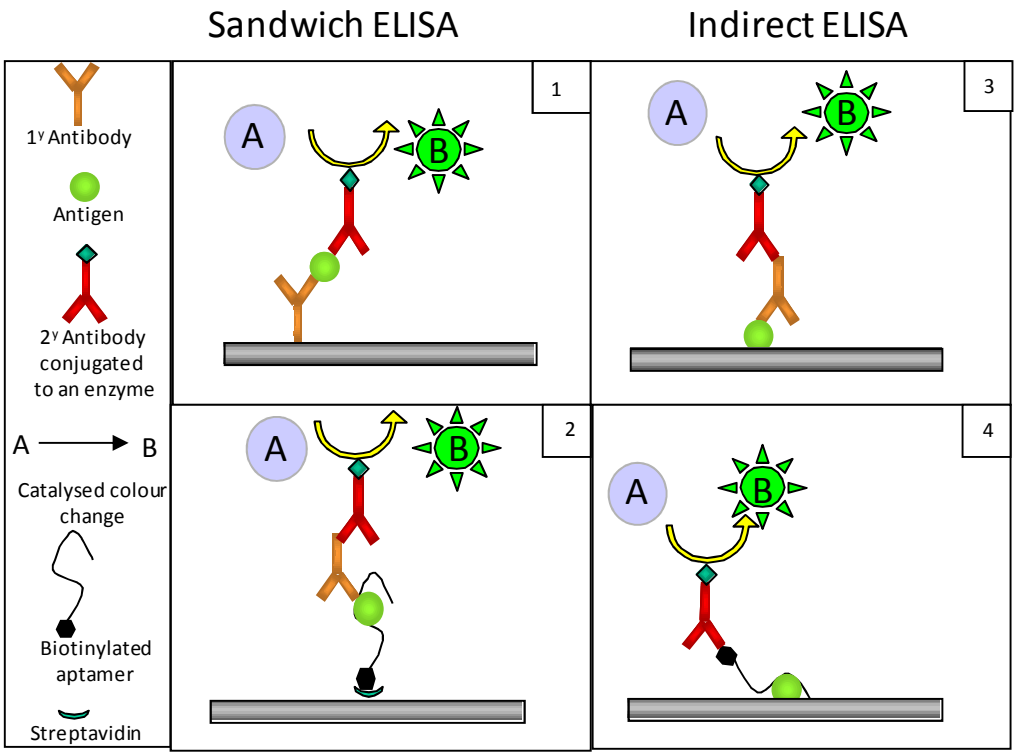

Figure 3.21: Illustration of different ELISA techniques.
In panel 1, a sandwich ELISA is being carried out using antibodies. In panel 2 an aptamer is used in place of an antibody to capture the target. In panel 3, an indirect ELISA is being performed to detect for the antibody against the target. Panel 4 illustrates an assay that can detect aptamers which interact with the target.

The main advantage of using an ELISA type technique to evaluate aptamers is the ability to screen a large pool of potential candidates and thus high affinity, selective and specific aptamers can be identified quickly. It can be used as a qualitative technique or quantitative technique through the use of standards of known concentration.

A large body of work was carried out in an attempt to create an ELISA to test the aptamers isolated from the SELEX work. The majority of experiments followed the same format as detailed below.

Amphetamine was immobilised on the surface (usually a microtitre plate coated with a particular functional group). The plate was then blocked in order to prevent un-reacted sites causing non-specific interactions. The aptamers (modified with a biotin group) were then

applied and incubated to allow binding to immobilised amphetamine. An enzyme conjugate (streptavidin alkaline phosphatase) was then added. The streptavidin binds to the biotin modification (a very strong interaction with an association constant of 10^{15} M^{-1})[173] on the aptamers and the enzyme catalysed a colour change when exposed to the substrate (added in the subsequent step). The colorimetric analysis was achieved through the catalytic colour change of BCIP / NBT from pale yellow to blue / purple.

The wells of the microtitre plate were coated with maleic anhydride which allowed surface immobilisation of the amphetamine. This was due to the formation of an amide bond, as shown in Scheme 3.2.

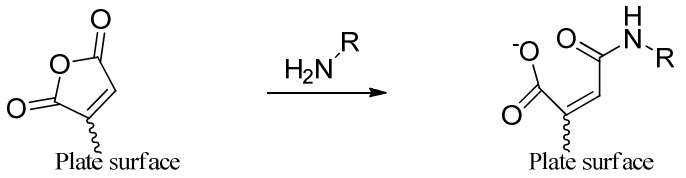

Scheme 3.2: Outline of reaction between maleic anhydride functionalised wells and a primary amine (as present in amphetamine).

The reaction between the enzyme and substrate is shown in Scheme 3.3.

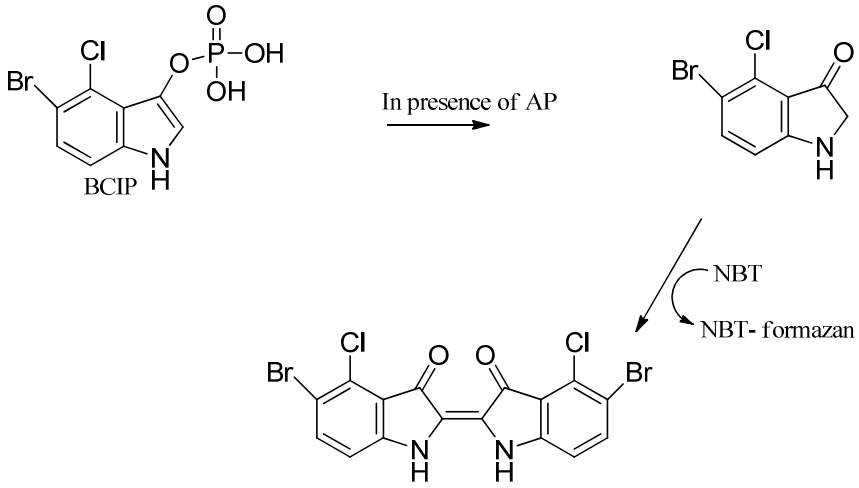

Scheme 3.3: Reaction between BCIP and NBT with alkaline phosphatase.
The enzyme cleaves the phosphate group and allows for dimerisation of the BCIP resulting in the blue / purple coloured product.

The results were interpreted by eye; observations noted and a digital photograph taken of each

plate. The formation of the precipitate meant UV-visible spectroscopic analysis would be problematic.

Due the qualitative nature of the BCIP / NBT detection system, a quantitative approach was investigated. Consequently, a different substrate was used. *p*-nitrophenyl phosphate disodium salt (pNPP) chosen as the detection method and used in place of BCIP/NBT. In the presence of AP, pNPP is catalytically converted to 4-nitrophenol (see Scheme 3.4) which is yellow in colour with a characteristic absorbance peak at 405 nm. The absorbance can be measured by absorption spectroscopy thus yielding quantitative data.

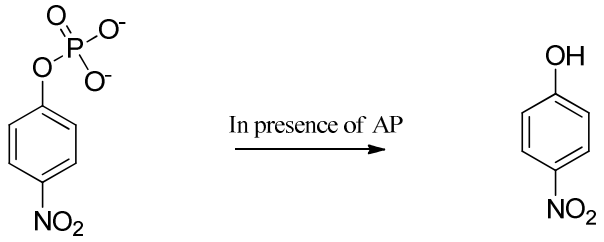

Scheme 3.4: Outline of conversion of pNPP to nitrophenol in the presence of AP.

Although a number of experiments were carried out, only one example is included below. In this experiment, a maleic anhydride surface was used and the pNPP detection system used. Figure 3.22 details the plan of the ELISA plate and lists the samples analysed.

1	***2***	***3***	***4***	***5***	***6***	***7***	***8***	
1A	19A	23A	30A	5B	10B	14B	19B	***A***
1A	19A	23A	30A	5B	10B	14B	19B	***B***
4A	20A	24A	2B	6B	11B	15B		***C***
4A	20A	24A	2B	6B	11B	15B		***D***
8A	21A	26A	3B	7B	12B	17B	Neg1	***E***
8A	21A	26A	3B	7B	12B	17B	Neg1	***F***
9A	1B	28A	4B	9B	13B	18B	Neg2	***G***
9A	17B	28A	4B	9B	13B	18B	Neg2	***H***

Figure 3.22: Summary of ELISA plate detailing the samples analysed.
(Neg 1 is the first negative sample in which no amphetamine was immobilised on the surface. Neg 2 is the second negative sample which contains no aptamer sample).

The ELISA experiment was carried out according to the protocol detailed previously. The pNPP substrate was added to the wells and the absorbance measured at 405 nm using a plate reader

after a 60 minute incubation. Photographs were also taken.

1	*2*	*3*	*4*	*5*	*6*	*7*	*8*	
0.418	0.276	0.28	0.315	0.325	0.314	0.291	0.184	***A***
0.437	0.156	0.33	0.225	0.44	0.373	0.321	0.576	***B***
0.282	0.248	0.295	0.587	0.284	0.318	0.315		***C***
0.417	0.268	0.296	0.261	0.225	0.236	0.245		***D***
0.384	0.31	0.317	0.35	0.318	0.292	0.315	0.396	***E***
0.492	0.507	0.431	0.23	0.357	0.288	0.289	0.282	***F***
0.467	0.368	0.322	0.326	1.324	0.267	0.225	2.332	***G***
0.644	0.451	0.569	0.425	0.821	0.198	0.369	1.74	***H***

Figure 3.23: Absorbance values at 405 nm for the samples in each of wells after addition of the substrate and 1 hour incubation.

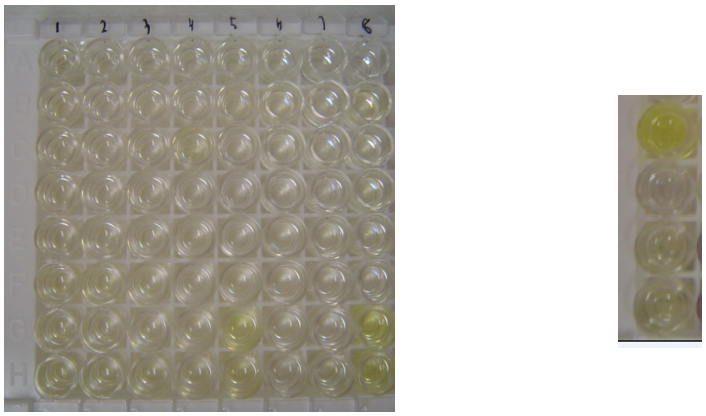

Figure 3.24after addition of the substrate and 1 hour incubation (left) and wells containing positive controls - decreasing concentration (top to bottom) of enzyme conjugate.

The most significant observation is the colour of the two negative controls. While the negative control with aptamer but no amphetamine did not produce high intensity colour change (see wells 8E and 8F), the negative control with amphetamine but no aptamer gave the strongest signals of all those analysed (see wells 8G and 8H). Of the aptamer samples analysed, wells 5G and 5H were coloured, originating from sample 9B. The work was attempted several times but reproducibility was never achieved. A recurring feature of the results was the high signals observed for the negative controls. Indeed, the majority of effort was focused on reducing the

background signal and optimising the blocking conditions.

Consequently, a number of parameters were investigated:

- Surface chemistry: maleic anhydride plates, Immulon 4BHX plates, commercial amphetamine detection kit and epoxide beads.
- Blocking buffer: BSA, ethylamine, ethanolamine, lysine, milk, commercial blocking reagent.
- Blocking conditions: room temperature / 4 °C, agitation / no agitation, Tween / no Tween.
- Detection method: BCIP/NBT, pNPP

Although a thorough investigation was undertaken, the attempts to generate an ELISA capable of assessing the aptamers proved unsuccessful. Consequently, other routes were investigated, namely, circular dichroism and surface plasmon resonance.

3.5.2 Circular dichroism

This work was carried out by Sharon Kelly, University of Glasgow

Circular dichroism (CD) is a spectroscopic technique used to study bio-molecules (and others). It uses the chirality of bio-molecules to assess their effect on plane polarised light and hence deduce conformational information. It is often used to study proteins, in particular to assign the extent of α helix and β sheet secondary structure present,[174] however it can be used to study DNA.[175]

Plane polarised light consists of two equal components; one left handed and one right handed, with circular dichroism being the differential between the two. Chiral molecules will absorb only one component and thus generate a CD spectrum. The difference in absorbance is converted to degrees and is measured as a function of wavelength.

It was theorised that changes in the conformation of the DNA aptamer in the presence of

amphetamine could be detected using CD.

The following sequence was tested using this method:

CDapt2 - ACGCCAAACAGCAGCACAACGACGACCGGCGCGTAGGAGGACGGGGAAGGTGGGCATAG

CDapt2 originated from the consensus sequence between CD.13.4 and CD.13.15. A solution of CDapt 2 (5 µM, 200 µL in 4-(2-hydroxyethyl)-1-piperazineethanesulfonic acid (HEPES buffer) was analysed, and then increasing concentrations of amphetamine added and the analysis repeated.

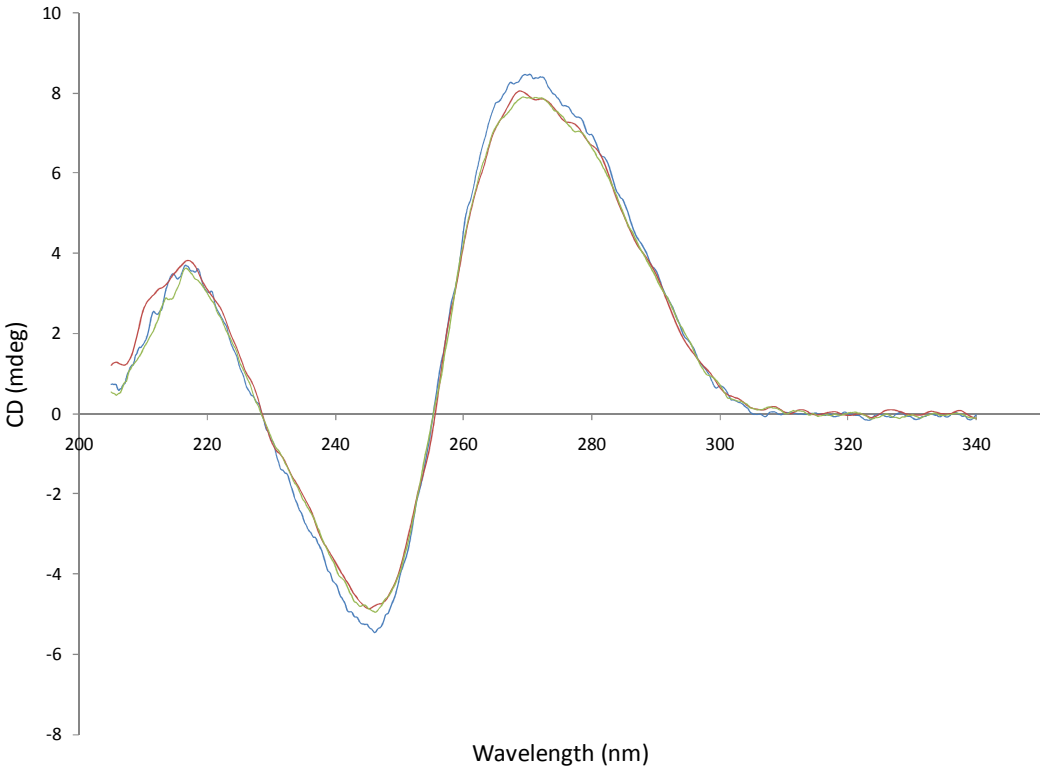

Figure 3.25: Overlaid CD spectra of CDapt2, 5 µM, 200 µL in the absence of amphetamine (blue), in the presence of 30 µM amphetamine (red) and 60 µM amphetamine (green).

As shown in Figure 3.25, no significant changes were observed. It could be that no binding occurred or that the binding of aptamer and target was not accompanied by a conformational change and thus surface plasmon resonance was attempted.

3.5.3 Surface Plasmon Resonance

This work was carried out by Dr Sharon Kelly, University of Glasgow.

Surface Plasmon resonance (SPR) is often the method of choice for biological samples due to its real time analysis capability, small volume and concentration requirements, its label free detection method and its compatibility with aqueous / biological buffers.[176] Consequently, it has been used in numerous aptamer studies.[177] [79] [178] It is based on changes in the refractive index on a layer of gold surface. This change is the result of accumulation of an analyte arising from an interaction between the analyte and a ligand immobilised on the gold surface. The change in refractive index is converted to response units (RU) and is measured against time to produce a sensogram. Analysis of the sensogram can give thermodynamic and kinetic information about the interaction; it is possible to calculate association and dissociation constants (K_A and K_D, respectively) in addition to on and off reaction rates (K_{on} and K_{off}).

The ligand is immobilised on a functionalised gold surface (using one of a number of different surface chemistries) and the analyte is flowed across the surface. In this work, a carboxymethylated dextran (CM) functionalised gold surface was used as this allowed for immobilisation of primary amines using EDC – NHS chemistry (as shown in Scheme 3.5).

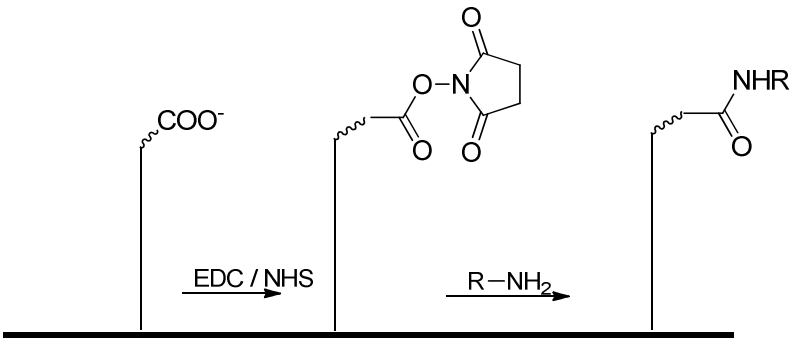

Scheme 3.5: Surface immobilisation of primary amine onto a CM chip.

In this work, amphetamine (ligand) was immobilised onto the surface on a CM chip and the following three different aptamers (analyte) flowed over the chip:

CDapt 1
ACCCCTTAGCAGCACAACGACGACCGGCGCGTAGGAGGACGGGGAAGGTGGGCATAG

CDapt 2 ACGCCAAACAGCAGCACAACGACGACCGGCGCGTAGGAGGACGGGGAAGGTGGGCATAG

CDapt 3 AAGAATAAGCCGCAATCAAAGTGCAGTACGAGATCAACCTTGGCCGTAATGCCACTCAGT

CDapt 1 originated from the consensus sequence from the top 7 sequence alignment in the negative SELEX, CDapt2 originated from the consensus sequence between CD.13.4 and CD.13.15 and CDapt3 originated from the consensus sequence between CD.16.59, CD.16.83 and CD.16.84.

Each of the four flow cells on the chip were modified differently;
Flow cell 1: control surface (ethanolamine)
Flow cell 2: amphetamine surface (low concentration, 10 μM)
Flow cell 3: amphetamine surface (high concentration, 1 mM)
Flow cell 4: unmodified surface

A number of experiments were attempted but all resulting sensograms indicated that no binding between the amphetamine and aptamer was observed.

3.6 Conclusion

A SELEX programme was carried out, with a total of 16 cycles completed involving the two drug targets, amphetamine and methamphetamine. In the first 13 cycles amphetamine columns were used and the aim was to enrich the aptamer pool towards amphetamine. Methamphetamine was then introduced as a negative selection step in SELEX 12, and the eluted aptamer pool retained for introduction into the first methamphetamine column. A total of three methamphetamine SELEX cycles were carried out. The overall aim was to generate three different pools of aptamers each with varying degrees of specificity toward amphetamine

and methamphetamine. There was potential, therefore, to generate sequences which targeted one drug over the other and / or which could detect both drugs simultaneously. Three sets of cloning were carried out and sequence analysis showed good consensus both within and between sets, however, mfold analysis revealed no obvious patterns in the secondary structure.

For the development of a single aptamer sequence, investigations were undertaken to devise an appropriate method to assess the binding of the cloned aptamer samples to amphetamine and methamphetamine. A screening method, whereby numerous samples could be analysed quickly was investigated. An ELISA based system had the capability of analysing numerous samples (and replicates of each sample through the use of 96 – well microtitre plates) and as such, this system was pursued. There were in excess of 45 cloned samples to be tested and so it would have been advantageous to reduce this number through such a screening process before continuing on with more in-depth analysis. Extensive method development into an ELISA was carried out but it was not possible to achieve a working system. It was therefore, necessary to explore other avenues. For the final stages, three sequences were chosen, one from each set of cloning and based on their sequence alignment, to proceed to circular dichroism and surface plasmon resonance analysis. The subsequent results, however, were not able to confirm an interaction between the aptamer and amphetamine. Small molecule binding assessment can be problematic due to the large size of the aptamer with respect to the drug target. The good consensus resulting from the sequence analysis does indicate the potential for identifying and aptamer for amphetamine, methamphetamine and/ or both. However, at this stage, it is necessary to conclude that no aptamer was produced.

4 The isolation of a DNA aptamer for the potential biocatalysis of the Diels - Alder reaction

4.1 Introduction

There is a constant need to develop catalysts for organic reactions. It is desirable to reduce temperature and pressure requirements in reactions, in addition to increasing product yields. Aptamers have shown catalytic ability,[65 67 66] indeed one of the first aptamers isolated was an RNA aptamer which catalysed the cleavage of DNA.[7] One of the aims of this project was to generate a DNA aptamer to catalyse the Diels-Alder reaction. This is an important organic reaction as it produces 2 carbon - carbon bonds and can generate four stereogenic centres. It is referred to as a cycloaddition reaction due to the formation of cyclic product via reaction between a diene and a dieneophile, as shown in Scheme 4.1.

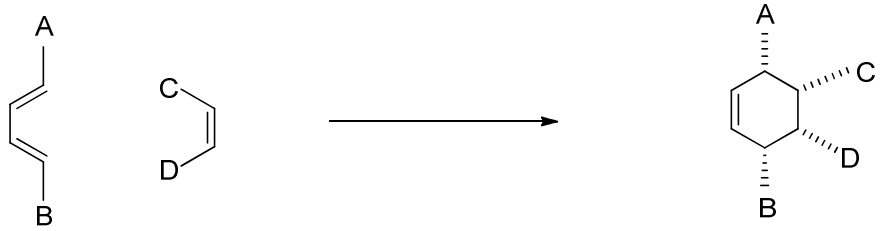

Scheme 4.1: Reaction of a diene (left) and dienophile (right) resulting in the formation of a cyclohexene (right hand side of equation).

The reaction is termed a 4π + 2π reaction as this indicates the electrons involved in the reaction (4π electrons from the diene and 2π electrons from the dieneophile).

The catalysis of the Diels-Alder reaction has been the subject of varied investigation in the literature with both an antibody[179] and an RNA aptamer[71] successfully isolated. Whilst the selection of an RNA aptamer was a significant development and overcame some of the issues

relating to antibody technology, the use of RNA in a general laboratory environment is not ideal and so the development of a DNA aptamer could prove more versatile. Additionally, the SELEX process involved the use of numerous metal co-factors, including aluminium, copper and manganese. The toxicity and associated cost of such metals is another disadvantage of this approach and could be overcome by the development of a SELEX process without the inclusion of co-factors. The efforts to develop a Diels - Alder DNA aptamer were an extension of cycloaddition work already carried out within the Graham Group.[180] The Diels - Alder reaction been used for bio-conjugation of DNA to a cell penetrating Tat peptide potential biosensor with cell penetrating properties.[181] In this work, 40 °C temperature requirements were necessary, the reaction had to be left overnight and poor reaction yields were produced when using fluorescently-labelled DNA sequences. Consequently, work was undertaken to isolate an aptamer to catalyse this reaction in aqueous buffer, without the use of co-factors and with a relatively short reaction time (under one hour). The focus of the research was the creation of a cyclohexadiene modified aptamer library and the subsequent reaction with biotin functionalised maleimide. This allowed for immobilisation onto streptavidin beads[173] and thus facilitated the separation of the cyclo-adduct from the aptamer library molecules during the SELEX process.

4.2 Generation of cyclohexadiene modified DNA aptamer library

Before commencing work on creating an aptamer to catalyse the Diels-Alder reaction, it was necessary to generate an aptamer library capable of participating in the reaction. In this work the reagents used were maleimide (dienophile) and cyclohexadiene (diene) (see Figure 4.1).

Figure 4.1: Structure of maleimide (left) and 1,3-cyclohexadiene (right).

The aptamer library was modified with cyclohexadiene at the 5'-terminus, achieved through the in-house synthesis of the reverse primer using a cyclohexadiene phosphoramidite.[181] This primer consisted of a complementary sequence to that of the primer binding region of the aptamer library. The DNA was modified with cyclohexadiene for a number of reasons. Biotin maleimide was commercially available as opposed to a biotin-modified cyclohexadiene. Also, DNA synthesis involves a deprotection step using conc. aqueous ammonia. This would hydrolyse the maleimide, thus modification of the DNA with cyclohexadiene was carried out. A custom made phosphoramidite was synthesised to prepare the cyclohexadiene modified DNA[181] (as shown in Figure 4.2).

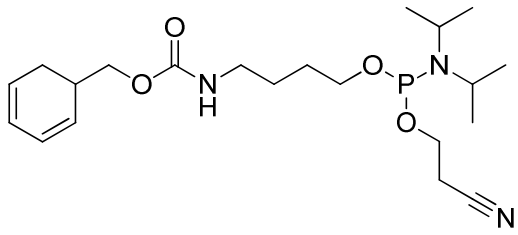

Figure 4.2: Structure of cyclohexadiene modified phosphoramidite.

PCR was carried out to produce double stranded DNA with 5' phosphate modification on one strand and a 5' cyclohexadiene modification on the complementary strand, as shown in Figure 4.3.

Figure 4.3: Illustration of PCR product showing the cyclohexadiene modified strand (top) and the biotinylated strand (bottom).

The standard procedure was carried out in order to produce the ss DNA aptamer library suitable for introduction in to the SELEX process. This involved PCR, gel electrophoresis, purification, rendering DNA ss, and finally ethanol precipitation, similar to the work carried out in Chapter 3. The only difference was the use of streptavidin beads to immobilise the target instead of epoxide resin, which is detailed in section 4.3

4.3 SELEX

The Diels-Alder SELEX process differed from that used in the amphetamine / methamphetamine work. The main contrast was the formation of a covalent bond during the Diels-Alder reaction (see Scheme 4.2). This differs from traditional SELEX, which is based on relatively weak interactions such as electrostatic, Van der Waals and hydrophobic interactions.

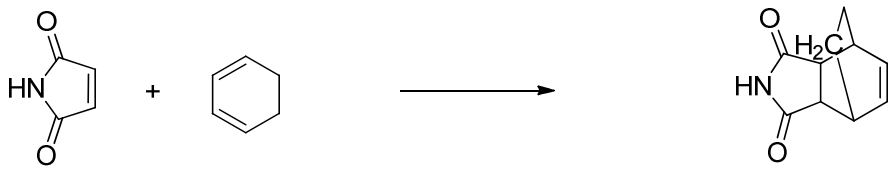

Scheme 4.2: Reaction between maleimide and 1,3-cyclohexadiene.

Scheme 4.2 illustrates a simplified version of the reaction carried out. The commercial biotin maleimide product used was a hydrazide derivative shown in Figure 4.4.

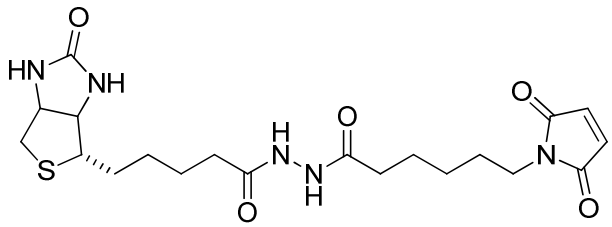

Figure 4.4: Structure of 6-(2,5-dioxo-2,5-dihydro-1H-pyrrol-1-yl)-N'-(5-((4S)-2-oxohexahydro-1H-thieno[3,4-d]imidazol-4-yl)pentanoyl)hexanehydrazide.

Table 4.1 details the work carried out and the results obtained. The counter SELEX was carried out to ensure that sequences did not bind to the host matrix i.e. the streptavidin beads. The aptamer library was incubated with unfunctionalised beads so that any sequences with affinity would be excluded from the first round of SELEX. The SELEX program was designed in order of decreasing time, that is, the aptamer library was exposed to the maleimide-functionalised beads for 2 hours and then decreased incrementally to 15 minutes. A total of 8 cycles of SELEX were carried out. The aptamer library was introduced into the streptavidin column

functionalised with maleimide and the cyclclohexadiene modified aptamer library allowed to react (in aqueous binding buffer). As with previous Diels Alder work, biotin maleimide was present in excess and reducing the reaction time was considered a more appropriate approach to increasing the stringency as opposed to decreasing concentration of target in the column (as carried out in Chapter 3). Table 4.1 summarises the SEL EX work carried out.

Table 4.1: Summary of SELEX work carried out.

SELEX no.	Incubation time (mins)	No. of PCR
Counter	10	-
1	10	1
2	5	1
3	5	2
4	5	1
5	5	2
6	2.5	2
Counter	2.5	-
7	5	2
8	2.5	2

A total of 8 cycles of SELEX were carried out in collaboration with Victoria Steven.

As shown in Table 4.1, a successful SELEX was carried out consisting of 8 cycles and 2 counter selections. In the first few rounds one PCR was sufficient to yield enough DNA to continue into the next round of SELEX, however, as the incubation time was decreased, it was necessary to carry out two PCR steps. After completion of round 8, cloning was carried out to separate the DNA pool into individual sequences in order to attempt to assess their catalytic properties.

4.4 Cloning

The cloning was carried out using the Perfectly Blunt® Cloning kit (Novagen), as detailed in section 3.3.

4.5 Sequence Analysis

4.5.1 Linear analysis

A total of 24 plasmid samples were sent for sequencing. The sequencing was carried out by the service at Dundee University. The instrument used was ABI 3730 Capillary DNA Sequencer (Appled Biosystems) using a T7 promoter. Five samples failed to be sequenced successfully. After data processing, the 60 base random region was identified for each sample and summarised in the Table 4.2.

This data was subject to sequence alignment software (Multalin)[168] in order to identify any consensus regions and the output is displayed in Figure 4.5.

Table 4.2: Summary of sequence results.

Sample name	Sequence of 60 base random regoin
CD.VS.1	GTGGGCCCTCGAGCTAACACGTGCGCGGCTGAGATAGTGTAGGTCCAATGTGGCAAGGT
CD.VS.2	GGGACCAGCAGATGTGCAGTTGCGGAGGGTGCGTTAGGTTGGTCACTAAGTTCTGAGGG
CD.VS.3	GGCGCAGGTAATGGGCACACGATAACAGTAGGTGTTGGTCGCACGGTTGTTGGGATAGGA
CD.VS.4	AGGCAAGGTACAGCGGGGGTTGCGGGTCAGGTCGTGTGTGTGTGGGGTGTCCCGTGCGGT
CD.VS.5	GCGCACAGGGGTAGCGGGTTGGATGGACGTAGCGCTGAGGTGGGACACGAGGGC
CD.VS.6	CGAGCTGGGTGGCTAATGCTCCGGTGGGGTTGCGGGGTTGTGTGGCAAGTAGATACTGG
CD.VS.7	AGGCATGCGTCGGGGTGCCCGTTTGTGCAAAGTGACATCGTACGGCCGCGTGTGTTGTT
CD.VS.8	TACCTGGTGTTGTGACAAGCATCGACGTAGTCAGCGTGGGCATCATCGGGGGGGTGGCGT
CD.VS.9	AACTACTGTAGGGCGGATCTTGTATTGGTGTTAGTAGTGCGTGGGGTGTGCCGCAGTTG
CD.VS.10	GTGACGTGCTGCCTATAGGGTTGGACGGTTATTTCCTTGCGGTGTTGTTGTTGGTGGTG
CD.VS.12	GGCGGCGTATTAGGCTACCTAGGTACGAATACATAGGTACATGGGTGGCTCGTAACATG
CD.VS.13	CCGCAGGCTCATATTATCTGCACTATGCCTGGATGCGGGTAGGATGGACGGGGGCCGAG
CD.VS.16	GTTGGGCTAGTAGGGCCAGTTCGGGTGTCGCGTATAGTCACCAGTGTCAGGCTGCGGCG
CD.VS.19	GTATCCCGGGGTCGTAGTGGTGATCGGGTGGCATTGGGAGGTCTACCACCTTGTCTACG
CD.VS.20	AAGCAACGTGCGCATTTGCCAGTGGGTGTCTCGTTGCAATGTCCCTACGGTTCAAGCAT
CD.VS.21	TGTTTGCAGTACGATACGTGCACTGTAGTTGGGGTTTGATCTCGCACCGGGCGGCTGCCT
CD.VS.22	ACGAGGGCAGTGTCGAGGTGGGTTGCGATCCTGGGCCAATTAGGTCGGTTGTTGCGCCC
CD.VS.23	CACTCACATACCCGTACGCTGGCCGGGTCAGCTCCGTCAGGCACAAAGAGCTGCGACCT
CD.VS.24	GTTGTCTGCAGGACACGGTGTCGCTCGTATGGCATCCGGTGTGTGTGTGCAGGGCGTT

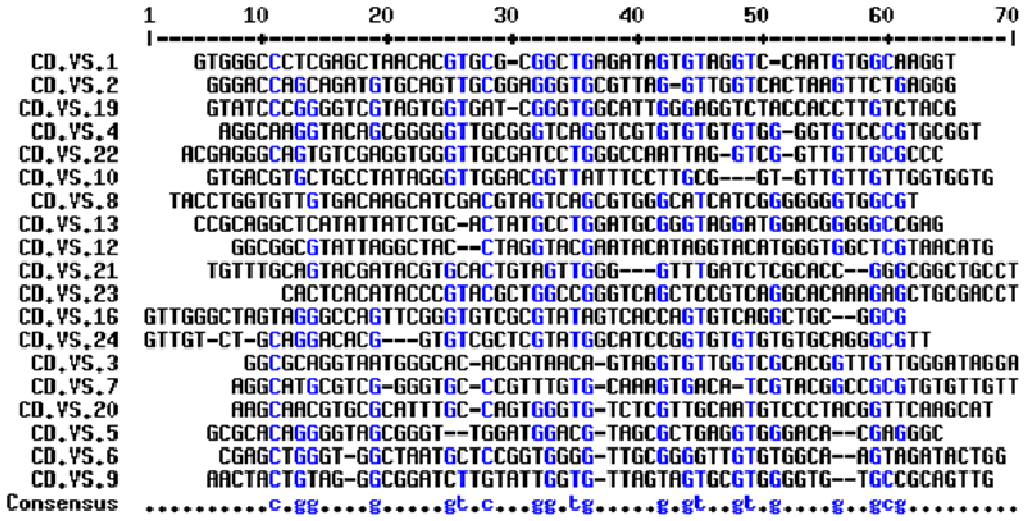

Figure 4.5: Alignment of all sequences

The blue areas represent partial matches with > 50% agreement. Although not present in the diagram above red areas represent full alignment i.e. >90%. The "N" signifies that the software was unable to assign a definite name to a base. The horizontal lines are gaps that have been inserted into the sequence by the algorithm. At a first glance, there would appear to be little consensus between the sequences. However, upon closer inspection, and with the aid of the software, a number of very similar pairs of sequences within the set were identified:

CD.VS.1 and CD.VS.2
CD.VS.4 and CD.VS.22
CD.VS.5 and CD.VS.6 and CD.VS.20
CD.VS.9 and CD.VS.10
CD.VS.16 and CD.VS.24
CD.VS.21 and CD.VS.23

The sequence alignment of all 6 sets is shown in Figure 4.6.

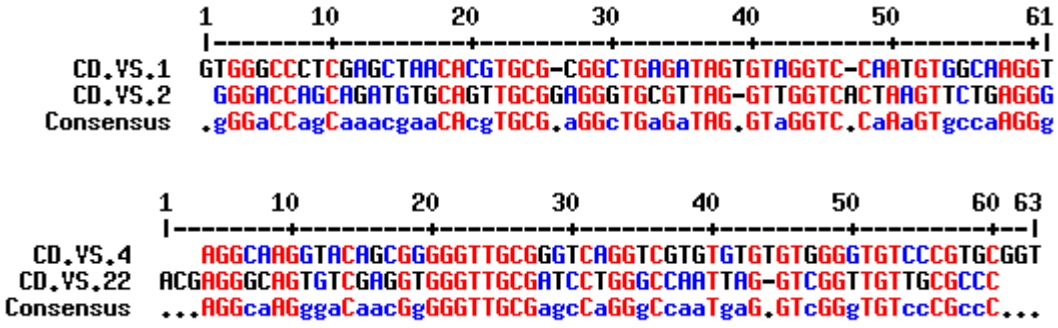

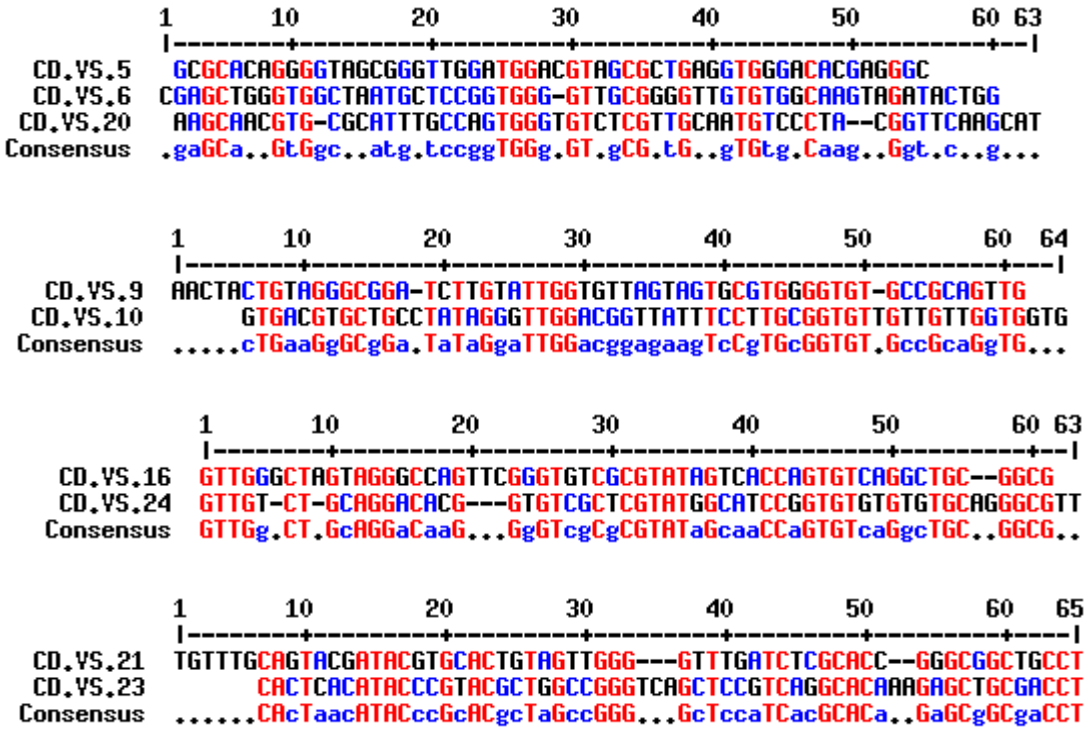

Figure 4.6: Grouping of sequences.

In all 6 sets of sequences, there is a large degree of consensus, as indicated by the blue and red areas. This is, however, only a linear analysis and so a more detailed analysis was necessary.

4.5.2 G- rich calculation

The formation of complex tertiary structures is dependent on numerous properties of DNA. G – quadruplexes are a common structural feature of DNA and often occur in G- rich sequences.[182] These are defined as sequences where the proportion of guanine residues is greater than random probability of G occurrences, > 25 %. For each sequence, the number of G residues was calculated and converted in to a percentage.

CD.VS.1	37 %	
CD.VS.2	42 %	
CD.VS.3	40 %	
CD.VS.4	50 %	*(This was ordered and used in subsequent work)

CD.VS.5	50 %
CD.VS.6	46 %
CD.VS.7	37 %
CD.VS.8	40 %
CD.VS.9	39 %
CD.VS.10	39 %
CD.VS.12	32 %
CD.VS.13	37 %
CD.VS.16	41 %
CD.VS.19	37 %
CD.VS.20	27 %
CD.VS.21	33 %
CD.VS.22	41 %
CD.VS.23	25 %
CD.VS.24	40 %

* CD.VS.4 was chosen and commercially synthesised for use in testing. Both the full 105 base and the 60 base variable region were ordered and used in subsequent work.

4.6 Catalytic investigation

Test Diels-Alder reactions were attempted in order to assess the biocatalytic potential of the isolated DNA sequences, with the work consisting of three main areas:

1. General Diels-Alder reaction carried out with biotin maleimide and cyclohexadiene in the presence of catalytic CD.VS.4 (catalytic quantity).

2. SELEX specific Diels-Alder reaction carried out with the cyclohexadiene modified primer (from 4.2) and biotin maleimide, in the presence of CD.VS.4 (catalytic quantity).

   5’ – X TCC ACG TTT TCC CAG TCA GAC GTA A – 3’

3. SELEX specific Diels Alder reaction with a different cylcohexadiene modified DNA sequence (VSDR 2 mid) and biotin maleimide, in the presence of CD.VS.4 (catalytic quantity)

5’ – CGC A***T***T CAG GAT – 3’

In each of the three approaches above, the reactions were carried out in SELEX conditions, that is, aqueous binding buffer, room temperature and reaction times ranging from 30 minutes to 1 hour. The detection methods employed varied from UV-vis spectroscopy, HPLC and mass spectrometry.

4.6.1 General Diels – Alder reaction / small molecule synthesis

For the initial work, some experiments were conducted using UV-vis spectroscopy to assess the suitability of this technique for monitoring the reaction.

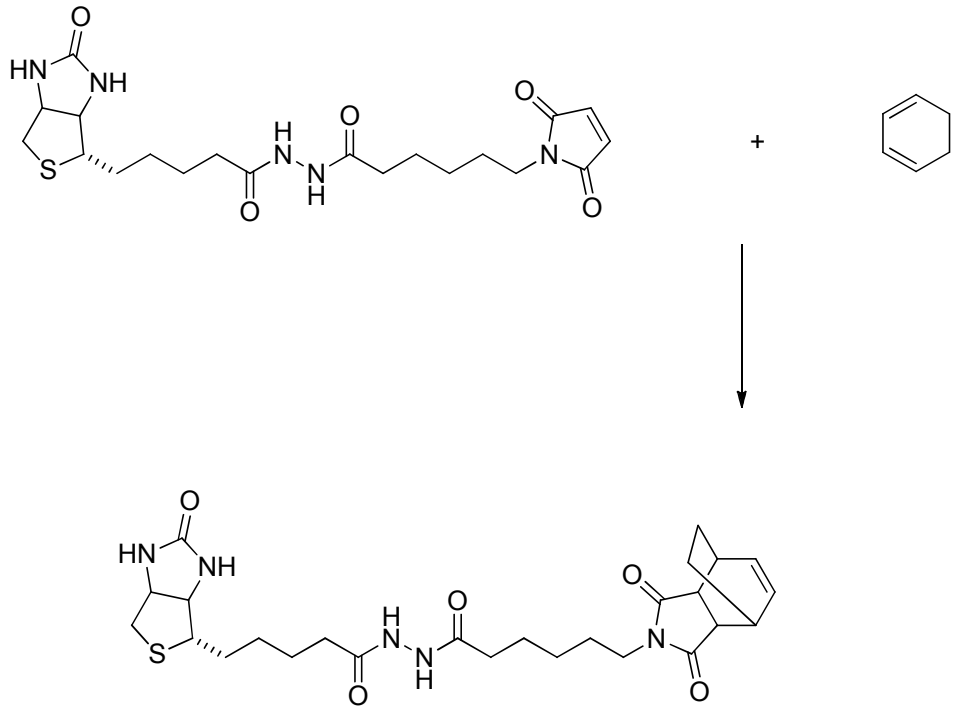

Scheme 4.3: Diels – Alder reaction between the commercial biotin maleimide product and cyclohexadiene.

Both reactants were analysed by UV-Vis spectroscopy and their traces overlaid to investigate

whether resolved peaks could be observed (see Figure 4.7).

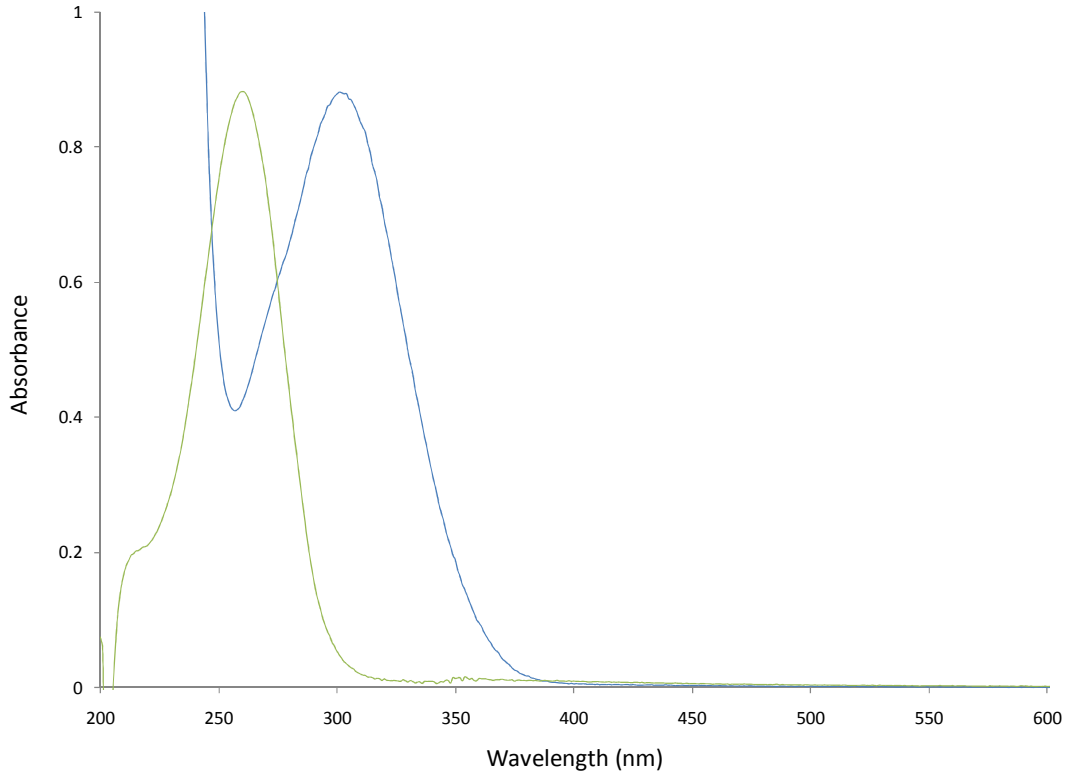

Figure 4.7: Overlaid UV-vis spectra of biotin maleimide, 1.5 mM in 70 % acetic acid (blue line) and cyclohexadiene, 1.5 mM in 10% methanol (green line).

As shown in Figure 4.7, biotin maleimide had a peak of maximum absorbance at 300 nm, whereas cyclohexadiene had a peak at 260 nm.

Both reactants were then analysed as a single solution under proposed reaction conditions, as shown in Figure 4.8.

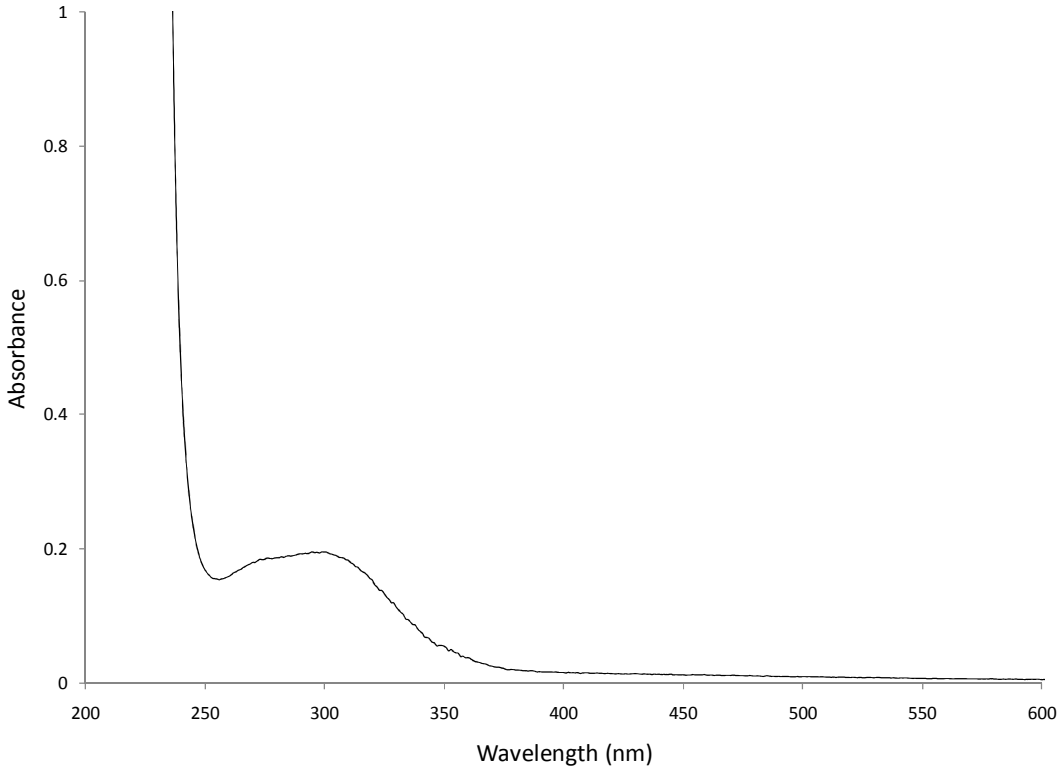

Figure 4.8: UV-Vis spectrum of biotin maleimide and cyclohexadiene (0.5 mM in binding buffer).

As expected, the two peaks were not well resolved and thus another route had to be investigated. High performance liquid chromatography (HPLC) and mass spectrometry were used in an attempt to identify any product formation arising from the Diels- Alder reaction of cyclohexadiene and maleimide, using the catalytic aptamer sequence. It was hoped that the sequence would display some catalytic ability and so formation of the cycloadduct could be monitored.

Biotin maleimide (10 eq.) and cyclohexadiene (1 eq.) were reacted together in the SELEX binding buffer and in the presence of the 105 mer CD.VS.4 (0.01 eq.). A further 2 samples were analysed as controls, the first containing no DNA and the other containing a control (non-aptamer) sequence of DNA. The mixture was allowed to react for 30 minutes then excess DNA was removed by centrifugal filtration and desalted to remove binding buffer salts *via* HPLC.

The overlaid HPLC traces of all three samples are shown in Figure 4.9.

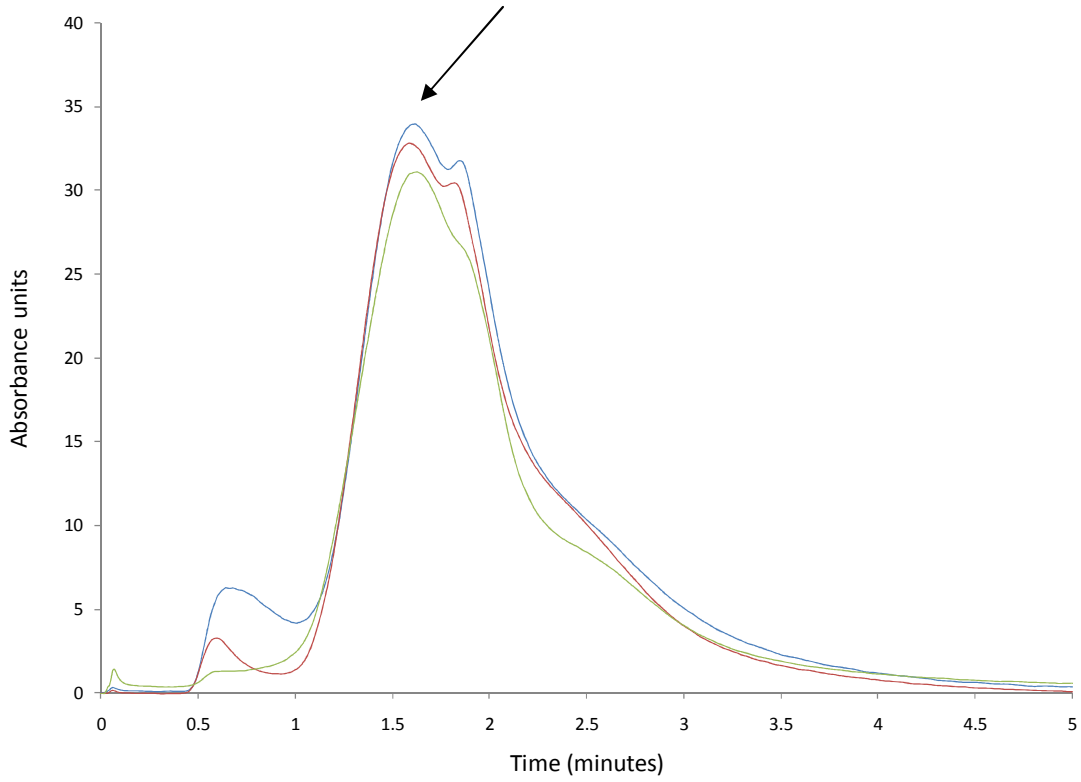

Figure 4.9: Overlaid HPLC traces of positive (blue), negative (green) and control (red) samples (the arrow indicates the fraction collected).

Both positive and control samples contained 2 peaks at 45 and 105 seconds. The negative sample contained only 1 peak. The extra peak is most probably due to excess DNA (as size exclusion chromatography was employed and thus the early fractions will contain large DNA fragments). Consequently, the second fragment of both the positive and control were collected and MALDI- TOF mass spectrometry analysis was carried out. However, the expected mass of the cycloadduct was not found.

4.6.2 SELEX specific Diels – Alder reaction using cyclohexadiene modified DNA (primer)

The initial catalytic investigation work carried out did not mimic the SELEX process, where the cyclohexadienyl modified DNA molecule was the substrate. Therefore, subsequent

experiments were attempted using a short cyclohexadienyl modified oligonucloetide as this was a closer match to the original SELEX experiment. A further difference in experimental technique was the use of silanised glassware. This technique is often carried out to prevent DNA sticking to the glass surface. Biotin maleimide (10 eq.) and cyclohexadiene modified primer (1 eq.) were reacted together in the SELEX binding buffer and in the presence of the 105 mer CD.VS.4 (0.01 eq.). A further 2 samples were analysed as controls, the first containing no DNA (referred to as the negative control) and the other containing a control fragment of DNA (referred to as the nonsense control). All three samples were analysed by HPLC after 30 minutes and 16 hours and the resulting traces shown in Figures 4.10 and 4.11.

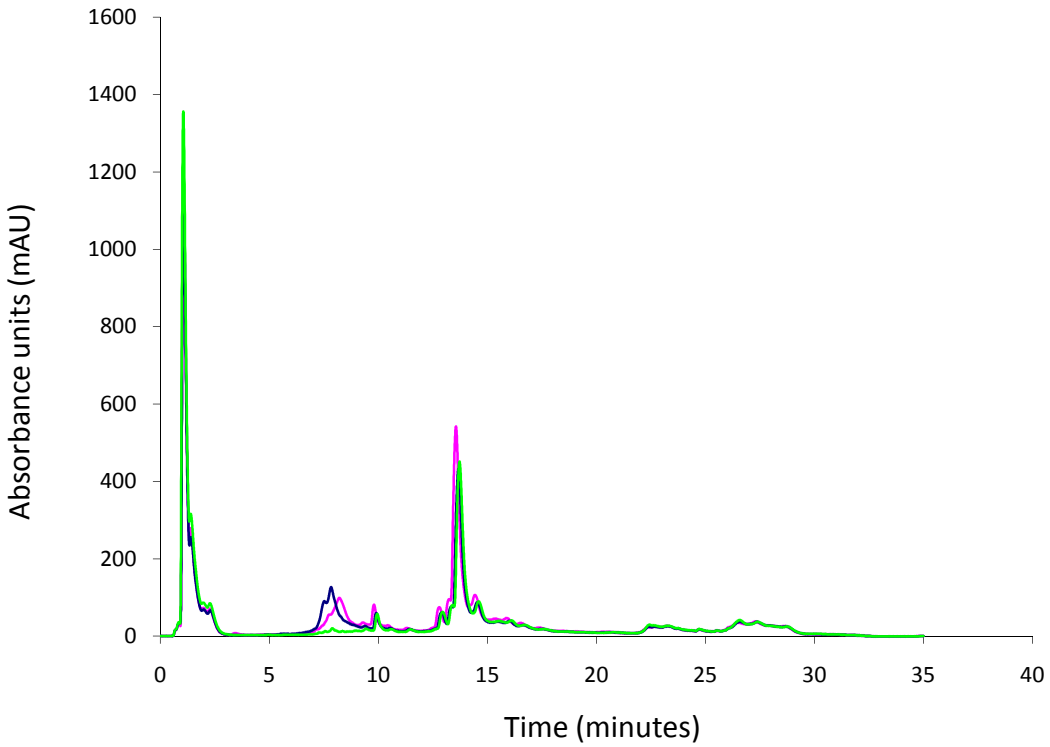

Figure 4.10: Overlaid HPLC traces of positive (blue line), negative control (green line) and nonsense control (pink line) after 30 minutes.

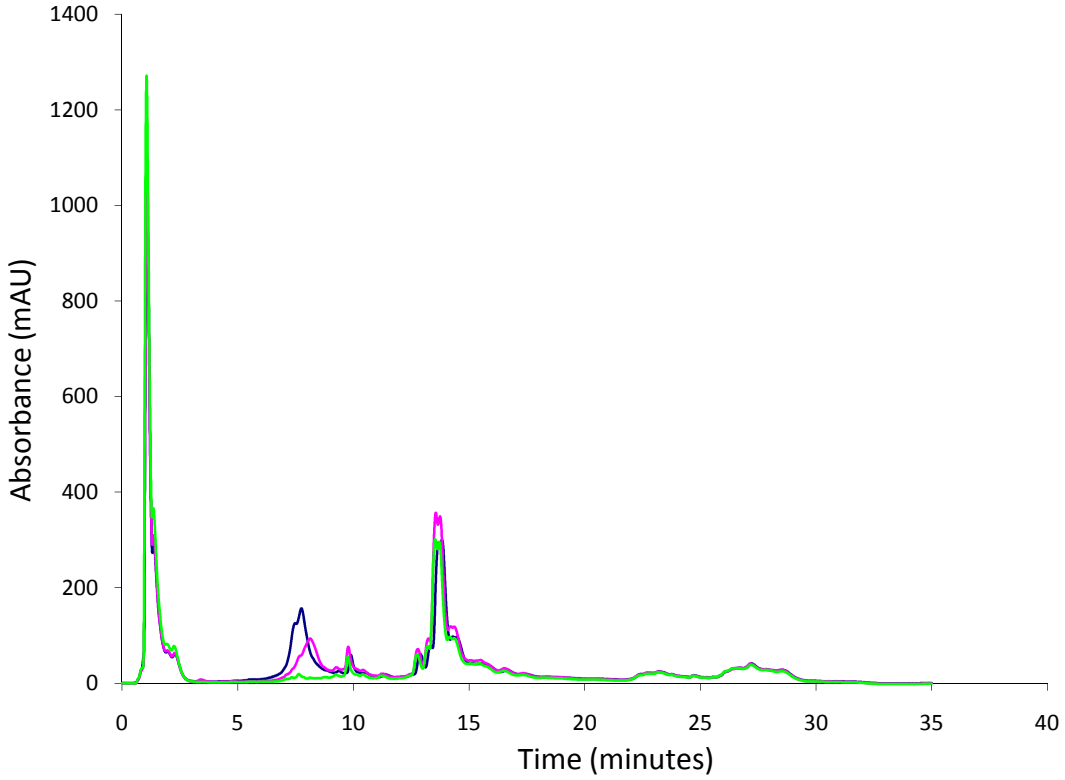

Figure 4.11: Overlaid HPLC traces of positive (blue line), negative control (green line) and nonsense control (pink line) after 16 hours.

As can be seen from Figures 4.10 and 4.11, there is very little change after allowing the mixture to react overnight. A product peak was not present and so no fractions were collected or analysed by mass spectrometry.

The experiment was carried out using the full 105 base aptamer DNA. It may have been that the 60 base aptamer should have been used as this would be lacking in the primer region of DNA which was complementary to the cyclohexadiene modified DNA used in the experiment. It was, therefore, necessary to repeat the work using the 60 base aptamer sequence (see entry CD.VS.4 in Table 4.2).

4.6.3 HPLC of DNA sequences

Before carrying out further work, it was necessary to analyse the 105 base aptamer, the 60 base aptamer and the modified DNA to be used in the reaction to ascertain their retention times and help identify peaks in subsequent HPLC analysis. Sample shortage meant that the modified primer used in PCR and the previous experiment was no longer a possible substrate and a different cyclohexadiene modified DNA sequence had to be used. The sequence consisted of 12 bases, with the cyclohexadiene modification in a mid-sequence position (as underlined in the sequence below), as opposed to at the 5' terminus:

5' – CGCA***T***TCAGGAT – 3' (VSDR2 mid)

All three DNA samples were analysed by reverse phase HPLC, using a previously optimised method.[183] The resulting HPLC traces are shown in Figure 4.12.

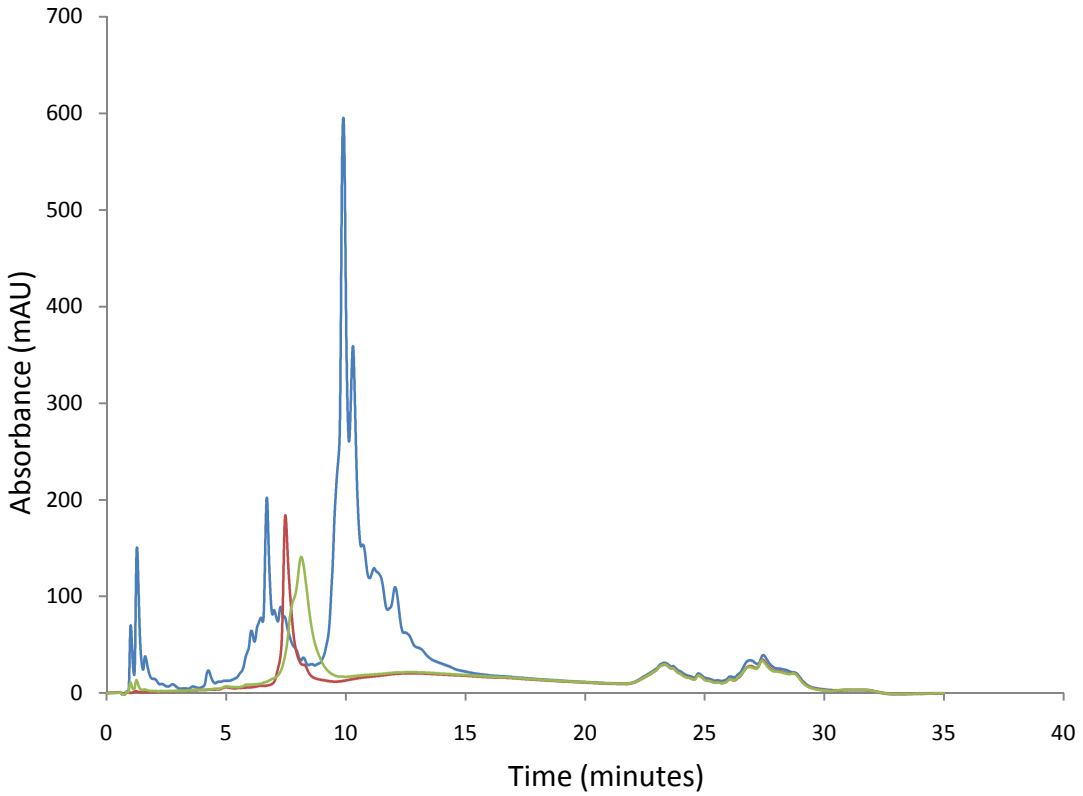

Figure 4.12: Overlaid HPLC spectra of VSDR2 mid (blue line), 60 base aptamer (red line) and 105 base aptamer (green line).

As shown in Figure 4.12, the two aptamer sequences elute at similar times, between 7 and 8 minutes. The analysis of the VSDR2 mid revealed that the sample was not pure as three distinct peaks were observed. Consequently, the full sample was purified using the same HPLC method, the three peaks collected and the final peak (between 10 and 12 minutes) analysed by MALDI – TOF mass spectrometry. The expected mass of the pure VSDR2 mid, 3820, was found.

4.6.4 SELEX specific Diels – Alder reaction using cyclohexadiene modified DNA (VSDR2 mid)

After purification and confirmation of the mid-sequence modified DNA sequence, two experiments were carried out, one with the 60 base aptamer and the other with the 105 base aptamer. 5 µM the cyclohexadenyl modifed DNA VSDR2 mid was reacted with 50 µM biotin

maleimide in the presence of 0.2 µM aptamer (both the 60 and 105 base sequences). The reaction was carried out in binding buffer for 1 hour and then analysed by HPLC. Both starting materials were also analysed.

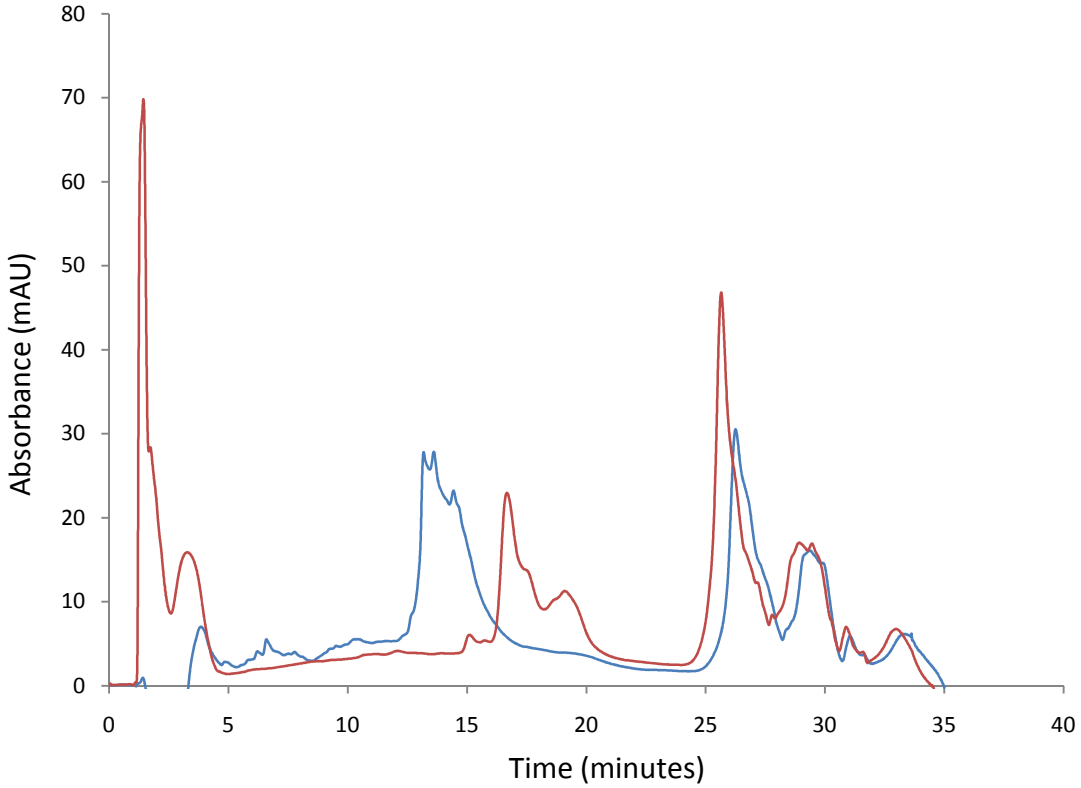

Figure 4.13: Overlaid HPLC spectra of VSDR2 mid (blue line) and biotin maleimide (red line).

The two reaction mixtures were then analysed and their respective HPLC traces are shown in Figures 4.14 and 4.15.

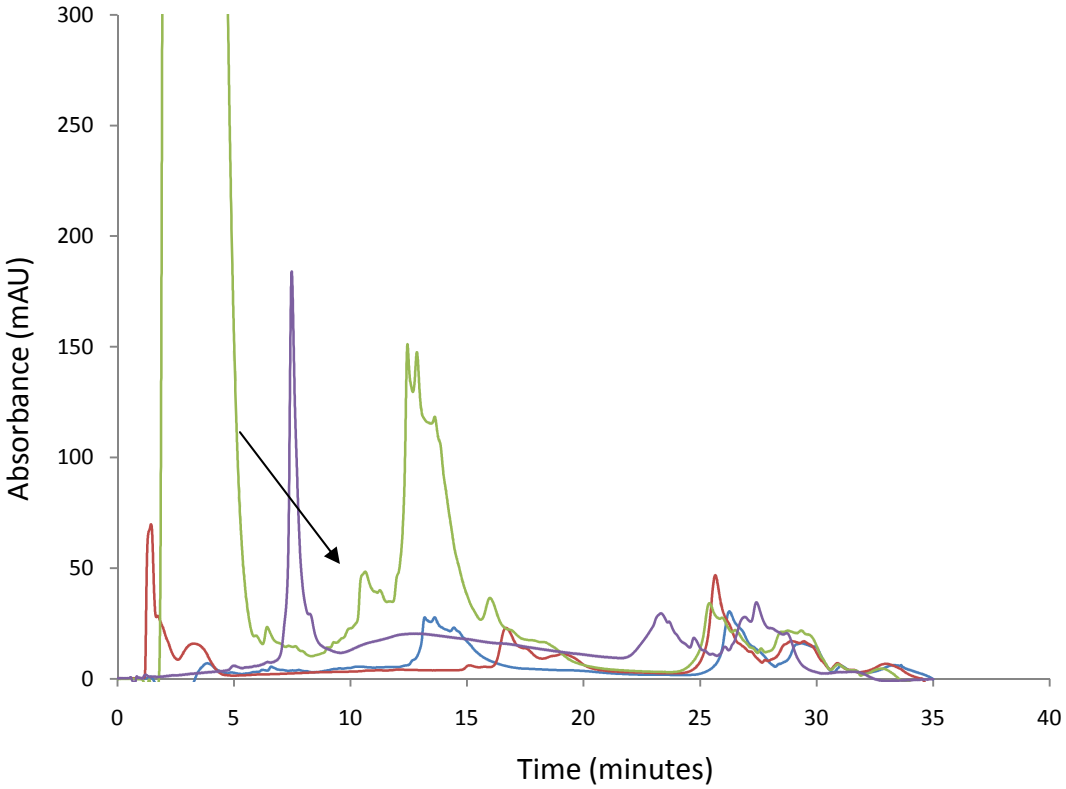

Figure 4.14: Overlaid spectra of the reaction mixture (green line) containing the 60 base aptamer catalyst, VSDR2 mid DNA (blue line), biotin maleimide (red line) and the 60 base aptamer (purple line).

There is a new peak in the reaction mixture (as highlighted by the arrow), which may have arisen from the formation of the Diels-Alder product. When compared with the other traces, this peak is not indicative of either starting materials or the catalytic 60 base aptamer. The fraction from 10 – 13 minutes was collected for MALDI – TOF analysis. The same experiment was carried out using the 105 base aptamer. The HPLC traces for this experiment are shown in Figure 4.15.

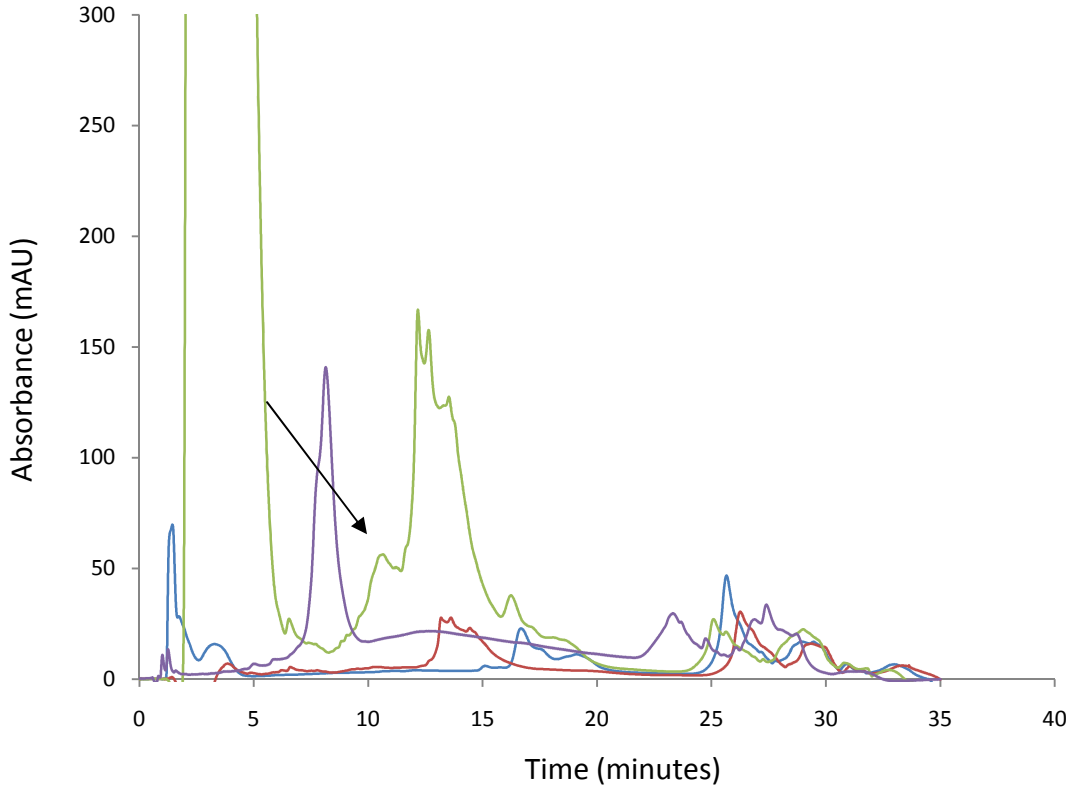

Figure 4.15: Overlaid spectra of the reaction mixture (green line) containing the 105 base aptamer catalyst, VSDR2 mid (blue line), biotin maleimide (red line) and the 105 mer aptamer (purple line).

As with the previous experiment involving the 60 base aptamer, there is a new peak in the reaction mixture (indicated with the arrow in Figure 4.15) which may be due to the presence of the Diels-Alder product. As with the previous experiment, the fraction from 10 – 13 minutes was collected and analysed by MALDI – TOF.

60 base aptamer expected mass 4272.1 mass found 4269.23

105 base aptamer expected mass 4272.1 mass found 4260.3 (this is a difference of 12 and so could be due to protonation of the 12 base phosphate backbone).

4.7 Conclusion

A SELEX program was designed for the selection of a potential biocatalytic DNA aptamer for the Diels-Alder reaction. This was carried out, involving a total of 8 cycles and two counter selections. Cloning and sequencing revealed 6 families and one sequence, CD.VS.4, was used in an investigation into its biocatalytic potential. A number of different experiments were attempted before HPLC was identified as a suitable analytical technique for assessment. Preliminary results by HPLC analysis indicated that the cycloadduct of a mid-sequence cyclohexadienyl modified DNA (VSDR2 mid) sequence and biotin maleimide had been formed in the presence of both the 60 mer and 105 mer CD.VS.4 aptamer sequences. This was confirmed by MALDI-TOF mass spectrometry. This was a significant result as aqueous buffer conditions were used and a short reaction time of one hour was necessary. It represents an improvement on current methods and whilst further confirmatory work is necessary, there is preliminary evidence that a potential biocatalytic DNA sequence for the Diels-Alder reaction may have been isolated. The next steps would be to analyse the biocatalytic potential of the aptamer using labelled DNA sequences and maleimide modified Tat peptide. Kinetic studies should also be carried out to investigate reaction rates.

5 Protein Kinase C aptamer conjugated nanoparticles for intracellular protein detection

5.1 Introduction

The detection and monitoring of protein interactions is of great importance in increasing our understanding of biological systems. The identification of protein function has major implications in, for example, the control and treatment of disease states. Nanoparticles are also being used in biological detection work due to the ease with which bioconjugation can be achieved and their superior spectroscopic properties with respect to fluorescence.[184] [185] [124] Protein Kinase C (PKC) is a negatively charged protein involved in many essential cellular processes.[186] [96] [187] There are a number of different isoforms including PKC α, β, μ and δ, but can all be classified as enzymes responsible for the cascade of reactions resulting in phospholipid hydrolysis.[188] [187] Specifically, PKC delta (δ) is activated by diacylglyceral and exhibits anti-proliferative and tumor suppressing properties.[189] PKC has been the subject of varied research, with most studies use immunofluorescence staining or fluorescent tracking of over expressed labelled PKC within the cell.[44] Over expression is necessary to produce enough protein to visualise using these techniques.

There are inherent disadvantages with these techniques as over expression is not the natural cellular state and the increased production of a protein can interfere with the endogenous enzymes. It is therefore desirable to investigate other detection methodologies. An aptamer for PKC δ has already been selected and so nanoparticle conjugates could be provide a platform for the development of a molecular probes. Indeed, this set-up has been reported previously for other targets.[190] [145] [191] The aim of this section of work was to use gold

nanoparticles modified with an aptamer that binds to PKC δ. The initial work involved the synthesis and characterisation of the nanoparticle conjugates. Later experiments were carried out in order to assess the aptamer functionalised - protein interaction and investigate whether the conjugates could be used as a biosensor for PKC δ. The work was limited to the delta isoform of PKC and so for simplicity is referred to PKC in subsequent sections. The ultimate aim of this area of the project was the intracellular detection of PKC.

5.2 Synthesis

Nanoparticle synthesis involved the use of citrate reduction of a gold salt to yield spherical nanoparticles approximately 18 nm in diameter with a surface layer of citrate.[192 193] This layer stabilises the nanoparticles by ensuring they are monodispersed by conferring an overall negative charge to the nanoparticles and thus preventing aggregation. For the attachment of DNA, a thiol modification was used as sulfur has an affinity for the gold surface and displaces the stabilising citrate layer to deposit the DNA on the surface. This was a modified protocol[194] based on work pioneered by Mirkin *et al*.[128] The PKC aptamer is a 31 base oligonucleotide with the following sequence.[44]

5' – ACACGACGGGAATACTGACTCTCCCCCATGT – 3'

This was synthesised commercially with a 5' thiol modification (thiohexyl group as shown in Figure 5.1) to allow attachment to the nanoparticle (illustrated in Figure 5.2). All thiolated DNA used in Chapters 5 and 6 were synthesised using the same modification. The protocol involved the addition of 2 nmoles of thiolated DNA to Au colloid (1 mL, 20 nM) and leaving overnight. Incremental salt addition was carried (31 µL, 2M NaCl) to a final concentration of 0.1 M. The nanoparticle conjugates were then resuspended in 0.3 M phosphate buffered saline (PBS).

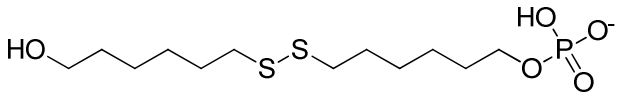

Figure 5.1: Thiol linker used in DNA synthesis.

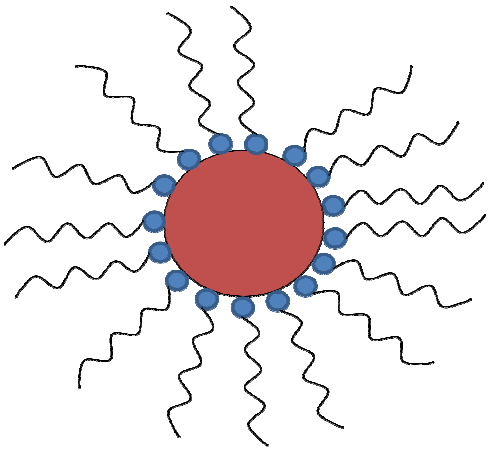

Figure 5.2: Illustration of thiolated DNA attachment to a gold nanoparticle producing PKC aptamer gold nanoparticle conjugate (PCK AGNCs).Blue circles represent the thiol modification on the DNA and the large red circle represents the nanoparticle (not to scale).

The generation of thiolated DNA GNCs *via* this method is well known but it was necessary to characterise the samples to gain insight into the effect on the surface plasmon resonance, the stability of the conjugates and to confirm the presence and quantify the number of aptamers on the surface. A number of techniques were used and are detailed in section 5.3.

5.3 Characterisation

5.3.1 UV – visible spectroscopy

The properties of nanoparticles are greatly affected by their size, shape, polydispersity, stabilising surface layer and dispersant medium.[138] One way of characterising nanoparticles is through UV-visible spectroscopy analysis. The surface plasmon resonance wavelength can give an indication of the environment surrounding the nanoparticles and as the nanoparticles are modified with DNA (or any other molecule) this is often accompanied by a shift in the plasmon and can be observed by UV- vis spectroscopy.

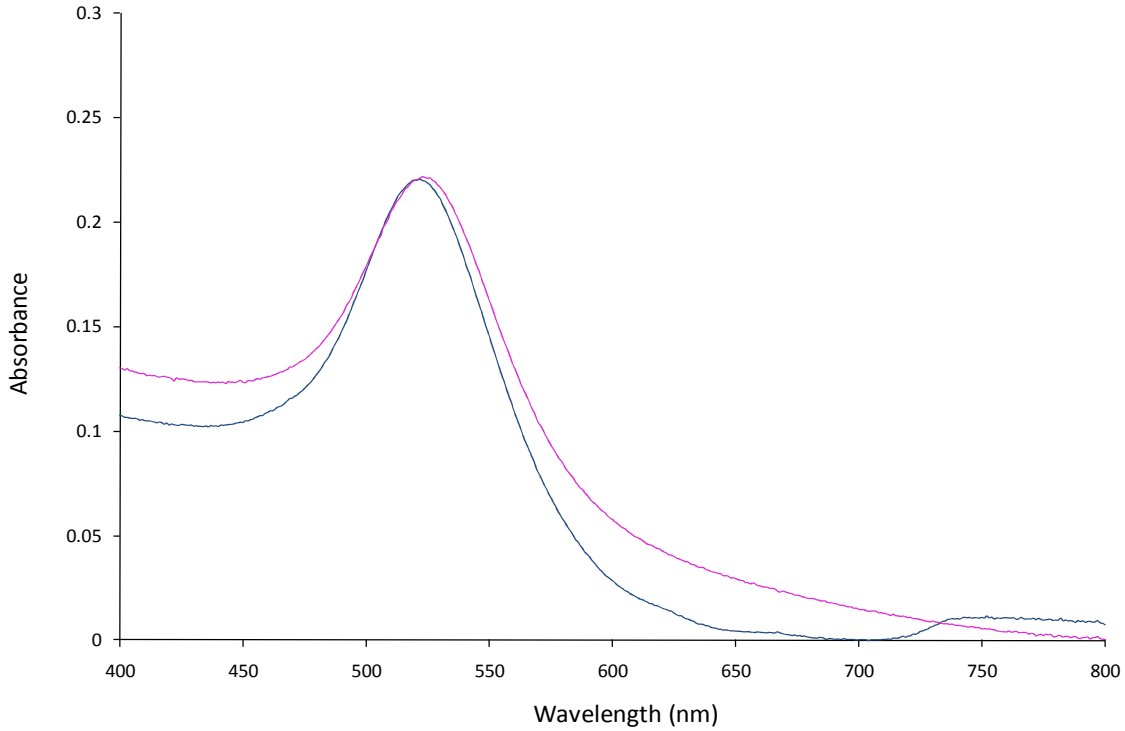

Figure 5.3: Comparison of bare nanoparticles (0.8 nM in H_2O, blue line) with PKC AGNC (0.8 nM in 0.3 M PBS, pink line).

As can be seen from Figure 5.3 there is a shift of a few nanometers (519 nm for colloid compared to 523 nm for the PKC AGNC). There is also a broadening of the peak, 90 nm at full width at half height (FWHH) for colloid compared to 105 nm for the conjugated nanoparticles. This phenomenon is observed in the literature[124 138] and although this shift is indicative of the presence of DNA on the surface of the nanoparticle, it is not significant enough to draw any firm conclusions and so further characterisation was necessary. It is worth noting that the stability of the conjugates in PBS is further evidence of the DNA attachment as unmodified nanoparticles would aggregate in such salt conditions.

5.3.2 Gel electrophoresis

There have been a number of studies in which gel electrophoresis has been used as a

characterisation method for nanoparticle functionalisation.[195] [196] [197] The purpose of this analysis was to investigate whether the DNA coated on the nanoparticles could be visualised using conventional molecular biology techniques.

A number of gel types were investigated throughout this project, with the different variables summarised below:

Agarose concentration (w/v):	2 %	1.5 %
Concentration of TBE buffer:	1×	0.5×
Loading buffer:	Tri colour (commercial)	glycerol (30 %)

The optimum conditions were found to be a 1.5 % gel made up in 0.5× TBE buffer, 0.5× TBE tank buffer and samples loaded using glycerol (7.5 % final concentration). All gels produced similar results and so for simplicity, an example gel is illustrated in Figure 5.4.

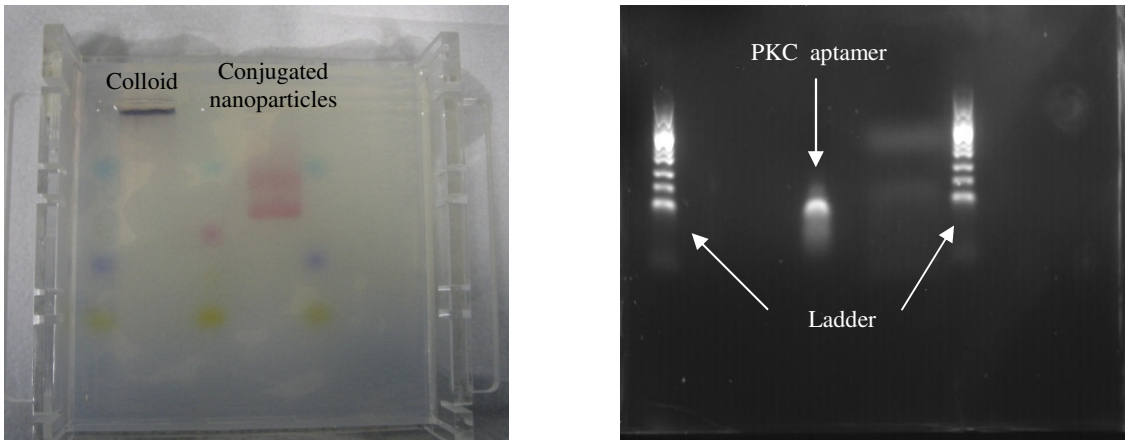

Figure 5.4: Gel electrophoresis of bare nanoparticles (13.4 nM), PKC AGNC (13.4 nM) and PKC DNA aptamer (2.5 µM) on a 1.5% agarose gel, white light image (left) and UV light image (right).

The first point to note is the difference between bare nanoparticles and PKC AGNC in the white light image, that is, only the latter migrated through the gel. It could be theorised that the TBE buffer used in the electrophoresis may cause the bare nanoparticles to precipitate and the resulting aggregates are too large to pass through the pores of the gel. Whereas, the DNA present in the conjugate sample stabilises the gold nanoparticles so that, when exposed to TBE, no aggregation occurs and the conjugates can migrate through the gel. From the UV image, the DNA on the nanoparticles can be observed. The DNA band present from the nanoparticles is

retarded in the gel when compared to the free DNA solution. This is due to the movement of DNA being dependant on its electrophoretic mobility only. However, steric hinderance, due to the presence of the nanoparticles affects the electrophoretic mobility of the conjugated nanoparticles. There is another, less intense DNA band in the conjugate sample. This is approximately the same size as the DNA sample which may originate from excess DNA in the conjugate sample. The results thus far suggested that the gold nanoparticles had been successfully modified with the PKC aptamer

5.3.3 Surface coverage determination

After indicating the presence of the aptamer on the nanoparticles it was necessary to better understand the surface coverage of the DNA on the nanoparticles. Ascertaining the density of DNA on the surface was crucial in order assess any steric hinderance issues that may affect the binding of aptamer and protein. The number of DNA molecules on the surface was quantified using a method developed by Mirkin *et al*.[198] Triplicates of the FAM modified PKC AGNCs were treated with dithiothreitol (DTT) (100 mM) and left overnight to completely aggregate. The DTT displaces the DNA molecules form the nanoparticle surface, thus releasing them into solution. The nanoparticles aggregate as the repelling forces between the nanoparticles (the negatively charged DNA) has been removed and so the nanoparticles form clusters. After centrifugation and two wash steps, the supernatants were removed and aliquots analysed in triplicate by fluorescence spectroscopy. A calibration curve was first generated (using the FAM modified PKC aptamer) and then used to quantify the DNA in the supernatants, which is shown in Figure 5.5.

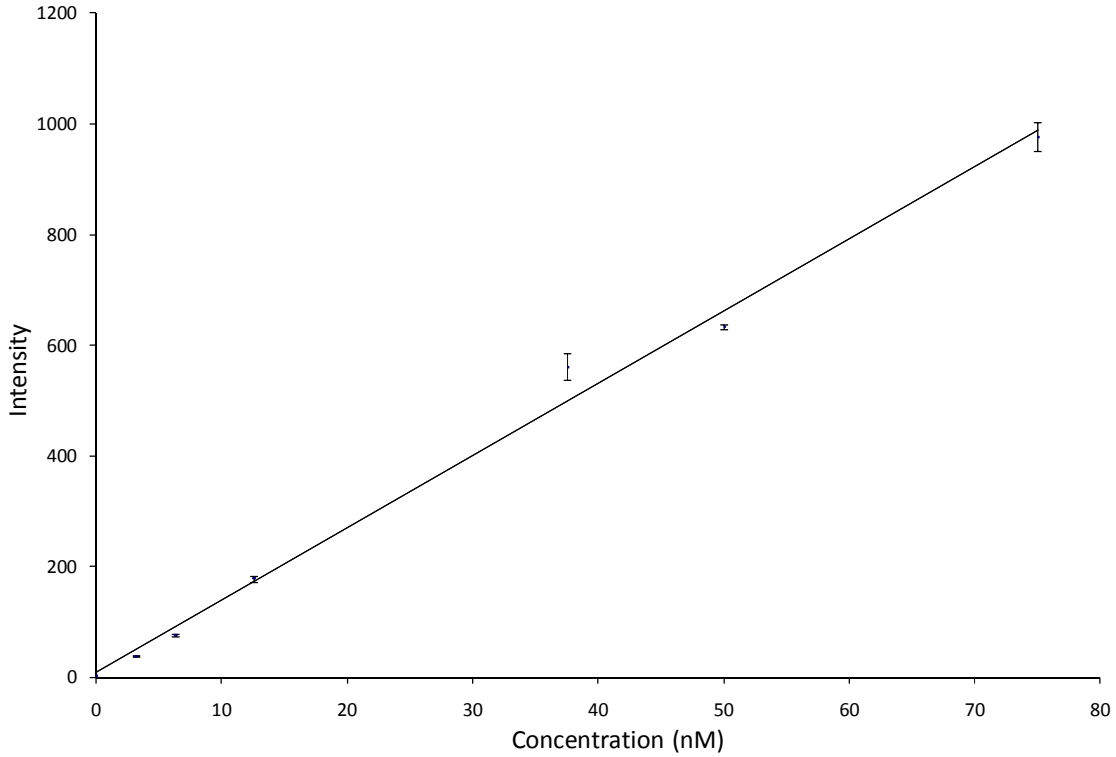

Figure 5.5: Calibration graph of fluorescently labelled PKC aptamer (emission recorded at 518 nm and the standard deviation of the three replicates used as the error bars).

Using this calibration data together with the fluorescence readings from the supernatant samples and the initial concentration of nanoparticles, it was calculated that there were 99 ± 13 DNA molecules per nanoparticle (18 nm diameter). This was in good agreement with other published results.[198 139 199]

5.3.4 UV- vis melt investigation

It was necessary to gain an understanding of the behaviour of the DNA whilst on the nanoparticle. Examination of the aptamer sequence indicated areas of self-complementarity (as underlined).

5' – ACACGACGGGAATACTGACTCTCCCCCATGT – 3'
3' – TGTACCCCTCTCAGTCATAAGGGCAGCACA – 5'

UV – vis melting experiments were carried out to investigate whether hybridisation of self-complementary regions could be monitored. A solution of the DNA PKC aptamer and PKC AGNC were analysed at 260 nm (with the nanoparticle sample also analysed at 520 nm as this was the characteristic peak for gold nanoparticles). The hyperchromicity of DNA dictates that upon denaturation, the absorbance of DNA at 260 nm increases. Whilst in a duplex formation, a "screening effect" takes place which prevents the individual bases from exerting their full contribution to the molar extinction coefficient. This effect does not occur in DNA when in the single stranded state. Since heating disrupts the hydrogen-bonding of the duplex and results in strand separation, an increase in the absorbance at 260 nm with temperature is indicative of duplex denaturation. Figures 5.6 and 5.7 show the three experiments carried out to investigate whether self-hybridisation was occurring on the nanoparticles.

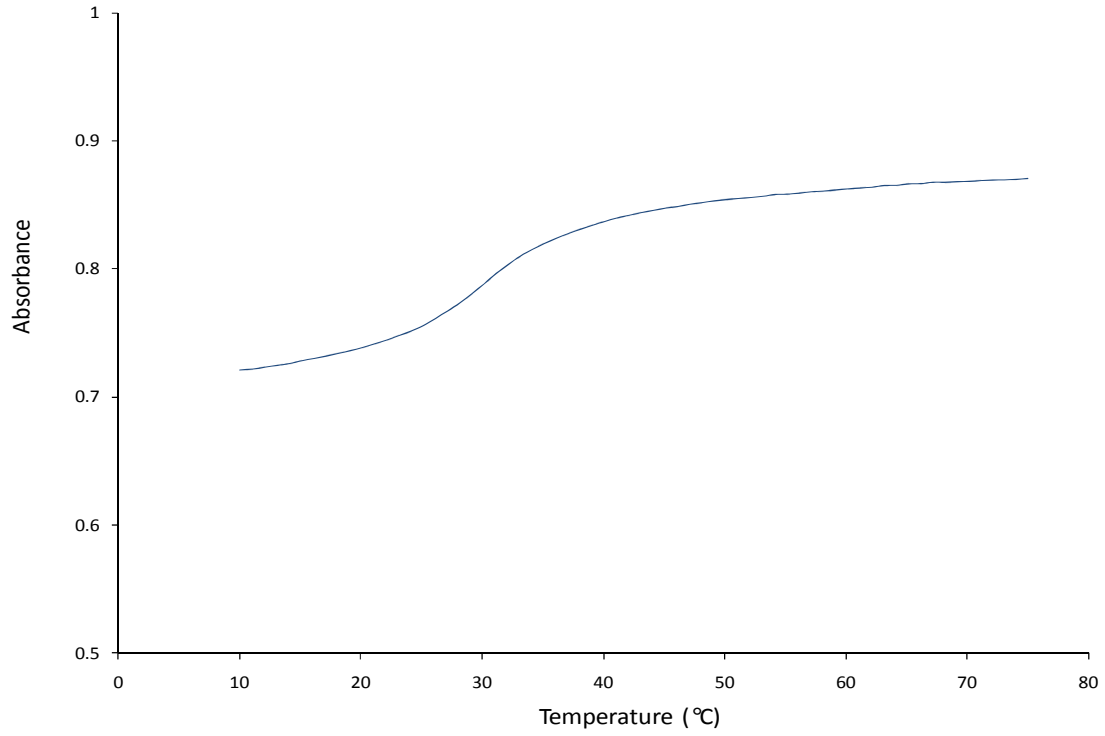

Figure 5.6: UV melting curve of thiolated PKC aptamer solution (2 µM in 0.3 M PBS) obtained at 260 nm.

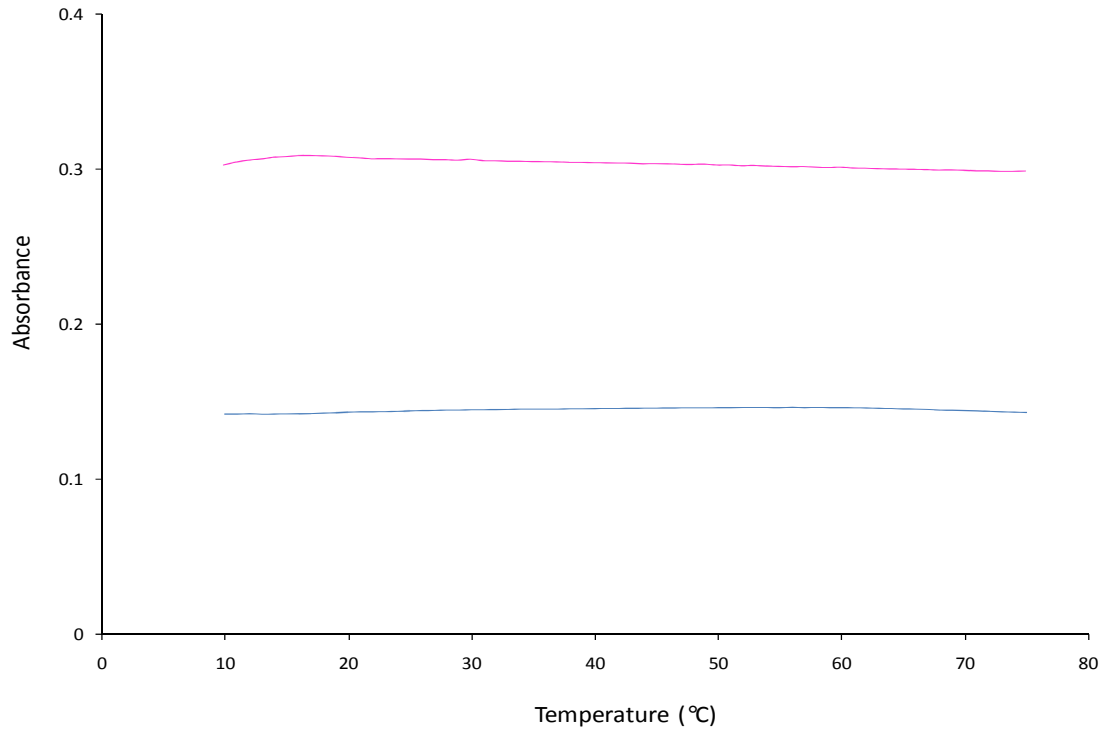

Figure 5.7: UV melting curve of PKC AGNC (1 nM in 0.3 M PBS) obtained 260 nm (pink line) and 520 nm (blue line).

As shown in Figure 5.6, a typical UV melting curve is observed for the DNA when free in solution. This confirms duplex formation in the absence of nanoparticles. However, when conjugated to nanoparticles (as shown in Figure 5.7) , the aptamer displays no such behaviour as no increase in absorbance is observed at 260 nm. DNA – gold nanoparticle conjugates can also be monitored at 520 nm for evidence of hybridisation. As with the lower wavelength monitoring, there should be an increase in absorbance as temperature increases if a duplex is present. At higher temperatures, the DNA is denatured and exists in a single stranded state thus ensuring the nanoparticles are monodispersed, thereby exhibiting a surface plasmon resonance at 520 nm. However, at temperatures below the melting temperature of the DNA sequence, hybridisation would cause the the particles to aggregate and their UV-vis absorbance contribution at 520 nm to decrease. However, no such phenomenon is observed at 520 nm for the conjugated samples. This result would seem to suggest that while self-complementary does exist in the sequence, the presence of the nanoparticles has an inhibitory effect and hybridisation does not occur. This may be due to densely packed DNA molecules on the surface

being restricted and unable to self-hybridise. In addition, DNA -nanoparticle conjugates are known to show high specificity for fully complementary targets over single base mismatch sequences.[200] In the case of the PKC aptamer, the self-complementarity is not complete and there may be insufficient complementarity to induce the hybridisation-induced aggregation of the nanoparticles.

5.4 Assays

In order to study the aptamer – protein interaction, UV-visible spectroscopy experiments were carried out to investigate whether a change in the plasmon of the nanoparticles coincided with the binding of the aptamer and protein. A number of assays were attempted and all followed a similar route: the AGNC and nonsense DNA GNC samples were incubated with PKC (or control protein), left for one hour and then analysed by UV – vis spectroscopy.

Figure 5.8 shows overlaid spectra of a number of different samples after an hour long incubation with PKC (and control protein bovine serum albumin (BSA)). This protein is often used as a control due to its stability, low cost and lack of interference in biological reactions. The nonsense DNA control was essential to ensure any observed phenomena originated from a specific aptamer protein interaction as opposed to a non specific DNA – protein interaction.

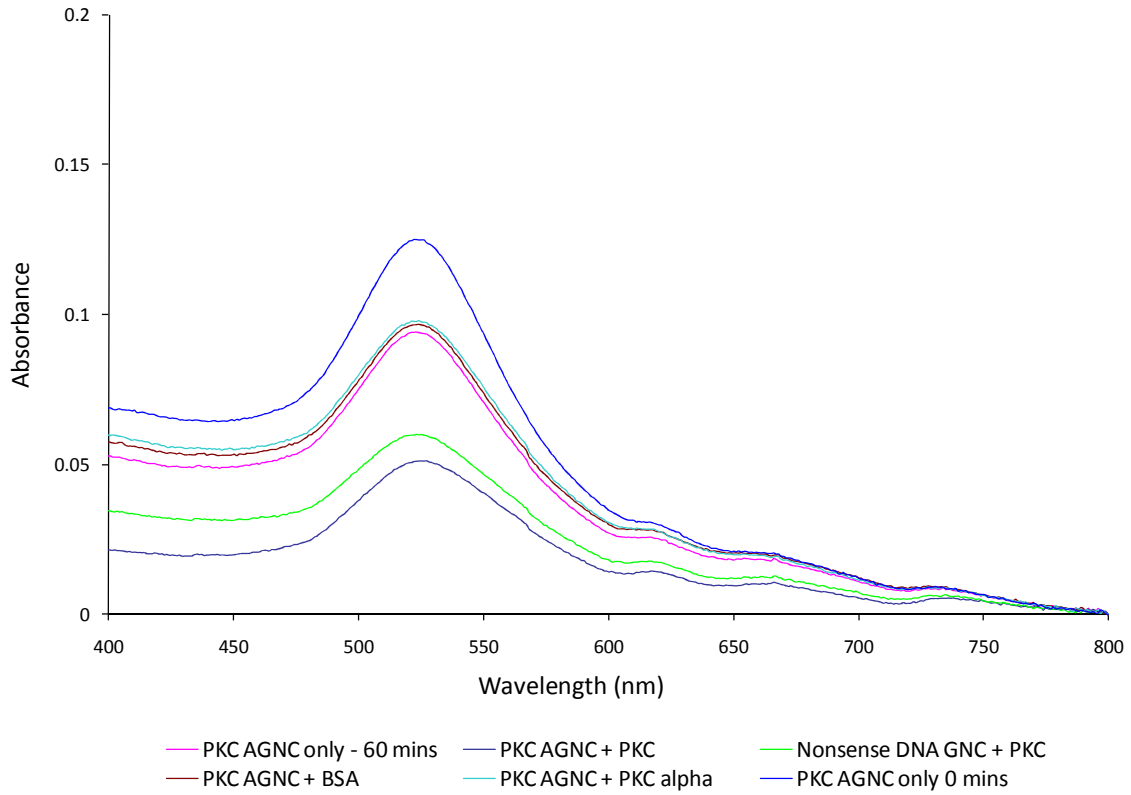

Figure 5.8: Overlaid spectra of different GNC (0.5 nM, 400 µL) in the presence of PKC and BSA (6.6 nM)

The aptamer was selected to be specific towards PKC delta and should not have an affinity for any other PKC isoform. The biggest shift in plasmon resonance does occur in PKC AGNC + PKC however, nonsense DNA GNC + PKC also shows a similar drop. No significant shift in the plasmon resonance occurs and the buffer seems to have an effect on the conjugates as there is a drop in absorbance when comparing PKC AGNC only 0 mins with PKC AGNC only 60 mins. This suggests that the change in plasmon resonance is not indicative of the specific interaction between aptamer and target. Crucially, there were no visible signs of aggregation and a shift and / or broadening of the plasmon resonance band was not observed. The PKC AGNC were monitored in the presence of PKC over a series of time intervals to identify whether an optimum incubation time existed. The conjugates were also monitored in the absence of PKC to assess their stability in the buffer.

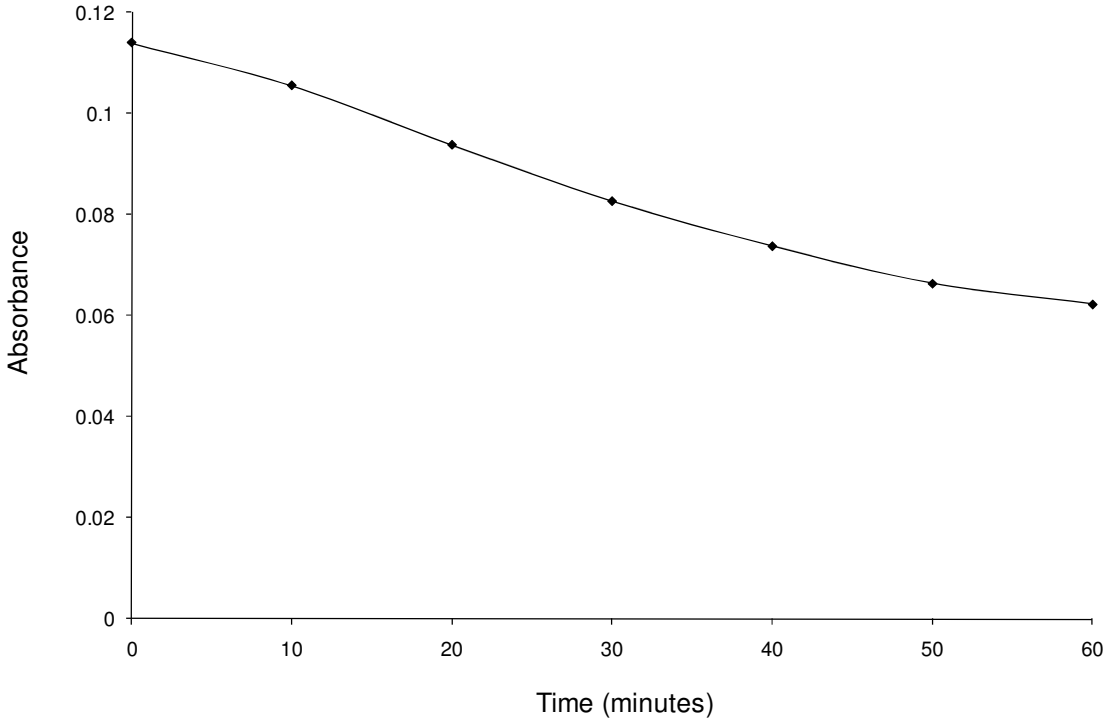

Figure 5.9: Plot of absorbance of PKC AGNC (0.4 nM) in the presence of PKC (13 nM) in 0.3 M PBS as a function of time. (Graph plotted using the data from Figure 5.8)

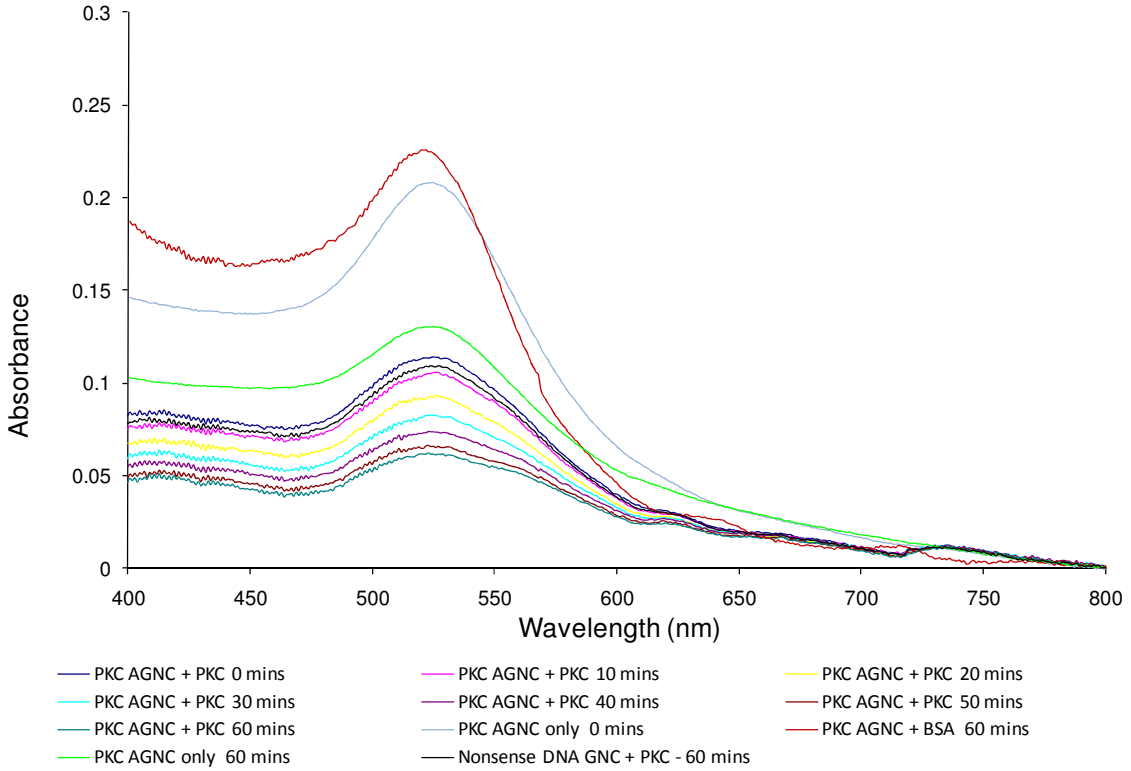

Figure 5.10: (Top) Overlaid spectra of PKC AGNC (and nonsense conjugate, 075 nM) in the presence of 13 nM PKC (and BSA) at 10 minute intervals.

The main observation to be made is that there appears to be a time dependence relationship when PKC is present in the sample. There is a steady drop in absorbance as time progresses from 0 – 60 minutes. It should also be noted that there is no such shift in the control protein sample (PKC AGNC + BSA 60 mins) but there is a drop in absorbance in the control DNA sample (nonsense DNA GNC + PKC 60 mins). There is a drop when no protein is present, that is, when the conjugates are resuspended in buffer only. However, the most significant drop is after 1 hour in the presence of PKC. However, as with the other experiments, no broadening or shift of the surface plasmon resonance was observed.

The data from the initial work proved inconclusive and so it was therefore necessary to attempt further study. The main areas of interest were to reduce / control the number of aptamers on the surface. It may be that there are too many DNA molecules on the surface. Indeed, the surface coverage data indicated that there were approximately 100 aptamers on the surface. Steric hindrance maybe an issue and thus could be preventing the aptamers from interacting

with the target. As such, a dual approach of using spacer groups was investigated. The first method comprised of the use of a small molecule which had an affinity for the nanoparticle surface and so by introducing this into the system together with the aptamer, a mixed layer of aptamer and small molecule could be created, thereby spacing out the aptamer on the nanoparticle surface (referred to a surface spacer). In work thus far, the aptamer sequence was directly attached to the surface of the nanoparticle. It may be that the first few bases of the sequence are crucial for binding and the close proximity of this region to the nanoparticle could inhibit the binding. As such, the second approach utilised a spacer group (incorporated into the aptamer sequence) which separated the aptamer moiety from the NP surface (referred to as a linking spacer). The work detailed in section 5.5 outlines the results of both approaches.

5.5 Control of Surface Coverage

5.5.1 Short thiol molecule attachment

Two different small thiol molecules (as shown in Figures 5.11 and 5.12) were used in order to bind to the surface of the nanoparticle and so compete with the aptamer.

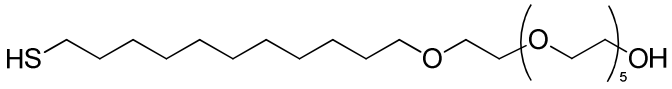

Figure 5.11: Structure of 11-Mercaptoundecyl hexa(ethylene glycol) (11- MHEG).

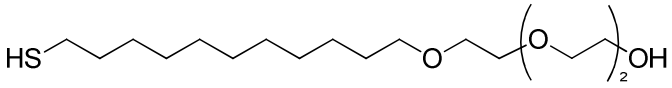

Figure 5.12: Structure of Triethylene glycol mono-11-mercaptoundecyl ether (11-MTEG).

The two different molecules varied in the length of the PEG; 2 and 5 units were used. A similar

method to the one used to synthesise the PKC AGNC was used where the aptamer was replaced with the 11- MHEG and 11-MTEG at varying concentrations (1.5, 3.0, 6.0, 15 and 30 μM). Unfortunately, it was not possible to obtain stable nanoparticle conjugates using this method. Instead, the possibility of using a short DNA sequence was investigated.

5.5.2 6 mer attachment

When considering the length of DNA to use as a surface spacer, care had to be taken as longer sequences could pose a problem by increasing the likelihood of DNA – DNA interactions between the spacer the aptamer. Shorter sequences, however, do not stabilise nanoparticles as effectively as longer sequences and so a stabilising group (hexaethylene gycol, HEG) was incorporated into the short, 6 mer, control sequence.

Spacer: 5' thiol (HEG)CTCTCT 3'
Aptamer: 5' thiol ACACGACGGGAATACTGACTCTCCCCCATGT 3'

The spacer was added in varying concentrations, relative to the aptamer, in order to space the aptamer out on the surface. Four different conjugates were prepared; 1:1, 1:2, 1:5, 1:9 (aptamer:spacer) and were named PKC AGNCs HEG 1, 2, 5 and 9 respectively.

A surface coverage study was carried out to establish what effect altering the ratio of aptamer to spacer had on the concentration of aptamer attached to the surface of the nanoparticle. A repetition of the experiment in 5.3.3 was carried out using triplicate samples of the four different conjugates. The results are summarised in Table 5.1.

Table 5.1: Summary of different conjugates.

Name of conjugate	No. of moles aptamer, spacer	No. of aptamers / nanoparticle
HEG 1	1.5, 1.5	62 ± 13
HEG 2	1.0, 2.0	3.1 ± 1.3
HEG 5	0.5, 2.5	1.0 ± 0.1
HEG 9	0.3, 2.7	0.5 ± 0.2

As highlighted in Table 5.1, there is a definite decrease in the number of aptamers attached to each nanoparticle with increasing concentration of spacer. This was to be expected, however, a steady drop reflected in the respective ratios was not observed. For example, the concentration of aptamer is 20 times larger when comparing HEG 1 with HEG 2, despite the fact a 1:1 ratio has been used as opposed to a 2:1 ratio. This can be rationalised by considering the HEG group present on the spacer DNA. Unlike DNA, this is a neutral molecule and so the lack of electrostatic repulsion confers better packing ability of the HEG modified DNA and so could preferentially attach to the nanoparticle surface when compared to the unmodified aptamer sequence.

Successful control of the aptamer density on the nanoparticle surface had been achieved and some of the previous work was repeated to investigate whether the alternative conjugates behaved differently to the fully saturated aptamer conjugates.

5.5.3 Stability study

Before carrying out any assays with PKC, the stability of the conjugates in the buffer had to be established. The PKC aptamer isolated by Tan *et al*. used HEPES buffer as the solution in their binding studies. This buffer had not been used in the work detailed previously as PBS buffer is often the preferred choice in biological analysis and nanoparticle work. However, since previous results had not indicated a successful aptamer-PKC interaction, it was decided to

investigate the preferred buffer. A stability study was set up using HEPES buffer to resuspend the conjugates.

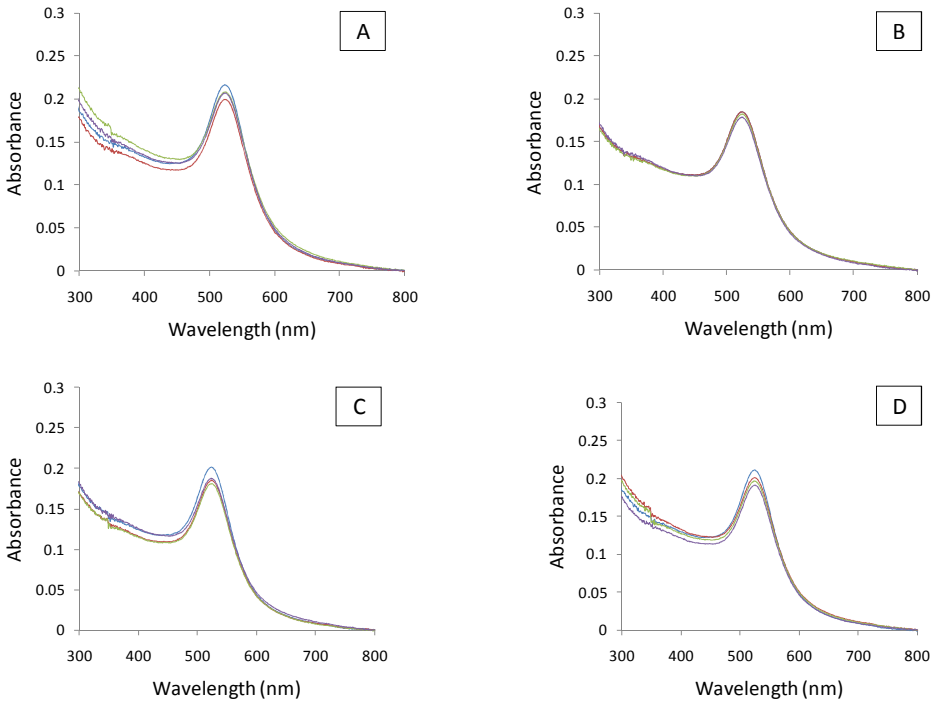

Figure 5.13: Overlaid spectra of 0.85 nM conjugates (A, HEG 1) (B, HEG 2) (C, HEG 5) (D, HEG 9) taken at 4 different time intervals (blue – t = 0 hours), (red – t = 1 hour), (green – t = 2 hours) and purple – t = 3 hours).

For each of the four conjugate samples, UV – vis spectra were taken after 0, 1, 2 and 3 hours. As indicted from the UV – vis spectra in Figure 5.13 no appreciable change was observed, indicating the conjugates were stable in the buffer. This allowed the work to progress towards the assay system.

5.5.4 PKC assay using HEG 2, 5 and 9 conjugates

After successfully synthesising nanoparticle conjugates with varying aptamer surface coverages, an assay was carried out to investigate whether the binding of aptamer and protein

in specific stoichiometries could be observed by UV- vis spectroscopy analysis. HEG 1 was not investigated as previous work with total aptamer coverage had proven unsuccessful (100 aptamers/NP for full surface coverage compared to 62 aptamers/NP achieved with HEG 1 conjugate). HEG 2, 5 and 9 had surface coverages of 3.1, 1.0 and 0.5 aptamers/NP respectively, thus providing the desired spacing on the surface of the nanoparticle. The PKC aptamer has not been well studied in the literature and thus no experimental data had been acquired to indicate the binding mechanism and / or stoichiometry of the aptamer – target complex. Consequently, a number of different concentrations were investigated.

For the three conjugates, the concentration of DNA was estimated using the concentration of nanoparticles and the calculated surface coverages. PKC was the added at different concentrations allowing for a variety of different ratios to be investigated (as summarised in Table 5.2).
The samples were left for 45 minutes and then analysed by UV-vis spectroscopy.

Table 5.2: Ratio of protein to aptamer used for each sample.

Sample	Protein : aptamer
1	5 : 1
2	2 : 1
3	1 : 1
4	1 : 2
5	1 : 5

The samples analysed ranged from the aptamer being in a 5× excess, to aptamer and protein being equimolar to PKC being in a 5× excess. The data, shown in Figure 5.14, indicates no change in the surface plasmon was observed for any of the five (HEG 2 AGNC) samples.

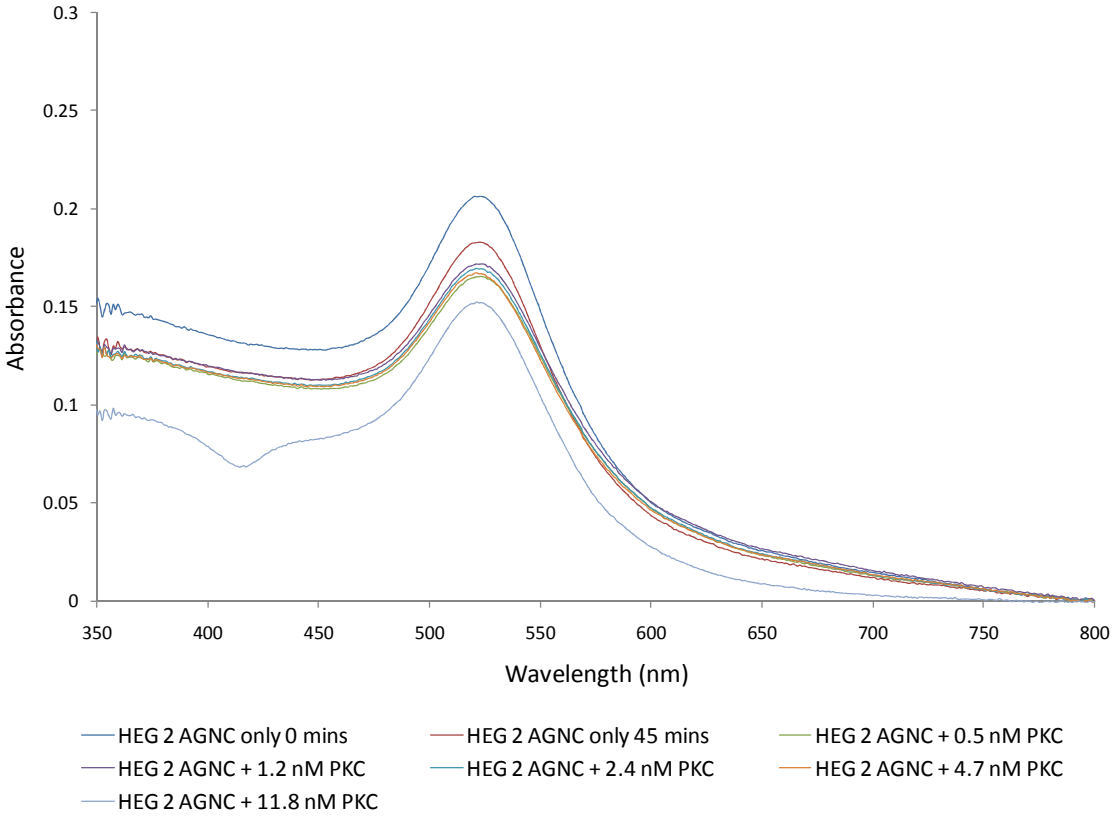

Figure 5.14: Overlaid spectra of HEG 2 conjugate (0.75 n M, 400 µL total volume in HEPES) in the presence of increasing concentrations of PKC.

As shown in Figure 5.14, there was a small drop in the absorbance when the HEG 2 PKC AGNC was incubated with 11.8 nM PKC (which corresponded to sample 1, protein : aptamer ratio of 5:1). For simplicity, no controls were included in this experiment. Had aggregation or a broadening of the plasmon occurred, a full assay (as carried out in section 5.4) would have been carried out. As was common to all experiments thus far, no observable shift in the plasmon resonance was observed for any of the samples. Figures 5.15 and 5.16 show the results obtained for the HEG 5 and HEG 9 PKC AGNC respectively.

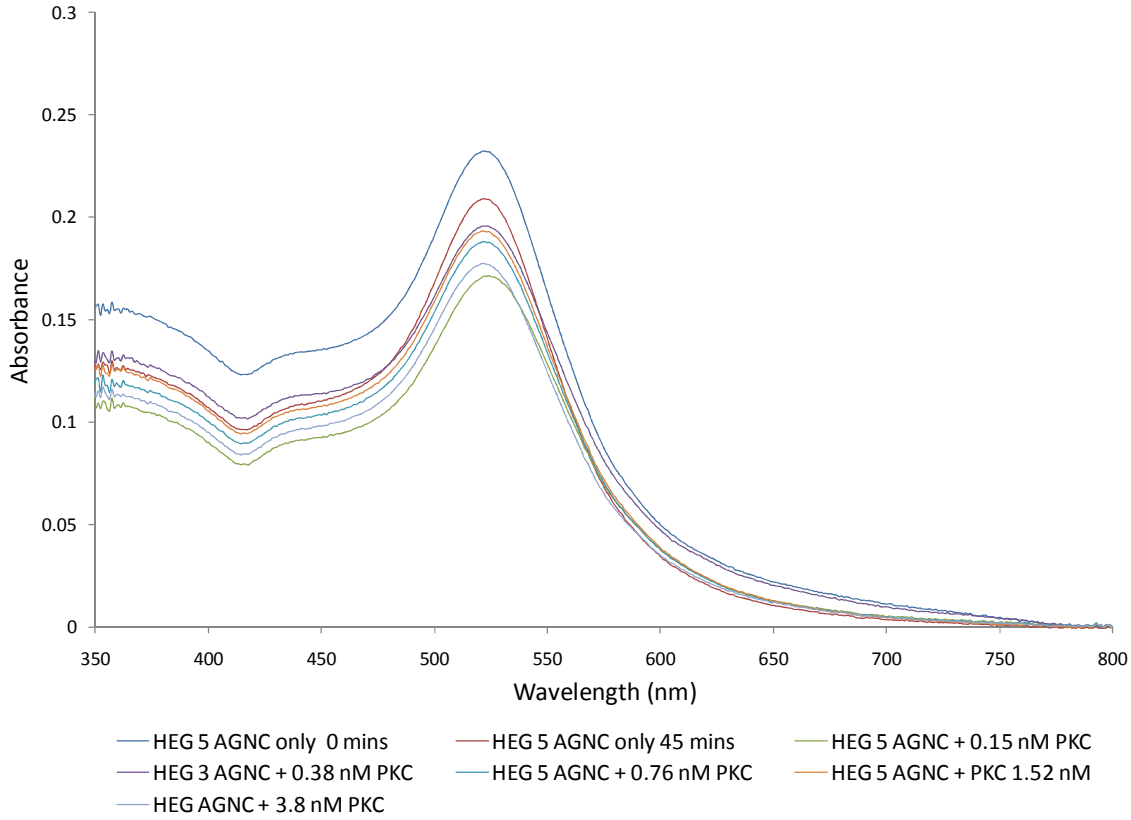

Figure 5.15: Overlaid spectra of HEG 5 conjugate (0.75 nM, 400 µL total volume in HEPES) in the presence of increasing concentrations of PKC.

No significant changes were observed in any of the samples. The largest drop occurred in HEG 5 PKC AGNC + 015 nM PKC (which corresponded to sample 5, protein : aptamer ratio of 1:5).

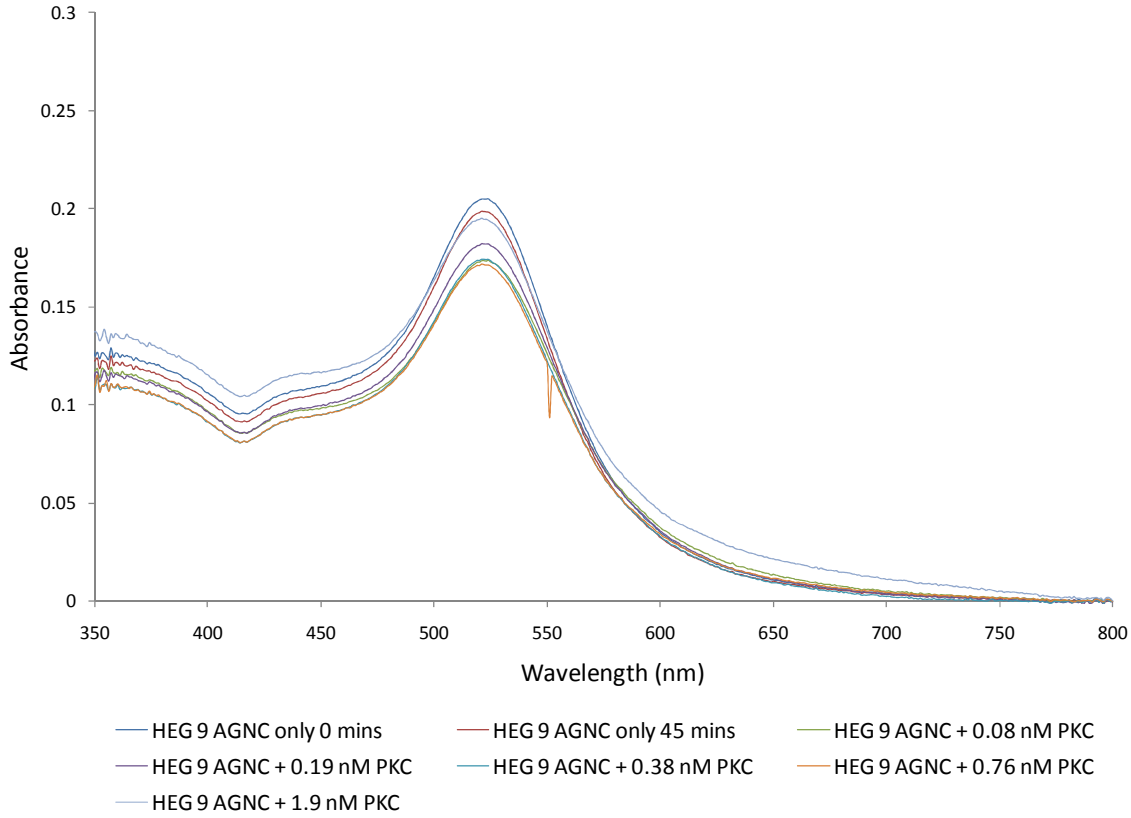

Figure 5.16: Overlaid spectra of HEG 9 conjugate ($7.6x10^{-10}$ M, 400 µL total volume in HEPES) in the presence of increasing concentrations of PKC.

As shown in Figure 5.16, the biggest drop in absorbance occurs in HEG 9 PKC AGNC + 0.76 nM. As with the results from the HEG 2 and HEG 5 conjugates, no shift in the wavelength of maximum absorbance is observed. It may be that there are still steric hindrance issues affecting the binding of aptamer and protein. The aptamer is directly attached to the nanoparticle and is surrounded by short 6 mer oligonucleotides. It could be theorised that the protein cannot "see" the full aptamer sequence and so binding is inhibited. This could be overcome by removing the aptamer sequence from the surface of the nanoparticle using spacer bases, for example 15 thymine bases at the 5' end.

5.5.5 15T spacer group work (linking spacer)

15 thymine bases were incorporated into the PKC aptamer sequence in addition to using the 6 mer hexaethylene glycol DNA (similar to the HEG 2 conjugates, see Table 5.2) to produce a mixed monolayer as shown in Figure 5.17. This was an attempt to incorporate both surface and linking spacers simultaneously.

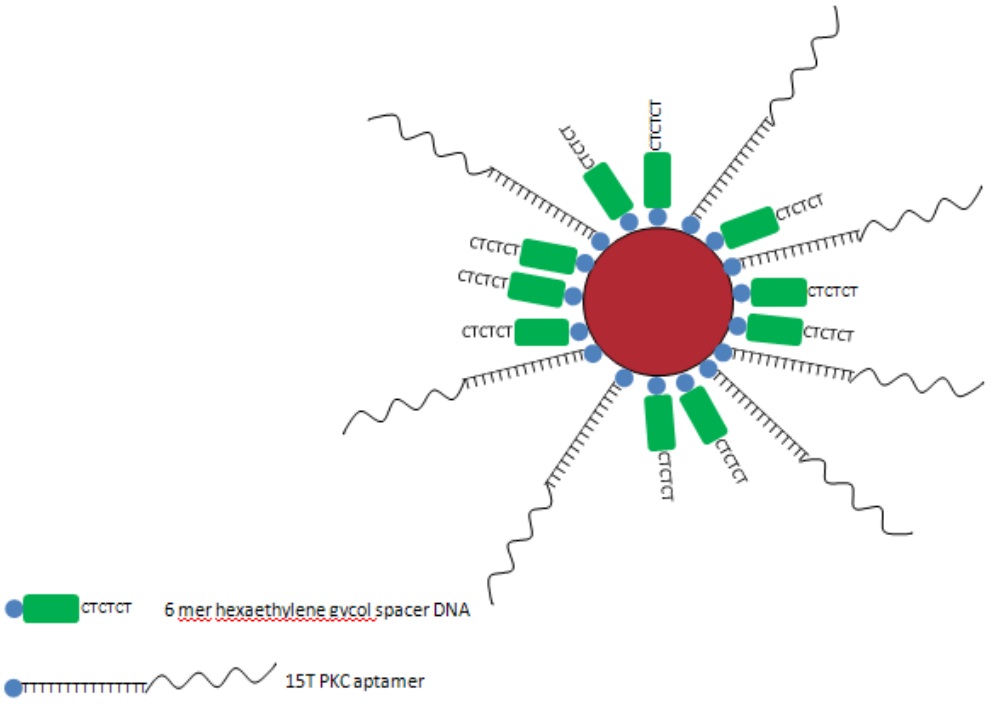

Figure 5.17: Illustration of I5T PKC AGNC HEG 2 (The blue circles represent the thiol modification and the green rectangles represent the HEG spacer).

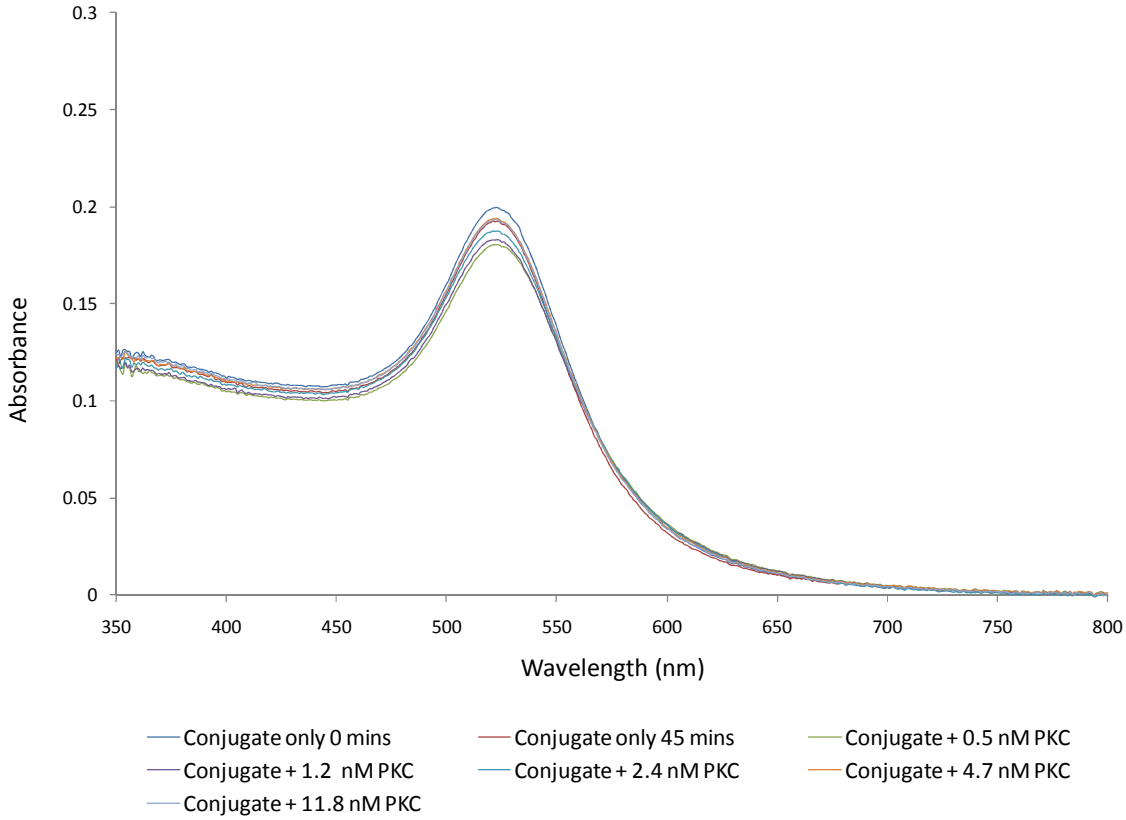

Figure 5.18: Overlaid spectra of 15T AGNC HEG 2 (7.6×10^{-10} M in HEPES) *in the presence of increasing concentrations of PKC.*

As with much of the work, there was no observable change in any of the spectra. As with the work carried out in section 5.5.4, no controls were analysed. Despite investigating a number of protein concentrations ranging from the aptamer being present at a 5× excess with respect to protein concentration to the protein being in a 5× excess with respect to aptamer concentration, no significant interactions were observed. It may be that significantly increasing the protein concentration, for example 50 or 100× excess may have caused a change in the surface plasmon resonance of the AGNC. However, limited supply of protein prevented this work from being attempted. It was, therefore, not possible to use UV-visible spectroscopy to monitor the interaction of aptamer and protein.

5.6 Conclusion

The successful conjugation of the PKC aptamer to gold nanoparticles was achieved and the presence of the DNA on the nanoparticle surface demonstrated using a variety of different characterisation techniques including UV-visible spectroscopy and gel electrophoresis. In addition, the quantification of the DNA on the nanoparticle surface was achieved using DTT displacement of fluorescently labelled aptamer molecules.

The number of aptamers attached to the surface of the nanoparticles was controlled through the use of a short six base DNA sequence. A total of four stable PKC AGNCs were successfully synthesised, with surface coverages ranging from 63 – 0.5 aptamers / NP.

Furthermore, simultaneous surface spacing using the 6 mer and the linker spacing using a 15T base group within the aptamer sequence was achieved.

A number of assays were carried out to determine whether UV-visible spectroscopy based detection of PKC could be achieved using the PKC AGNCs. All conjugate samples were investigated at a number of different concentrations but it was not possible to get a working assay based on this detection system. It may be that upon binding to PKC, the aptamer does not undergo a conformational change resulting in a change in the surface plasmon resonance of the nanoparticles and so a detection method based on UV- vis spectroscopy was not appropriate. It will be necessary to investigate other detection methods. Furthermore, it may be necessary to carry out fundamental work into the nature of the binding between aptamer and protein in order to gain a greater understanding. A technique such as isothermal titration calorimetry (ITC) could be useful. On the other hand, a solid phase detection approach (whereby the AGNC or the protein is immobilised) as opposed to a solution phase based method may overcome some of the problems encountered thus far.

6 Development of a Surface Enhanced Resonance Raman Scattering (SERRS) assay using thrombin aptamer gold and silver nanoparticle conjugates

6.1 Introduction

Aptamers have been combined with metallic nanoparticles in order to allow manipulation of optical, electronic and magnetic properties.[191, 201 191] Indeed, Chapter 5 detailed the potential use of gold nanoparticles functionalised with a PKC aptamer for use as a protein detection probe. There are also numerous studies in the literature in which gold nanoparticle – aptamer conjugates been used to detect a wide variety of targets, including thrombin,[121] adenosine[202] and cocaine.[203] One of the main advantages of using nanoparticles is the simplicity of detection, as a qualitative approach can be employed which exploits the colour change between aggregated and unaggregated particles. This type of study utilises molecular recognition events between aptamer and target, thus bringing nanoparticles into close proximity and causing aggregation. Another advantage of using nanoparticles is the ability to couple the analytical technique to surface enhanced resonance Raman scattering (SERRS) using a Raman active dye.

Silver and gold metallic nanoparticles have been used in extensively in biological type experiments and have been the subject of numerous reviews.[140 124 204] There are a number of reasons for this including the inert nature of the metals, the ability to control the size of

the nanoparticles[205] and the ease with which biomolecules can be attached.[206] Furthermore, gold nanoparticles are often preferred over silver. One of the main reasons is their increased stability (compared to silver).[139] [140] Another critical factor when studying biological interactions is cytoxicity. Gold is often the metal of choice as it is biocompatible and does not cause acute cytoxicity.[207] [208] In this chapter, thrombin aptamer functionalised nanoparticles were investigated as a potential biosensor to detect thrombin using SERRS analysis. Thrombin is an essential protein involved in the coagulation of blood and plays a regulatory role in other physiological processes.[209] It is a biologically relevant target and it is also one of the most well studied aptamers in the literature. Consequently, a great deal of data regarding the aptamer / protein complex has been aquired making it an ideal candidate for the development of a nanoparticle based detection system. The intial work into developing a novel thrombin detection system started with gold nanoparticles as optimisation would be easier. It would also be advantagoues to compare gold and silver nanoparticles in the same system to investigate which is the better substrate for enhancement.

The synthesis of the aptamer nanoparticle conjugates were carried out using a method detailed in Chapter 5 where thiolated DNA was direcly attached to the surface of the gold.

The thrombin protein has 2 DNA binding sites[146] and so could bind to two aptamers from two different nanoparticles thus inducing aggregation. It should be noted that the nanoparticles are labelled with many DNA molecules which is necessary for stablisation in the buffer. This phenomenon was expolited by Wilner *et al*. when they used DNA functionalised gold nanoparticles to indicate binding to thrombin through a change in the plasmon coupling. This shift can be monitored by UV – vis spectroscopy and is accompanied by a colour change. The experiments carried out by Wilner *et al*.[121] were used as the basis for the initial work, although some modifications to their assay were carried in order to simplify the protocol.

6.2 Au nanoparticle work

6.2.1 Synthesis of aptamer gold nanoparticle conjugates

The synthesis of gold colloid and the preparation of thrombin aptamer functionalised gold nanoparticle conjugates (AGNCs) were carried out as described in section 5.2. They were resuspended in 0.3 M PBS and their concentration determined by UV-visible spectroscopy.

6.2.2 Initial experiment

Although 0.3 M PBS was used to resuspend the AGNCs, the buffer used in the experiment originated from the work of Wilner *et al*. , as did the incorporation of 15T bases into the aptamer sequence.

Buffer: 34 mM Tris-HCl (pH = 7.4), 233 mM NaCl, 8.5 mM KCl, 1.7 mM CaCl2, 1.7 mM MgCl2, 8.5 % glycerol (v/v)

Sequence 5' - (thiol) TTTTTTTTTTTTTTTGGTTGGTGTGGTTGG – 3'

$6x10^{-10}$ M thrombin AGNCs were incubated with increasing concentrations of thrombin; 0 - 200 nM. The samples were left for 45 minutes and then their UV-vis spectra taken. It was necessary to include a protein control and a DNA control to ensure any experimental observations were attributable to specific aptamer – protein recognition as opposed to a non-specific protein – DNA interaction.

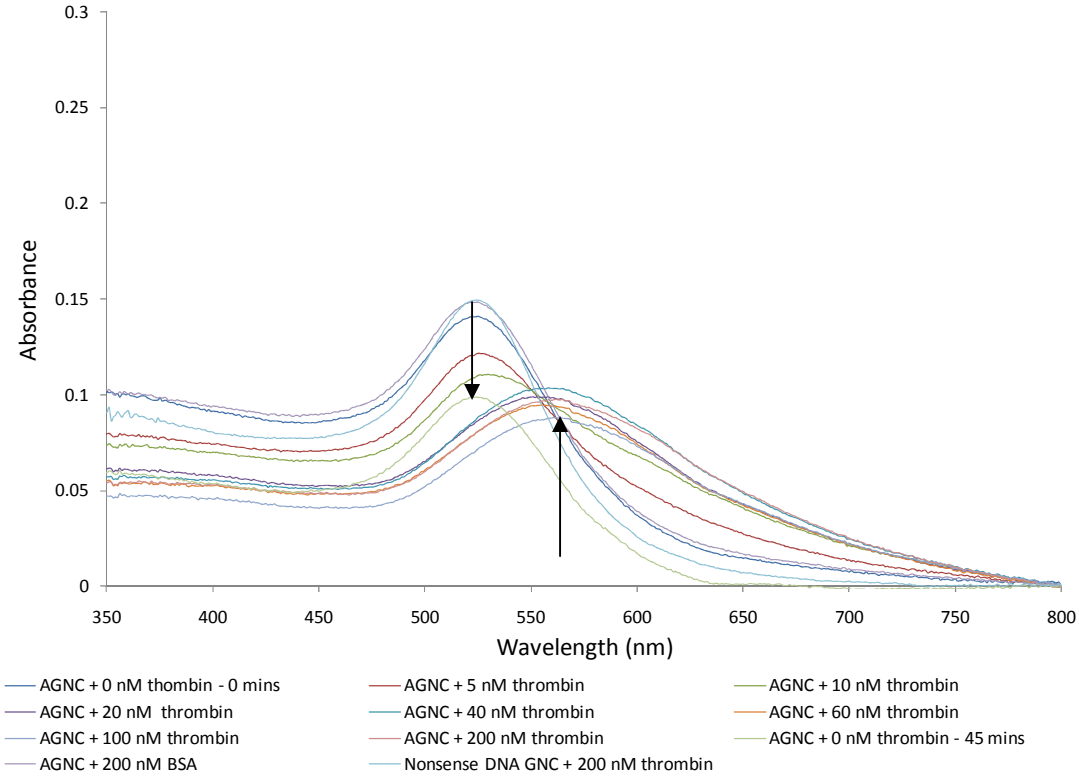

Figure 6.1: Overlaid spectra of AGNCs (0.6 nM) with increasing concentrations of thrombin.

There is a steady shift in the plasmon resonance peak of the nanoparticle sample as the concentration of thrombin increases. Indeed, a significant change occurs after the addition of 60 nM thrombin. As shown by the arrows, a decrease in the peak at ~ 520 nm occurs in addition to the emeregence of a peak at ~ 560 nm. In the presence of a control protein, BSA, no such change is observed indicating that a specific reaction between thrombin and aptamer is taking place. The other control, the use of nonsense DNA GNCs incubated with 200 nM thrombin showed no aggregation. Again, this reinforces the theory that a specific reaction is occurring between the aptamer and protein. The other noteworthy comment from this experiment is the stability of the conjugates. When comparing 0 nM - 0 mins with 0 nM - 45 mins, it would appear that in the absence of thrombin, there is a drop in the peak, indicating that the buffer itself is causing some aggregation. Buffer induced aggregation does pose a problem for nanoparticles due to the presence of metal cations and counter ions. The charged particles can interfere with the repelling forces between the nanoparticles, disrupt monodispersity and cause aggregation. Consequently, other buffers were investigated to

overcome this problem.

6.2.3 Phosphate buffered saline experiment

When studying biological interactions, it is necessary to mimic physiological conditions. Phosphate buffered saline (PBS) is often used for this purpose due to its desirable pH range and the presence of NaCl. Sodium chloride is an essential component of nanoparticle buffers as it facilitates high surface coverage of DNA onto the nanoparticle. As before, the conjugates were resuspended in the buffer of interest (PBS), thrombin added, incubated for 45 mins and analysed by UV – vis spectroscopy.

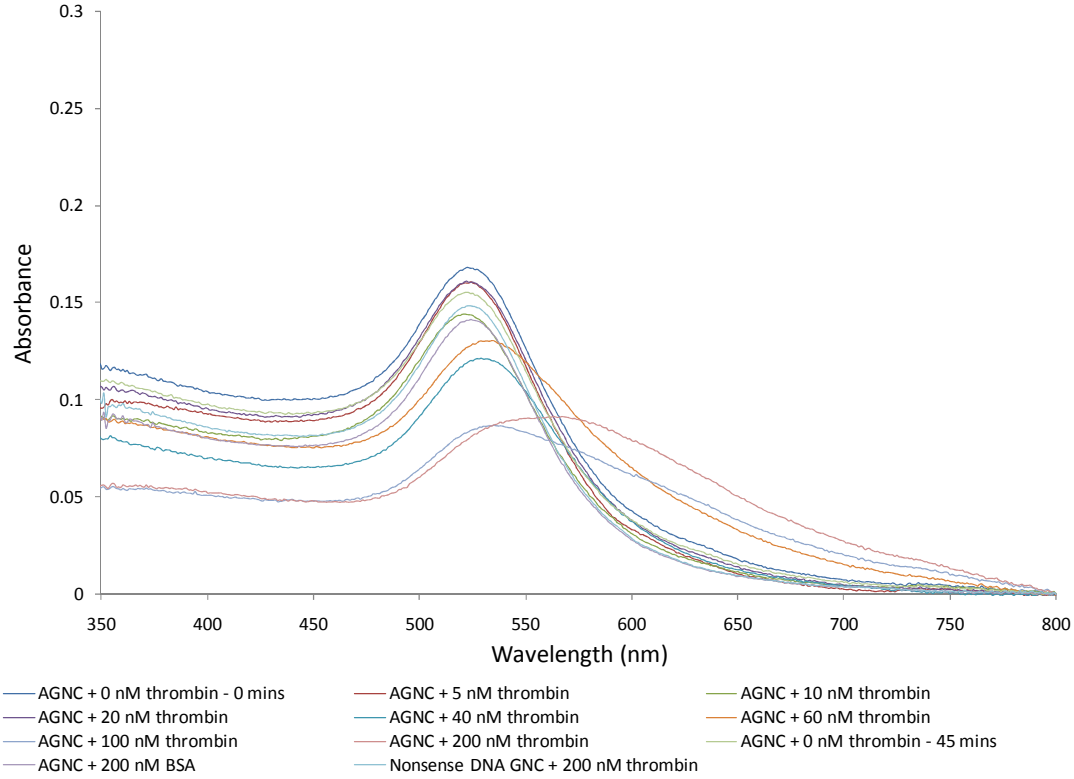

Figure 6.2: Overlaid spectra of thrombin AGNCs (0.6 nM in 0.3 M PBS) in the presence of increasing concentrations of thrombin.

The stability of the conjugates has seen a marked improvement when comparing the results

from Figure 6.2 with Figure 6.1. In the absence of thrombin, there is very little change in the conjugates after the 45 minute incubation (when comparing 0 nM – 0 mins to 0 nM – 45 mins) indicating no aggregation is taking place in the buffer. This is obviously an improvement however; there is compromise between stability and sensitivity. In the previous experiment (see Figure 6.1), 60 nM thrombin was sufficient to cause a significant shift in the plasmon. In this experiment, however, a similar shift is only observed after the addition of 100 nM. Several studies indicate that the presence of potassium ions is essential for the formation of the characteristic G – quartet present when the thrombin aptamer binds to the protein.[210 211] As such, an experiment investigating varying concentrations of KCl was carried out in order to increase the sensitivity of the assay.

6.2.4 KCl optimisiation

In this study, 3 different concentrations of KCl (in 0.3 M PBS) were attempted. In each experiment, 3 samples were made up; AGNC in the absence of thrombin at time = 0 and at time = 45 minutes and AGNC in the presence of 60 nM thrombin at time = 45 minutes. The concentration of thrombin was chosen as previous work (summarised in Figure 6.1) indicated that this concentration caused a significant change in the plasmon resonance of the nanoparticles. The samples were also analysed in the absence of thrombin in order to assess the stability of the conjugates in ach of the buffers.

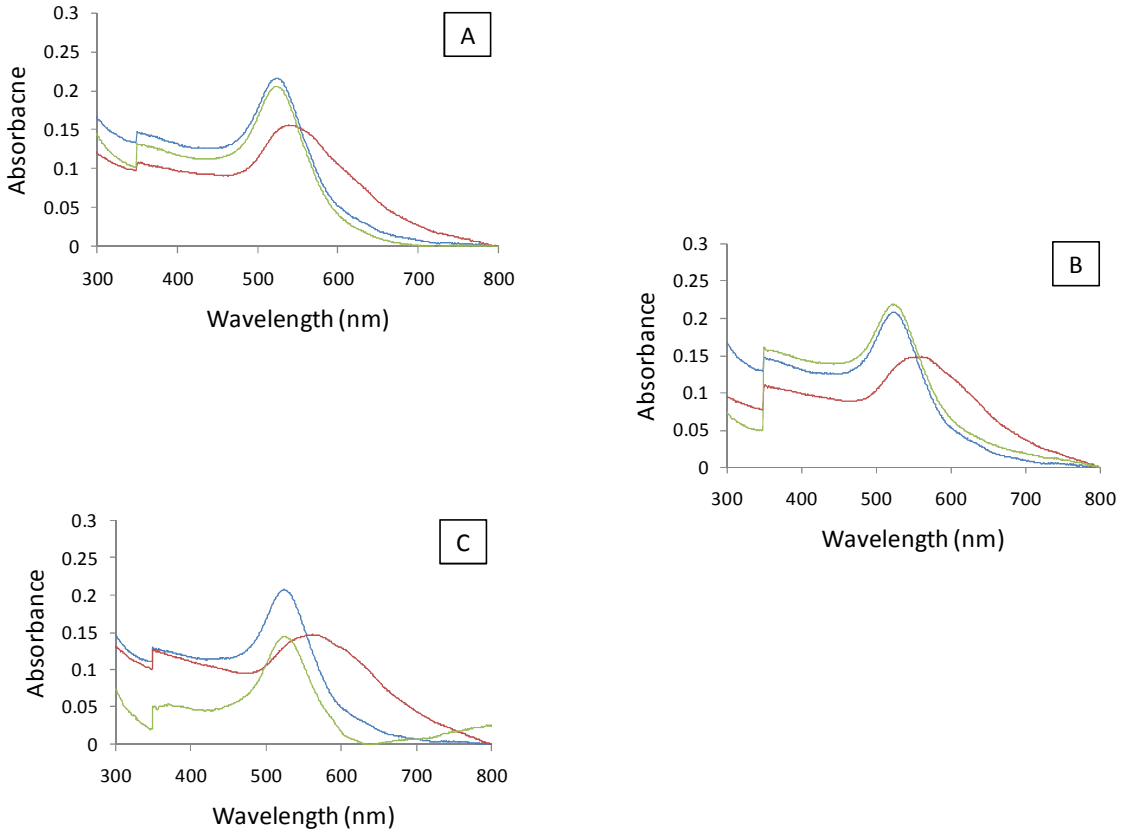

Figure 6.3: Graphs of the different KCl buffers A - 0.01 M, B – 0.1 M and C – 0.3 M. Blue line AGNC only @ t = 0 mins, green line AGNC only @ t = 45 mins and red line AGNC + 60 nM thrombin @ t = 45 mins.

There was no real difference between 0.01 and 0.1 M KCl (comparing A and B). However, upon increasing the concentration of KCl to 0.3 M there is a decrease in stability of the conjugates. The concentration of KCl used in all subsequent work was 0.01 M as no real advantage was gained by using the higher (0.1 M) concentration and it is generally desirable to have a low concentration of cations in buffers used for nanoparticle work. Similar work was carried out with $CaCl_2$ and MgCl. No real benefit was achieved by the introduction of more cations and so the optimised buffer was found to be 0.21 M NaCl, 0.01 M KCl, 9 mM Na phosphate buffer pH 7.5. All subsequent experiments were carried out in this buffer and referred to as thrombin binding buffer.

6.2.5 Optimised buffer assay

Thrombin binding buffer, 0.21 M NaCl, 0.01 M KCl, 9 mM Na phosphate buffer pH 7.5, was compared to the buffers used earlier by repeating the assay with increasing concentrations of thrombin, as detailed in section 6.2.2.

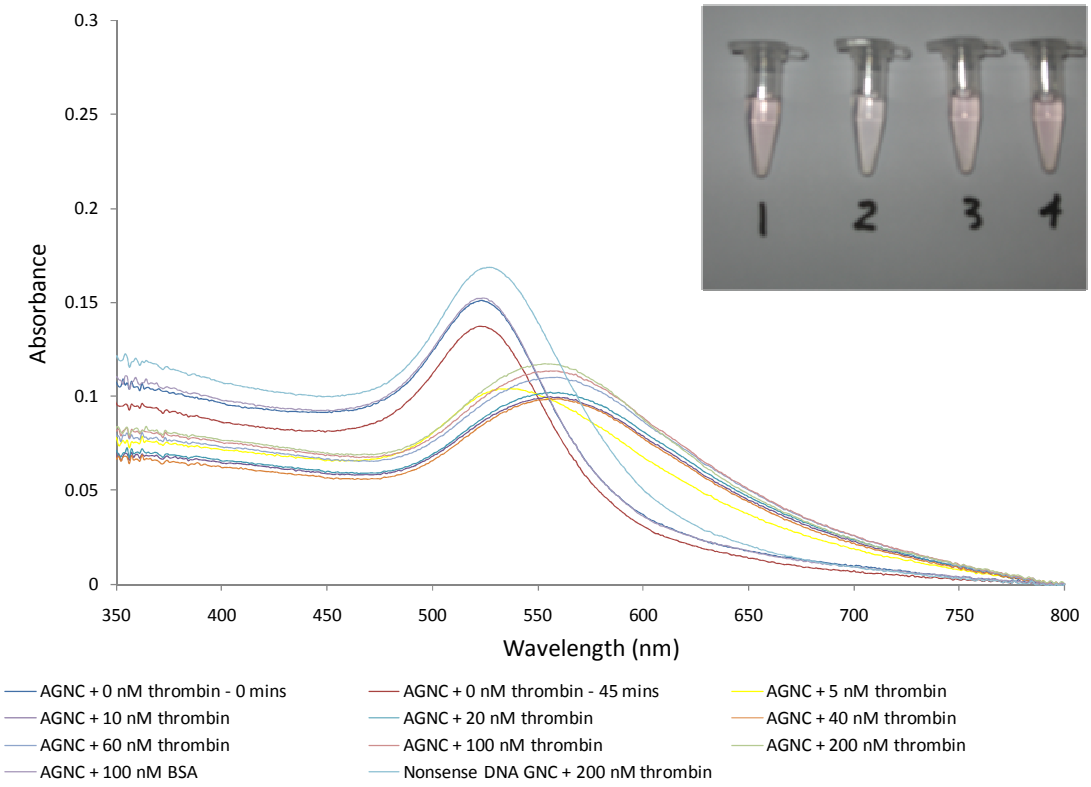

Figure 6.4: Overlaid spectra of thrombin AGNCs (400 µL, 0.6 nM in thrombin binding buffer) in the presence of increasing concentrations of thrombin. Insert, photograph of 1) conjugate in presence of buffer only, 2) conjugate in the presence of 200 nM thrombin, 3) conjugate in the presence of 200 nM BSA and 4) nonsense conjugate in the presence of 200 nM thrombin.

In thrombin binding buffer, the conjugates appear to be relatively stable as there is little difference in the sample after being exposed to the buffer for 45 minutes (comparing 0 nM – 0mins with 0 nM – 45 mins). Both DNA and protein control samples do not show evidence of aggregation and significant aggregation occurs after the addition of only 5 nM. The use of this buffer does increase sensitivity as in previous work a concentration of thrombin in excess of 60 nM was required to cause similar aggregation. The photograph indicates the visible colour

change arising from the thrombin induced aggregation. This was a significant result and improved on the work carried out by Wilner *et al*. Our method was more sensitive as their system required in excess of 100 nM thrombin to achieve aggregation as opposed to 5 nM in our system. In addition, our method was simpler and involved fewer steps, allowing for a quicker analysis. Due to the success of the gold nanoparticle work, it was decided to attempt similar work using silver nanoparticles.

6.3 Ag nanoparticle work

6.3.1 Introduction

There was a number of reasons why it would be advantageous to expand the concept to silver nanoparticles. Gold nanoparticle studies feature extensively in the literature and so it would be useful to investigate another metal. Silver nanoparticles have a greater extinction coefficient and so are inherently more sensitive.[138] Consequently, analytical techniques could be improved by substituting silver in place of gold nanoparticles.

As discussed in the Introduction, nanoparticles allow for the incorporation of SERRS analysis (providing a chromophore is present either in the analyte or incorporated as a label). The silver conjugates used in the subsequent section of work originated from previous studies carried out within the Graham group.[212 213] The silver nanoparticles were coated with a mixed monolayer containing the DNA aptamer and a benzotriazole dye, as shown in Figure 6.5.

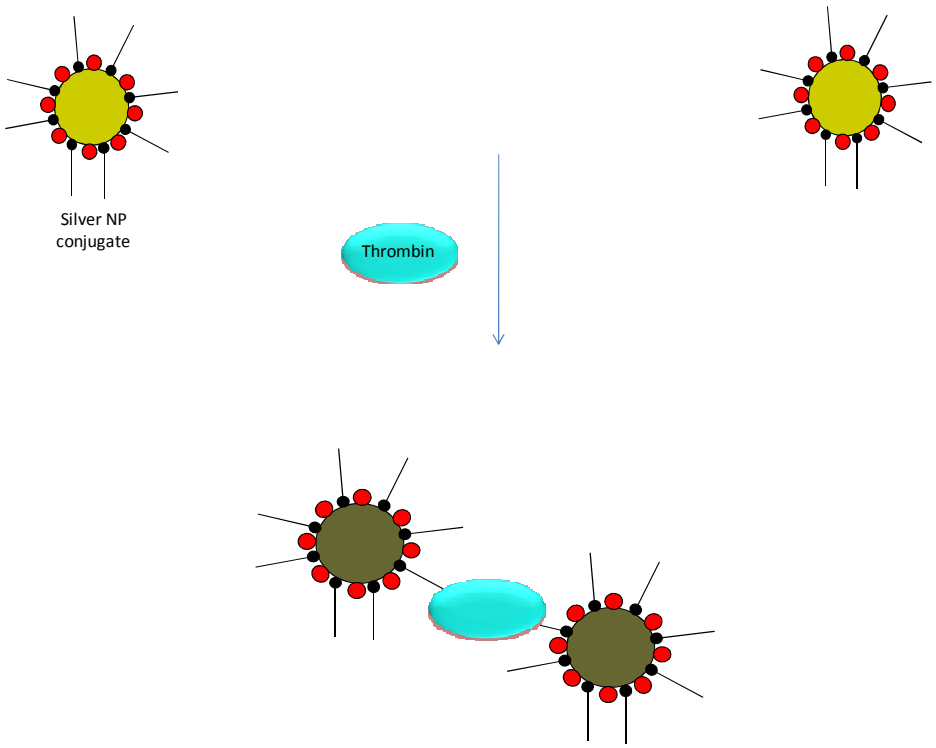

Figure 6.5: In the presence of thrombin, two nanoparticles are brought into close proximity causing aggregation and producing a colour change. (Aptamer shown in black and dye shown in red, not to scale).

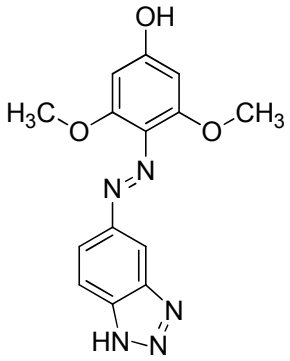

Figure 6.6: Structure of (E)-4((1H-benzo[d] [1,2,3] triazole-5-yl) diazenyl)-3,5-dimethoxy phenol (BDTDD), the SERRS active dye.

The benzotriazole moiety present on the BDTDD dye (as shown in Figure 6.6) has a high affinity for the silver surface so direct attachment of the label was achieved through this surface seeking group. Thiolated DNA was also directly attached thus creating a mixed monolayer on

the surface of the nanoparticle. In theory, the aggregation caused in the presence of thrombin should produce a large increase in SERRS intensity. The SERRS process is very complex and there are many factors affecting the enhancement. It consists of both a surface enhancement (due to the presence of the nanoparticles) and a resonance enhancement (from the dye). It is generally accepted that the enhancement factor (EF) can be greatly increased through the aggregation of such dye coated nanoparticles.[154] It is due to the formation of areas of high electric field in between the aggregated nanoparticles (so called "hot spots") which is responsible for the SERRS enhancement.[214] [215] [216] Indeed this phenomenon is observed in the system when applied to DNA – DNA hybridisations. Before SERRS could be carried out, it was necessary to ensure the UV-visible spectroscopic data observed with gold were also observed with silver. The work was repeated, however, with a lower concentration of nanoparticles. As mentioned previously, silver nanoparticles have a higher extinction coefficient than gold and consequently a lower concentration is required.

6.3.2 Synthesis of aptamer functionalised Ag nanoparticle conjugates

Silver nanoparticle synthesis involved the citrate reduction of a silver salt to yield spherical nanoparticles approximately 40 nm in diameter.[217] The synthesis of thrombin aptamer functionalised silver conjugates (ASNCs) were carried out using thiolated DNA a Raman active dye according to published methods.[212] Briefly, colloidal silver was functionalised with dye (1 μM final concentration) and left overnight. Thiolated DNA (10 nmoles) was then added and left overnight. Sodium phosphate and salt additions were carried out gradually over 3 days before the conjugates were resuspended in 0.3 M PBS. Silver nanoparticle conjugation had been carried out extensively in house and numerous studies indicate that a 3 day process is optimal. UV – vis analysis was carried out to compare "bare" colloid with the DNA conjugated nanoparticles.

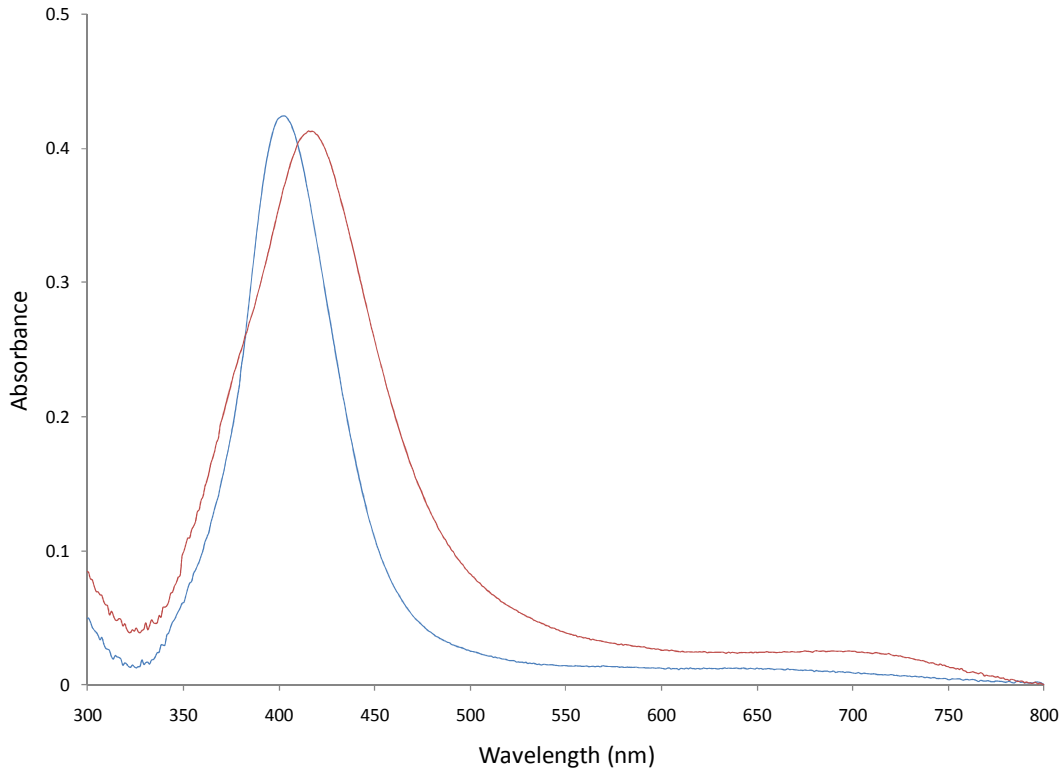

Figure 6.7: Overlaid spectra of silver colloid (15 pM in water, blue line) and thrombin ASNC (15 pM in PBS, red line).

There is a slight shift in the wavelength of maximum absorbance which corresponds to the change in the environment of the nanoparticles that is the attachment of DNA and dye molecules onto the surface.

6.3.3 UV – vis spectroscopy assay

The assays carried out with AGNCs were repeated with ASNCs, with a slight variation on the concentrations used; 10 pM silver conjugate compared with 600 pM of Au conjugate. Consequently, a lower concentration of thrombin was also used: 0, 1, 2, 5, 7, 10 and 20 nM.
Two control samples were also analysed:

Control DNA - 5’ SH AAAAAAAAAATCTCTACTC

Control protein - BSA

The DNA sequence used for the control sample was chosen as this conjugate was in use in the group so and the sample was known to be stable. As before, all samples were left to incubate at room temperature for 45 minutes and then a UV – Vis spectrum was recorded.

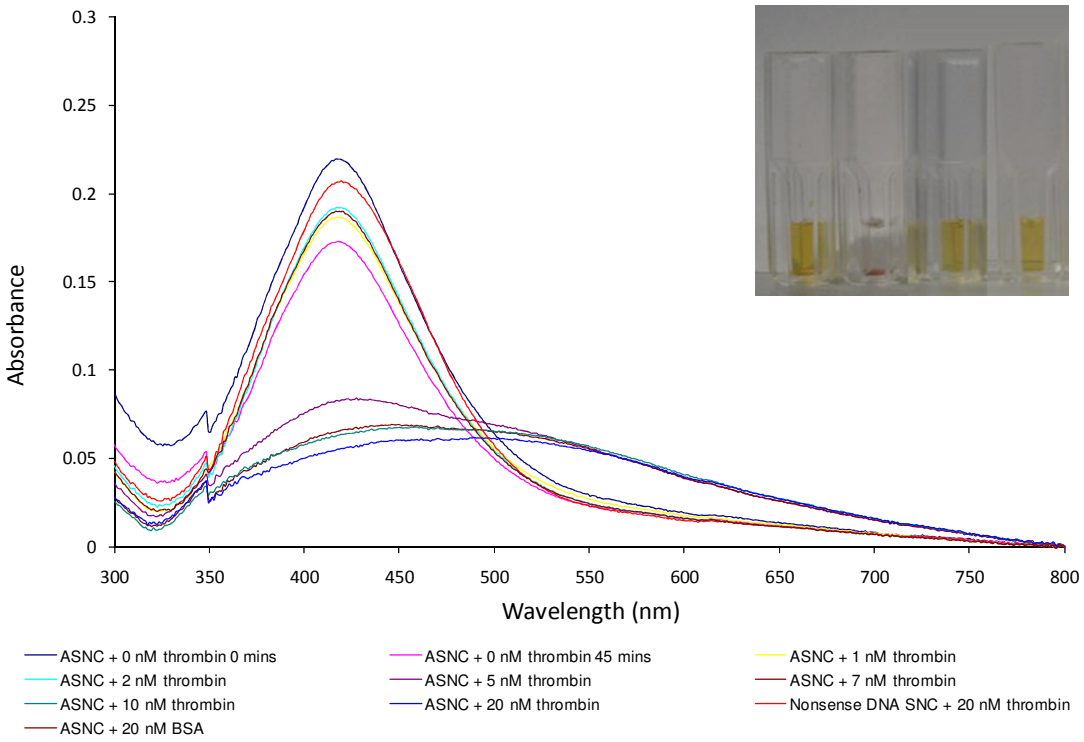

Figure 6.8: Overlaid spectra of ASNCs (10 pM in thrombin binding buffer) with increasing concentrations of thrombin. Insert, photograph of (from left to right) conjugate in presence of buffer only, conjugate in the presence of 20 nM thrombin, conjugate in the presence of 20 nM BSA and control DNA SNC in the presence of 20 nM thrombin.

This was a good result as significant aggregation is observed from a low thrombin concentration, 5 nM, indicating it is a sensitive technique. No such aggregation was seen in the nonsense DNA control or when the thrombin ASNC were exposed to a non specific protein (BSA). In the absence of thrombin (comparing 0 nM – 0 mins with 0 nM – 45 mins) a small drop in absorbance occurred. This result offered significant advantages over the gold work. There is a large increase in sensitivity in this system; there was a 60 fold decrease in conjugate concentration when comparing ASNC with AGNC. The aggregation is also accompanied by a

colour change (also present in the gold work) but the colour change is far more pronounced and easier to see with the naked eye (compare with insert from Figure 6.4). Although a detection limit of 5 nM was quoted, this was based on an arbitrary point of aggregation chosen, that is, the point at which the absorbance dropped below 0.1 accompanied by a broadening of the peak. A detection limit experiment was performed using replicate samples in order to calculate the lowest concentration at which thrombin could be detected.

6.3.4 Visual limit of detection study

In this study, 10 pM of thrombin ASNC was incubated with 0, 2, 5, 10, 20 and 30 nM thrombin, left for 45 mins and then analysed. All samples were made up in 5 replicates with the results shown in Table 6.1 and plotted and displayed in Figure 6.9.

Table 6.1: Data arising from the concentration study

Concentration of thrombin (nM)	0^a	0^b	2	5	10	20	30
Average absorbance	0.2892	0.2648	0.2551	0.2428	0.2009	0.0817	0.0784
Standard deviation	0.0163	0.0191	0.0136	0.0126	0.0297	0.0130	0.0090
Change in absorbance*		0.0244	0.0341	0.0464	0.0883	0.2075	0.2107

a – absorbance of ASNC at t = 0minutes
b - absorbance of ASNC at t = 45minutes
* - calculated as $0^a - x$ (where x is the maximum absorbance of the ASNC in varying concentrations of thrombin)

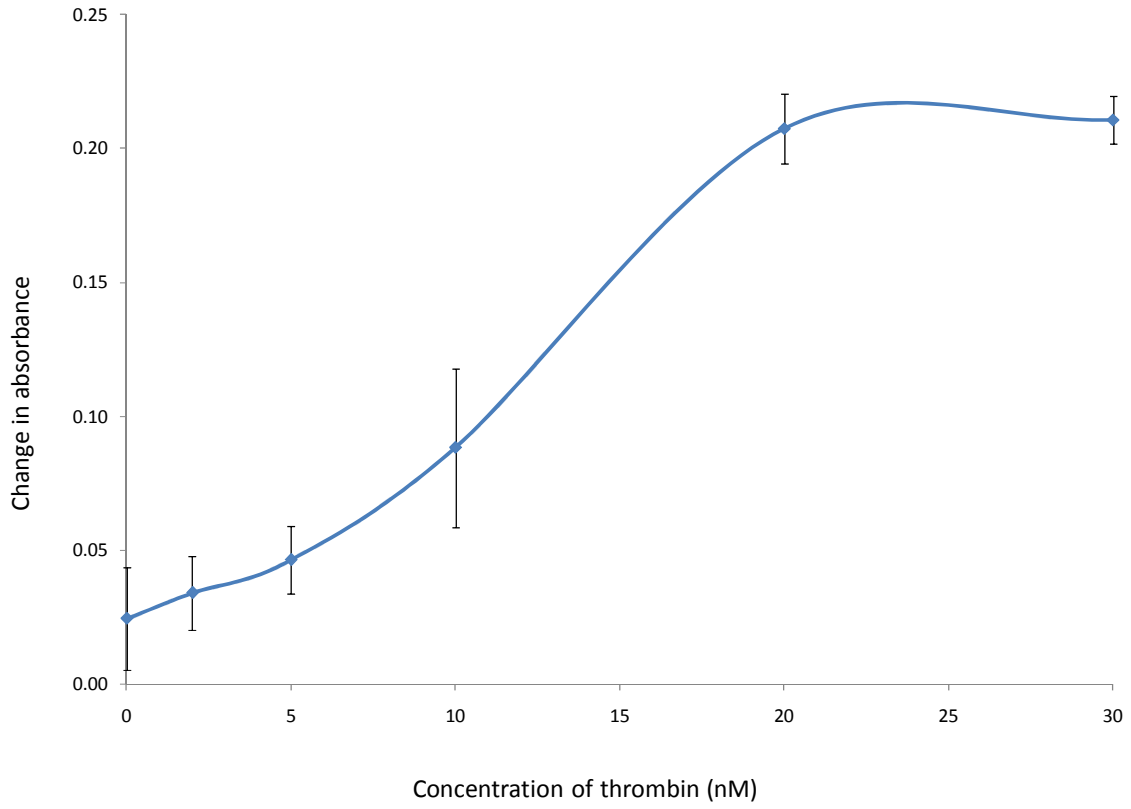

Figure 6.9: Plot of change in absorbance of ASNC (10 pM) as a function of thrombin concentration. (The error bars are the standard deviation).

The change in absorbance in the absence of thrombin i.e. absorbance at t = 0 minutes – absorbance at t = 45 minutes is set as the background signal. Three times the background change (3 x 0.0244) 0.0732 is taken as the visual limit of detection and therefore indicated that 10 nM thrombin is the lowest detectable concentration.

6.3.5 Time study

An investigation into the performance of the conjugates over time was carried out. This could indicate the nature of the aggregation process and the optimum incubation time necessary to observe significant aggregation. As with previous work, 10 pM was incubated with 20 nM thrombin and analysed by UV-vis spectroscopy every 5 mins from 0 – 90 mins.

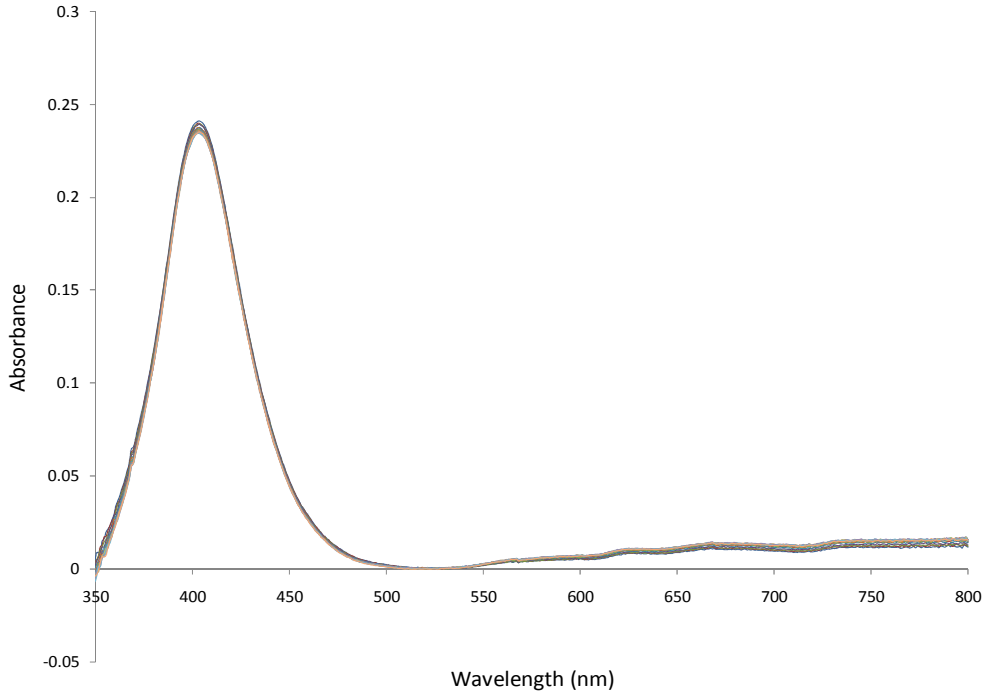

Figure 6.10: Overlaid spectra of ASNC (10 pM) in buffer only over a series of time intervals (0 – 90 minutes).

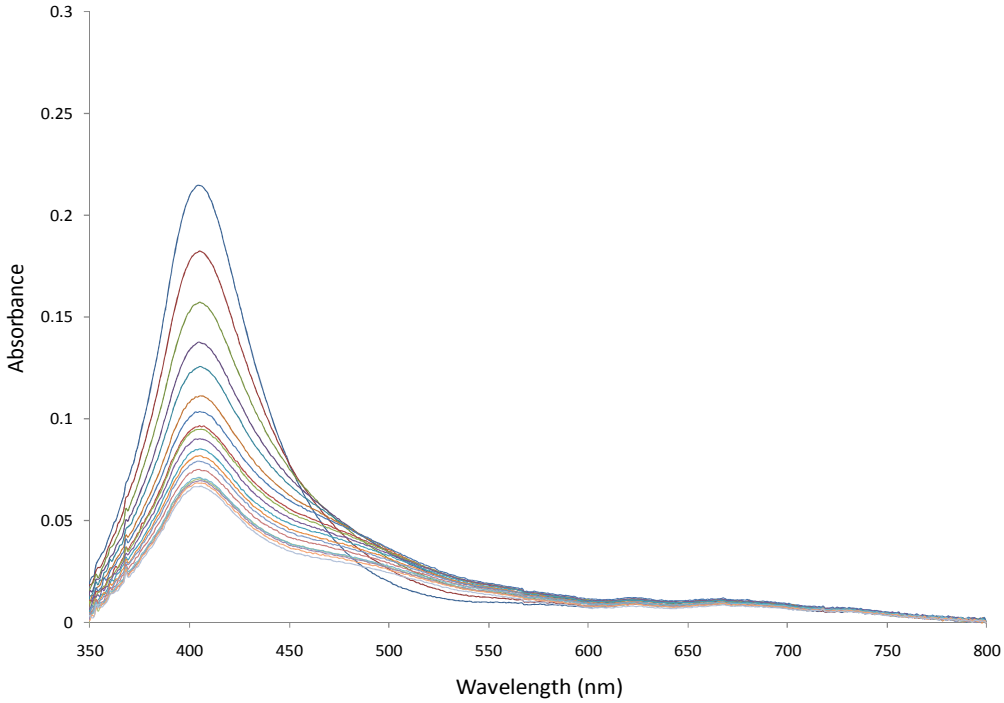

Figure 6.11: Overlaid spectra of ASNC (10 pM) in the presence of 20 nM thrombin over a series of time intervals (0 – 90 minutes).

As shown in Figure 6.11, there is a steady drop in the plasmon of the sample as a function time. It would appear that leaving the conjugates for 90 minutes does result in a greater degree of aggregation though a 45 minute incubation time does result in significant aggregation.

After an extensive study into UV – visible spectroscopic analysis, a new detection method was investigated, namely, SERRS.

6.3.6 Initial SERRS work

The ultimate aim of this body of work was to create a SERRS assay to detect thrombin. The requirements for such analysis are a roughened surface, a chromophore and laser light of a wavelength that closely matches the wavelength of the maximum absorbance of the dye and the surface plasmon resonance of the aggregated nanoparticles. There is often a compromise between access to lasers of different wavelengths, and matching it with the other variables. Figure 6.12 summarises the relationship between the components in the experimental set-up.

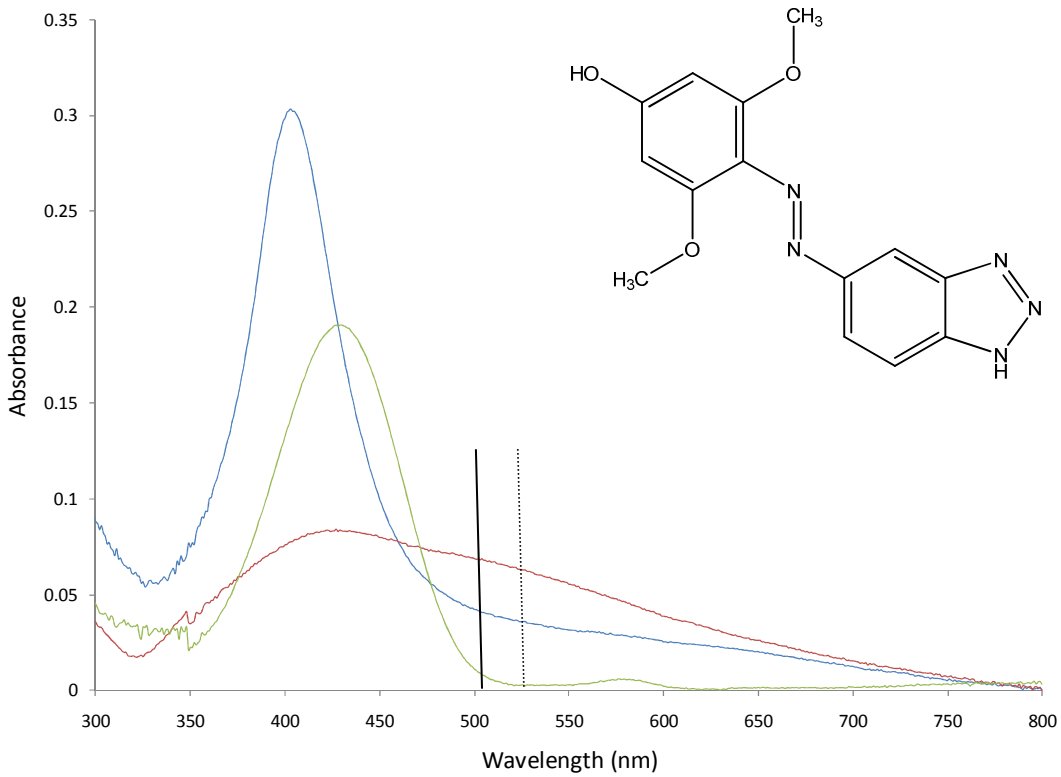

Figure 6.12: Overlaid spectra of BDTDD dye (10 µM, green line), silver nanoparticles, (15 pM in 0.3 M PBS, blue line) and thrombin induced aggregation of ASNC, (15 pM in thrombin binding buffer, red line). The structure of BDTDD dye is shown in the insert and the lines indicate laser excitation wavelengths (514.5 nm, solid line and 532 nm, dashed line).

Aggregated nanoparticles have an absorption maximum at ~ 430 nm (as opposed to the un-aggregated nanoparticles at ~ 400 nm). The wavelength of the absorption maximum of the dye closely matches that of the aggregated nanoparticles. The two available laser excitation wavelengths were 532 and 514.5 nm, as indicated in Figure 6.12. Although not coincident with the surface plasmon resonance of the aggregated nanoparticles and the dye, there is sufficient absorption at both laser lines for SERRS to be a viable technique.

The initial SERRS experiments were carried out to investigate the optimum laser wavelength and most appropriate analysis format, as summarised in Table 6.2.

Table 6.2: Summary of different SERRS experiments.

Wavelength (nm)	***Analysis format***
523	Cuvette
514.5	Microtitre plate
514.5	Cuvette

When analysing the results, the following parameters were considered; good signal to noise ratio, well pronounced characteristic peaks and the absence of interference from plastic. A selection of results from the optimisation work is illustrated in Figures 6.13 and 6.14.

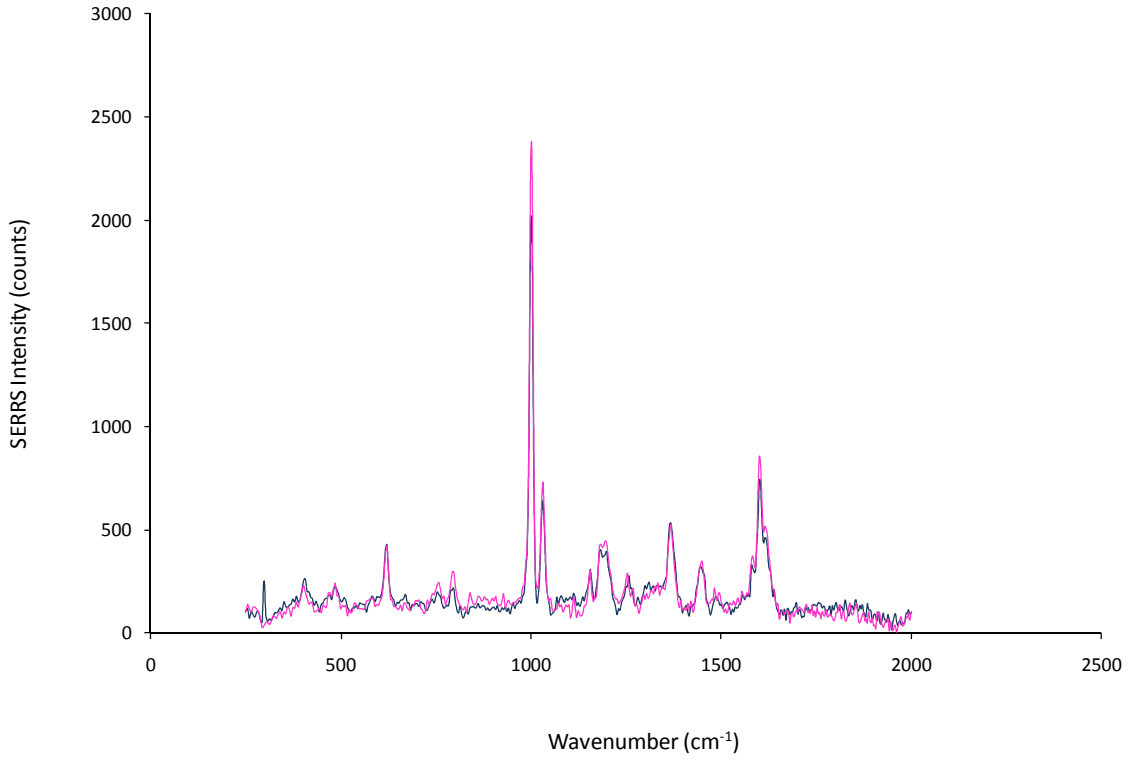

Figure 6.13: Overlaid SERRS spectra (recorded using 532 nm laser excitation and cuvette based sample analysis) of 50 pM conjugate with 0 nM thrombin (blue line) and 5 nM thrombin (pink line).Measurements recorded after 45 minutes.

Figure 6.13 illustrates the issues regarding signal to noise ratio. There is poor signal to noise

ratio present especially in the region 1500 – 2000 cm^{-1}. In addition, the largest peak (located at 1000 cm^{-1}) is due to plastic interference.

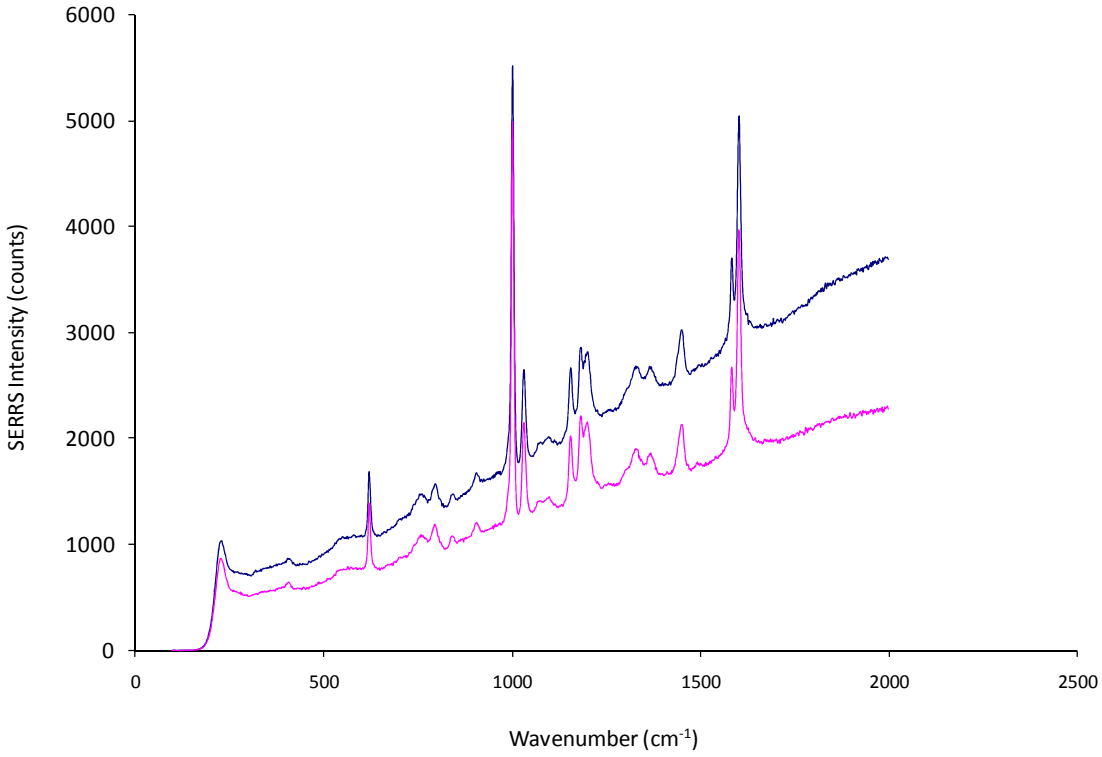

Figure 6.14: Overlaid SERRS spectra (recorded using 515.4 nm laser excitation and microtitre plate based sample analysis) of 50 pM conjugate with 0 nM thrombin (blue line) and 5 nM thrombin (pink line.) Measurements recorded after 45 minutes.

Figure 6.14 highlights another problem observed in the optimisation work. Baseline "drift" was present, whereby the baseline was elevated. Ideally, a flat baseline should be observed and this can be achieved using background correcting software. This is not an automatic process and can introduce additional variation into the sample analysis if the correcting is not carried out exactly the same way each time. As with the spectra in Figure 6.13, a plastic peak is also present.

Results indicated that the 514.5 laser line combined with cuvette based analysis was the most appropriate. In addition, cuvette based analysis is more reproducible, possibly due to the fact that the bulk solution is sampled during analysis as the laser passes through the whole cuvette

as opposed to microtitre plate analysis where only the top surface of the liquid is sampled.

6.3.7 Cuvette based SERRS at 514.5 nm

Numerous experiments were carried out using SERRS analysis at 514.5 nm. Included below is a selection of results summarising the findings. Initially, samples were analysed in triplicate and their spectra plotted.

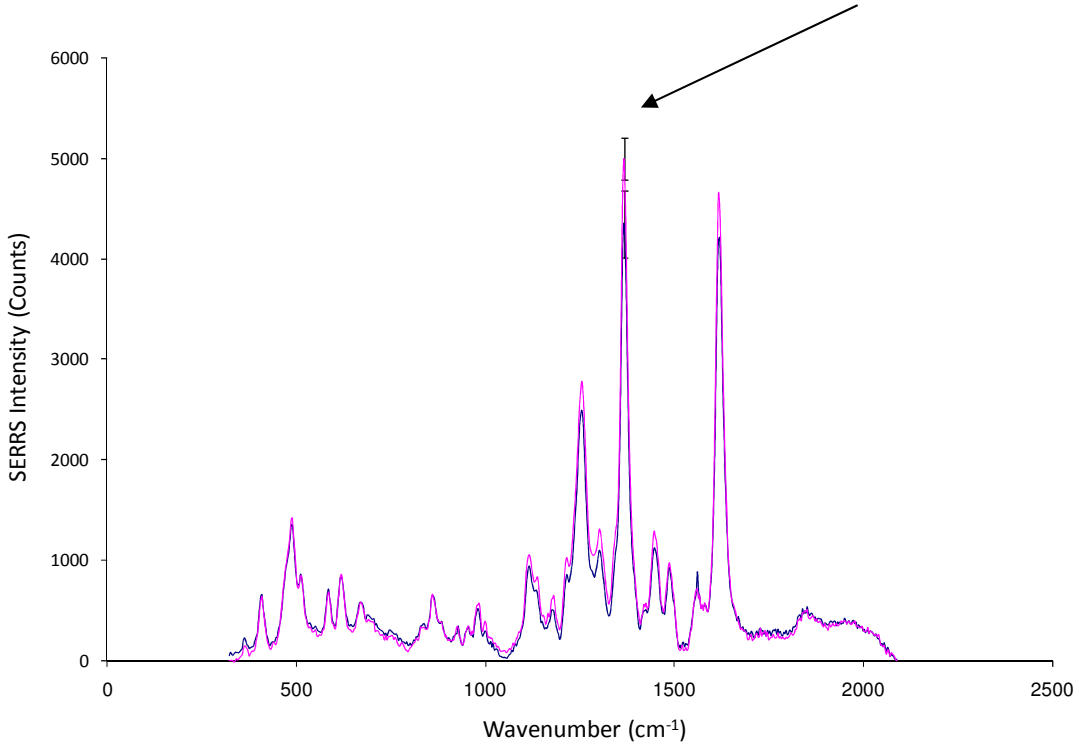

Figure 6.15: Overlaid SERRS spectra of 50 pM conjugate with 0 nM thrombin (blue line) and 5 nM thrombin (pink line). Error bars plotted using standard deviation of the intensity at 1368 cm^{-1} marked with an arrow).

SERRS analysis was carried out after 45 minutes and upon visual inspection, the sample containing thrombin did aggregate. However, a large increase in SERRS intensity did not accompany the aggregation. Incubation time was investigated as although 45 minutes was suitable for the UV-vis spectroscopy analysis, this may not have been ideal for SERRS analysis.

Consequently, a time study was set-up to determine the optimum length of incubation time which would produce a SERRS signal with the greatest intensity from the aggregated nanoparticles. A study was carried out which analysed the ASNC samples (50 pM) and nonsense DNA SNC samples in the absence of thrombin, control protein and absence of thrombin at 0, 5, 15, 30, 45, and 60 minute time intervals.

Five replicate samples were analysed, 2 different thrombin concentrations were investigated and two control samples were also included.

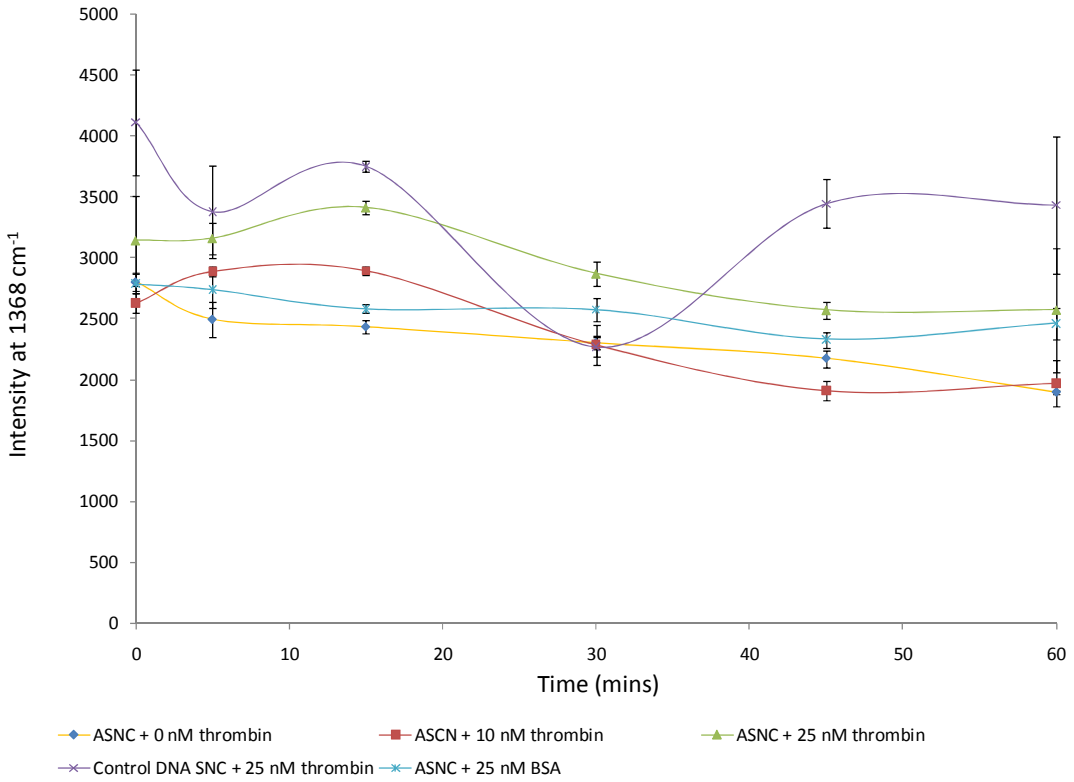

Figure 6.16: Plot of SERRS intensity at 1368 cm^{-1} against time. All five samples were overlaid with the standard deviation represented by the error bars.

There is very little difference between all five samples. The large error bars indicate that he signals observed were variable and no enhancement was observed for the "positive" thrombin samples.

Before considering other options and to complete this section of work, a concentration study

was set up to see if there was an optimal concentration of thrombin which would produce a large SERRS response.

Although, concentration studies were carried out in the UV – vis experiments, it was necessary to repeat the work with SERRS. As with the time studies, the peak at 1368 cm^{-1} was chosen and its intensity monitored after the addition of increasing concentrations of thrombin. 10 pM ASNC was incubated with 0 – 10 nM thrombin for 45 minutes and then analysed by SERRS.

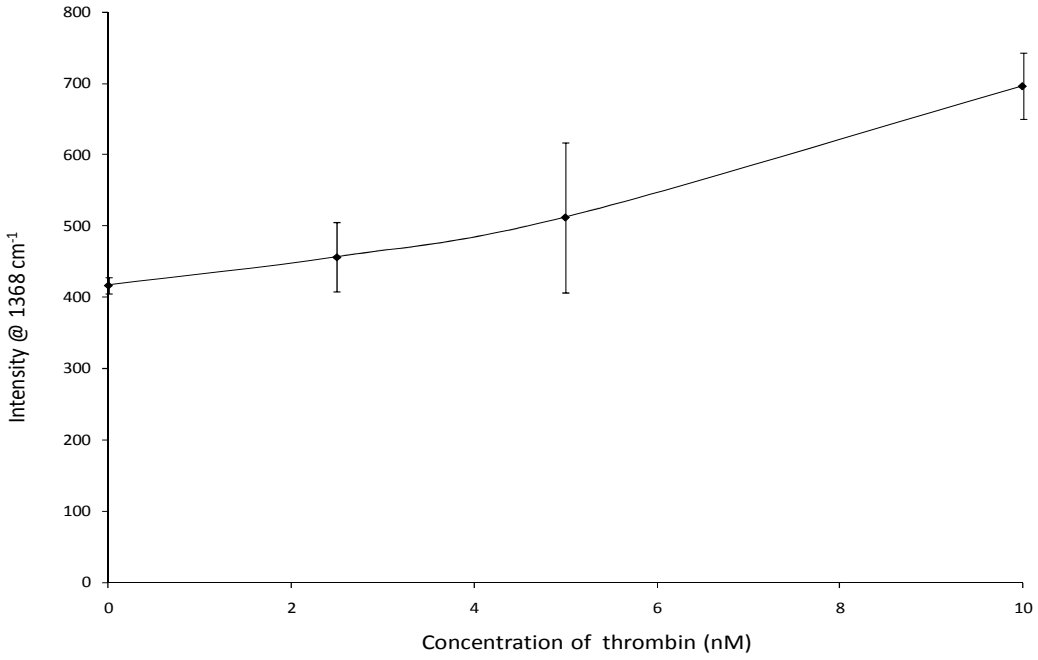

Figure 6.17: Plot of SERRS intensity at 1368 cm^{-1} against thrombin concentration. The error bars were the standard deviation for each sample.

There does appear to be a concentration dependence as the intensity does increase with increasing thrombin concentration. The large error bars indicate the problem with reproducibility. The aggregation of the nanoparticles does not result in a large SERRS intensity, a feature common to all experiments thus far. In all work, addition of thrombin caused aggregation while all control samples displayed no aggregation. However, for the SERRS effect to be "turned on", there should be at least a 2 fold increase in signal from an aggregated sample compared to a monodispersed sample.

The data acquired thus far had been inconclusive and so sophisticated statistical analysis was

attempted to investigate whether subtle changes in the SERRS spectrum could be elucidated.

6.3.8 Automatic Time Study

The problems of reproducibility featured in all SERRS data and in order to address those issues, an automatic time study was set up which incorporated replicate sampling and analysis. Buffer only, DNA and protein control and thrombin samples were all made up in 5 replicate samples (10 pM ASNC) and each sample analysed 5 times. This would help assess variation between samples and inherent instrumental error.

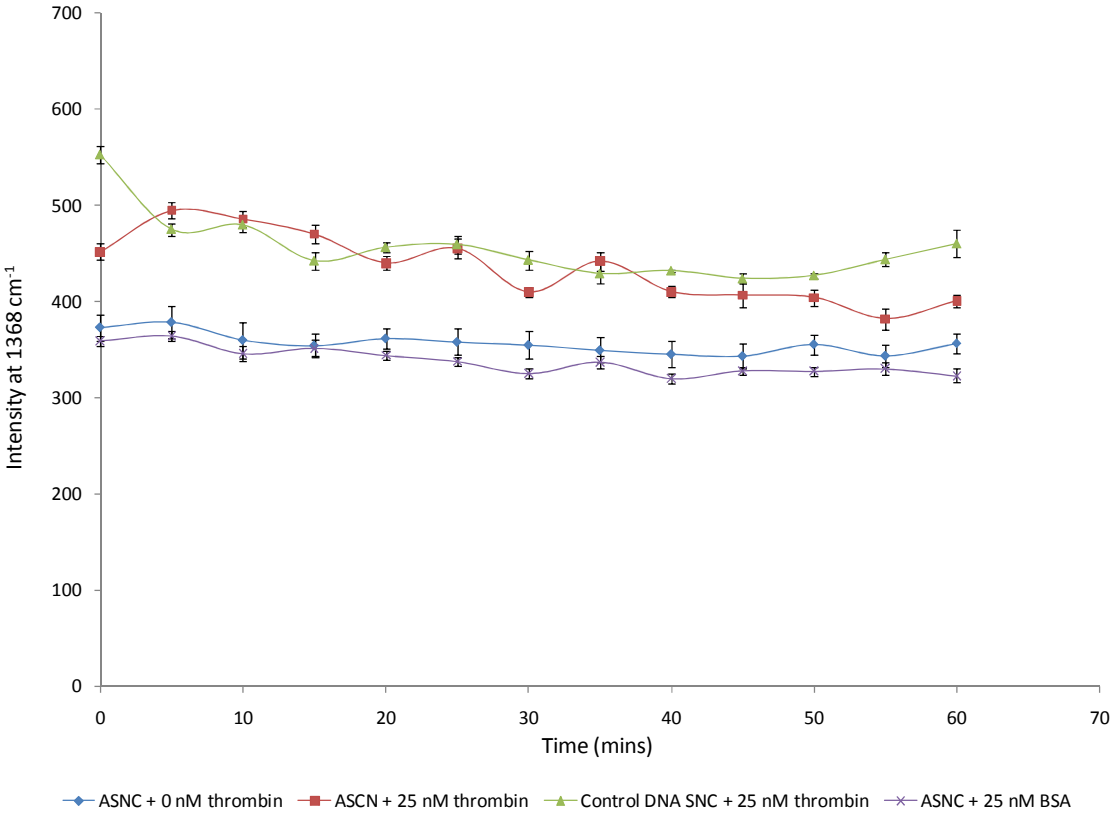

Figure 6.18: Plot of SERRS intensity at 1368 cm^{-1} against time. All four samples are overlaid with the standard deviation represented by the error bars.

The main observation from the data in Figure 6.18 is that there appears to be no difference in

SERRS intensity over time in any samples. It was therefore necessary to compare different samples at set time intervals.

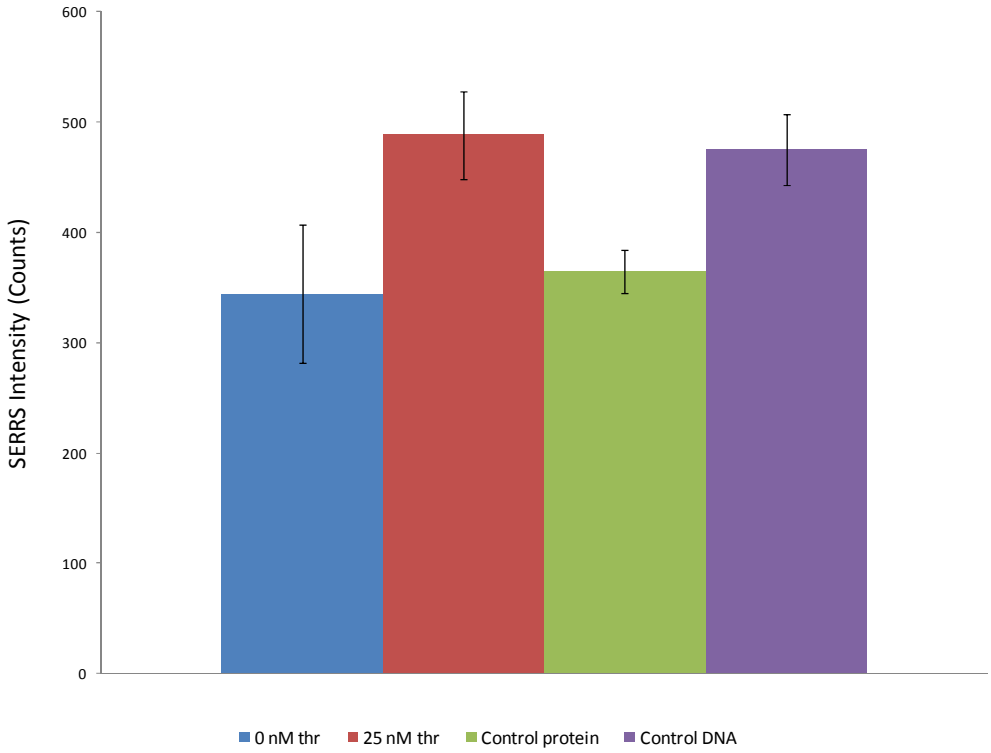

Figure 6.19: Comparison of SERRS intensity after 5 minutes.

The SERRS intensity is greater after 5 mins when 25 nM thrombin is present. It is also greater than the control protein. However, the SERRS intensity of ASCN in the presence of thrombin and in the presence of nonsense DNA is similar despite the fact that aggregation of the nanoparticles only occurred in the ASNC sample.

Other statistical analysis was carried out (by collaborators at Glasgow University) on the data presented in Figures 6.18 and 6.19, using Bayesian analysis and Markov chain Monte Carlo algorithm, but proved inconclusive.

The initial work did show some potential but it was necessary to conduct further work in order to address the reproducibility issues and attempt to achieve better discrimination between unaggreagated and aggregated samples.

6.3.9 Alternative aptamer sequence

The SERRS phenomenon is dependant on numerous factors including, the type of nanoparticles used, the nature and concentration of the dye, the degree of aggregation and (most crucially) the distance between the nanoparticles. It is the formation of "hot spots" between the nanoparticles which give rise to intense SERRS bands. These "hot spots" are areas of high electric fields and allow for great enhancement. There are a number of ways to alter the distance between the nanoparticles. The most common is to vary the length of spacer DNA used. This DNA is an area of nonsense sequence (in the work so far it has consisted of 15 thymine bases) which removed the aptamer sequence from the surface of the nanoparticle. This is deemed necessary as direct attachment of the aptamer sequence to the nanoparticle could inhibit binding due to steric hindrance.

There was an attempt to vary the spacer sequence used. Hexaethylene gycol (HEG) units were incorporated into the 5' end of the aptamer sequence as a replacement for the 15 thymine bases. Unfortunately, it was not possible to obtain stable nanoparticles using the HEG modified DNA. Previous work with short thiol organic molecules had proved unsuccessful when attempting to create stable gold conjugates (see Chapter 5) and so alternative routes were investigated.

As mentioned in the Introduction, there have been two different DNA aptamers[12 97] and one RNA aptamer[20] selected against thrombin. The alternative DNA aptamer sequence isolated by Tasset *et al*. exhibits different binding to thrombin compared to the Bock aptamer.[97] Consequently, the aggregation induced by thrombin binding could produce nanoparticles which are closer together and thus produce greater SERRS signals.

The initial UV-vis spectroscopy analysis of Tasset ASNC in the presence and absence of thrombin mirrored the results obtained with Bock ASNC, and for simplicity are not shown. Consequently, the focus switched to developing the SERRS assay with the new conjugates. In addition, another dye (ROX isothiocyanate (ROX- ITC)) was also investigated in attempt to increase the SERRS signal originating from the aggregated ASNC. The ROX-ITC dye conjugates

were synthesised in a similar way to the BDTDD dye conjugates with the exception that the dye functionalisation with ROX-ITC occurred after DNA functionalisation.

Figure 6.20 compares the UV-vis absorption profile of both dyes with aggregated and monodispersed ASCN.

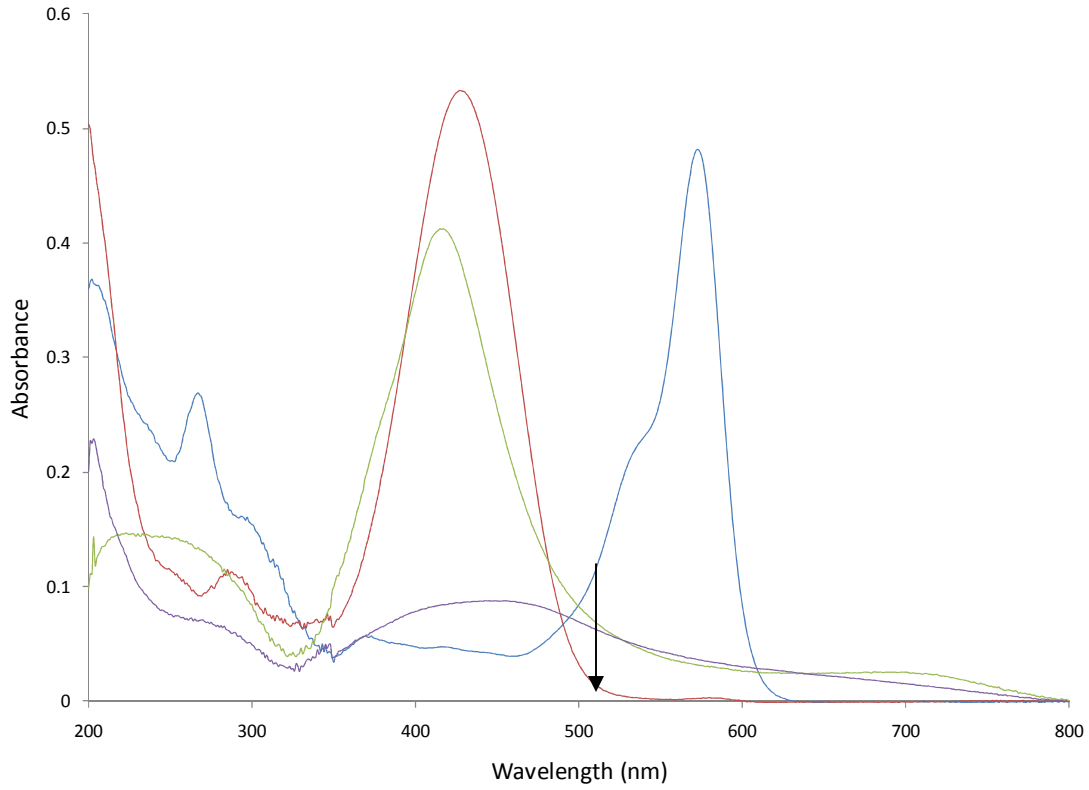

Figure 6.20: Overlaid spectra of both dyes (ROX-ITC, 7.7 µM, blue and BDTDD , 15 µM, red) with aggregated ASNC, 15 pM (purple) and monodispersed ASNC , 15 pM (green).

As shown in Figure 6.20, the dyes differ in their wavelength of maximum absorption by ~ 150 nm (ROX-ITC, 570 nm compared with BDTDD 427 nm). As indicated by the arrow, there is significant overlap between both dyes and the surface plasmon resonance of aggregated nanoparticles at 514 nm (laser light wavelength). Consequently, ASNC were prepared with both Bock and Tasset aptamers and both dyes (four conjugates in total were attempted) and work carried out using the same SERRS experimental set-up as detailed in section 6.37.

Before carrying out SERRS analysis on the different conjugate samples, it was necessary to

analyse both dye conjugates in order to identify the characteristic spectrum of each and observe the enhancement from aggregation. Figures 6.21 – 6.23 show the SERRS spectra of silver nanoparticles conjugated with dye only, no aptamer functionalised was included.

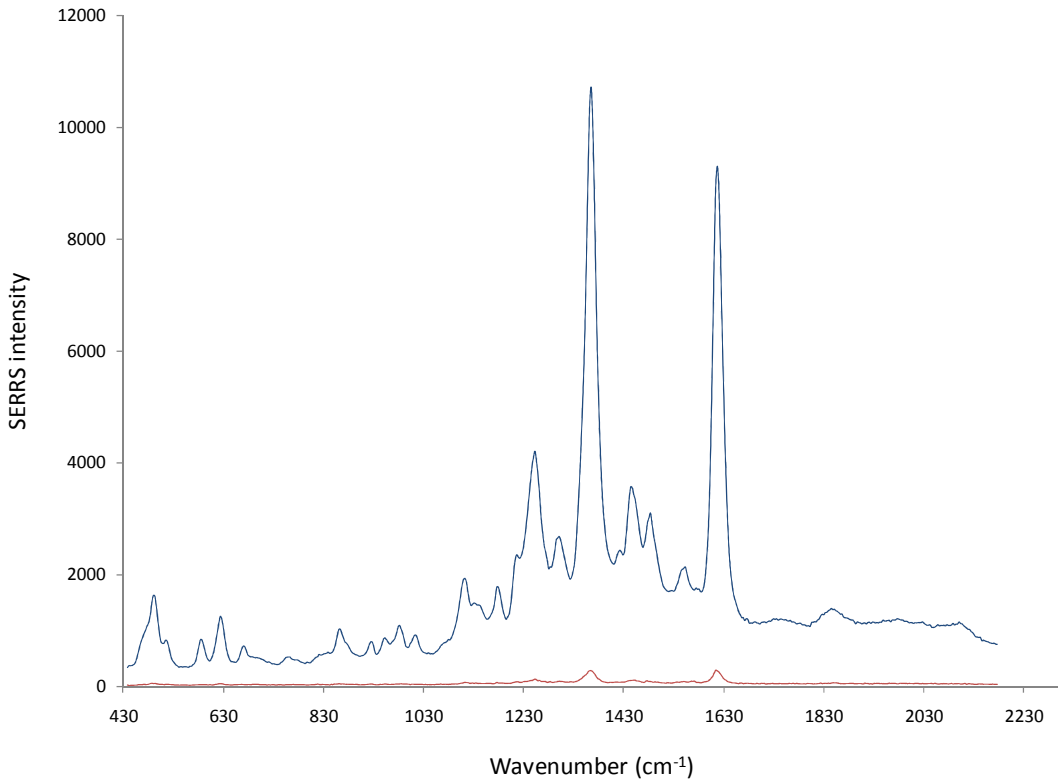

Figure 6.21: Overlaid spectra of BDTDD dye functionalised nanoparticles (neat colloid functionalised with 100 nM dye, final concentration in water). Monodispersed – red, aggregated - blue. Aggregation caused by the addition of NaCl (0.22 M final concentration).

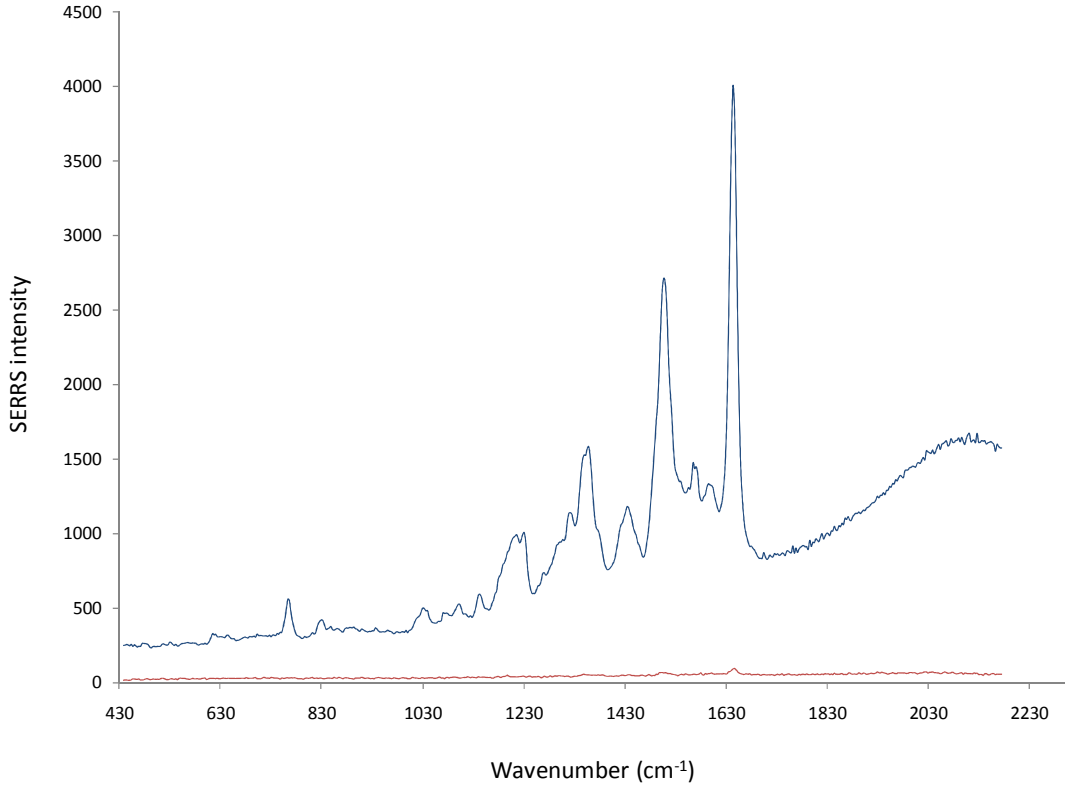

Figure 6.22: Overlaid spectra of ROX-ITC dye functionalised nanoparticles (neat colloid functionalised with 100 nM dye, final concentration in water). Monodispersed – red, aggregated - blue. Aggregation caused by the addition of NaCl (0.22 M final concentration).

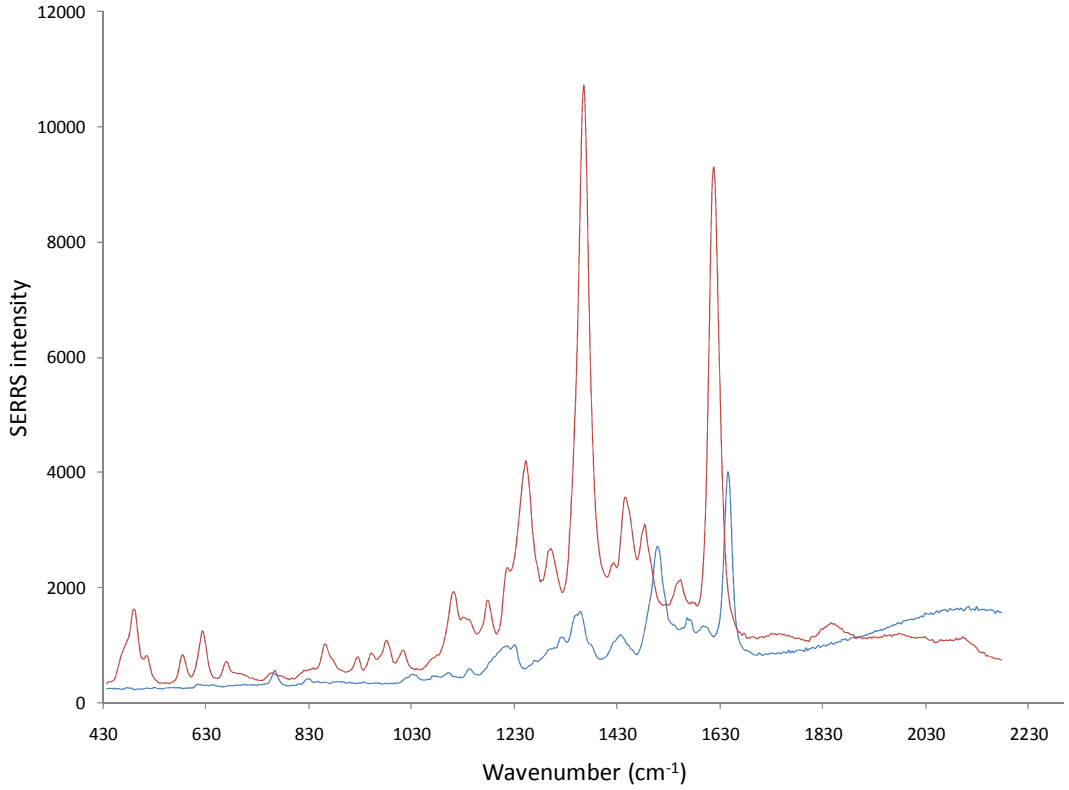

Figure 6.23: Overlaid spectra of aggregated dye functionalised nanoparticles (data from Figures 25 and 26. (ROX-ITC, blue and BDTDD,red).

As observed from Figures 6.21 – 6.23, good enhancement is observed for both dyes when subjected to sodium chloride induced aggregation. Figure 6.23 highlights how the BDTDD dominates over the ROX-ITC signal. It was therefore necessary to prepare four different sets of nanoparticles using both dyes and both aptamer sequences and to analyse them individually and in different combinations.

Of the four possible combinations of aptamer and dye nanoparticle conjugates, only three were synthesised successfully. It was not possible to synthesise the Bock ASNC with BDTDD dye, despite earlier work being successful.

Different combinations of the conjugates were analysed by SERRS but no enhancement was observed for any samples.

In order to progress and explore other possible investigation routes, it was necessary to gain an understanding of the surface coverage of both aptamer and dye on the nanoparticle. As with work carried out in the Chapter 5, the ability to control the surface coverage was investigated

with the aim of achieving good SERRS enhancement.

6.3.10 Surface coverage

It was necessary to quantify both the DNA and dye concentration on the surface of the nanoparticles. The conjugate chosen was Bock ASNC with ROX-ITC dye as the BDTDD dye was not fluorescent and so could not be quantified using the previous method (fluorescence spectroscopy). Another issue present in this work which differed from the PKC surface coverage work was the necessity of having two fluorphores (from the dye and the DNA label).

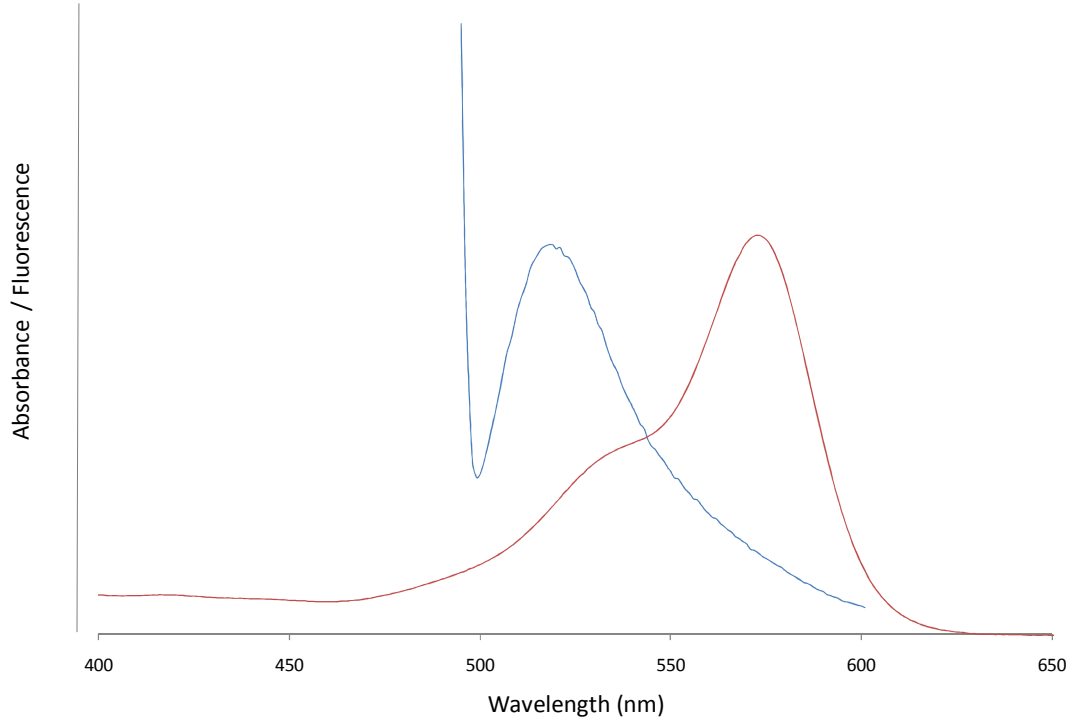

Figure 6.24: Overlaid fluorescence emission spectrum of FAM (blue line) with the UV-vis absorption spectrum of ROX dye (red line).

There is significant overlap between the fluorescence emission of FAM and the absorbance of ROX-ITC. This would lead to a decrease in the observed fluorescence of FAM and so would

prevent the accurate comparison of conjugate samples with the calibration data. In order to overcome the problems with the use of the two fluorophores, two separate experiments were carried out in order to quantify the concentration of DNA and dye separately.

The first involved the use of FAM labelled DNA and an exonuclease enzyme to digest the DNA and release the fluorophore into the solution.[218] The ROX dye therefore remains on the surface and will not interfere with the fluorescence of the DNA label and allow the concentration of DNA to be quantified. The other experiment involved the displacement of the dye and DNA from the nanoparticle surface using DTT (as in Chapter 5). There was no fluorophore present on the DNA and so only the ROX dye present in the supernatant would contribute to the fluorescence of the sample.

Part A - Exonuclease Assay

A series of standards (FAM labelled Tasset aptamer sequence) at varying concentrations were prepared and analysed in order to create a calibration graph.

The nanoparticle samples were made up in triplicate, resupended in (commercial) Exonulease Buffer, concentration determination carried out and then enzyme added. The samples were incubated at 37 °C for 16 hours and the spun down. The supernatant was removed, the nanoparticles washed and the combined supernatant and washings analysed. The fluorescence readings were then converted to molar concentrations using the equation of the line.

The average number of DNA / NP was calculated to be 2420 ± 370. Although, the RSD was relatively large this number is consistent with the size of the nanoparticles (approx 35 nm in diameter) and with results in the literature.[213] [139]

Part B - DTT Assay

A series of standards (ROX ITC) at varying concentrations were prepared and analysed in order to create a calibration graph.

The nanoparticle samples were made up in triplicate, resupended in PBS buffer, concentration determination carried out and DTT added to a final concentration of 100 mM. The samples were left for 16 hours, supernatant removed and then washed. The combined supernatant and washings were analysed. The fluorescence readings were then converted to molar concentrations using the equation of the line.

The average number of ROX molecules/NP was calculated to be 246 ± 19. There is approximately a 10 fold excess of DNA compared to dye. This is likely to originate from the preparation method as the DNA functionalisation takes place first and then dye is added to "fill in the gaps" on the nanoparticle surface. It may be that to improve the SERRS enhancement, the concentration of dye could be increased.

6.4 Conclusion

Successful synthesis of thrombin aptamer gold nanoparticle conjugates (AGNCs) was achieved through direct attachment of thiolated Bock aptamer to gold nanoparticles, producing stable conjugates.

The UV- vis spectroscopy assay set up developed by Wilner *et al*. was modified with a resulting increase in sensitivity and simplicity of thrombin detection.

In addition, successful synthesis of thrombin aptamer sliver nanoparticle conjugates (ASNCs) was achieved using the Bock aptamer and a benzotriazole dye (BDTDD). UV-visible spectroscopy was used to detect the interaction between aptamer and protein and substitution of AGNCs with ASNCs led to an increase in sensitivity.

Extensive research into developing a SERRS assay was carried out with the Bock ASNC but proved unsuccessful. A further two different conjugates were prepared, using the Tasset aptamer and ROX-ITC dye but continued effort did not result in a working SERRS assay to detect thrombin. Successful quantification of the number of both the aptamer and dye molecules on the nanoparticle surface indicated that manipulation / optimisation of their relative surface coverage (similar to that carried out in chapter 5) could be an area to investigate in further work. Indeed, a great deal of preliminary work was carried out to establish a solid platform upon which future efforts can be focussed.[219]

7 Conclusions and further work

Since its discovery in 1990, aptamer technology has made a significant impact in the literature and while rapid growth in this area has taken place, the field is still very much in the early stages. Consequently, there are a number of issues which have to be resolved in order to fully exploit the potential applications of aptamers. This thesis is a reflection of such a position with work focussed on preliminary investigations into the potential selection of novel aptamers for targets and the development of novel assays for use in biologically relevant applications using existing aptamers.

A SELEX programme was developed and executed for the selection of amphetamine and methamphetamine aptamers. Both drug targets were incorporated into the process, with a "split" SELEX carried out from cycle 12 onwards. Three different pools of potential aptamers were isolated and sequence analysis showed good consensus both within and between sets, indicating the potential for an aptamer sequence to be elucidated. Although a great deal of effort was concentrated towards developing an ELISA based binding assay, it was not possible to confirm the affinity and specificity of the isolated sequences towards amphetamine and methamphetamine using an ELISA. As an alternative approach, SPR analyses were carried out on three sequences, but results indicated that no interaction between the aptamer and target occurred. Similarly, CD analysis was unable to prove binding between the aptamer and drug. Going forward, it will be necessary to develop a screening method capable of assessing the aptamer binding to small molecules such as amphetamine and methamphetamine. One potential method would be to carry out affinity chromatography such that amphetamine columns were created and individual, labelled aptamer samples passed through. Binding could then be indicated through the difference between the starting, unbound and eluted concentrations. Indeed, this method was used for a similar small drug molecule, namely cocaine.[220] If an aptamer sequence could be identified it would then be essential to test the detection limits and compare to existing methods and assess its compatibility with real clinical samples originating from blood, urine, saliva etc.

For the development of catalytic aptamers for the Diels-Alder reaction, a novel SELEX programme was designed using cyclohexadiene modified aptamer library and maleimide with a biotin moiety immobilised onto streptavidin beads. The SELEX system was designed to complement and augment existing bio-conjugation work carried out within the group with the aim to attach cell penetrating TAT peptide to DNA. In that respect, unlike conventional Diel-Alder reactions, the reaction was carried out in aqueous buffer, at room temperature and without the use of heavy metal co-factors. The devised SELEX system was carried out and potential sequences isolated and identified. To test the efficacy of the isolated aptamers, the Diels-Alder reaction was carried out on a cyclohexadiene modified oligonucloetide in the presence of one of the aptamer sequences identified. A 60 base aptamer region was used and analysis *via* MALDI – TOF MS indicated the desired cycloadduct had been formed. This work is very much in the preliminary stages but an interesting avenue of research would be to investigate the rate of reaction in order to gain kinetic information. It would also be advantageous to extend the methodology to the aptamer catalysed bio-conjugation of TAT peptide to an oligonucleotide.

In an attempt to create novel assays using previously published aptamers, an aptamer specific for PKC was conjugated to gold nanoparticles. A number of different conjugate types were synthesised in order to investigate optimum DNA surface coverage and spacer effects. UV-visible spectroscopy analysis was carried out with the effort focussed on investigations into buffer systems and identification of optimum protein concentration. Although attempts proved unsuccessful, the preliminary research can provide a good platform for further research. Before continuing, however, it would be necessary to gain a better understanding of the nature of the aptamer – protein interaction with respect to stoichiometry, reaction rate and potential conformational changes arising from the interaction. Future assays could then be specifically tailored and appropriate detection methods selected.

The concept of UV-visible spectroscopy assays investigated in the PKC area of research was mirrored and expanded to incorporate SERRS analysis with the aim of creating a novel detection system for thrombin and improving on the sensitivity of pre-existing methodologies. Both gold and silver nanoparticle conjugates were applied successfully in UV-visible

spectroscopy assays with good selectivity and sensitivity achieved using silver conjugates.[219] For the creation of a SERRS based thrombin detection assay, different combinations of dye labelled silver conjugate samples were created using two different aptamer sequences and two different dyes (BDTDD and ROX-ITC). Analysis of individual conjugates and conjugate mixtures in the assay proved unsuccessful and thus the creation of a novel solution phase assay using a SERRS detection system was not achieved. There has been little research into the SERRS analysis of DNA - protein interactions and so further work may be required including optimisation of dye coverage and DNA coverage. It can be problematic developing solution phase assays due to the dynamic nature of the environment and so it may be necessary for future work to focus on surface-based assays.

8 Experimental

8.1 General

Chemicals were purchased from Sigma Aldrich, UK, unless stated otherwise. All UV-visible analysis was performed on a Varian Cary Bio 300 spectrophotometer fitted with a 6 x 6 cell changer and Peltier temperature controller, using quartz glass cuvettes with a path length of 1 cm. Fluorescence analysis was performed on a Varian Cary Eclipse spectrophotometer. All PCR experiments were carried out using a Minicycler ™ thermocycler, MT Research. All centrifugation was carried out on a bench-top centrifuge at 13000 rpm unless stated otherwise. All agarose gels were photographed using a BioDoc-It^{TM} Imaging System on the 365 nm setting. Ion exchange HPLC was carried out using a Dionex UVD170U detector fitted with a P680 pump through a Resource Q column. Size exclusion HPLC was carried out using a Dionex UVD170U detector fitted with a P680 pump through a HiTrap™ Desalting Column. Reverse phase HPLC was carried out using a Dionex UVD170U detector fitted with a P680. Specific HPLC method details are specified in the text. Amphetamine and methamphetamine salts were obtained in mg quantities form Lynn Curran, University of Strathclyde. MilliQ water (MWQ, Millipore) was used unless otherwise stated.

8.2 Amphetamine / methamphetamine SELEX

8.2.1 PCR amplification of aptamer library

Aptamer library TCCACGTTTTCCCAGTCACGACGT - 60 N -CGTTAATCATGGTCATAGCTG (MWG Eurofins) was amplified using a universal forward primer with a phosphate modification and a universal reverse primer (MWG Eurofins). The PCR mixture was made up as described in Table 8.1 and run on the following temperature program:

10 minutes	@ 94°C	
20 seconds	@94°C	x 15
20 seconds	@ 53°C	
20 seconds	@72°C	
30 seconds	@ 94°C	
1 minute	@ 53°C	
5 minutes	@ 72°C	
2 hours	@ 4 °C	

Table 8.1: List of PCR reagents

Component	Amount (µL)	Notes
Buffer B	25.0	MasterAmp 2X PCR Pre-Mix (Epicentre)*
U Forward primer (P)	1.0	Stock at 100 pmol μl^{-1} Phosphorylated 5'
U Reverse primer	1.0	Stock at 100 pmol μl^{-1}
Aptamer template	1.0	Stock at 10 pmol μl^{-1}
KOD Polymerase	0.5	KOD 1 unit μl^{-1} A hotstart proof reading enzyme[#]
Sterile water	19.0	Sigma PCR water, sterile nuclease free

8.2.2 Preparation of DNA for SELEX

Gel electrophoresis - All gels used throughout this project (unless otherwise stated) were 2% (w/v) of agarose in 1x Tris Borate EDTA (TBE) buffer (Sigma). Once set, the gel was pre-soaked in ethidium bromide (0.5 µg/mL in TBE buffer) for 15 minutes and placed in an electrophoresis tank containing 1xTBEbuffer. The PCR product generated in 8.2.1 was combined and 10 µL of the mixture was retained as a pre-purified standard. The remainder was loaded in a well with 1/10 volume of tricolour loading buffer (Bioline). 5 µL of Hyperladder V

[#] The KOD stock is expressed in units ($1u.\mu l^{-1}$). "One unit is defined as the amount of enzyme that will catalyse the incorporation of 10 nmol of dNTP into acid insoluble form in 30 minutes at 75°C in a reaction containing 20 mM Tris-HCl (pH 7.5 at 25°C), 8 mM MgCl, 0.5 mM DTT, 50 µg/ml BSA, 150 µM each dATP, dCTP, dGTP, dTTP (a mix of unlabelled and [^{3}H]-dTTP) and activated calf thymus DNA." Definition provided by Novagen®.

* The MasterAmp 2X PCR PreMix contains 100 mM Tris-HCl (pH 8.3), 100 mM KCl, and 400 mM each dNTP. The concentrations of MgCl2 (3-7 mM)

(Bioline) was also run on the gel (in a separate well). The electrophoresis was run at 120 V for 50 minutes and then photographed. To extract the DNA, the gel was visualised using a transilluminator (UVP) on the lower power setting. The band at ~100 bp was excised using a clean scalpel and placed in a sterile pre-weighed 15ml Falcon tube.

Purification – The excised gel band was purified using QIAquick gel extraction kit (Qiagen) through the use of silica columns and according to the following protocol (modified from the manufacturers' guidelines). Three gel volumes of QG buffer was added to the agarose gel slice and heated at 50°C. Once dissolved, 1 gel volume of isopropanol was added and then mixed. This mixture was placed in the silica columns (750 µL max volume each) and centrifuged for 1 minute. The flow through was discarded and this step was repeated until the all the gel mixture had been added. However, care was taken to ensure that the columns did not become over saturated with DNA (maximum binding capacity of 10 µg DNA). The columns were washed twice with 700µl an ethanol containing buffer. The columns were transferred to 1.5 mL microcentrifuge tube and centrifuged for 5 minute to remove traces of ethanol. The DNA was eluted from the columns using 50µl DEPC water (Bioline) followed by a 1 minute centrifugation step. The flow through from all columns was then pooled. A 10 µL aliquot was removed from the pooled sample above and run on an analytical gel together with 10 µL of the pre-purified standard.

Single stranded –ss DNA was produced *via* enzyme digestion of the phosphorylated strand using lamda exonuclease (Epicentre). The following mixture was made up: ds purified product (1 volume), 10x λ exonuclease buffer (1/10 volume), λ exonuclease enzyme (10 units, 5 units/µL).
The sample was mixed, spun down on a centrifuge, placed in the thermocycler and subjected to the following conditions: 30 minutes @ 37°C and 10 minutes @ 72°C.

Ethanol precipitation – The following reagents were placed in a 1.5 mL microcentrifuge tube: ss DNA (1 volume), sodium acetate (1/10 volume, 3 M), Gen Elute LPA (1 µL) and ethanol (2.5 volumes, 100 %). The tube was mixed thoroughly and then centrifuged for 10 mins, 13000 rpm.

This resulted in the formation of a pellet of DNA. The supernatant was carefully removed and the pellet was then washed with 1 mL ethanol (70 %) then 500 µL ethanol (100 %). The pellet was spun down for 1 minute, 13000 rpm and the lid removed and allowed to air dry for 5 minutes. The pellet was resuspeded in 100 – 200 µL in DEPC water.

Concentration determination – The concentration of the DNA sample was determined using UV absorbance reading carried out using a biophotometer (Eppendorf) on the ss DNA program.
The aptamer library was then ready to be introduced into the SELEX process

8.2.3 SELEX

Throughout the process, four buffers were used:

- Coupling buffer $NaHCO_3$ / Na_2CO_3 (0.1 M pH 9.0)
- Binding buffer Tris HCl (20 mM), NaCl (300 mM), $MgCl_2$ (5 mM)pH 7.6
- Low pH buffer sodium acetate (0.2M) NaCl (0.2M) pH 4.0
- High pH buffer Tris HCl (0.1M) pH 8.0

Counter selection - 1 g of the Epoxy activated Sepharose 6B™ (GE Healthcare) was washed through a glass sinter with 200 mL of MQW, left to vacuum dry for a few minutes and then resuspended in 1 mL MQW. Ethanolamine (1 M, 4mL, in coupling buffer) was then added to the resin and incubated for 16 hours at 37 °C with gentle agitation. Once completed, the resin was transferred into a 10 mL syringe (plugged with cotton wool) and washed as follows: The column was then washed with 3 cycles (10 mL each) of alternating low pH and high pH buffer before a final wash step of binding buffer (30 mL). The purified single stranded aptmer library was then introduced into the column (x M, 4 mL, in binding buffer according to Table 8.2) and allowed to incubate for 2 hours at room temperature. Unbound aptamers were eluted with 4 mL binding buffer and this fraction was kept for introduction into the first round of amphetamine SELEX.

SELEX – 1 g of resin was washed as before and then incubated with amphetamine sulfate solution (x M, 4 mL in coupling buffer, according to Table 8.2) for 16 hours at 37 °C with gentle agitation. The washing steps with low pH, high pH and binding buffer were then carried out. The eluted aptamer library from the counter selection step was then introduced into the column and allowed to incubate at room temperature for 1 hour. Unbound aptamers were removed through washing the column with binding buffer (30 mL). Competition elution (using a higher amphetamine concentration) was used to remove the bound aptamers from the column. The bound fraction was concentrated to a volume of ~ 3 mL using a rotary evaporator and then dialysed (D-Tube^{TM} dialyser Molecular Weight Cut Off (MWCO) value of 12-14 kDa, Merck Biosciences) to remove amphetamine. The sample was further concentrated, reuspended in 1 mL DEPC water and used as template for PCR. The process of amplification and purification of the DNA as outlined in section 8.2.1 and 8.2.2 was repeated in order to prepare the aptamer library for the next round of SELEX.

Negative SELEX - As indicated in Table 8.2, the first negative election was carried out after SELEX 7. Prior to elution of the bound aptamer library during SELEX 7, the column was washed with aniline (2.5 μM, 4 mL) and discarded before elution of the bound aptamers with a higher concentration of amphetamine.

Table 8.2: Summary of SELEX work carried out

SELEX no.	Aptamer library concentration (μM)	Column loading (μM)	Elution concentration of target (μM)
1	5.0	10	12
2	12.8	10	12
3	11.3	5	7
4	11.9	5	7
5	10.2	5	7
6	10.7	5	7
7	5.1	2.5	4
Negative*	7.4	2.5	10
8	7.3	5	7
9	8.2	2.5	4
10	8.6	1	3
11	10.0	1	3
12*	10.4	1	2.5 (meth)
13	15.2	2	4
14	9.3	5	50 (amp) 50 (meth)
15	6.3	5	80 (amp) 80 (meth)
16*	5.8	2.5	100 (amp)

As shown in Table 8.2, a total of 16 SELEX cycles were carried out. From SELEX 12 onwards, a split process was carried out where both amphetamine and methamphetamine were introduced into the process. In SELEX 12, negative selection was carried out with

methamphetamine. The fraction of aptamers which bound to methamphetamine were retained and then used in a further 3 methamphetamine cycles, namely 14, 15 and 16. Amphetamine was then used to elute the remaining aptamer fraction from SELEX 12 which was then taken through to a final amphetamine column in SELEX 13.

8.2.4 Cloning

Agar plate preparation – Growth medium was made up by dissolving one sachet (~ 18 g) S-Gal / Luria Broth (LB) Agar blend powder (containing 5 g tryptone, 2.5 g yeast extract, 5.0 g NaCl, 6 g agar, 0.15 g S-Gal, 0.25 g ferric ammonium citrate and 0.015 g IPTG) in 500 mL MQW, sterilised via autoclaving, melted until fully dissolved and left to cool. Once "hand hot" carbenicillin (5 µL, 100 mg mL^{-1}). The media was then poured into Petri dishes (40 mL in each one) and allowed to cool and set.

The cloning protocol was carried out using a commercial kit (Perfectly Blunt Cloning kit, Novagen) and consisted of six steps; end conversion, ligation, transformation, colony selection, outgrowth and DNA preparation.

End conversion – The following mixture was made up in a 200 µL PCR tube, mixed and placed in a thremocycler:

dsPCR product 2 µL, end conversion mix 2 µL sterile water 3 µL

It was subjected to the following temperature conditions: 22 °C for 15 mins and 75 °C for 5 mins. The tube was cooled on ice for 2 minutes immediately prior to the next step, ligation.

Ligation - The following reagents were added to the tube from the previous step and then placed in the thermocycler:

Blunt vector 1 µL, T4 DNA ligase 1 µL

It was subjected to the following temperature conditions: 22 °C for 15 mins.

Transformation – One tube of NovaBlue Singles Competent cells was thawed on ice for 2 – 5 minutes. They were gently agitated before adding 2 µL of ligation reaction mixture and then incubated on ice for 5 minutes. The tube was then placed in a water bath at 42 °C for 30

seconds and then immediately returned to ice. 250 µL SOC medium was added to the tube and then placed in a water bath at 37 °C for 30 seconds. This mixture was then spread onto the pre-prepared agar plates (10 – 100 µL) and incubated for 16 hours at 37 °C.

Colony selection – Upon visual examination of the plates, hundreds of colonies were present. Using a sterile pipette, colonies were picked and then dropped into sterile tubes containing 5 mL LB. A total of 24 colonies were picked and taken to the outgrowth step.

Outgrowth – The tubes were incubated for 16 hours at 37 °C, with agitation.

DNA preparation – This was carried out using QIAprep® Miniprep Kit (Qiagen). All buffers used in the protocol were commercial ones supplied with the kit.

1.5 mL of overnight culture was transferred into microcentrifuge tubes and spun down for 1 minute. The supernatant was removed, leaving a pellet of cells which were resuspended in buffer (100 µL, SpinPrep Resuspension Buffer). They were then vortexed to ensure complete reuspension. Lysis buffer (200 µL) was then added and the tubes inverted 6 times to ensure proper mixing. Tubes were not to be vortexed. The tubes were incubated at room temperature for 5 minutes before adding 400 µL neutralisation buffer. Again the tubes were inverted 6 times. The samples were then centrifuged for 10 minutes before transferring the supernatant into a column unit and spinning again for 30 seconds. The column was washed with 0.75 mL Buffer PE, centrifuged again for 1 minute to remove any residual wash buffer. The column was transferred into a separate tube and the plasmid DNA eluted by addig 50 uL DEPC water to the column and centrifuged for 1 minute. The samples were then ready for sequence analysis.

The samples were assigned individual numbers as follows:

Negative SELEX → CD.N.1, 3, 4, 5, 8, 9, 19, 20, 21, 22, 23, 24, 25, 26, 27, 28, 29, 30 (18 samples)

SELEX 13 → CD.13.1, 2, 3, 4, 5, 6, 7, 8, 9, 10, 11, 12, 13, 14, 15, 16, 17, 18, 19, 20 (20 samples)

SELEX 16 → CD.M.48, 51, 52, 55, 56, 58, 59, 60, 61, 63, 64, 67, 71, 74, 75, 80, 82, 83, 84, 85, 89 (21 samples)

8.2.5 Sequence analysis

Sequencing - Sequence analysis for the first two sets of samples i.e. Negative SELEX and SELEX

13 were carried by Rothwell Tate, Strathclyde Institute of Pharmacy and Biomedical and Studies, University of Strathclyde using an Applied Biosystems 3100-Avant Genetic Analyser. Sequence analysis for the final set, SELEX 16 was carried out by The DNA Sequencing Service, Medical Sciences Institute, University of Dundee using an Applied Biosystems 3730 Capillary DNA Sequencer.

Raw data analysis – the sequencing data consisted of a long list of A, T, G and C's approx 1000 bases in length. The first step was location of the *EcoR*I site GAATTC. The reverse primer (TCCACGTTTTCCCAGTCACGACGT) is located immediately after this followed by the 60 base random region and the forward primer inverted sequence (CGTTAATCATGGTCATAGCTG). The opposite case could also be found i.e. the forward primer was encountered first, then the 60 base random region followed by the inverted reverse primer. For each sample the 60 base sequence was isolated and inverted if necessary, depending on which set of primers were present.

Multialin – An algorithm, freely available on the internet (http://multalin.toulouse.inra.fr/multalin/multalin.html) was used to identify regions of sequence consensus and group sequences into hierarchal clusters.[168] The 60 base random region extracted from the raw data analysis was entered into the website and the output displayed.

M- fold - An algorithm, freely available on the internet (http://www.bioinfo.rpi.edu/applications/mfold) was used to predict DNA secondary structure.[169] The 60 base random region extracted from the raw data analysis was entered into the web server and the structures displayed as PDF files.

8.2.6 Binding analysis – ELISA using maleic anhydride plates

The following buffers were used:

- 1× Phosphate buffered saline {1xPBS}

- 2× bind and wash (B/W) buffer {2.0 M NaCl, 10 mM Tris-HCl, 1 mM EDTA pH 7.5}
- Binding buffer {Tris HCl (20 mM), NaCl (300 mM), $MgCl_2$ (5 mM)pH 7.6}
- 5× TBS buffer {30.25 g Tris, 8.76 g NaCl pH 7.5}
- TBST {1× TBS buffer plus 0.2% (v/v)Tween 20}
- Blocking solution (BS) {TBST plus 5% (w/v) Marvel milk powder}

Two negative controls were used; the first without immobilisation of amphetamine and the second using a nonsense biotinlyated DNA sequence.

The wells were washed twice with 200 µL 1× PBS buffer. Amphetamine solution (100 µL, 12.5 µg/mL in 1x PBS buffer) was added to each well. The plate was covered and incubated at 37 °C on a shaker for 1 hour. The wells were washed with 2x200 µL BS. A further 200 µL of blocking solution was added. This was incubated at room temperature for 1 hour (with no shaking).The wells were rinsed with 3x200 µL TBST solution. Biotinylated aptamer solution (0.15 µM in binding buffer) was added to each well and incubated for 1 hour at room temperature. The wells were then rinsed with 3x200 µL TBST buffer. Streptavidin AP solution (0.1 µg/mL in 1×B/W buffer) was prepared from 0.1 mg/mL stock solution (Pierce) and 100 µL added to each well. This was incubated for 30 minutes and then washed with 4x200 µL 1×B/W buffer. Colorimetric analysis was then carried out using a commercial AP enzyme detection kit (Pierce). The substrate solution was made up BICP and 20 µL nitro blue tetrazolium NBT in 5 mL 1×AP buffer), 200 µL added to each well and then incubated at room temperature for 10 minutes. A photograph or scan of the microtitre plate was taken at several time intervals.

8.2.7 Blocking investigation

Wells were washed with 2x200 µL 1×PBS and then 300 µL blocking solution added (as detailed in Table 8.3). The plate was incubated for varying lengths of time, at two different temperatures (also listed in Table 8.3). BS was removed and the wells washed with 6 x 300 µL (1x PBS). The antibody/AP conjugate was then added to each well (100 µL, 1000× diluted

Rabbit polyclonal to goat (AbCam) and allowed to incubate at room temperature for 2 hours. Once completed, all wells were washed with TBST (3x200 µL) and the colorimetric analysis carried out as detailed previously. A photograph or scan of the microtitre plate was taken at several time intervals.

Table 8.3: Summary of blocking conditions investigated.

Solution	Ethylamine (1 M)	Ethanolamine (1 M)	Lysine (0.5 M)	BSA (10 % w/v)
Incubation time	1 hour	2 hours	16 hours	
Agitation	Y	N		
Temperature	RT	4		

8.2.8 Binding analysis – ELISA using Immulon 4BHX plates

The blocking investigation carried out previously was repeated with the exception of Immulon 4BHX plates (Thermo Scientific) being used in place of maleic anhydride plates.

8.2.9 Binding analysis – ELISA using commercial amphetamine detection kit

1st experiment - A reduction amphetamine assay was carried out i.e. aptamers were used to capture amphetamine and a commercial kit containing strips of functionalised wells and all reagents (Amphetamine Direct ELISA kit, Calbiotech) used to monitor the drop in amphetamine concentration. Two biotinylated aptamer samples were analysed; 21A and 26A. The following solutions were made up for each of the two aptamer samples and left to incubate for 1.5 hours:

1. 80 pmol aptamer (2.5 µM, 32 µL) added to 20 pmol amphetamine (0.2 µM, 100 µL)
2. 5 pmol aptamer (2.5 µM, 2 µL) added to 20 pmol amphetamine (0.2 µM, 100 µL)

Streptavidin beads (40 µL, 4 mg /mL, New England Biolabs) were then added, left to incubate

for 30 minutes and placed on a magnetic separator. The supernatant (10 µL) was removed and applied to the commercial plate. The enzyme conjugate (supplied with the kit) was then added to each well (100 µL) and incubated for 1 hour at room temperature. All wells were washed (6x 350 µL MQW) before inverting the plate and using absorbent paper to remove any residual moisture. The substrate was then added (100 µL) and left to incubated for 30 minutes. Once completed, stop solution was added to each well (100 L) and absorbance reading recorded at 450 nm on iEMS Reader MF (Labsystems). A positive and negative control (also supplied wit the kit) was run with each experiment.

2nd experiment – The above experiment was repeated wit the exception that nine aptamer samples were analysed; CD.N.19, CD.N.20, CD.N.21, CD.N.26, CD.13.7, CD.13.9, CD.13.11, CD.13.15 and CD.13.19. For each sample, two solutions were made up

1. 0.4 pmol aptamer (0.25 µM, 1.6 µL) added to 0.1 pmol amphetamine (1nM, 100 µL)
2. $2.5x10^{-14}$ mol aptamer (0.25 µM, 0.1 µL) added to 0.1 pmol amphetamine (1nM, 100 µL)

8.2.10 Binding analysis – ELISA using epoxide beads

0.825 mL Dynabeads® M-450 Epoxy (Invitrogen) were washed with3x1 mL Borax buffer pH 9.4 using a magnetic separator to remove the supernatant each time and then the beads were resuspended in amphetamine solution (6.5 µM, 0.825 mL in Borax buffer). They were left to incubate overnight. The beads were washed with Borax buffer (3x1 mL) to remove excess amphetamine and then a 25 µL aliquot sample placed into the wells of a microtitre plate. The plate was placed on a magnetic separator, the supernatant removed and the beads resuspended in biotinylated aptamer solution (60 µL, 80 nM in binding buffer). The plate was left for 2 hours at room temperature with shaking. Once completed, the wells were washed with binding buffer (4x200 µL) and then the enzyme conjugate was added, strepatvidin HRP (Pierce) (100 µL, 1 µg/mL). This was left to incubate for one hour at room temperature with shaking. The wells were then washed with binding buffer (6x 200 µL) before adding 50 µL tetramethylbenzidine (TMB solution). After 15 minutes, 50 µL stop solution was added and the

absorbance reading at 450 nm recorded, as detailed in 8.2.9.

8.2.11 Binding analysis – Circular Dichroism

All experiments were carried out by Sharon Kelly at Glasgow University using a J-810 Spectropolarimeter on the following settings:

- 5 scans
- 50 nm/min
- 0.5 s response
- 1 band width
- 0.2 data pitch
- 0.2 cm path length

Three samples were analysed:

1. CDapt 2 (5 μM, 200 μL in HEPES)
2. CDapt 2 (5 μM, 200 μL in HEPES) with amphetamine (30 μM, final concentration)
3. CDapt 2 (5 μM, 200 μL in HEPES) with amphetamine (60 μM, final concentration)

Both samples 2 and 3 were left to incubate for 0.5 hours before analyses.

8.2.12 Binding analysis – surface plasmon resonance

Analysis carried out by Sharon Kelly at Glasgow University using a Biacore™ 2000 and a carboxymethylated dextran (CM5) chip. The following DNA samples were analysed:

CDapt 1 – ACCCCTTAGCAGCACAACGACGACCGGCGCGTAGGAGGACGGGGAAGGTGGGCATAG

CDapt 2 – ACGCCAAACAGCAGCACAACGACGACCGGCGCGTAGGAGGACGGGGAAGGTGGGCATAG

CDapt 3 – AAGAATAAGCCGCAATCAAAGTGCAGTACGAGATCAACCTTGGCCGTAATGCCACTCAGT

Flow cell 1: control surface (ethanolamine)

Flow cell 2: amphetamine surface (low concentration, 10 μM)

Flow cell 3: amphetamine surface (high concentration, 1 mM)

Flow cell 4: unmodified surface

There were 2 buffers used; HEPES and SELEX binding buffer

A total of 11 experiments were carried out:

1. Control experiment to investigate whether the DNA had any affinity for the chip surface. CD apt 2 was flowed over the chip (5 μM , 500 μL, 40 μL / min) an unactivated chip.
2. The chip was activated with EDC (750 mg/mL) and NHS (115 mg/mL) and allowed to react for 7 minutes (5 μL/min). The chip was then blocked with ethanolamine for 7 minutes (1 M, 5 μL/min). CD apt 2 was flowed over the chip (5 μM, 500 μL, 40 μL / min).
3. The chip was activated with EDC / NHS as before and then reacted with amphetamine (10 μM, 5 μL/min, 7 mins). It was then blocked as before with ethanolamine. CD apt 2 was flowed over the chip (5 μM, 500 μL, 40 μL /min). Flow cell 2 monitored.
4. Same as 3 except Flow cell 2 – flow cell 1 was monitored.
5. Chip was re-activated and then reacted with amphetamine (100 M, 5 μL/min). CD apt 2 was flowed over the chip (10 μM, 500 μL, 40 μL/min). Flow cell 2 monitored.
6. Same as 5 except CD apt 3 was flowed over chip and flow cell 2- flow cell 1 monitored.
7. Chip activated as previously on flow cell 3 and then amphetamine reacted on the surface (1 mM, 5 μL/min, 30 mins). The surface was blocked with ethanolamine and CD apt 2 was flowed over the chip (2.5 μM , 40 μL/min, 5 mins).
8. Chip was regenerated through trial and error of numerous reagents; NaCl, NaOH, EDTA, Glycine with EDTA (0.1 M, 5 μL/min, 10 mins) proving successful at regeneration.
9. Repetition of 7 with the exception of monitoring the difference against all flow cells; 3 - 1, 2 - 1, and 4 - 1.
10. Repetition of 9 with the exception of an increased concentration of DNA (5 μM).
11. Repetition of 10, with the presence of Mg^{2+}(50 mM) in the coupling buffer.

8.3 Diels Alder

8.3.1 PCR amplification of aptamer library

As detailed in Section 8.2.1. The exception was the use of a cyclohexadiene modified DNA oligonucleotide in place of the universal reverse primer, synthesised by Victoria Steven, University of Strathclyde:[181]

5' – X TCC ACG TTT TCC CAG TCA GAC GTA A – 3'

Where X is the cyclohexadienyl modification

All remaining steps for the preparation of the DNA aptamer library were carried out as described in Section 8.2.1 with the exception of the PCR mixture, as summarized in Table 8.4.

Table 8.4: List of PCR reagents

Component	Amount (µL)	Notes
Buffer B	25.0	MasterAmp 2X PCR Pre-Mix (Epicentre)
U Forward primer (P)	1.0	Stock at 100 pmol μl^{-1} Phosphorylated 5'
U Reverse cyclo	1.0	Stock at 100 pmol μl^{-1}
Aptamer template	2.0	Stock at 10 pmol μl^{-1}
KOD Polymerase	0.5	KOD 1 unit μl^{-1} A hotstart proof reading enzyme
Sterile water	20.5	Sigma PCR water, sterile nuclease free

8.3.2 SELEX

Counter SELEX - 375 µL magnetic streptavidin beads (4 mg/mL in PBS, New England Biolabs) were washed with 3x500 µL sterile binding buffer (20 mM Tris HCl, 0.3 M NaCl, 5 mM $MgCl_2$ pH 7.6 sterilised using 0.22 µm syringe filter (Millipore). ss DNA aptamer library solution made up to 300 µL using binding buffer. The washed beads were resuspend in DNA solution and incubated for 1 hour. The supernatant was removed and added directly to biotin maleimide

functionalised beads (prepared in the subsequent step).

SELEX - 375 µL streptavidin beads were washed with 3x500 µL binding buffer. The beads were resuspended in biotin malemide (100 µL, 15 µM in binding buffer prepared from a 150 µM biotin maleimide stock solution in 70 % acetic acid) and incubated for 0.5 hours. The beads were washed with 3x300 µL binding buffer to remove unbound biotin malemide. The counter SELEX supernatant (or DNA aptamer library from previous SELEX) was then added to the beads and incubated for x hour (according to Table 8.5).The supernatant was removed and the beads washed with 3x300 µL binding buffer and kept for analysis to determine the concentration of unbound DNA. The beads were resuspended in 100 µL DEPC water and used as template for PCR.

Table 8.5: Outline of SELEX.

Type	Incubation time (minutes)
Counter SELEX	60
SELEX 1	120
SELEX 2	120
SELEX 3	60
SELEX 4	60
SELEX 5	30
SELEX 6	30
Counter SELEX	60
SELEX 7	15
SELEX 8	15
SELEX 9	5
SELEX 10	5

8.3.3 Progress towards subsequent SELEX

After the completion of each round of SELEX, PCR, gel electophoresis, conversion to ssDNA and ethanol precipitation had to be carried out. This was done as outlined in sections 8.2.1 – 8.2.2 with the only difference being the mixture used in the PCR, as summarized in Table 8.6.

Table 8.6: List of PCR reagents

Component	Amount (µL)	Notes
Buffer B	50.0	MasterAmp 2X PCR Pre-Mix (Epicentre)
U Forward primer (P)	2.0	Stock at 100 pmol μl^{-1} Phosphorylated 5'
U Reverse primer	2.0	Stock at 100 pmol μl^{-1}
Template	20.0	Streptavidin beads from SELEX
KOD Polymerase	1.0	KOD 1 unit μl^{-1} A hotstart proof reading
Sterile water	25.0	Sigma PCR water, sterile nuclease free

8.3.4 Cloning

As detailed in Section 8.2.4 with the following samples cloned successfully:

CD.VS.1, 2, 3, 4, 5, 6, 7, 8, 9, 10, 12, 13, 16, 19, 20, 21, 22, 23, 24 ➔ 19 in total

8.3.5 Sequence analysis

As detailed in Section 8.2.5

8.3.6 Catalytic Investigation

The two DNA aptamer sequences (MWG Eurofins, 100 µM) used in this section were as follows:

CD.VS.4_60:
5' - AGGCAAGGTACAGCGGGGGTTGCGGGTCAGGTCGTGTGTGTGTGGGGTGTCCCGTGCGGT- 3'

CD.VS.4_105 :
5'TCCAGCTTTTCCCAGTCACGACGTAGGCAAGGTACAGCGGGGGTTGCGGGTCAGGTCGTGTGTGTGT
GGGGTGTCCCGTGCGGTCGTAATCATGGTCATAGCTG - 3'

Two other DNA sequences were used, namely, the cycloheadiene modified (5' end) primer detailed in section 8.3.1 and a cyclohexadiene modified oligonucleotide (mid sequence on T underlined below).

5' – CGCA***T***TCAGGAT – 3'

Prior to MADLI – TOF analysis, DNA samples were purified and concentrated by the use of ZipTip™ C18 pipette tips and eluted directly in matrix solution. The matrix solution was prepared by dissolving 3-hydroxypiccolinic acid in 50:50 acetonitrile / MQW (50 mg/mL) and mixing in a 9:1 ratio with ammonium citrate in MQW (50 mg/mL). The analysis was carried out by Patricia Keating, University of Strathclyde, and performed on a Shimadzu Axima-CFR in linear negative mode. Calibration was achieved through the use of DNA standard solutions (Bruker Daltonics).

8.3.7 General Diels Alder reaction – small molecule synthesis

Serial dilutions of a biotin maleimide stock solution (15 mM, 3 mL in 70 % acetic acid) were carried out to prepare 1.5, 0.15 and 0.015 mM biotin maleimide solutions (3 mL in binding buffer).

Serial dilutions of a cyclohexadiene stock solution (97 % solution, density 0.84 g/mL , 15 mM in methanol) were carried out to prepare 1.5, 0.15 and 0.015 mM biotin maleimide solutions (3 mL in binding buffer).

A mixture solution was made up (400 µL 1.5 mM biotin maleimide, 400 µL cyclohexadiene, 1.5 mM final volume 2 mL in binding buffer).

All solutions were analysed by UV-vis spectroscopy.

Cyclohexadiene (1 molar eq 0.3 mM, 200 µL binding buffer prepared by 100 x dilution of 30 mM stock solution in methanol) was reacted with 10 molar eq. of biotin maleimide (3 mM, 200 µL binding buffer prepared by 10 x dilution of 30 mM stock solution in 70 % acetic acid) in the presence of 105 mer aptamer DNA 0.01 molar eq (6 µL, 100 µM neat solution). Two control experiments were also carried out where:

1). The aptamer solution was replaced with binding buffer and

2). A different 100 base DNA solution was used.

The three solutions were left to react for 30 minutes and then purified (to remove the DNA) through centrifugal filtration (MWCO 10,000, Millipore) of 4x5 minutes spins at 13000 rpm.

The buffer salts were removed via size exclusion HPLC on the following program:

Eluent: 100 % H_2O at 3 mL / min for 10 minutes

The fractions were concentrated *in vauo* and resuspended in 1 mL water and analysed by LC-MS.

8.3.8 SELEX specific Diels – Alder reaction using cyclohexadiene modified DNA (primer)

All glassware was silanised using 10 % trimethyl silane chloride (TMS-Cl) solution prior to use.

As per 8.3.7 except cyclohexadiene replaced with cyclohexadiene modified primer.

The samples were left to react for 30 minutes and then analysed via reverse phase HPLC on the following program:

Buffer A: TEEA (0.1 M, pH 7) Buffer B: CH_3CN

T=0 , 95 % A, 5 % B

With a gradient increase of 1 %/min B over 15 minutes and held at 20 % B for 5 minutes at a flow rate of 1 mL/min.

No fractions were collected.

8.3.9 HPLC of DNA sequences (analytical)

The two aptamer solutions (CD.VS.4_60 and CD.VS.4_105) and mid sequence cyclohexadiene modified DNA (VSDR 2 mid) were analysed by reverse phase HPLC using program in 8.3.8.

8.3.10 SELEX specific Diels – Alder reaction (VSDR2 mid)

Preparative HPLC was carried out on VSDR2 mid (30 µL unknown concentration made up to 1 mL water) via 2x500 µL injections and using the same column and program as detailed in section 8.3.8. Fractions were collected, freeze dried, resuspended in 1 mL water and analysed by MALDI – TOF MS:

8.3.11 Final 2 HPLC reactions with MALDI analysis

Two reactions were carried out each in the presence of either CD.VS4_60 or CD.VS4_105 aptamers (100 µM). Biotin maleimide (10 molar eq.) VSDR 2 mid (1 molar eq.) and aptamer solution (0.04 molar eq). in binding buffer, 500 µL total volume were allowed to react for 30 minutes and then injected onto a reverse phase column and HPLC carried out using the program as detailed in section 8.3.8. Fractions were collected (taking into account delay time), freeze dried, resuspended in 1 mL water and analysed by MALDI-TOF MS.

8.4 PKC

All PKC AGNC were prepared in the same way. All centrifugation was carried out using a bench top centrifuge at 5000 rpm or 20 minutes. Resuspension buffer was 0.3 M PBS (10 mM Na phosphate pH 7, 0.3 M NaCl). All DNA was purchased from ATDbio or MWG Eurofins.

8.4.1 Gold nanoparticle synthesis

18 nm diameter gold nanoparticles were prepared *via* citrate reduction of $HAuCl_4$ [193] [192] and the concentration was estimated using UV – vis spectroscopy based on the absorbance at

wavelength of 520 nm and an extinction coefficient of 2.7×10^8 M^{-1} cm^{-1}.

8.4.2 Nanoparticle – conjugate synthesis

Aptamer - modified gold nanoparticles were prepared using standard gold / thiol chemistry[128] and according to the following protocol. 20 nM Au colloid (for example, 355 µL, 5.6 µM) reacted with 3 nmoles thiol - modified DNA PKC aptamer (95 µL, 31.6 µM) made up to 1 mL total volume with water. Phosphate buffer was then added to a final concentration of 10 mM (200 µL, 60 mM) and left for 16 hours. Gradual salt additions were then carried out, 31 µL, 2M NaCl (0.05 M NaCl, final concentration) immediately after the 16 hour phosphate incubation and then 32 µL 2M NaCl (0.1 M NaCl, final concentration) 6 hours after original salt addition. After 24 hours, the sample was centrifuged, the supernatant removed and the pellet resuspended in 1 mL 0.3 M PBS. The concentration of AGNC was then determined by UV – vis spectroscopy.

8.4.3 Gel electrophoresis

All gels were prepared using agarose powder in Tris Borate EDTA (TBE) buffer, stained with GelStar Gel Stain (Lonza) and allowed to run for 1 hour at 120 V. Gel Pilot 50 bp ladder was used as the DNA size marker and the gels photographed. Both 1.5 % and 2 % (w/v) agarose gels were used and both Tri colour loading buffer (Bioline) and glycerol (7.5 %, v/v final concentration) were used to load the samples onto the gel.

8.4.4 Surface coverage

Samples were made up and analysed in triplicate. Conjugate samples were prepared as described previously, with the exception of the use of a 3' fluorescent label (FAM) modification

in addition to the 5‘ thiol required for nanoparticle attachment. Once resuspended in 0.3 M PBS, the sample was washed twice by repeated centrifugation and resuspension in 0.3 M PBS. The nanoparticle concentration was then determined by UV-Vis spectroscopy before displacement of the DNA molecules using Dithriothetol (DTT) (100 mM, final concentration) and left for 16 hours to completely aggregate.[198] The samples were spun down, the supernatant removed and resuspended in buffer. This was repeated a further two times and the washings kept and combined. Aliquots of each triplicate sample were analysed on a CaryEclipse Fluorimeter under the following conditions:

Monitor:	emission
Excitation:	485 nm
Emission:	495 – 600 nm
Slit size:	10 nm
PMT voltage:	medium

A calibration graph was first created using solutions of the FAM labelled DNA at varying concentrations. These were analysed, plotted using excel and the equation of the line used to determine the concentration of fluorescent DNA in the nanoparticle samples. In combination with the dilution factor (from the washing steps) and the concentration of the nanoparticles, it was possible to calculate the number of DNA molecules attached to the surface of the nanoparticles.

8.4.5 UV- melts

PKC aptamer solution (2 µM final volume using 31.61 µM stock solution in 2 mL 0.3 M PBS) was analysed using the thermal program on the UV-vis spectrophotometer under the following conditions:

Monitor:	260 nm
Start:	10 °C
Stop:	25 °C
Advanced collect:	6 stages (alternating cycles of 75 °C and 10 °C)
Rate:	1 °C / min

Gold nanoparticle conjugates (1.0 nM, 400 µL in PBS) were made up in duplicate (one for each

wavelength) and analysed using the thermal program on the UV-vis spectrophotometer under the following conditions:

Monitor:	260 or 520 nm
Start:	10 °C
Stop:	25 °C
Advanced collect:	6 stages (alternating cycles of 75 °C and 10 °C)

8.4.6 Mixed surface coverage – thiol PEG spacer

The two small thiol molecules, 11-Mercaptoundecyl tri ethylene glycol (11- MHEG) and 11-Mercaptoundecyl hexa ethylene glycol (11 MTEG) were added to gold colloid (20 nM, 1 mL final volume) at increasing concentrations 1.5, 3.0, 6.0, 15 and 30 µM. All were left for 16 hours, centrifuged and resuspended in 0.3 M PBS.

8.4.7 Short DNA sequence

The following DNA sequences were used and added to gold colloid (as outlined in 8.4.2) in different ratios according to Table 8.7:

5'- ACACGACGGGAATACTGACTCTCCCCCATGT - 3'	PKC aptamer, 33.8 µM
5' (HEG)CTCTCT -3'	6 mer spacer, 45.6 µM

Table 8.7: Summary of different conjugate samples.

Sample	Aptamer (no. of n moles)	6 mer spacer (no of n moles)	Ratio
HEG 1	1.5	1.5	1:1
HEG 2	1.0	2.0	1:2
HEG 5	0.5	2.5	1:5
HEG 9	0.3	2.7	1:9

8.4.8 Thymine spaced aptamer sequence

The following sequence were used

5' 15TACACGACGGGAATACTGACTCTCCCCCATGT – 3'	15T PKC aptamer, 100 μM
5' (HEG)CTCTCT -3'	6 mer spacer, 45.6 μM

The I5T PKC AGNC HEG 2 was prepared ss per HEG 2 conjugate as outlined in 8.4.7 with the exception of the 15 T PKC aptamer used in place of the PKC aptamer.

8.4.9 General assays

All assays were carried out in a similar way; AGNC (400 μL, 5 – 8.5 $x10^{-10}$ M) were incubated with PKC delta (Biosource, 8.26 μM stock solution) at varying concentrations (6.6 – 13 nM). Samples were left to incubate for 45 minutes and then analysed by UV-Vis spectroscopy. In all experiments, a control protein (BSA) was analysed in the presence of the PKC aptamer conjugates and a control DNA GNC (5' – TTTTTTTTTTTTTTTGGTTGGTGTGGTTGG - 3') was analysed in the presence of PKC. The conjugates were also analysed in the absence of any protein.

8.4.10 Time study

$8x10^{-10}$ M PKC AGNC was analysed in the presence of 13 nM PKC (400 μL total volume in 0.3 M PBS) from 0 – 60 minutes using UV-visible spectroscopy.

8.4.11 Stability study

HEG 1, HEG 2, HEG 5 and HEG 9 AGNC were diluted in HEPES buffer (10 mM HEPES, 1 mM $MgCl_2$, 16 mM KCl, pH 8.1) to a final concentration of 0.85 nM in 1 mL and their UV- vis spectra recorded time intervals of 1, 2, 3 and 4 hours.

8.4.12 Concentration study

HEG 1, HEG 2, HEG 5 and HEG 9 AGNC (400 µL, $7.6x10^{-10}$ M, in HEPES) were incubated with six different concentrations of PKC as detailed below:

Conjugate 2: 11.8, 4.7, 2.4, 1.2, 0.5 and 0 nM

Conjugate 3: 3.8, 1.52, 0.76, 0.38, 0.15 and 0 nM

Conjugate 4: 1.9, 0.76, 0.38, 0.19, 0.08 and 0 nM

The samples were left for 45 minutes and then analysed by UV-vis spectroscopy.

8.4.13 Concentration study (15T PKC AGNC)

A repetition of the assay outlined in 8.4.12 was repeated using I5T PKC AGNC HEG 2 with 11.8, 4.7, 2.4, 1.2, 0.5 and 0 nM PKC.

8.5 Thrombin

8.5.1 Thrombin aptamer gold nanoparticle conjugate synthesis

The synthesis of thrombin AGNC carried out as described in Section 8.4.1 and 8.4.2 with the following sequence:

Bock aptamer: 5 - TTTTTTTTTTTTTTTGGTTGGTGTGGTTGG- 3

8.5.2 Initial experiments

With the exception of time study experiments, all samples were left to incubate for 45 minutes before analysis. Unless stated otherwise nanoparticle samples were made up to a total volume of 400 µL in a variety of buffers and final concentration of 600 pM of AGNC and incubated with thrombin (Human alpha, 8.16 µM stock solution) a variety of final concentrations (0, 5, 10, 20, 40, 60, 100, 200 nM). Two control samples were also prepared;

1.) control protein where 200 nM BSA was added in place of thrombin and

2.) 600 pM control GNP with nonsense DNA (5' – thiol ACACGACGGGAATACTGACTCTCCCCCATGT – 3') in place of the thrombin GNP.

The following buffers were used:

1. Wilner buffer: 34 mM Tris-HCl (pH = 7.4), 233 mM NaCl, 8.5 mM KCl, 1.7 mM CaCl2, 1.7 mM MgCl2, 8.5 % glycerol (v/v)
2. PBS

8.5.3 KCl buffer optimisation experiment

AGNC (600 pM) were incubated with thrombin 0 and 60 nM thrombin in made up to 400 µL final volume in the following buffers:

1. PBS, 0.01 M KCl
2. PBS, 0.1 M KCl
3. PBS, 0.3 M KCl

8.5.4 $CaCl_2$ experiment

As per 8.5.3 using the following buffers:

1. PBS, 0.01 M KCl, 0.5 mM $CaCl_2$
2. PBS, 0.01 M KCl, 1 mM $CaCl_2$

3. PBS, 0.01 M KCl, 2 mM $CaCl_2$
4. PBS, 0.01 M KCl, 4 mM $CaCl_2$

8.5.5 $MgCl_2$ experiment

As per 8.5.3 using the following buffers:

1. PBS, 0.01 M KCl, 0.5 mM $MgCL_2$
2. PBS, 0.01 M KCl, 1 mM $MgCL_2$
3. PBS, 0.01 M KCl, 2 mM $MgCL_2$

8.5.6 Optimised buffer assay

The assay carried out on section 8.5.2 was repeated but the buffer used was 0.21 M NaCl, 0.01 M KCl, 9 mM Na phosphate buffer pH 7.5 (thrombin binding buffer). Once analysis by UV-vis spectroscopy was carried out, the samples were transferred to 0.2 mL plastic tubes and photographed.

8.5.7 Silver nanoparticle synthesis

Silver colloid was prepared using published methods[217] via citrate reduction of silver nitrate.

8.5.8 Synthesis of thrombin aptamer silver nanoparticle conjugates

The synthesis of thrombin ASNC was developed with reference to previously published method.[212]

Bock aptamer: 5 - Thiol TTTTTTTTTTTTTTTGGTTGGTGTGGTTGG- 3

Tasset aptamer: 5 - Thiol TTTTTTTTTTTTTTTAGTCCGTGGTAGGGCAGGTTGGGGTGACT -3

BDTDD conjugation

The benzotriazole dye (E)-4((1H-benzo[d] [1,2,3] triazole-5-yl) diazenyl)-3,5-dimethoxy phenol (BDTDD), synthesised by David Thompson[213] (10 µL, 1 mM) was added to silver colloid (990 µL, neat). This was left for 24 hour before the addition of DNA was carried out (10 nmoles e.g. 100 µL, 100 µM stock solution) to the dye functionalised nanoparticles. After another 24 hours, sodium phosphate buffer (60 mM, 200 µL) was then added (10 mM final concentration). Salt additions were carried out in 0.05 M increments to a final concentration of 0.1 M over a 24 hour period. The samples was then centrifuged for 20 minutes at 4000 rpm and then resuspended in 500 µL resuspension buffer (0.3 M PBS).

ROX conjugation[194]

DNA aptamer (10 nmoles e.g. 100 µL, 100 µM stock solution) was added to silver colloid (1 mL, neat) and left for 24 hours. Sodium phosphate buffer (60 mM, 200 µL) was then added (10 mM final concentration) and left for 24 hours. Salt additions were carried out in 0.05 M increments to a final concentration of 0.1 M over a 24 hour period. The samples was then centrifuged for 20 minutes at 4000 rpm and then resuspended in 500 µL resuspension buffer (0.3 M PBS). A ROX isothiocyanate (ROX ITC, Invitrogen) stock solution was made up (1 mM, methanol) and 1 µM solution aq. then made from the stock solution. The dye solution was then added to the DNA functionalised nanoparticles (500 µL, 1 µM).

8.5.9 UV-visible spectroscopy analysis

With the exception of time study experiments, all ASNC were left to incubate for 45 minutes before analysis. Unless stated otherwise samples were made up in thrombin binding buffer to a total volume of 400 µL and final concentration of 10 pM of ASNC and x nM thrombin. The concentration of thrombin was varied and so specific concentrations will be stated for each experiment.

8.5.10 Time study

ASNC (10 pM) was incubated with 0 and 20 nM thrombin (8.26 µM stock solution) (400 µL total volume in thrombin binding buffer) and then analysed by UV-visible spectroscopy using the automatic time study setting. A scan (200 – 800 nm) was taken every 5 minutes for a total of 90 minutes.

8.5.11 Visual limit of detection limit study

Five replicate samples of ASNC (10 pM) were incubated with 0, 2, 5, 10 and 20 nM thrombin (400 µL total volume). The sample containing no thrombin was analysed immediately after dilution in buffer and then again after a 45 minute incubation. All other samples were made up and analysed after 45 minutes.

8.5.12 Surface coverage determination

Only one set of nanoparticle conjugates were used namely, ROX Bock and both DNA and dye coverages were calculated.

Part A (DNA coverage) – this method was based on published methods.[218] The following DNA sequence was used: 5 – TTTTTTTTTTTTTTTGGTTGGTGTGGTTGG FAM – 3.

All samples and calibration standards were made up in triplicate.

The samples were prepared as set out in section 8.5.8 (ROX conjugation) with the exception of the resuspension buffer being replaced with DNase I reaction buffer (10mM Tris-HCl, 2.5 mM MgCl2, 0.5 mM CaCl2, pH 7.6, New England BioLabs) for treatment with DNAse I. The samples were analysed by UV-vis spectroscopy to determine the nanoparticle concentration using a molar extinction coefficient for Ag of 2.78 x 10^{10} M^{-1} cm^{-1}. DNAse I (final concentration 125 units/mL, New England BioLabs) was added to the DNA-nanoparticle conjugates. The samples were left for 16 hours at 37 °C and then centrifuged for 20 minutes at 5000 rpm. The

supernatant was extracted and analysed by fluorescence spectroscopy using an excitation wavelength of 495 nm. The following samples of FAM labelled DNA solutions (2 mL, x M) were used as the standard solutions for the calibration graph:

1.6, 3.1, 11.0, 18.0, 25.0, 37.5, 40.0, 50.0 nM

The experimental set up for the fluorimeter was as follows:

Monitor: emission
Excitation: 485 nm
Emission: 495 – 600 nm
Slit size: 10 nm
PMT voltage: medium

Part B (Dye coverage) - this method was based on published methods.[5] The following DNA sequence was used :

5 – TTTTTTTTTTTTTTTTGGTTGGTGTGGTTGG - 3

All samples and calibration standards were made up in triplicate.

The method detailed in section 8.4.4 was carried out here with the exception of the use of non fluorescent DNA and ROX dye solutions used as the calibration standards:

5.0, 10.0, 20.0, 30.0, 50.0, 60.0, 70.0, 80.0 nM

The experimental set up for the fluorimeter was as follows:

Monitor: emission
Excitation: 575 nm
Emission: 585 – 650 nm
Slit size: 10 nm
PMT voltage: medium

8.5.13 SERRS experimental - general

SERRS analysis was carried out on a variety of instruments including different wavelengths (532 and 514.5 nm) and sample set – up (microtitre plate and cuvette based).Microtitre plate analysis was carried out using a 96-well plastic plate and samples were made up to a total volume of 200 μL in thrombin binding buffer. Cuvette analysis was carried out in 1 cm path length plastic cuvettes and samples were made up to 400 μL in thrombin binding buffer. In

general , the following samples were investigated:

1. TASNC (with either Bock or Tasset sequence and either ROX or Rb dye) only.
2. TASNC (with either Bock or Tasset sequence and either ROX or Rb dye) in the presence of varying concentrations of thrombin.
3. ASNC (with either Bock or Tasset sequence and either ROX or Rb dye) in the presence of control protein (BSA).
4. Nonsense DNA SNC in the presence of thrombin.

8.5.14 Initial experiments

Two different instruments were used in the initial experiments:

1. Renishaw 2000 Raman Microprobe spectrometer with a charge-coupled device (CCD). The excitation was provided by a Spectra-Physics Model 2020 argon-ion laser with a wavelength of 514.5 nm and 3 mW of power at the source. Samples were analysed in a plastic microtitre plate using a 350× objective, an acquisition time of 1 second and the grating was centred at 1350cm^{-1}.
2. Renishaw 2000 Raman Microprobe spectrometer with a charge-coupled device (CCD). The excitation was provided by a Spectra-Physics Model 2020 argon-ion laser with a wavelength of 532 nm and 3 mW of power at the source. Samples were analysed in plastic cuvettes, with a 1 second acquisition time and the grating centred at 1400 cm^{-1}.

Triplicate samples of 10 pM TASNCs were incubated with in 0 and 10 nM thrombin (400 µL total volume in thrombin binding buffer) for 45 minutes and then analysed.

8.5.15 Cuvette based SERRS at 514 nm

1st experiment - Renishaw 2000 Raman Microprobe spectrometer with a charge-coupled device (CCD). The excitation was provided by a Spectra-Physics Model 2020 argon-ion laser with a

wavelength of 514.5 nm and 3 mW of power at the source. Samples were analysed in plastic cuvettes, with a 1 second acquisition time and the grating centred at 1400 cm^{-1}.

The samples (listed below) were made up and analysed in triplicate in plastic cuvettes.

1. 50 pM ASNCs, 0 nM thrombin
2. 50 pM ASNCs, 5 nM thrombin

2^{nd} experiment - Time study carried out at 5 minute intervals for 60 minutes. All samples were made up in triplicate as follows:

1. 10 pM ASNC, 0 nM thrombin
2. 10 pM ASNC, 10 nM thrombin
3. 10 pM ASNC, 25 nM thrombin
4. 10 pM Nonsense DNA SNC, 25 nM thrombin
5. 10 pM ASNCs, 25 nM BSA

3^{rd} experiment concentration study - Triplicate samples of ASNCs (10 pM) was incubated with increasing concentrations of thrombin (in a total volume of 400 µL in thrombin binding buffer) 0 nM thrombin. The samples were left for 45 minutes and analysed as detailed in 8.5.14. The thrombin concentrations used were: 0, 2, 5 and 10 nM.

8.5.16 Automatic time study

An automatic time study was carried out. The following four samples were made up in five replicates and analysed individually. The analysis was carried out every 5 seconds for 60 minutes.

1. 10 pM TASNCs, 0 nM thrombin
2. 10 pM TASNCs, 25 nM thrombin
3. 10 pM NDSNCs, 25 nM thrombin
4. 10 pM TASNCs, 25 nM BSA

8.5.17 Aggregation study of ROX – ITC and BDTDD dye functionalised nanoparticles

Each dye solution (40 µL, 1 µM aq.) was added to silver colloid (360 µL, neat) and analysed immediately (as in section 8.5.15). The samples were then centrifuged (20 minutes @ 6000 rpm), the supernatant removed and the samples resuspended in 400 µL water. This was then analysed by SERRS. Salt addition was then carried out (50 µL, 2 M) to aggregate the nanoparticles and a final SERRS analysis carried out.

9 References

1. K. B. Mullis, F. A. Faloona and W. Ray, *Method Enzymol.*, 1987, **155**, 335.
2. A. J. Jeffreys, V. Wilson and S. L. Thein, *Nature*, 1985, **314**, 67.
3. J. C. Venter, M. D. Adams, E. W. Myers, P. W. Li, R. J. Mural, G. G. Sutton and H. O. Smith, *Science*, 2001, **291**, 1304.
4. S. E. Osborne, I. Matsumura and A. D. Ellington, *Curr. Opin. Chem. Biol.*, 1997, **1**, 5.
5. A. D. Ellington and J. W. Szostak, *Nature*, 1990, **346**, 818.
6. R. D. Jenison, S. C. Gill, A. Pardi and B. Polisky, *Science*, 1994, **263**, 1425.
7. D. L. Robertson and G. F. Joyce, *Nature*, 1990, **344**, 467.
8. C. Tuerk and L. Gold, *Science*, 1990, **249**, 505.
9. J. F. Lee, J. R. Hesselberth, L. A. Meyers and A. D. Ellington, *Nucl. Acids Res.*, 2004, **32**, D95.
10. J. Ciesiolka, J. Gorski and M. Yarus, *RNA*, 1995, **1**, 538.
11. I. Hirao, S. Yoshinari, S. Yokoyama, Y. Endo and A. D. Ellington, *Nucleic Acids Symp. Ser.*, 1997, 283.
12. L. C. Bock, L. C. Griffin, J. A. Latham, E. H. Vermaas and J. J. Toole, *Nature*, 1992, **355**, 564.
13. Z. Tang, D. Shangguan, K. Wang, H. Shi, K. Sefah, P. Mallikratchy, H. W. Chen, Y. Li and W. Tan, *Anal. Chem.*, 2007, **79**, 4900.
14. A. Geiger, P. Burgstaller, H. von der Eltz, A. Roeder and M. Famulok, *Nucl. Acids Res.*, 1996, **24**, 1029.
15. N. C. Pagratis, C. Bell, Y. F. Chang, S. Jennings, T. Fitzwater, D. Jellinek and C. Dang, *Nat. Biotechnol.*, 1997, **15**, 68.
16. P. A. Levene, *J. Biol. Chem.*, 1919, **40**, 415.
17. J. D. Watson and F. H. C. Crick, *Nature*, 1953, **171**, 737.
18. R. E. Franklin and R. G. Gosling, *Nature*, 1953, **172**, 156.
19. M. H. F. Wilkins, A. R. Stokes and H. R. Wilson, *Nature*, 1953, **171**, 738.
20. M. F. Kubik, A. W. Stephens, D. Schneider, R. A. Marlar and D. Tasset, *Nucleic Acids Res.*, 1994, **22**, 2619.
21. P. Colas, B. Cohen, T. Jessen, I. Grishina, J. McCoy and R. Brent, *Nature*, 1996, **380**, 548.
22. M. Crawford, R. Woodman and P. K. Ferrigno, *Brief. Funct. Genomic Proteomic.*, 2003, **2**, 72.
23. B. A. Cohen, P. Colas and R. Brent, *P. Natl. Acad Sci. USA*, 1998, **95**, 14272.
24. K. Butz, C. Denk, B. Fitscher, I. Crnkovic-Mertens, A. Ullmann, C. H. Schroder and F. Hoppe-Seyler, *Oncogene*, 2001, **20**, 6579.
25. P. Colas, B. Cohen, P. K. Ferrigno, P. A. Silver and R. Brent, *P. Natl. Acad. Sci.USA*, 2000, **97**, 13720.
26. M. N. Stojanovic, P. de Prada and D. W. Landry, *J. Am. Chem. Soc.*, 2000, **122**, 11547.
27. J.-L. He, Z.-S. Wu, H. Zhou, H.-Q. Wang, J.-H. Jiang, G.-L. Shen and R.-Q. Yu, *Anal. Chem.*, 2010, **82**, 1358.
28. X. Zuo, Y. Xiao and K. W. Plaxco, *J. Am. Chem. Soc.*, 2009, **131**, 6944.
29. C.-y. Zhang and L. W. Johnson, *Anal. Chem.*, 2009, **81**, 3051.
30. M. Bogusz, R. Aderjan, G. Schmitt, E. Nadler and B. Neureither, *Forensic Sci.Int.*, 1990,

48, 27.
31. K. A. Moore, C. Werner, R. M. Zannelli, B. Levine and M. L. Smith, *Forensic Sci. Int.*, 1999, **106**, 93.
32. W. M. Asselin and J. M. Leslie, *J. Anal. Toxicol.*, 1992, **16**, 381.
33. E. Meyer, J. F. VanBocxlaer, I. M. Dirinck, W. E. Lambert, L. Thienpont and A. P. DeLeenheer, *J. Anal. Toxicol.*, 1997, **21**, 236.
34. H. Kimura, J. L. Yuan, G. L. Wang, K. Matsumoto and M. Mukaida, *J. Anal. Toxicol.*, 1999, **23**, 11.
35. P. Lillsunde and T. Korte, *J. Anal. Toxicol.*, 1991, **15**, 71.
36. K. Hara, S. Kashimura, Y. Hieda and M. Kageura, *J. Anal. Toxicol.*, 1997, **21**, 54.
37. R. Meatherall, *J. Anal. Toxicol.*, 1995, **19**, 316.
38. A. Solans, M. Carnicero, R. Delatorre and J. Segura, *J. Anal. Toxicol.*, 1995, **19**, 104.
39. R. Stoltenburg, C. Reinemann and B. Strehlitz, *Biomol. Eng.*, 2007, **24**, 381.
40. M. T. Bowser, *Analyst*, 2005, **130**, 128.
41. D. W. Drolet, L. MoonMcDermott and T. S. Romig, *Nat. Biotechnol.*, 1996, **14**, 1021.
42. C. Ferreira, K. Papamichael, G. Guilbault, T. Schwarzacher, J. Gariepy and S. Missailidis, *Anal. Bioanal. Chem.*, 2008, **390**, 1039.
43. S. J. Lee, B.-S. Youn, J. W. Park, J. H. Niazi, Y. S. Kim and M. B. Gu, *Anal. Chem.*, 2008, **80**, 2867.
44. P. Mallikaratchy, R. V. Stahelin, Z. H. Cao, W. H. Cho and W. H. Tan, *Chem. Commun.*, 2006, 3229.
45. R. Stoltenburg, C. Reinemann and B. Strehlitz, *Anal. Bioanal. Chem.*, 2005, **383**, 83.
46. D. Nieuwlandt, M. Wecker and L. Gold, *Biochemistry*, 1995, **34**, 5651.
47. Z. Cao, S. W. Suljak and W. Tan, *Current Proteomics*, 2005, **2**, 31.
48. J. S. Swensen, Y. Xiao, B. S. Ferguson, A. A. Lubin, R. Y. Lai, A. J. Heeger, K. W. Plaxco and H. T. Soh, *J. Am. Chem. Soc.*, 2009, **131**, 4262.
49. M. N. Stojanovic and D. W. Landry, *J. Am. Chem. Soc.*, 2002, **124**, 9678.
50. N. Kawazoe, Y. Ito and Y. Imanishi, *Biotechnol. Prog.*, 1997, **13**, 873.
51. F. Li, J. Zhang, X. Cao, L. Wang, D. Li, S. Song, B. Ye and C. Fan, *Analyst*, 2009, **134**, 1355.
52. J. W. Liu, D. Mazumdar and Y. Lu, *Angew. Chem. Int. Ed.*, 2006, **45**, 7955.
53. S. Pakakasama, S. Kajanachumpol, S. Kanjanapongkul, N. Sirachainan, A. Meekaewkunchorn, V. Ningsanond and S. Hongeng, *Int. J. Lab. Hematol*, 2008, **30**, 286.
54. F. Michor, T. P. Hughes, Y. Iwasa, S. Branford, N. P. Shah, C. L. Sawyers and M. A. Nowak, *Nature*, 2005, **435**, 1267.
55. S. Raskin, J. A. Phillips, G. Kaplan, M. McClure and C. Vnencak-Jones, *Genome Res.*, 1992, **2**, 154.
56. R. K. Saiki, S. Scharf, F. Faloona, K. B. Mullis, G. T. Horn, H. A. Erlich and N. Arnheim, *Science*, 1985, **230**, 1350.
57. K. B. Jensen, B. L. Atkinson, M. C. Willis, T. H. Koch and L. Gold, *Proc. Natl. Acad. Sci.*, 1995, **92**, 12220.
58. L. Green, S. Waugh, J. P. Binkley, Z. Hostomska, Z. Hostomsky and C. Tuerk, *J. Mol. Biol.*, 1995, **247**, 60.
59. R. N. Veedu and J. Wengel, *Mol. Biosyst.*, 2009, **5**, 787.
60. D. A. Braasch and D. R. Corey, *Chem. Biol.*, 2001, **8**, 1.
61. J. Wengel, *Acc. Chem. Res.*, 1999, **32**, 301.
62. S. Kluszmann, A. Nolte, R. Bald, V. A. Erdmann and J. P. Furste, *Nat. Biotech.*, 1996, **14**,

1112.
63. K. P. Williams, X.-H. Liu, T. N. M. Schumacher, H. Y. Lin, D. A. Ausiello, P. S. Kim and D. P. Bartel, *Proc. Natl. Acad. Sci*, 1997, **94**, 11285.
64. B. Wlotzka, S. Leva, B. EschgfÃ¤ller, J. Burmeister, F. Kleinjung, C. Kaduk, P. Muhn, H. Hess-Stumpp and S. Klussmann, *PNAS*, 2002, **99**, 8898.
65. S. Tsukiji, S. B. Pattnaik and H. Suga, *J. Am. Chem. Soc.*, 2004, **126**, 5044.
66. E. H. Ekland and D. P. Bartel, *Nature*, 1996, **383**, 192.
67. K. E. McGinness and G. F. Joyce, *Chem. Biol.*, 2002, **9**, 297.
68. J. R. Prudent, T. Uno and P. G. Schultz, *Science*, 1994, **264**, 1924.
69. S. Baskerville and D. P. Bartel, *Proc. Natl. Acad. Sci*, 2002, **99**, 9154.
70. V. R. Jadhav and M. Yarus, *Biochemistry*, 2001, **41**, 723.
71. B. Seelig and A. Jäschke, *Chem. Biol.*, 1999, **6**, 167.
72. L. A. Holeman, S. L. Robinson, J. W. Szostak and C. Wilson, *Fold. Des.*, 1998, **3**, 423.
73. D. Mann, C. Reinemann, R. Stoltenburg and B. Strehlitz, *Biochem. Bioph. Res. Co.*, 2005, **338**, 1928.
74. S. Gopinath, *Anal. Bioanal. Chem.*, 2007, **387**, 171.
75. S. Sekiya, K. Noda, F. Nishikawa, T. Yokoyama, P. K. R. Kumar and S. Nishikawa, *J. Biochem.*, 2006, **139**, 383.
76. S. C. B. Gopinath, T. S. Misono, K. Kawasaki, T. Mizuno, M. Imai, T. Odagiri and P. K. R. Kumar, *J. Gen. Virol.*, 2006, **87**, 479.
77. S. C. B. Gopinath, Y. Sakamaki, K. Kawasaki and P. K. R. Kumar, *J Biochem*, 2006, **139**, 837.
78. M. Blank, T. Weinschenk, M. Priemer and H. Schluesener, *J. Biol. Chem.*, 2001, **276**, 16464.
79. T. S. Misono and P. K. R. Kumar, *Anal. Biochem.*, 2005, **342**, 312.
80. S. N. Krylov and M. Berezovski, *Analyst*, 2003, **128**, 571.
81. A. P. Drabovich, M. Berezovski, V. Okhonin and S. N. Krylov, *Anal. Chem.*, 2006, **78**, 3171.
82. J. C. Cox and A. D. Ellington, *Bioorg. Med. Chem.*, 2001, **9**, 2525.
83. G. Hybarger, J. Bynum, R. F. Williams, J. J. Valdes and J. P. Chambers, *Anal. Bioanal. Chem.*, 2006, **384**, 191.
84. N. Ferrara and W. J. Henzel, *Biochem. Bioph. Res. Co.*, 1989, **161**, 851.
85. D. Jellinek, L. S. Green, C. Bell and N. Janjic, *Biochemistry*, 1994, **33**, 10450.
86. D. Jellinek, L. S. Green, C. Bell, C. K. Lynott, N. Gill, C. Vargeese, G. Kirschenheuter, D. P. C. McGee and P. Abesinghe, *Biochemistry*, 1995, **34**, 11363.
87. L. S. Green, D. Jellinek, C. Bell, L. A. Beebe, B. D. Feistner, S. C. Gill, F. M. Jucker and N. Janji, *Chem. Biol.*, 1995, **2**, 683.
88. J. Ruckman, L. S. Green, J. Beeson, S. Waugh, W. L. Gillette, D. D. Henninger, L. Claesson-Welsh and N. Janjic, *J. Biol. Chem.*, 1998, **273**, 20556.
89. J. M. Healy, S. D. Lewis, M. Kurz, R. M. Boomer, K. M. Thompson, C. Wilson and T. G. McCauley, *Pharm. Res.*, 2004, **21**, 2234.
90. L. Gryziewicz, *Adv. Drug Deliver. Rev.*, 2005, **57**, 2092.
91. C. A. Trujillo, A. A. Nery, J. M. Alves, A. H. Martins and H. Ulrich, *Clin. Ophthalmol.*, 2007, **1**, 393.
92. M. G. Theis, A. Knorre, B. Kellersch, J. r. Moelleken, F. Wieland, W. Kolanus and M. Famulok, *Proc. Natl. Acad. Sci*, 2004, **101**, 11221.

93. G. n. Mayer, M. Blind, W. Nagel, T. BÃ¶hm, T. Knorr, C. L. Jackson, W. Kolanus and M. Famulok, *Proc. Natl. Acad. Sci.*, 2001, **98**, 4961.
94. S. J. Klug, A. Huttenhofer, M. Kromayer and M. Famulok, *Proc. Natl. Acad. Sci.*, 1997, **94**, 6676.
95. R. C. Conrad, L. Giver, Y. Tian and A. D. Ellington, 1996, **267**, 336.
96. U. Kikkawa, H. Matsuzaki and T. Yamamoto, *J. Biochem.*, 2002, **132**, 831.
97. D. M. Tasset, M. F. Kubik and W. Steiner, *J. Mol. Biol.*, 1997, **272**, 688.
98. L. C. Griffin, G. F. Tidmarsh, L. C. Bock, J. J. Toole and L. L. Leung, *Blood*, 1993, **81**, 3271.
99. A. DeAnda, Jr., S. E. Coutre, M. R. Moon, C. M. Vial, L. C. Griffin, V. S. Law, M. Komeda, L. L. Leung and D. C. Miller, *Ann. Thorac. Med.*, 1994, **58**, 344.
100. W. X. Li, A. V. Kaplan, G. W. Grant, J. J. Toole and L. L. Leung, *Blood*, 1994, **83**, 677.
101. C. P. Rusconi, J. D. Roberts, G. A. Pitoc, S. M. Nimjee, R. R. White, G. Quick, E. Scardino, W. P. Fay and B. A. Sullenger, *Nat. Biotechnol.*, 2004, **22**, 1423.
102. M. Srivastava and H. B. Pollard, *J. FASEB*, 1999, **13**, 1911.
103. A. G. Hovanessian, F. Puvion-Dutilleul, S. Nisole, J. Svab, E. Perret, J.-S. Deng and B. Krust, *Exp. Cell. Res.*, 2000, **261**, 312.
104. C. R. Ireson and L. R. Kelland, *Mol. Cancer Ther.*, 2006, **5**, 2957.
105. P. J. Bates, J. B. Kahlon, S. D. Thomas, J. O. Trent and D. M. Miller, *J. Biol. Chem.*, 1999, **274**, 26369.
106. Y. Saijo, B. Uchiyama, T. Abe, K. Satoh and T. Nukiwa, *Jpn. J. Cancer Res.*, 1997, **88**, 26.
107. S. Yasuo, U. Bine, A. Tatsuya, S. Ken and N. Toshihiro, *J. Jpn. Cancer Res.*, 1997, **88**, 26.
108. M. Famulok and G. Mayer, *Chem. Bio. Chem*, 2005, **6**, 19.
109. G. Mayer, *Angew. Chem. Int. Ed.*, 2009, **48**, 2672.
110. S. Yamazaki, L. Tan, G. Mayer, J. S. Hartig, J.-N. Song, S. Reuter, T. Restle, S. D. Laufer, D. Grohmann, H.-G. Kräusslich, J. Bajorath and M. Famulok, *Chem. Biol.*, 2007, **14**, 804.
111. M. Hafner, A. Schmitz, I. Grune, S. G. Srivatsan, B. Paul, W. Kolanus, T. Quast, E. Kremmer, I. Bauer and M. Famulok, *Nature*, 2006, **444**, 941.
112. L. S. Green, D. Jellinek, R. Jenison, A. Ostman, C.-H. Heldin and N. Janjic, *Biochemistry*, 1996, **35**, 14413.
113. P. Leveen, M. Pekny, S. Gebre-Medhin, B. Swolin, E. Larsson and C. Betsholtz, *Genes Dev.*, 1994, **8**, 1875.
114. H. Bostrom, K. Willetts, M. Pekny, P. Leveen, P. Lindahl, H. Hedstrand, M. Pekna, M. Hellstrom, S. GebreMedhin, M. Schalling, M. Nilsson, S. Kurland, J. Tornell, J. K. Heath and C. Betsholtz, *Cell*, 1996, **85**, 863.
115. R. F. Doolittle, M. W. Hunkapiller, L. E. Hood, S. G. Devare, K. C. Robbins, S. A. Aaronson and H. N. Antoniades, *Science*, 1983, **221**, 275.
116. G. Powis, M. J. Seewald, D. Melder, M. Hoke, C. Gratas, T. A. Christensen and D. E. Chapman, *Cancer Chemoth. Pharm.*, 1992, **31**, 223.
117. R. Conrad and A. D. Ellington, *Anal. Biochem.*, 1996, **242**, 261.
118. K. A. Davis, B. Abrams, Y. Lin and S. D. Jayasena, *Nucl. Acids Res.*, 1996, **24**, 702.
119. Y. Xiao, A. Lubin, A., A. Heeger, J. and K. Plaxco, W., *Angew. Chem.*, 2005, **117**, 5592.
120. H. Pandana, K. H. Aschenbach and R. D. Gomez, *IEEE Sens. J.*, 2008, **8**, 661.
121. V. Pavlov, Y. Xiao, B. Shlyahovsky and I. Willner, *J. Am. Chem. Soc.*, 2004, **126**, 11768.
122. C. C. Huang, Y. F. Huang, Z. H. Cao, W. H. Tan and H. T. Chang, *Anal. Chem.*, 2005, **77**, 5735.
123. C. D. Medley, J. E. Smith, Z. Tang, Y. Wu, S. Bamrungsap and W. Tan, *Anal. Chem.*, 2008,

80, 1067.
124. M. C. Daniel and D. Astruc, *Chem. Rev.*, 2004, **104**, 293.
125. M. Faraday, *Philos. Trans. R. Soc. Lond.*, 1856, **146**, 159.
126. J. D. Aiken and R. G. Finke, *J. Mol. Catal. A-Chem.*, 1999, **145**, 1.
127. C. J. Johnson, N. Zhukovsky, A. E. G. Cass and J. M. Nagy, *Proteomics*, 2008, **8**, 715.
128. C. A. Mirkin, R. L. Letsinger, R. C. Mucic and J. J. Storhoff, *Nature*, 1996, **382**, 607.
129. E. Suprun, V. Shumyantseva, T. Bulko, S. Rachmetova, S. Rad'ko, N. Bodoev and A. Archakov, *Biosens. Bioelectron.*, 2008, **24**, 825.
130. K. Kerman and E. Tamiya, *J. Biomed. Nanotechnol.*, 2008, **4**, 159.
131. J. Liu and Y. Lu, *Angew. Chem. Int. Ed. Engl.*, 2006, **45**, 90.
132. J. Zhang, L. H. Wang, D. Pan, S. P. Song, F. Y. C. Boey, H. Zhang and C. H. Fan, *Small*, 2008, **4**, 1196.
133. Y. Li, H. Qi, Y. Peng, J. Yang and C. Zhang, *Electrochem. Commun.*, 2007, **9**, 2571.
134. S. Zhang, J. Xia and X. Li, *Anal. Chem.*, 2008, **80**, 8382.
135. J.-W. Chen, X.-P. Liu, K.-J. Feng, Y. Liang, J.-H. Jiang, G.-L. Shen and R.-Q. Yu, *Biosens. Bioelectron.*, 2008, **24**, 66.
136. L. Fabris, M. Dante, T. Q. Nguyen, J. B. H. Tok and G. C. Bazan, *Adv. Funct. Mater.*, 2008, **18**, 2518.
137. C. Jiwei, J. Jianhui, G. Xing, L. Guokun, S. Guoli and Y. Ruqin, *Chem-Eur. J.*, 2008, **14**, 8374.
138. J. Yguerabide and E. E. Yguerabide, *Anal. Biochem.*, 1998, **262**, 137.
139. J. A. Dougan, C. Karlsson, W. E. Smith and D. Graham, *Nucl. Acids Res.*, 2007, **35**, 3668.
140. L. S. Nair and C. T. Laurencin, *J. Biomed. Nanotechnol.*, 2007, **3**, 301.
141. B. D. Chithrani, A. A. Ghazani and W. C. W. Chan, *Nano. Lett.*, 2006, **6**, 662.
142. P. H. Yang, X. S. Sun, J. F. Chiu, H. Z. Sun and Q. Y. He, *Bioconjugate Chem.*, 2005, **16**, 494.
143. V. Dixit, J. Van den Bossche, D. M. Sherman, D. H. Thompson and R. P. Andres, *Bioconjugate Chem.*, 2006, **17**, 603.
144. Z. W. Tang, D. Shangguan, K. M. Wang, H. Shi, K. Sefah, P. Mallikratchy, H. W. Chen, Y. Li and W. H. Tan, *Anal. Chem.*, 2007, **79**, 4900.
145. J. E. Smith, C. D. Medley, Z. Tang, D. Shangguan, C. Lofton and W. Tan, *Anal. Chem.*, 2007, **79**, 3075.
146. K. Padmanabhan, K. P. Padmanabhan, J. D. Ferrara, J. E. Sadler and A. Tulinsky, *J. Biol. Chem.*, 1993, **268**, 17651.
147. C. V. Raman and K. S. Krishnan, *Nature*, 1928, **121**, 501.
148. M. Fleischmann, P. J. Hendra and A. J. McQuillan, *Chem. Phys. Lett.*, 1974, **26**, 163.
149. S. Nie and S. R. Emory, 1997, **275**, 1102.
150. M. G. Albrecht and J. A. Creighton, *J. Am. Chem. Soc.*, 1977, **99**, 5215.
151. C. L. Haynes and R. P. Van Duyne, *J. Phys. Chem. B*, 2001, **105**, 5599.
152. G. M. Wallraff and W. D. Hinsberg, *Chem. Rev.*, 1999, **99**, 1801.
153. M. Moskovits, *Rev. Mod. Phys.*, 1985, **57**, 783.
154. P. L. Stiles, J. A. Dieringer, N. C. Shah and R. P. Van Duyne, *Annu. Rev. Anal. Chem*, 2008, **1**, 601.
155. W. E. Smith and G. Dent, *Modern Raman Spectroscopy; A Practical Approach*, 2005.
156. T. Vo-Dinh, L. R. Allain and D. L. Stokes, *J. Raman Spectrosc.*, 2002, **33**, 511.
157. M. Culha, D. Stokes, L. R. Allain and T. Vo-Dinh, *Anal. Chem.*, 2003, **75**, 6196.

158. K. Faulds, F. A. McKenzie, E. W. Smith and D. Graham, *Angew. Chem. Int. Ed.*, 2007, **46**, 1829.
159. L. Sun, C. Yu and J. Irudayaraj, *Anal. Chem.*, 2008, **80**, 3342.
160. M. Green, F.-M. Liu, L. Cohen, P. Kollensperger and T. Cass, *Faraday Discuss.*, 2006, **132**, 269.
161. X. X. Han, Y. Kitahama, Y. Tanaka, J. Guo, W. Q. Xu, B. Zhao and Y. Ozaki, *Anal. Chem.*, 2008, **80**, 6567.
162. T. Li, L. Guo and Z. Wang, *Anal. Sci.*, 2008, **24**, 907.
163. P. Douglas, R. J. Stokes, D. Graham and W. E. Smith, *Analyst*, 2008, **133**, 791.
164. H. Cho, B. R. Baker, S. Wachsmann-Hogiu, C. V. Pagba, T. A. Laurence, S. M. Lane, L. P. Lee and J. B. H. Tok, *Nano. Lett.*, 2008, **8**, 4386.
165. M. S. P. A. R. Bizzarri and M. S. P. S. Cannistraro, *Nanomed.-Nanotechnol.*, 2007, **3**, 306.
166. A. J. Bonham, G. Braun, I. Pavel, M. Moskovits and N. O. Reich, *J. Am. Chem. Soc.*, 2007, **129**, 14572.
167. M. L. Darnaud, *PhD Thesis*, University of Strathclyde, 2008.
168. F. Corpet, *Nucl. Acids Res.*, 1988, **16**, 10881.
169. M. Zuker, *Nucl. Acids Res.*, 2003, **31**, 3406.
170. B. K. Van Weemen and A. H. W. M. Schuurs, *FEBS Lett.*, 1971, **15**, 232.
171. E. Engvall, K. Jonsson and P. Perlmann, *Biochem. Biophys. Acta*, 1971, **251**, 427.
172. E. Engvall and P. Perlmann, *Immunochemistry*, 1971, **8**, 871.
173. L. Chaiet and F. J. Wolf, *Arch. Biochem. Biophys*, 1964, **106**, 1.
174. S. M. Kelly and N. C. Price, *Curr. Prot. Pept. Sci.*, 2000, **1**, 349.
175. R. Marty, C. N. N'Soukpoe-Kossi, D. Charbonneau, C. M. Weinert, L. Kreplak and H.-A. Tajmir-Riahi, *Nucl. Acids Res.*, 2009, **37**, 849.
176. U. Jonsson, L. Fagerstam, B. Ivarsson, B. Johnsson and R. Karlsson, *Biotechniques*, 1991, **11**, 620.
177. M. N. Win, J. S. Klein and C. D. Smolke, *Nucl. Acids Res.*, 2006, **34**, 5670.
178. A. S. R. Potty, K. Kourentzi, H. Fang, G. W. Jackson, X. Zhang, G. B. Legge and R. C. Willson, *Biopolymers*, 2009, **91**, 145.
179. C. J. Suckling, M. C. Tedford, L. M. Bence, J. I. Irvine and W. H. Stimson, *Bioorg. Med. Chem. Lett.*, 1992, **2**, 49.
180. V. Steven, *PhD Thesis*, University of Strathclyde, 2010.
181. V. Steven and D. Graham, *Org. Biomol. Chem.*, 2008, **6**, 3781.
182. V. Dapic, V. Abdomerovic, R. Marrington, J. Peberdy, A. Rodger, J. O. Trent and P. J. Bates, *Nucl. Acids Res.*, 2003, **31**, 2097.
183. J. Dougan, 2009.
184. S. G. Penn, L. He and M. J. Natan, *Curr. Opin. Chem. Biol.*, 2003, **7**, 609.
185. N. L. Rosi and C. A. Mirkin, *Chem. Rev.*, 2005, **105**, 1547.
186. A. C. Newton, *Chem. Rev.*, 2001, **101**, 2353.
187. S. R. Cerda, R. Mustafi, H. Little, G. Cohen, S. Khare, C. Moore, P. Majumder and M. Bissonnette, *Oncogene*, 2006, **25**, 3123.
188. Y. Nishizuka, *J. FASEB*, 1995, **9**, 484.
189. Z. Lu, A. Hornia, Y. W. Jiang, Q. Zang, S. Ohno and D. A. Foster, *Mol. Cell. Biol.*, 1997, **17**, 3418.
190. C.-C. Huang, S.-H. Chiu, Y.-F. Huang and H.-T. Chang, *Anal. Chem.*, 2007, **79**, 4798.
191. W. A. Zhao, W. Chiuman, M. A. Brook and Y. F. Li, *Chembiochem.*, 2007, **8**, 727.

192. J. Turkevich, P. C. Stevenson and J. Hillier, *Discuss. Faraday Soc.*, 1951, **11**, 55.
193. G. Frens, *Nature (London), Phys. Sci.*, 1973, **241**, 20.
194. F. A. McKenzie, *PhD Thesis*, University of Strathclyde, 2010.
195. P. Sandstrom, M. Boncheva and B. Akerman, *Langmuir*, 2003, **19**, 7537.
196. M. Hanauer, S. Pierrat, I. Zins, A. Lotz and C. Sonnichsen, *Nano. Lett.*, 2007, **7**, 2881.
197. T. Pellegrino, R. A. Sperling, A. P. Alivisatos and W. J. Parak, 2007, **2007**, 26796.
198. L. M. Demers, C. A. Mirkin, R. C. Mucic, R. A. Reynolds, R. L. Letsinger, R. Elghanian and G. Viswanadham, *Anal. Chem.*, 2000, **72**, 5535.
199. H. D. Hill, J. E. Millstone, M. J. Banholzer and C. A. Mirkin, 2009, **3**, 418.
200. F. McKenzie, K. Faulds and D. Graham, *Small*, 2007, **3**, 1866.
201. J. Liu and Y. Lu, *J. Am. Chem. Soc.*, 2007, **129**, 8634.
202. J. L. Liu, Y., *Angew. Chem. Int. Ed.*, 2006, **45**, 90.
203. Z. Juan, W. Lihua, P. Dun, S. Shiping, Y. C. B. Freddy, Z. Hua and F. Chunhai, 2008, **4**, 1196.
204. R. A. Sperling, P. R. Gil, F. Zhang, M. Zanella and W. J. Parak, *Chem. Soc. Rev.*, 2008, **37**, 1896.
205. A. Van Hoonacker and P. Englebienne, *Curr. Nanosci.*, 2006, **2**, 359.
206. R. Wilson, *Chem. Soc. Rev.*, 2008, **37**, 2028.
207. E. E. Connor, J. Mwamuka, A. Gole, C. J. Murphy and M. D. Wyatt, *Small*, 2005, **1**, 325.
208. C. J. Murphy, A. M. Gole, J. W. Stone, P. N. Sisco, A. M. Alkilany, E. C. Goldsmith and S. C. Baxter, *Acc. Chem. Res*, 2008, **41**, 1721.
209. L. C. Griffin, G. F. Tidmarsh, L. C. Bock, J. J. Toole and L. L. K. Leung, *Blood*, 1993, **81**, 3271.
210. K. Y. Wang, S. McCurdy, R. G. Shea, S. Swaminathan and P. H. Bolton, *Biochemistry*, 1993, **32**, 1899.
211. R. F. Macaya, P. Schultze, F. W. Smith, J. A. Roe and J. Feigon, *Proc. Natl. Acad. Sci.*, 1993, **90**, 3745.
212. D. G. Thompson, A. Enright, K. Faulds, W. E. Smith and D. Graham, *Anal. Chem.*, 2008, **80**, 2805.
213. D. Graham, D. G. Thompson, W. E. Smith and K. Faulds, *Nature Nanotech.*, 2008, **3**, 548.
214. D. Cunningham, R. E. Littleford, W. E. Smith, P. J. Lundahl, I. Khan, D. W. McComb, D. Graham and N. Laforest, *Faraday Discuss.*, 2006, **132**, 135.
215. I. Khan, D. Cunningham, D. Graham, D. W. McComb and W. E. Smith, *J. Phys. Chem. B*, 2005, **109**, 3454.
216. I. Khan, D. Cunningham, R. E. Littleford, D. Graham, W. E. Smith and D. W. McComb, *Anal. Chem.*, 2005, **78**, 224.
217. P. C. Lee and D. Meisel, *J. Phys. Chem.*, 1982, **86**, 3391.
218. F. McKenzie, V. Steven, A. Ingram and D. Graham, *Chem. Commun.*, 2009, 2872.
219. D. Graham, R. Stevenson, D. G. Thompson, B. L., C. Dalton and K. Faulds, *Faraday Discuss.*, 2010, **149**, 1.
220. M. N. Stojanovic, *Personal communication*, 2009.

10 Appendix

M-fold structures - see attached CD